CARBON FLOW THROUGH INSHORE MARINE ENVIRONMENTS OF THE VESTFOLD HILLS, EAST ANTARCTICA

by

John Andrew Edwin Gibson B.Sc. (Hons), M.Sc.

Submitted in fulfilment of the requirements for the degree of Doctor of Philosophy

Antarctic CRC

and

Institute of Antarctic and Southern Ocean Studies

University of Tasmania

Hobart

Australia

March, 1997

For

My parents and family

and

Kerrie

in appreciation of their love and support

DECLARATION

This is to certify that the material composing this thesis has never been accepted for any other degree or award in any tertiary institution and, to the best of my knowledge and belief, is solely the work of the author, and contains no material previously published or written by another person, except where due reference is made in the text.

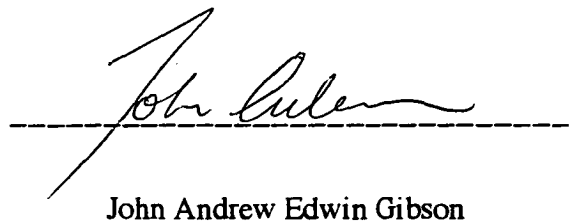

John Andrew Edwin Gibson

AUTHORITY OF ACCESS

This thesis may be made available for loan and limited copying in accordance with the Copyright Act 1968.

John Andrew Edwin Gibson

ABSTRACT

The first integrated study in the Antarctic region of the marine carbon cycle over an entire annual period, including organic carbon formation, remineralisation, sedimentation and burial, was undertaken during two summers and the intervening winter from December 1993 to February 1995 at two sites in the Vestfold Hills region, East Antarctica: offshore at O'Gorman Rocks and in semi-enclosed Ellis Fjord.

A single peak in uptake of dissolved inorganic carbon (DIC) occurred at the O'Gorman Rocks site in the first summer, while three peaks, resulting from different phytoplankton communities, were observed in the second. Net organic carbon (OC) production calculated from the uptake of DIC reached 2.1 mg kg^{-1}. The sum of particulate and dissolved OC was typically only 30 % of the calculated total, suggesting rapid sedimentation of OC or transfer to higher trophic levels. After the end of OC production in autumn the concentrations of DIC and nutrients increased slowly and steadily to late winter maxima, primarily as the result of remineralisation rather than nutrient supply by deep-water upwelling.

Sediment trap flux of OC at O'Gorman Rocks totalled 10 g m^{-2} $year^{-1}$, with peak sedimentation coinciding with maximum OC production, but with a significant proportion (30 %) occurring outside summer. The development of a bottom ice algal community in October contributed a pulse of sedimentation which was characterised by OC with high $\delta^{13}C$ (-13 ‰ compared to the annual average -19 ‰). Comparison of the fluxes with the OC content of a sediment core showed that 2 g m^{-2} $year^{-1}$ OC was buried, with the majority (80 %) remineralised by the benthic community.

In Ellis Fjord DIC and nutrient uptake began earlier and ended later than at O'Gorman Rocks, though total DIC uptake and annual OC sedimentation were similar to those offshore. Early in summer the C:N uptake ratio calculated from concentrations in the

water column reached 40, considerably higher than the expected Redfield Ratio of 16:1. Sedimentation of bottom ice algae again resulted in the transfer of particulate matter with high $\delta^{13}C$ to the sediment.

This study shows that OC production in the nearshore Antarctic environment does not necessarily occur in a single pulse after the loss of the ice cover, but rather can begin under the ice and continue after refreezing. Furthermore, OC production can be of similar magnitude in ice-covered systems to areas which are ice-free for part of the summer. Bottom ice algae play an important role in total OC production, and are a source of OC for sedimentation before and after the period of peak water column production. This community is also important in the formation of OC with elemental ratios and $\delta^{13}C$ different to material produced in open water. Interannual variability in OC production and the algal and phytoplankton communities, however, can be large. These factors must be taken into account when developing biological carbon uptake estimates from models of nutrient utilisation, in interpreting sedimentary isotope records, and considering the effects of climate change on Antarctic ecosystems.

ACKNOWLEDGMENTS

My sincere thanks go to my supervisors Tom Trull, Tom McMeekin and Peter Franzmann for supporting and encouraging my work over the last four years.

The winter expeditioners at Davis Base in 1994 helped immensely with the fieldwork. Special thanks are due to Kerrie Swadling, Graham Smith, Helen Cooley, Terry Newton, Dale Hughes, Trevor Bailey and Jenny Skerratt (for that first day) for their patience and support. Station Leaders Michael Carr and Diana Patterson made it possible to get out into the field to collect samples with the minimum of fuss. The assistance of the Australian Antarctic Division with logistics was appreciated.

The help of the following people was also greatly appreciated: Mark Pretty and Bronte Tilbrook (CSIRO Division of Oceanography, Hobart), who provided assistance with the determination of total DIC and also provided standards; Brian Popp and Terri Rust (University of Hawaii), who measured $\delta^{13}C$ in some samples; Mike Power and Chris Cooke (Central Science Laboratory, University of Tasmania), who assisted with $\delta^{13}C$ measurements in Hobart, Graham Rowbottom (Central Science Laboratory, University of Tasmania) for microanalytical work; Roger Francey, Colin Allison and Emily Welch (CSIRO Division of Atmospheric Research), who provided flasks and a pump unit for the collection of air samples and for analysis of the samples; Andrew McMinn (IASOS, University of Tasmania) provided identifications for some diatoms; Professor Frank Millero (University of Miami) provided a computer program for calculation of carbonate parameters; Professor Bob Byrne (University of South Florida) for clarification of pH measurement techniques; and John Cox (Australian Antarctic Division), who drafted some of the figures. I also wish to thank Kerrie Swadling, Harry Burton, Andrew Davidson, Harvey Marchant, Bronte Tilbrook and Dennis Mackey for discussions on various aspects of the work. The card players in the Chemistry Department, University of Tasmania, also deserve a special mention. I

would like to acknowledge the financial assistance of the Antarctic CRC, University of Tasmania, and the Australian Postgraduate Award scheme.

Finally I would like to thank Kerrie Swadling and all members of my family for their continued support throughout the past four years.

ABBREVIATIONS

Standard SI unit and prefix abbreviations are used, and are not listed except for some less common units.

μatm	microatmosphere
μE	microeinstein
μequiv	microequivalent
Alk_T	total alkalinity
ANSTO	Australian Nuclear Science and Technology Organisation
BOD	biological oxygen demand
chl *a*	chlorophyll *a*
chl *b*	chlorophyll *b*
DIC	dissolved inorganic carbon
DO	dissolved oxygen
DOC	dissolved organic carbon
fCO_2	fugacity of CO_2
mS	millisiemen (unit of electrical conductance)
Gt	gigatonne (10^{15} g)
OC	organic carbon
pH_f	pH measured on the free hydrogen scale
POC	particulate organic carbon
POM	particulate organic matter
psu	practical salinity unit
S	salinity
SDL	submersible data logger
WW	winter water

TABLE OF CONTENTS

ABSTRACT i

ACKNOWLEDGMENTS iii

ABBREVIATIONS v

TABLE OF CONTENTS vi

FIGURES xii

TABLES xviii

1 INTRODUCTION 1
1.1 Introduction 1
1.2 The global biogeochemical carbon cycle 2
1.3 The role of the Antarctic region in the global carbon cycle 7
1.4 Components of the Antarctic carbon cycle 8
1.4.1 Measurements of fCO_2 8
1.4.2 Primary production: conversion of CO_2 to organic material 10
1.4.3 Carbon export: sediment trap studies 13
1.4.4 Carbon export: advection 15
1.5 The themes of this thesis 16

2 O'GORMAN ROCKS SITE: LOCATION, PREVIOUS STUDIES AND PHYSICAL OCEANOGRAPHY 18
2.1 Introduction 18
2.2 The Vestfold Hills 23
2.3 The inshore marine environment of the Vestfold Hills 23
2.4 The climate of the Vestfold Hills 26
2.5 Physical oceanography at the O'Gorman Rocks site, December 1993 - February 1995 28
2.5.1 Ice cover 28
2.5.3 Water temperature 29
2.5.4 Water salinity 31
2.6 Conclusions 36

3 PHYTOPLANKTON AT THE O'GORMAN ROCKS SITE: SEASONAL CYCLE AND INTERANNUAL VARIABILITY 37
3.1 Introduction 37
3.2 Results 38
3.2.1 Seasonal phytoplankton cycle 38
3.2.1.1 Cryptomonad A 40
3.2.1.2 Diatoms 42
3.2.1.3 *Phaeocystis* cf. *antarctica* 44
3.2.1.4 Dinoflagellates 45

3.2.1.5 *Pyramimonas gelidicola* 46
3.2.2 Chlorophyll *a* 46
3.3 Discussion 47
3.3.1 Comparison of the seasonal cycle to previous studies 47
3.3.2 Factors contributing to variation in the phytoplankton community 50
3.3.3 What effect could phytoplankton variability have on carbon export? 54
3.4 Conclusions 57

4 ORGANIC MATTER PRODUCTION AND ATMOSPHERIC CO_2 UPTAKE AT O'GORMAN ROCKS 58
4.1 Introduction 58
4.2 Results 58
4.2.1 Dissolved inorganic carbon 58
4.2.2 Dissolved organic carbon 59
4.2.3 Particulate organic carbon 60
4.2.4 Carbon isotope ratios 62
4.2.5 pH 62
4.2.6 Chlorophyll *a* 63
4.2.7 Dissolved oxygen 64
4.2.8 Nutrients 66
4.2.9 Calculated carbon parameters 68
4.2.9.1 Total alkalinity 69
4.2.9.2 The fugacity of CO_2 70
4.2.10 Atmospheric carbon dioxide: concentration and isotopic ratio 70
4.3 Discussion 71
4.3.1 Seasonal cycles of primary production and related parameters 71
4.3.1.1 The general seasonal cycle of primary productivity 71
4.3.1.2 DIC and nutrients 73
4.3.1.3 Dissolved oxygen 76
4.3.1.4 pH 77
4.3.1.5 Total alkalinity 78
4.3.1.6 fCO_2 79
4.3.2 Correlations: DIC, nutrients and dissolved oxygen 80
4.3.2.1 Correlation of DIC and the nutrients 80
4.3.2.2 Correlations of dissolved oxygen with DIC and the nutrients 84
4.3.3 Carbon budget calculations and correlation of measured and calculated organic carbon 88
4.3.3.1 Carbon budget calculations 88
4.3.3.2 Correlation of calculated and measured organic carbon 93
4.3.4 Is the Ocean at O'Gorman Rocks a sink of CO_2 for the atmosphere? 96
4.3.4.1 Calculation of the amount of CO_2 taken up by the ocean 96
4.3.4.2 Evidence for CO_2 uptake 97

4.4 Conclusions 102

5 ORGANIC MATTER SEDIMENTATION AND BURIAL AT O'GORMAN ROCKS 104
5.1 Introduction 104
5.2 Results 104
5.2.1 Total sedimentation 104
5.2.2 Organic carbon sedimentation 106
5.2.3 The problem of resuspension 108
5.2.4 Carbon to nitrogen mole ratio of the sedimenting material 109
5.2.5 The $\delta^{13}C$ of the sedimenting organic carbon 110
5.2.6 Characteristics of the sedimenting material 111
5.2.7 Carbon in the sediment 113
5.3 Discussion 114
5.3.1 Sediment trap design 114
5.3.2 The cycle of sedimentation 115
5.3.3 Sedimentation inventories and rates: comparison to other Antarctic studies 119
5.3.4 The $\delta^{13}C$ of the sedimenting organic carbon 122
5.3.5 Factors influencing $\delta^{13}C$ of the sediment trap material 126
5.3.6 Carbon in the sediment 131
5.3.7 A model of carbon remineralisation and burial 133
5.4 Conclusions 137

6 ELLIS FJORD SITE: LOCATION, PREVIOUS STUDIES AND PHYSICAL OCEANOGRAPHY 139
6.1 Introduction 139
6.2 Ellis Fjord 139
6.3 Physical Characteristics of the Ellis Fjord site, May 1994 - February 1995 145
6.3.1 Ice cover 145
6.3.2 Water temperature 145
6.3.3 Water salinity 148
6.3.4 Mixing and water body sources in Ellis Fjord 149
6.3.4.1 Winter cooling 149
6.3.4.2 The isolated bottom water 151
6.3.4.3 Summer warming and salinity decrease 152
6.4 Conclusions 156

7 ORGANIC MATTER PRODUCTION AND PHYTOPLANKTON IN ELLIS FJORD 157
7.1 Introduction 157
7.2 Results 157
7.2.1 Dissolved inorganic carbon 157
7.2.2 Dissolved organic carbon 159
7.2.3 Particulate organic carbon 159
7.2.4 The $\delta^{13}C$ of inorganic and organic carbon 161

7.2.5 pH 162
7.2.6 Chlorophyll 163
7.2.7 Dissolved oxygen 164
7.2.8 Nutrients 166
7.2.9 Calculated carbon parameters 168
7.2.9.1 Total alkalinity 168
7.2.9.2 fCO_2 169
7.2.10 Phytoplankton 169
7.3 Discussion 172
7.3.1 Seasonal cycles of primary production and related parameters 172
7.3.1.1 The general cycle of primary productivity 172
7.3.1.2 Seasonal cycle of phytoplankton 173
7.3.1.3 Seasonal cycle of DIC, nutrient and oxygen concentrations 177
7.3.1.4 Alkalinity 178
7.3.1.5 The fugacity of CO_2 181
7.3.1.6 Nutrients, DIC and dissolved oxygen at 70m 181
7.3.2 Correlations: DIC, nutrients and dissolved oxygen 182
7.3.3 Organic carbon production and budgets 188
7.3.3.1 Estimates of net organic carbon production 188
7.3.3.2 The magnitude of organic carbon production 190
7.3.3.3 Correlation of calculated and measured organic carbon 192
7.3.4 Carbon isotope chemistry: nutrient correlations and the effects of primary production 193
7.4 Conclusions 196

8 ORGANIC CARBON SEDIMENTATION AND BURIAL IN ELLIS FJORD 198
8.1 Introduction 198
8.2 Results 198
8.2.1 Total sedimentation 199
8.2.2 Organic carbon sedimentation 202
8.2.3 Carbon to nitrogen mole ratio of the sedimenting material 204
8.2.4 $\delta^{13}C$ of the sedimenting organic carbon 207
8.2.5 Characteristics of the sedimenting material 207
8.2.6 Carbon in the sediment 210
8.3 Discussion 211
8.3.1 The cycle of sedimentation 211
8.3.2 The $\delta^{13}C$ of the sedimenting organic carbon 215
8.3.3 The relationship between $\delta^{13}C$ of the sediment trap material and DIC in the water column 217
8.3.4 Trends in $\delta^{13}C_{oc}$ and the C:N mole ratio of the sediment trap material 218
8.3.5 Carbon in the sediment 220
8.3.6 A model of organic carbon production, remineralisation and burial 221

8.4. Conclusions 226

9 CONCLUSIONS 227

APPENDICES

A EXPERIMENTAL METHODOLOGY 234
A.1 Introduction 234
A.2 Sampling dates and times 234
A.3 Collection of water samples 234
A.4 Physical parameters 236
A.4.1 Water temperature and electrical conductivity 236
A.4.2 Water salinity and density 238
A.5 Dissolved inorganic carbon and related parameters 238
A.5.1 Dissolved inorganic carbon 238
A.5.2 Measurement of pH 239
A.5.3 Calculation of related parameters 241
A.6 Organic carbon 242
A.6.1 Dissolved organic carbon 242
A.6.2 Particulate organic carbon 244
A.7 Carbon isotopic ratios in the DIC pool 245
A.7.1 Measurement of the $^{13}C/^{12}C$ ratio of DIC 245
A.7.2 Measurement of the $^{14}C/^{12}C$ ratio of DIC 246
A.8 Chlorophyll 246
A.9 Dissolved oxygen 247
A.10 Nutrients 247
A.11 Phytoplankton 248
A.12 Sediment traps 249
A.12.1 Sediment trap design and deployment 249
A.12.2 Total and organic sedimentation rates 252
A.12.3 C:N molar ratio of the organic material 252
A.12.4 Determination of $\delta^{13}C$ of the sediment trap material 253
A.12.5 Description of material caught in sediment traps 253
A.13 Sediment cores 254
A.13.1 Percentage of organic carbon 254
A.13.2 Determination of inorganic carbon content 254
A.13.3 $\delta^{13}C$ of organic material from the sediment cores 255
A.13.4 $\delta^{13}C$ of carbonate material from the sediment cores 255
A.14 Atmospheric CO_2 concentration and isotope signature 255

B WEATHER CONDITIONS AT DAVIS STATION: DECEMBER 1993 - FEBRUARY 1995 256
B.1 Introduction 256
B.2 Air temperature 256
B.3 Wind 256
B.4 Sunlight 258

C O'GORMAN ROCKS: CHEMICAL AND PHYSICAL DATA 259

D O'GORMAN ROCKS: SEDIMENT TRAP AND CORE DATA 265

E O'GORMAN ROCKS: PHYTOPLANKTON CELL COUNTS 275

F ELLIS FJORD: CHEMICAL AND PHYSICAL DATA 277

G ELLIS FJORD: SEDIMENT TRAP AND CORE DATA 285

REFERENCES 288

FIGURES

1.1 The global biogeochemical carbon cycle. The amount of carbon in each reservoir (in gigatonnes (Gt)) and the estimated annual fluxes of carbon (Gt yr^{-1}) between reservoirs are given. The numbers in brackets are estimated annual changes in the stocks resulting from anthropogenic CO_2 input. The stocks and fluxes are from Post et al. (1990), Siegenthaler and Sarmiento (1993) and Suzuki (1995). Abbreviations: LC, land clearing; DF, deforestation. 3

2.1 Location of the study area: (a) A map of the Antarctic continent indicating the position of Prydz Bay and Davis Station, as well as a number of other locations mentioned in this thesis. Ice sheets are indicated by shading; (b) A map of the Prydz Bay region, showing depth contours in metres, and the locations of Davis Station, the Amery Ice Shelf and the West Ice Shelf; (c) A map of the Vestfold Hills region. The locations of Davis Station and Ellis Fjord are indicated; (d) A bathymetric map of the waters offshore from Davis Station showing the position of the O'Gorman Rocks site. The depth contours are again in metres. 19

2.2 Ice and snow thickness (metres) at the O'Gorman Rocks site, March 1994 - January 1995. 28

2.3 Water temperature (°C) at the O'Gorman Rocks site, December 1993 - February 1995. Temperature was recorded every metre. 30

2.4 Temperature and salinity at 10 m at the O'Gorman Rocks site. The jump in salinity in winter discussed later in the chapter is arrowed. 30

2.5 Water salinity (psu) at the O'Gorman Rocks site from December 1993 to February 1995. Salinity was recorded each metre. 32

2.6 $\delta^{13}C_{DIC}$ and $\Delta^{14}C_{DIC}$ at 10 m at the O'Gorman Rocks site. Calculated error bars are shown for the $\Delta^{14}C_{DIC}$ data. Full details of the $\Delta^{14}C_{DIC}$ data are given in Appendix D. The arrow indicates the approximate timing of the salinity jump (Figure 2.4) 35

3.1 Seasonal cycle of phytoplankton at 10 m, O'Gorman Rocks, December 1993 - March 1995: (a) Cell abundances of 5 species or species groups; (b) The same data expressed as percentages of total phytoplankton abundance. 39

3.2 Abundance of 5 species or groups of phytoplankton, O'Gorman Rocks, December 1993 - February 1995. The shaded area represents the range of cell abundances recorded. Note the logarithmic vertical scale. 41

3.3 Integrated chl *a* (to 23 m), O'Gorman Rocks, December 1993 - February 1995. 47

3.4 The relationship between nitrate and silicate concentrations (normalised to S = 35 psu) in January (closed symbols) and February (open symbols), 1995. 53

4.1 DIC (μmol kg^{-1}), O'Gorman Rocks site, December 1993 - February 1995: (a) all data; (b) the same data over a smaller concentration range. The symbols used in this and all similar plots in this chapter are: 0 or 2 m, □; 5 m, ◇; 10 m, ○; 15 m, Δ and 20 m, ✪. The lighter shading shows the minimum value for the parameter on the sampling date, and the darker shading the range of the data. The periods during which ice covered the sampling site are also indicated. 59

4.2 DOC (μmol kg^{-1}), O'Gorman Rocks site, November 1994 - February 1995. 61

4.3 POC (μmol kg^{-1}), O'Gorman Rocks site, November 1994 - February 1995. Concentrations greater than 150 μmol kg^{-1} occurred in early December, and are detailed in the text. 61

4.4 $\delta^{13}C_{DIC}$ (‰) at 10 m, O'Gorman Rocks site, March 1995 - February 1995. 62

4.5 pH, O'Gorman Rocks site, December 1993 - February 1995. 63

4.6 Chl *a* (mg m^{-3}), O'Gorman Rocks, December 1993 - February 1995. 64

4.7 Dissolved oxygen (μmol kg^{-1}), O'Gorman Rocks site, December 1993 - February 1995. 65

4.8 Dissolved oxygen saturation (%), O'Gorman Rocks site, December 1993 - February 1995. The dashed line indicates saturation . 65

4.9 Nitrate (μmol kg^{-1}), O'Gorman Rock site, December 1993 - February 1995. 66

4.10 Phosphate (μmol kg^{-1}), O'Gorman Rocks site, December 1993 - February 1995. 67

4.11 Silicate (μmol kg^{-1}), O'Gorman Rocks site, December 1993 - February 1995. 67

4.12 Calculated total alkalinity (μequiv kg^{-1}) O'Gorman Rocks site, December 1993 - February 1995. The data are normalised to a salinity of 35 psu. 69

4.13 Calculated fCO_2 (μatm), O'Gorman Rocks site, December 1993 - February 1995. The approximate concentration of CO_2 in the atmosphere is indicated by the dashed line. 70

4.14 Concentration (μatm, squares) and $\delta^{13}C$ (‰, circles) of atmospheric CO_2, Davis Station, March 1994 - March 1995. 71

4.15 Schematic diagram of the sedimentation and remineralisation of organic material. Any nutrients and DIC formed by remineralisation above the maximum depth of mixed WW layer will be mixed evenly throughout the WW at the end of winter. Any carbon, nitrogen, phosphorus and silicate that is lost from the WW must be replaced by entrainment of deeper water into the WW for a long term balance to be maintained. 76

4.16 Normalised nutrient correlation plots: (a) DIC and nitrate; (b) DIC and phosphate; and (c) nitrate and phosphate. Data obtained when the site was ice covered are represented by closed squares, and during periods of open water by open squares. Anomalously low DIC concentrations have been excluded from the plots (see text). 82

4.17 Correlation plot of the concentrations of DIC and dissolved oxygen. All concentrations have been normalised to S = 35 psu. Data obtained when site was ice covered are represented by closed squares, and during periods of open water by open squares. Anomalously low DIC concentrations have been excluded from the plots (see text). The regression line shown is for data points from when the sampling site was ice covered Also shown are the trends resulting from photosynthesis, respiration, DO degassing and CO_2 uptake. 85

4.18 Oxygen degassing. The upper panel shows the average measured oxygen supersaturation along with that calculated from the concentration of nitrate. The lower panel shows the mean oxygen deficit per kg of seawater. 87

4.19 The net OC production (μmol kg^{-1}) calculated from the concentrations of nitrate and phosphate plotted against net OC production calculated from the concentration of DIC. The 1:1 equivalence line is also shown. 89

4.20 Calculated net OC production (μmol kg^{-1}) for each sampling date and depth (crosses) and integrated calculated OC (g m^{-2}, line). 90

4.21 Calculated rates of OC production at the O'Gorman Rocks site. 91

4.22 Plot of measured total OC against calculated OC for discrete depths: (a) All data; (b) The same plot with an expanded vertical axis. Shown are the 1:1 line (dashed) and the regression line discussed in the text. The data not considered in calculation of the regression line are shown as crosses. 93

4.23 A plot of the calculated DIC surplus (assuming a C:N assimilation ratio of 6.6) against calculated dissolved oxygen deficit for the ice free period from 16 January 1995 until the end of the study. 99

4.24 A plot of DIC (normalised to S = 35 psu) against $\delta^{13}C_{DIC}$. The low $\delta^{13}C_{DIC}$ data from August and September have not been plotted. 101

5.1 Total sedimentation rates (columns, left hand axis) and cumulative sedimentation (line, right hand axis) at the O'Gorman Rocks site between April 1994 and April 1995. 105

5.2 Sedimentation rate of OC (columns, left hand axis) and cumulative OC sedimentation (line, right hand axis) at the O'Gorman Rocks site between April 1994 and April 1995. 106

5.3 The percentage of OC in the sedimenting material. The symbols used in this and all similar figures in this chapter are: 5m, ◇; 10 m, ○; 15 m, △; and 20 m, ✣. The line is the average of the data. Superimposed on the graphs are the rates of OC sedimentation from Figure 5.2. 107

5.4 The carbon to nitrogen mole ratio of the sedimenting material. The dashed line represents the Redfield Ratio. See Figure 5.3 for an explanation of the plot symbols and background. 110

5.5 Seasonal trend in the $\delta^{13}C$ of organic carbon in the sedimenting material. See Figure 5.3 for an explanation of the plot symbols and background. 111

5.6 Chemical characteristics of the short sediment core obtained from the O'Gorman Rocks site. The C:N mole ratio and the $\delta^{13}C_{OC}$ are for the organic fraction of the core. 113

5.7 The $\delta^{13}C_{OC}$ of the sedimenting material plotted against the water temperature at the trap depth on the day of recovery. Also shown is the relationship (Equation 5.2) found by Rau et al. (1991c) to relate $\delta^{13}C_{OC}$ and water temperature in another Antarctic study. 127
5.8 The $\delta^{13}C_{OC}$ of the sedimenting material plotted against the calculated $[CO_{2(aq)}]$ on the date of trap recovery. Also shown is the lines defined by Equation 5.3 The various plot symbols are described in the text. 129
5.9 A schematic representation of the model used to calculate the magnitude of carbon burial and remineralisation. The abbreviations and subscripts used are defined in Table 5.2. Also shown are the OC sedimentation and burial fluxes measured or calculated using the model. 134
6.1 Ellis Fjord (a) A bathymetric map of the fjord showing the location of the sampling site. (b) A cross-sectional view of the fjord, highlighting the presence of a series of shallow sills. 140
6.2 Water temperature (°C), Ellis Fjord site, May 1994 - February 1995. The ice cover in this and all similar plots of data from Ellis Fjord is represented by the thin white area at the top of the plot. 146
6.3 Temperature and salinity at 10 m at the Ellis Fjord site. 146
6.4 Temperature (°C), salinity (psu) and *in situ* density (kg m^{-3} - 1000) profiles, Ellis Fjord, 7 May 1994. 147
6.5 Water salinity (psu) at the Ellis Fjord site, May 1994 - February 1995. 148
6.6 A schematic diagram of the formation of brine as the result of ice formation near the edge of Ellis Fjord, and the mixing of the brine flowsinto the mid-depth water. 150
6.7 A plot of temperature versus salinity at the Ellis Fjord site from 12 December 1994 to the end of the study, indicating the close correlation between these parameters. Data from 2 m is not included in this plot. 153
6.8 Temperature increase between sampling dates as a function of water depth between 5 and 40 m at the Ellis Fjord site from December 1994 to February 1995. 155
7.1 DIC (μmol kg^{-1}), Ellis Fjord site, May, 1994 - February 1995: (a) all data; (b) the same data over a smaller concentration range. The symbols used in these and all similar plots in this section are: 2 m, □; 5 m, ◇; 10 m, ○; 20 m, Δ and 40 m, ✣. The lighter shading shows the minimum value (0 - 40 m) for the parameter on the sampling date, and the darker shading the range of the data. Data from 70 m is represented by inverted triangles joined by a line. 158
7.2 DOC (μmol kg^{-1}), Ellis Fjord site, May 1994 - February 1995. 160
7.3 POC (μmol kg^{-1}), Ellis Fjord site, May 1994 - February 1995. 160
7.4 $\delta^{13}C_{DIC}$ in water at 10 m, Ellis Fjord site, June 1994 - January 1995. 161
7.5 pH_f, Ellis Fjord site, May 1994 - February 1995. 162
7.6 A contour plot of the concentration of chl *a* (mg m^{-3}), Ellis Fjord site, May 1994 - February 1995. 163
7.7 Dissolved oxygen (μmol kg^{-1}), Ellis Fjord site, May 1994 - February 1995. 165
7.8 Percentage saturation of dissolved oxygen, Ellis Fjord site, May 1994 - February 1995. 166

7.9 Nitrate (μmol kg^{-1}), Ellis Fjord site, May 1994 - February 1995. 167
7.10 Phosphate (μmol kg^{-1}), Ellis Fjord site, May 1994 - February 1995. 167
7.11 Silicate (μmol kg^{-1}), Ellis Fjord site, May 1994 - February 1995. 168
7.12 Total alkalinity (μequiv kg^{-1}) normalised to S = 35 psu, Ellis Fjord site, May 1994 - February 1995. 169
7.13 fCO_2 (μatm), Ellis Fjord site, May 1994 - February 1995. The dashed line indicates the concentration of CO_2 in the atmosphere. 170
7.14 General cycle of dominant phytoplankton at the Ellis Fjord site. Green represents dominance by dinoflagellates, yellow diatoms, and red the flagellates cryptomonad A and/or *Pyramimonas gelidicola*. Orange essentially reflects mixed communities of diatoms and flagellates. Few viable phytoplankton were observed in samples from 70 m. 171
7.15 Total alkalinity (μequiv kg^{-1}) plotted against DIC (μmol kg^{-1}) for the Ellis Fjord site. All data have been normalised to S = 35 psu. Also shown is the relationship between these parameters expected (assuming an initial alkalinity of 2490 μequiv kg^{-1} and DIC of 2320 μmol kg^{-1}) if carbonate precipitation occurred. The dashed lines indicate the joint effect of carbonate precipitation and the production of organic material with C:N mole ratios ranging from 7.4 to 30. 179
7.16 Correlation plots of the concentrations (normalised to S = 35 psu) of (a) DIC and nitrate; (b) DIC and phosphate; (c) DIC and silicate; (d) DIC and dissolved oxygen; (e) nitrate and phosphate and (f) nitrate and silicate. Low concentrations of DIC and high concentrations of dissolved oxygen have not been included (see text). 184
7.17 Net organic carbon production (g m^{-2}) calculated from the concentrations of DIC, nitrate (N), phosphate (P) and dissolved oxygen (O). 189
7.18 Calculated rate of organic matter production (or remineralisation) for the entire water column to 40 m. 191
7.19 Plot of the calculated and measured concentrations of organic carbon in Ellis Fjord. 193
7.20 The correlation between DIC (normalised to S = 35 psu) and $\delta^{13}C_{DIC}$ for samples from 10 m. The data represented by crosses were not included in the calculation of the regression line. 194
7.21 A plot of $\delta^{13}C_{DIC}$ against DIC calculated from the concentrations of phosphate and nitrate (normalised to S = 35 psu) and the relationships given in Table 7.1. The slope of the regression line was used to calculate the isotopic fractionation of carbon during organic matter production. The data points equivalent to those shown by crosses in Figure 7.20 are arrowed. 195
8.1 Total sedimentation rates (mg m^{-2} day^{-1}) recorded in traps deployed at the Ellis Fjord site from June 1994 and June 1995. 200
8.2 Trends in the variation in rates of sedimentation at various depths in Ellis Fjord. 201
8.3 Resuspension and sediment focussing in Ellis Fjord. The cross section of the fjord at the sampling site has no vertical exaggeration. 201
8.4 Organic carbon sedimentation rates (mg m^{-2} day^{-1}) recorded in traps deployed at the Ellis Fjord site from June 1994 and June 1995. 203

8.5 Seasonal variations in the percentages of organic carbon in the material caught in the sediment traps at the Ellis Fjord site. The rate of OC sedimentation (Figure 8.4) is plotted in the background for comparison. 205
8.6 The seasonal cycle of the carbon to nitrogen mole ratio in the organic fraction of the sedimenting material. The dashed line is the Redfield Ratio. The rate of OC sedimentation (Figure 8.4) is plotted in the background for comparison. 206
8.7 Seasonal variation in the $\delta^{13}C$ of the organic fraction of the material caught in the sediment traps at the Ellis Fjord site. The rate of OC sedimentation (Figure 8.4) is plotted in the background for comparison. 208
8.8 Organic carbon content (percent) of a sediment core recovered from the Ellis Fjord sampling site. 210
8.9 The $\delta^{13}C$ of the sedimenting material plotted against the calculated $[CO_{2(aq)}]$ at the trap depth on the date of recovery. Also shown are the lines suggested by Rau et al. (1991c) to relate the $\delta^{13}C$ of particulate organic matter and $[CO_{2(aq)}]$ in other Antarctic studies (Equation 5.3). The data plotted as crosses are discussed in the text. 217
8.10 Plot of $\delta^{13}C$ versus the C:N mole ratio for sediment trap material from Ellis Fjord (squares) and O'Gorman Rocks (crosses). The solid line is the trend line for the data from the Ellis Fjord site, and the dashed lines represent trends in the data from the O'Gorman Rocks site during the periods indicated. 219
8.11 A schematic diagram of the carbon fluxes into and out of the n^{th} box in the model. 222
8.12 Annual carbon flow (g m^{-2}) through the water column and to the sediment at the Ellis Fjord site calculated using the data in Table 8.1 and Section 8.3.6 and the models described in this section and in Chapter 5. The numbers in the rectangles are the net change in 'trappable' OC in the boxes. 223
A.1 Diagram of the apparatus used to filter water samples for dissolved organic carbon analysis. 243
A.2 Design of the sediment trap arrays: (a) Side view of sediment traps in bracket; (b) Plan view of bracket. 250
B.1 Monthly maximum (squares), minimum (diamonds) and average (circles) temperatures, Davis Station, December 1993 - February 1995. Long term average monthly temperatures are indicated by the dashed line. 257
B.2 Monthly average wind speeds, Davis Station, December 1993 - February 1995. Long term average monthly wind speeds are indicated by the dashed line. 257
B.3 Average daily sunlight hours, Davis Station, December 1993 - February 1995. Long term average monthly sunlight hours are indicated by the dashed line. 258

TABLES

3.1 List of diatom species (with authorities) and genera observed during the study. Diatoms were identified after Priddle and Fryxell (1985) and Medlin and Priddle (1990). 43

4.1 Details of regressions between the concentrations of DIC, nutrients and DO (all normalised to a salinity of 35 psu). Anomalously low concentrations of DIC and DO during the ice free periods were excluded from the calculations (see text). The standard errors for the regressions are given. 81

4.2 Estimated end of winter values for the parameters used in the calculation of net OC production. 89

5.1 OC fluxes in year long studies of sedimentation in the Antarctic region. The surface fluxes were calculated using Equation 5.1. 121

5.2 Components of the model of carbon sedimentation and burial. 135

7.1 Details of regressions between the concentrations of DIC, nitrate (N), phosphate (P), silicate (Si) and DO (all normalised to S = 35 psu). The errors given are the standard errors for the regressions. All regressions were significant at the 1 % level. 183

7.2 Estimated end of winter values for the parameters used in the calculation of net OC production. 188

7.3 Calculated isotopic fractionation during the production of organic matter calculated as described in the text. 195

8.1 Annual inventories (g m^{-2} yr^{-1}) of total and carbon sedimentation for each trap depth separated into resuspended (Res) and newly formed material (New). The percentage of carbon in each of the pools is also given. 202

A.1 Sampling dates, O'Gorman Rocks, December 1993 - February 1995 235

A.2 Sampling dates, Ellis Fjord, May 1994 - June 1995. The site was covered by ice throughout the study. 236

A.3 A summary of the methods used for analysis of nutrients.Estimates of the detection range and accuracy (at the concentration given in brackets) of the methods is also given (Parsons et al., 1984). 248

C.1 Total cell counts (cells L^{-1}) at the O'Gorman Rocks site. 259

C.2 Cryptomonad A cell counts (cells L^{-1}) at the O'Gorman Rocks site. 260

C.3 Diatom cell counts (all species) (cells L^{-1}) at the O'Gorman Rocks site. 261

C.4 *Phaeocystis* cf. *antarctica* cell counts (cells L^{-1}) at the O'Gorman Rocks site. 261

C.5. Dinoflagellate cell counts (all species) (cells L^{-1}) at the O'Gorman Rocks site. 262

C.6 *Pyramimonas gelidicola* cell counts (cells L^{-1}) at the O'Gorman Rocks site. 263

D.1 Temperature, salinity and concentrations of nitrate, phosphate, silicate and dissolved oxygen at the O'Gorman Rocks site. 265

D.2 Further chemical parameters for samples from the O'Gorman Rocks Site. Chl *a*, pH_f and DIC were measured experimentally, while $[CO_{2(aq)}]$ fCO_2 and Alk_T were calculated as described in Appendix A. 269

D.3 Concentrations of DOC, POC and total organic carbon at the O'Gorman Rocks site. 272
D.4 $\delta^{13}C_{DIC}$ and $\Delta^{14}C_{DIC}$ at the O'Gorman Rocks site. Also given are the estimated 1σ counting error in the $\Delta^{14}C_{DIC}$ value and the ANSTO sample number. All samples were collected from 10 m. 273
E.1 Sediment flux and chemical data for the sediment trap array positioned at the O'Gorman Rocks site. The C:N mole ratio and $\delta^{13}C$ are for the organic fraction of the sediment trap material. 275
E.2 Chemical characteristics of the short sediment core recovered from the O'Gorman Rocks site. The C:N mole ratio and the $\delta^{13}C$ are for the organic fraction of the core. 276
F.1 Temperature, salinity and concentrations of nitrate, phosphate, silicate and dissolved oxygen at the Ellis Fjord site. 277
F.2 Further chemical parameters for samples from the Ellis Fjord Site. Chlorophyll *a*, pH_f and DIC were measured experimentally, while the concentration of $CO_{2(aq)}$, fCO_2 and Alk_T were calculated as described in Appendix A. 280
F.3 Concentrations of DOC, POC and total organic carbon at the Ellis Fjord site. 282
F.4 $\delta^{13}C_{DIC}$ at the Ellis Fjord site. All samples were collected from 10 m. 284
G.1 Sediment flux and chemical data for the sediment trap array positioned at the Ellis Fjord site. The C:N mole ratio and $\delta^{13}C$ are for the organic fraction of the sediment trap material. 285
G.2 Organic carbon content of the short sediment core recovered from the Ellis Fjord site. 287

CHAPTER 1

INTRODUCTION

1.1 Introduction

This thesis describes the first integrated study of the carbon cycle undertaken in the Antarctic region over an entire annual period. The study investigated the seasonal variation in as many aspects of the carbon cycle as possible, including the concentration of carbon dioxide (CO_2) in the atmosphere, the fugacity of CO_2 (fCO_2) in the ocean, production of organic carbon (OC) by phytoplankton, sedimentation of particulate organic carbon (POC), and burial and preservation of both organic and inorganic carbon in the sediment. The results obtained from these measurements provide insight into the relative importance of the processes which determine the role of neritic regions of the Southern Ocean in the uptake of anthropogenic CO_2 from the atmosphere and its transfer to longer term carbon repositories.

The study described in this thesis was carried out at two sites close to Australia's Davis Station in the Vestfold Hills, East Antarctica. One site was offshore at O'Gorman Rocks, and the other in semi-enclosed Ellis Fjord. The fjord site was chosen to provide a location where water mass advection was less likely to influence the dynamics of the carbon cycle. Chapter 2 reviews the physics, chemistry and biology previously recorded at or near the offshore site, and presents and discusses the physical oceanography recorded at the site during the study. Chapter 3 discusses the phytoplankton communities at this site responsible for primary production, and Chapters 4 and 5 describe the production, sedimentation and burial of organic matter at this site. Chapter 6 reviews the physics, chemistry and biology of Ellis Fjord, and presents and discusses the physical oceanography recorded during the study. Chapters 7 and 8 deal with the production and sedimentation of organic matter at the fjord site.

Finally, Chapter 9 summarises the data, and discusses a number of conclusions from the study that have particular relevance either to the uptake of CO_2 from the atmosphere or other Antarctic studies. Appendix A provides details of the experimental methods used in the study, Appendix B summarises the weather recorded at Davis Station during the study, and all experimental results are presented in tabular form in Appendices C - F.

1.2 The Global Biogeochemical Carbon Cycle

Processes such as burning of fossil fuels, cement production and deforestation have increased the concentration of CO_2 in the atmosphere from *circa* 280 microatmospheres (μatm) in the 18th century to over 360 μatm in the mid-1990s (Siegenthaler and Oeschger, 1987; Keeling, 1993). This change in the chemistry of the atmosphere has lead many scientists to predict an increase in global temperatures due to enhancement of the natural greenhouse effect. The processes which have added CO_2 to the atmosphere are often termed 'anthropogenic', as it is actions of mankind which have mobilised CO_2 from long term geological repositories, such as limestone and deeply buried coal and oil (Figure 1.1), and added it to the more fluxional oceanic, terrestrial and atmospheric carbon pools.

Only approximately half of the calculated amount of anthropogenic CO_2 has remained in the atmosphere (Keeling, 1973; Rotty, 1977), resulting in the observed increase in concentration (Tans and Bakwin, 1995). The rest of the CO_2 must have been absorbed into other carbon pools through uptake by the ocean, a process which has long been recognised as capable of removing anthropogenic CO_2 from the atmosphere (Suess and Revelle, 1957; Machta, 1972; Broecker and Peng, 1982), or by increased growth of the terrestrial biota. The percentages of anthropogenic CO_2 taken up by these processes is uncertain, and is the centre of continuing debate (Tans et al., 1990; Watson et al., 1991; Quay et al., 1992; Siegenthaler and Sarmiento, 1993; Keeling et

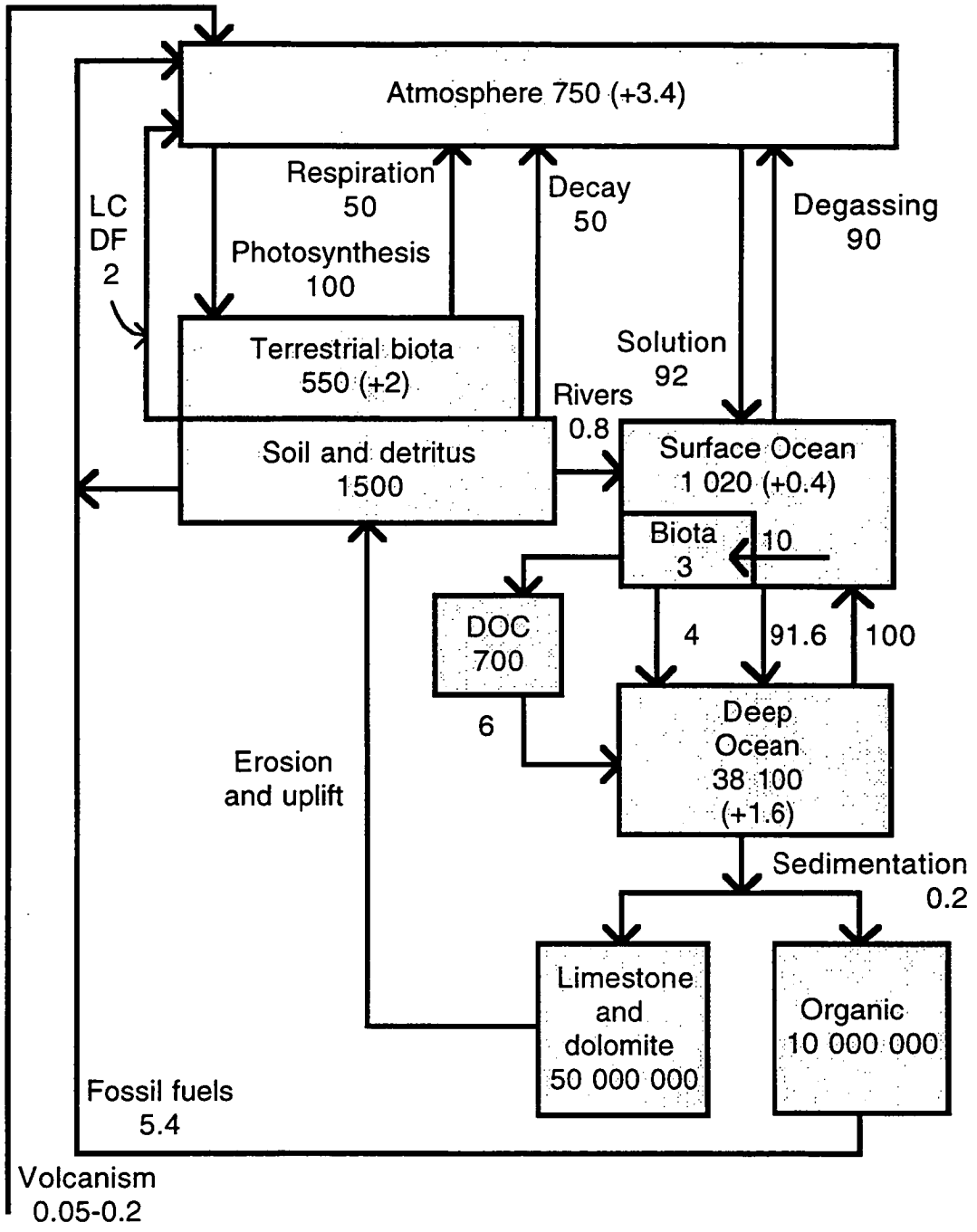

Figure 1.1. The global biogeochemical carbon cycle. The amount of carbon in each reservoir (in gigatonnes (Gt)) and the estimated annual fluxes of carbon (Gt yr^{-1}) between reservoirs are given. The numbers in brackets are estimated annual changes in the stocks resulting from anthropogenic CO_2 input. The stocks and fluxes are from Post et al. (1990), Siegenthaler and Sarmiento (1993) and Suzuki (1995). Abbreviations: LC, land clearing; DF, deforestation.

al., 1996). Therefore it is important to understand the factors which influence the magnitude of CO_2 uptake into and loss from these pools, especially the physical, biological and chemical processes which result in the absorption of anthropogenic CO_2 by the ocean.

The ocean is the largest non-geological global repository of carbon (Figure 1.1). Most of the carbon contained in this pool is present as dissolved inorganic carbon (DIC) in the deep ocean (Siegenthaler and Sarmiento, 1993), which is isolated from the atmosphere by surface waters for periods that average over 1500 years. The oceanic reservoir is much larger than that contained in the atmosphere and in the terrestrial biota and soil (Figure 1.1), and, importantly, is capable of absorbing further CO_2 (Tans and Bakwin, 1995). Prior to the beginning of the industrial revolution the ocean would have been in a steady state with respect to carbon (Smith and Hollibaugh, 1993): The amount of carbon entering the ocean either through absorption from the atmosphere or in river input would have matched losses by outgassing and burial in the sediment. Furthermore, transport of carbon from the surface waters to the deep ocean by downwelling or sedimentation of organic and inorganic carbon would have equalled the flux brought to the surface by upwelling.

The increased contemporary concentration of CO_2 in the atmosphere resulting from anthropogenic input has resulted in a net flux into the ocean estimated to be 2 Gt C yr^{-1} (Siegenthaler and Sarmiento, 1993; Sundquist, 1993), which represents approximately 25 % of the anthropogenic CO_2 added to the atmosphere per year (Houghton et al., 1992). Of this, 0.4 Gt C yr^{-1} remains in the surface waters, while 1.6 Gt C yr^{-1} is transported to the deep ocean. The flux of anthropogenic CO_2 into the ocean is only a small proportion of the total CO_2 flux. Thus it would take only a relatively small increase in the flux of CO_2 into the ocean or the efficiency of the transfer of carbon to longer term repositories, such as the deep ocean and the sediment, to stabilise the concentration of the gas in the atmosphere.

Absorption and outgassing of CO_2 by the ocean vary both spatially and temporally. The distribution and strengths of sink and source areas of CO_2 in the oceans (where absorption and outgassing, respectively, occur) is still imperfectly known (Takahashi, 1989), and is the centre of continuing research through such international programs as the Joint Global Oceanic Flux Study (JGOFS). Transport of carbon dioxide from the atmosphere to the surface ocean (or *vice versa*) is driven by the difference in the fCO_2 at the air - sea interface. (fCO_2 is numerically similar to the partial pressure of the gas (pCO_2), but takes into account non-ideal behaviour (Stumm and Morgan, 1981)). Since fCO_2 in the atmosphere is nearly constant on the time scale of gaseous exchange, changing physical, chemical and biological conditions in the surface waters of the ocean effectively determine the magnitude and direction of the exchange.

The wind-mixed surface layers of the ocean are typically near saturation with respect to atmospheric CO_2 (Tans et al., 1990). In contrast, water in the deep ocean is supersaturated with respect to the atmosphere. Thus, areas such as the equatorial Pacific Ocean where deep water is brought to the surface by upwelling and is subsequently warmed (which increases fCO_2), are regions of strong CO_2 outgassing from the ocean. As the deep ocean water currently being brought to the surface has been isolated from the atmosphere for over 1000 years, it contains little if any anthropogenic CO_2. In contrast, colder regions where water is cooled and deep water formation occurs, such as the north Atlantic Ocean, are regions of absorption of atmospheric, and anthropogenic, CO_2.

CO_2 (and nutrients) in surface waters can also be used by photosynthetic organisms in the production of organic material, which results in a decrease in fCO_2. On death, this material is either recycled within the surface waters or is exported by sedimentation through the water column to the deep ocean. Some of the material reaches the sediment and is buried, thus entering the very long term geological carbon repository. The rest of the material is remineralised in the deep ocean by heterotrophic organisms, which

release CO_2 back into the water column. The supersaturation of the deep water with respect to the atmosphere indicates that this process, often termed the biological pump, is an important mechanism for the transport of carbon from the surface into the deep ocean, and for creating a CO_2 deficit in the surface waters.

As mentioned above, CO_2 in the surface ocean is in approximate equilibrium with the atmosphere, and, even though this water is capable of absorbing further anthropogenic CO_2, its relatively small volume and short turnover time with respect to gas exchange with the atmosphere (*circa* 10 yrs) limit the efficacy of this water in sequestering anthropogenic CO_2. For longer term removal of anthropogenic CO_2, greater amounts of carbon must be transferred to the deep ocean, either by increasing the rate of carbon transfer during downwelling, reducing CO_2 outgassing during deep convection, or increasing the magnitude of the biological pump.

Increased carbon transport could be achieved during downwelling by increasing the rate of this process (Broecker and Peng, 1993) or by increasing wind speeds (which increases the rate of gas exchange) over areas of downwelling, especially in polar regions where the lower water temperatures decrease fCO_2 in the water column resulting in greater absorption by the ocean (Keir, 1993). The amount of the gas lost after upwelling and during deep convection will be reduced by the increased concentration of CO_2 in the atmosphere, as the difference in fugacities between the aqueous and gaseous phases will be reduced. This process is particularly important in buffering the ocean against loss of CO_2 to the atmosphere, and is possibly the most important mechanism for retaining anthropogenic CO_2 in the deep ocean. The strength of the biological pump, however, is likely to remain relatively constant, as it is the concentration of micro- or macronutrients rather than the availability of CO_2 that limit production and export of organic carbon in most of the surface ocean. Therefore, the biological pump remains an important mechanism by which carbon is transferred from

the surface to deepwater, but in itself is not responsible for the enhanced uptake of anthropogenic CO_2 (Smith and Mackenzie, 1991).

1.3 The Role of the Antarctic Region in the Global Carbon Cycle

The ocean surrounding the Antarctic continent is likely to play an important role in the redistribution between the surface and the deep ocean (Budd, 1991), as it is an area where significant exchange occurs between surface and deep waters due to thermohaline convection (Foster and Carmack, 1976), and which, in places, is highly biologically productive (El-Sayed, 1988; Knox, 1990; Smith and Sakshaug, 1990). Furthermore, it is expected that the climate of the Antarctic region will be affected to a greater extent during global warming than those of temperate and tropical regions, and this could play an important role in the carbon cycle in the Southern Ocean (Budd, 1991; Sarmiento and Le Quéré, 1996).

At present, detailed knowledge of the physical, biological and chemical processes that influence the uptake and transport of carbon from the atmosphere to the deep oceans in the Antarctic region is incomplete, largely due to the difficult logistic and environmental conditions. No integrated study over a complete year of the carbon cycle, including atmospheric, oceanic and sedimentary aspects, has been reported from the Antarctic region (Takahashi et al., 1993). If the role of this region in the uptake of CO_2 from the atmosphere is to be completely understood, such studies are necessary in order that the processes occurring during all months of the year are taken into account (Takahashi et al., 1993).

A number of studies has investigated various aspects of the carbon cycle in the Antarctic region over an annual cycle, but this research has often been an adjunct to other studies, and has not had the carbon cycle as its primary focus (e.g. Bunt, 1960; Shabica et al., 1977; Krebs, 1983; Fukuchi et al., 1984, 1985; Tokarczyk, 1986;

Watanabe et al., 1986; Matsuda et al., 1987a; Perrin et al., 1987; Fischer et al., 1988; Wefer et al., 1988; Domanov and Lipksi, 1990; Clarke and Leakey, 1996). Many other studies have considered shorter periods of the year, usually summer, as this is the period often thought most important and also is logistically the easiest time of the year to undertake work from Antarctica research bases or from research vessels (see reviews such as Knox, 1990 and Smith and Sakshaug, 1990). Two distinct types of studies are discernible: Those that attempt to gain information from a large area (giving good spatial but little temporal detail), and others that are undertaken at a single site over a period of time (yielding good temporal data but no spatial information). A few studies (e.g. the RACER program (Huntley et al., 1991b)) have attempted to integrate spatial and temporal scales, however most long term studies are limited to coastal areas where year round access to sampling sites is feasible.

1.4 Components of the Antarctic Carbon Cycle

The carbon cycle in the Antarctic region can be broken down into a number of constituent parts, for which the current state of knowledge is discussed below. This section provides a background against which the results presented in this thesis can be viewed.

1.4.1 Measurements of fCO_2

Measurement of fCO_2 both in the atmosphere and in the surface ocean is an important aspect of carbon cycle studies, as it is the difference between these parameters that will determine whether CO_2 is taken up by or released from the ocean. fCO_2 in the ocean can either be calculated from experimentally measured pCO_2 values, or from any two of three interrelated parameters: total alkalinity; pH; and the concentration of DIC (i.e. the sum of the concentrations of dissolved CO_2, carbonic acid, carbonate and bicarbonate) (Stumm and Morgan, 1981).

There have been few measurements of fCO_2 (or pCO_2) reported for the surface waters of the oceans south of 55 °S. Takahashi et al. (1993) plotted the distribution of the difference between atmospheric and surface water pCO_2 for the Southern Atlantic Ocean recorded on divers cruises, and detected a strong summer sink for atmospheric CO_2 in the Weddell Sea, with other areas closer to equilibrium. Beggs (1995) summarised all available data, and found that in most studies fCO_2 ranged from near equilibrium to considerable undersaturation with respect to the atmosphere. Little data, however, has been reported from the ice pack or close to the Antarctic continent in winter, and no data for the months from April to September.

The work of Beggs (1995) extended fCO_2 measurements to the marginal ice zone in the Australian sector of the Southern Ocean, and also recorded some data from south of 55 °S for all months from October to April. Although fCO_2 was found to be near equilibrium over much of the area studied, significant reductions in fCO_2 occurred close to the continent, with the most pronounced sinks being associated with coastal phytoplankton blooms, especially during summer. Similar low fCO_2 values were measured during summer in the Bransfield Strait region by Karl et al. (1991).

There remains no annual data set of the cycle of fCO_2 in surface waters in any part of the Antarctic region (Takahashi et al., 1993). The data of Beggs (1995) provided some indication of this cycle, as it appeared that fCO_2 was strongly anti-correlated with the concentration of chlorophyll *a* (chl *a*). If this relationship held throughout the year, it would be expected that fCO_2 would drop rapidly in spring with the onset of uptake of DIC by phytoplankton (outweighing the effects of limited surface warming), and then return to winter levels in February and March as the bloom disappeared. Thus, summer would be predicted to be the season during which most CO_2 was taken up from the atmosphere.

1.4.2 Primary Production: Conversion of CO_2 to Organic Material

Once absorbed by the ocean, CO_2, whether anthropogenic or not, can either remain as inorganic forms such as carbonate and bicarbonate ions, or can be converted by phytoplankton to organic carbon during photosynthesis (also termed primary production). This conversion removes carbon from the equilibria set up between CO_2 in the aqueous and gaseous phases, and is therefore an important step in the biological pump.

It was long thought that the ocean south of the Antarctic Convergence was highly productive, partially due to the high concentrations of nutrients and biomass of metazoan predators present. It is now realised, however, that the majority of this area experiences relatively low levels of primary productivity even during the peak period of phytoplankton activity in spring and summer (El-Sayed, 1988). A number of factors influence the development of phytoplankton blooms in the Southern Ocean, and these are discussed below.

Irradiance plays a major role in controlling primary production in polar regions. During winter, day length is short (or zero), and the low angle of the sun above the horizon further reduces penetration of light into the water column. During summer, however, daily irradiance is as high, if not higher, than in temperate and equatorial regions. Polar phytoplankton typically can adjust rapidly to altering light conditions, and can survive and continue to photosynthesise at very low irradiances (Palmisano et al., 1985, 1986).

Wind stress and stratification also play important roles in determining the irradiance experienced by an individual phytoplankton cell. Increased wind stress will result in deeper mixing, decreasing the time a cell spends above the 'critical depth' for net OC production (*sensu* Sverdrup, 1953). The deep mixing typically present in the Southern

Ocean is probably a major factor limiting primary production in open water areas. Strengthening stratification, on the other hand, reduces the mixed layer depth and increases average irradiance to the surface phytoplankton population, and therefore primary productivity (Sullivan et al., 1988).

The nutrients nitrate, phosphate and silicate rarely become depleted during the spring-summer phytoplankton bloom in the pelagic waters of the Southern Ocean. This has been attributed to limitation of phytoplankton resulting from deep mixing and the concomitant decrease in the average irradiance experienced by individual phytoplankton cells (Sakshaug and Holm-Hansen, 1984), and, more recently, the absence of important micronutrients, such as iron, in the water (Martin et al., 1990; de Baar et al., 1990, 1995).

Water temperature in the Southern Ocean ranges from -1.87 °C (the freezing point of seawater) to about 6 °C. The rate of primary productivity will be greater at higher temperatures, but the relatively small range means this effect will minor. This will be particularly so close to the Antarctic continent, where the temperature range is reduced.

There are two important special cases in which primary production is enhanced compared to a typical, open water, situation. The first is the marginal ice zone, where during spring and summer input of freshwater from melting sea ice results in enhanced stratification of the surface water and the development of a phytoplankton bloom (e.g. Hart, 1934; Smith, 1987; Sakshaug and Skjoldal, 1989). The bloom typically follows the retreating ice edge from north to south, and results in far higher rates of productivity than in open water or under a complete ice cover. More recently it has become apparent that the intensities of the blooms at the ice edge are affected by the position of oceanic fronts and the continental shelf. It has been estimated that ice-edge blooms account for up to 40 % of primary productivity in the Southern Ocean (Smith and Nelson, 1986). This figure does not include ice algal productivity. Primary

production in the water column under the ice away from the ice edge is generally thought to be minimal.

The second special case is production that occurs either in brine channels within the fabric of the ice, or in mats at the bottom of the ice cover (Garrison et al., 1987). A number of species of phytoplankton is adapted to these environments, in which they are held at higher light levels than experienced in the underlying water column. These communities are not influenced by water column mixing, and can thus develop early in spring and also in newly formed ice in autumn. Seeding of the water column by cells sedimenting from ice communities is one mechanism by which blooms can develop (Ackley and Sullivan, 1994; McMinn, 1996), though advection of cells from open water areas also is important (Palmisano et al., 1986).

Primary production in neritic areas is also significantly greater than in pelagic regions. Nutrient concentrations are often reduced to a much greater extent than in the open ocean, and on occasions are exhausted (Fukui et al., 1986; Perrin et al., 1987; Holm-Hansen et al., 1989; McMinn et al., 1995). The enhanced productivity can be attributed to a number of factors, in particular increased stratification, and therefore reduced mixed layer depth, resulting from greater meltwater input, and higher micronutrient concentrations due to aeolian input in areas near ice free oases or resuspension of sediment material (Nolting et al., 1991).

Any discussion of primary production is not complete without consideration of the remineralisation of organic matter resulting from the activity of heterotrophic organisms ranging from bacteria to metazoan zooplankton and larger animals. The activity of these organisms will result in the reconversion of organic carbon back into DIC. Thus, remineralisation will short circuit the biological pump - if newly formed organic material is remineralised before it can be transported from the surface waters, there will be no net effect on the distribution of carbon within the ocean.

1.4.3 Carbon Export: Sediment Trap Studies

Numerous sediment trap studies have been undertaken in the Antarctic region (summarised by Karl et al., 1991). Most of these studies have been carried out for short, typically summer periods, and only a small number have lasted for an entire year (Platt, 1979; Dunbar, 1984; Fischer et al., 1988; Wefer et al., 1988; DeMaster et al., 1992; Nedwell et al., 1993). The technology currently available for sediment trap design, however, does mean that data can be obtained throughout the year at sites in the open ocean distant from the continent without the necessity for attendance by scientists and research vessels.

Sedimentation in the pelagic Southern Ocean generally has the following characteristics (Honjo, 1990):

(i) Organic carbon and calcite fluxes are low compared to other oceans;
(ii) Diatom frustules, often packaged in faecal pellets of metazoan zooplankton dominate the sedimenting material to the exclusion of coccolithophores;
(iii) A strong seasonal pulse associated with passage of the ice front occurs;
(iv) Sedimentation during winter is negligible.

These conclusions are consistent with known aspects of the physical and biological oceanography of Southern Ocean waters. Firstly, the sediment flux peaks with the passing of the ice edge, when reduced mixing depth results in maximum productivity and tends to lead to an 'export community' (*sensu* Peinert et al., 1989)). At other times of the year, productivity is much lower or negligible, and the deeper surface mixed layer results in a recycling community out of which little material is exported (Peinert et al., 1989). The dominance of diatoms reflects the importance of these organisms among Antarctic phytoplankton and the high concentration of silicate in Antarctic

waters. The absence of reflects calcite the near absence of coccolithophores south of the Antarctic convergence.

The magnitude of the export of carbon in the pelagic regions of the Southern Ocean also appears to be strongly correlated to the distribution of krill (*Euphausia superba* Dana) (Smetacek et al., 1990). The export flux is typically much higher in areas where krill dominate, and in these cases the sedimenting material consists nearly entirely of krill faecal pellets, which sediment rapidly and are sufficiently robust to survive transport. In contrast, sedimentation in areas where krill are absent is much lower (Fischer et al., 1988), and a far greater percentage of organic carbon is recycled within the surface waters either by protists of the microbial loop or by smaller metazoan grazers that produce less robust pellets.

Sedimentation fluxes of carbon measured in the neritic waters of the Antarctic continent are typically higher than for pelagic regions, though the general seasonal cycle of sedimentation is the same. In the neritic environment, mass sedimentation of diatoms during blooms is important, and, especially close to the coast, production of faecal pellets by euphausids is limited. The shallow(er) water depths mean that regeneration of organic material will not occur as completely, as the sedimenting material reaches the sediment (and the sediment traps) more quickly and water column stratification is more marked. Thus, the neritic region is a zone of carbon export from the surface waters, even though there is less production of krill faecal pellets than in some pelagic regions.

Sediment trap studies indicate that the strength of the biological pump, and thus the potential to transport anthropogenic carbon to deep water, is not great throughout the majority of the pelagic Southern Oceans, but that the occurrence of krill and other large grazing organisms can result in enhanced sedimentation and therefore pumping. In contrast, export in the neritic water surrounding Antarctica can be significant. This

export occurs not only in the primary sedimentation of organic material, but also in carbon-rich 'winter outbursts', which result from the entrainment of organic material and DIC from the sediment during the flow of dense bottom waters formed by brine rejection from thickening sea ice over the shelf region (Anderson and Jones, 1991), and which thereby transfer organic matter to the deep ocean.

1.4.4 Carbon Export: Advection

In the Southern Ocean formation of bottom water occurs as a result of either deep convection (which probably occurs intermittently) or bottom water formation by shelf processes involving heat exchange with ice shelves. The role of deep convection is as yet uncertain, though the current high concentration of atmospheric CO_2 will reduce the outgassing of CO_2-rich deep waters convected to the surface. Bottom water formation transports both water and anthropogenic CO_2 from the surface to the deep ocean. However, it is necessary for CO_2 in the water to be saturated with respect to the atmosphere prior to subduction for transport of anthropogenic CO_2 to occur. As mentioned in the previous Section, winter outbursts could also be important.

Most studies of the distribution of anthropogenic CO_2 in the Southern Ocean have been carried out in the Weddell Sea, which is an important area of bottom water formation. It has been estimated that 0.024 Gt yr^{-1} anthropogenic C is transported to the deep ocean in this area, out of an estimated total 0.05 Gt yr^{-1} for the entire Southern Ocean (Anderson and Jones, 1991). The distribution of anthropogenic CO_2 in the Weddell Sea shows that it is present either in the surface water to a depth of *circa* 200 m resulting from the equilibration of this water with the atmosphere (Poisson and Chen, 1987), or a thin layer down the shelf slopes and at the bottom of basins, reflecting the importance of bottom water formation and winter outbursts (Anderson and Jones, 1991).

1.5 The Themes of this Thesis

Many questions remain to be answered about the biogeochemical carbon cycle in the ocean surrounding the Antarctic Continent. The study described in this thesis was designed to provide insight into a number of these questions, including:

(1) What is the seasonal cycle of carbon uptake and regeneration in neritic Antarctic waters? How much primary production occurs under the ice prior to the arrival of the ice edge at the coast? Can a balanced budget be developed incorporating organic carbon production calculated from the concentrations of organic and inorganic forms of carbon, and sediment fluxes?

(2) What effect does biological production during summer have on fCO_2, and how quickly and to what extent does fCO_2 recover during winter? Furthermore, is there any evidence for the actual uptake of CO_2 by the ocean during periods of low fCO_2 (as distinct from uptake calculated from empirical formulae)?

(3) Does the seasonal cycle of phytoplankton species composition and biomass follow a predictable seasonal cycle or is there interannual variability, and what effect could interannual variation have on the efficiency of the biological pump?

(4) Is the seasonal cycle of sedimentation in neritic waters similar to that described for pelagic regions, and what are the characteristics of the sedimenting material? What can the material tell us about the environment in which it was formed?

(5) Finally, to what degree can the understanding developed of nearshore Southern Ocean OC production and sedimentation enable us to predict how they are likely to respond to climate change?

These questions provide the themes for this thesis, and are discussed throughout the subsequent chapters.

CHAPTER 2

O'GORMAN ROCKS SITE: LOCATION, PREVIOUS STUDIES AND PHYSICAL OCEANOGRAPHY

2.1 Introduction

The O'Gorman Rocks sampling site was located at 68° 34.2'S 77° 56.4'E (Figure 2.1), and was named due to its proximity to O'Gorman Rocks, a group of small islands rising a few metres above sea level. The site was in an extensive area of near constant water depth of around 20-25 m, with the depth at the sampling site 23 m. The sampling site was chosen so that it would be accessible for as long as possible during the period of ice deterioration and break out in summer. Previous observations (Gibson et al., 1990a) indicated that deeper sites further offshore (Figure 2.1) would be inaccessible for extended periods from the time of ice break out in these areas until the shoreline at Davis Station became ice free. As the fast ice between the mainland and Anchorage Island often breaks out within a single day (J. Gibson, unpublished observations, 1987, 1994), the sampling site was located in this area in order to minimise the period of inaccessibility.

This chapter gives a brief description of the Vestfold Hills area (including the local climate), and reviews previous physical, chemical and biological studies undertaken in the inshore region near Davis Station. The chapter is concluded with a description of the physical oceanography recorded at the O'Gorman Rocks site between December 1993 and February 1995.

Figure 2.1. Location of the study area: (a) A map of the Antarctic continent indicating the position of Prydz Bay and Davis Station, as well as a number of other locations mentioned in this thesis. Ice sheets are indicated by shading; (b) A map of the Prydz Bay region, showing depth contours in metres, and the locations of Davis Station, the Amery Ice Shelf and the West Ice Shelf; (c) A map of the Vestfold Hills region. The locations of Davis Station and Ellis Fjord are indicated; (d) A bathymetric map of the waters offshore from Davis Station showing the position of the O'Gorman Rocks site. The depth contours are again in metres.

(a)

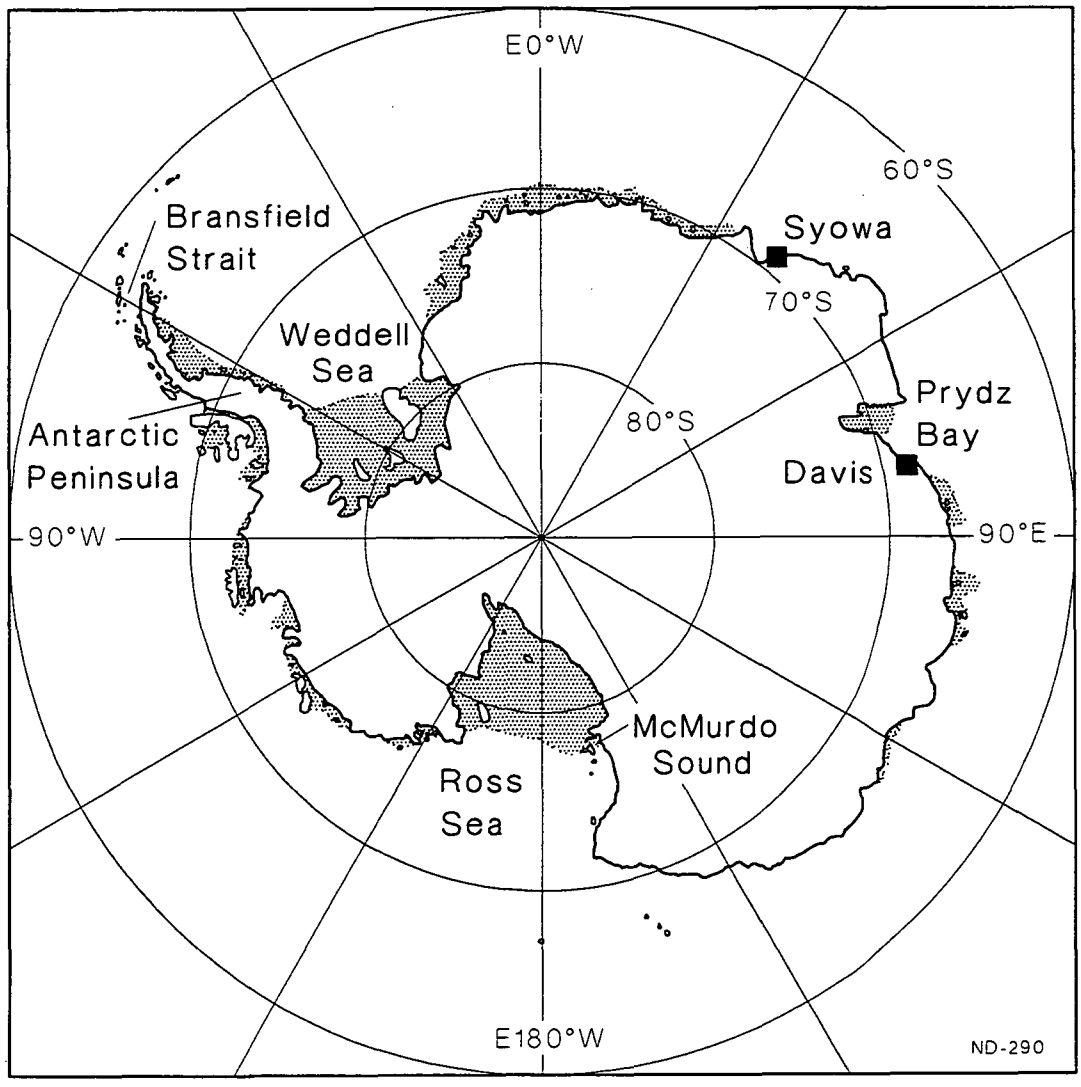

Figure 2.1. (b) A map of the Prydz Bay region, showing depth contours in metres, and the locations of Davis Station, the Amery Ice Shelf and the West Ice Shelf.

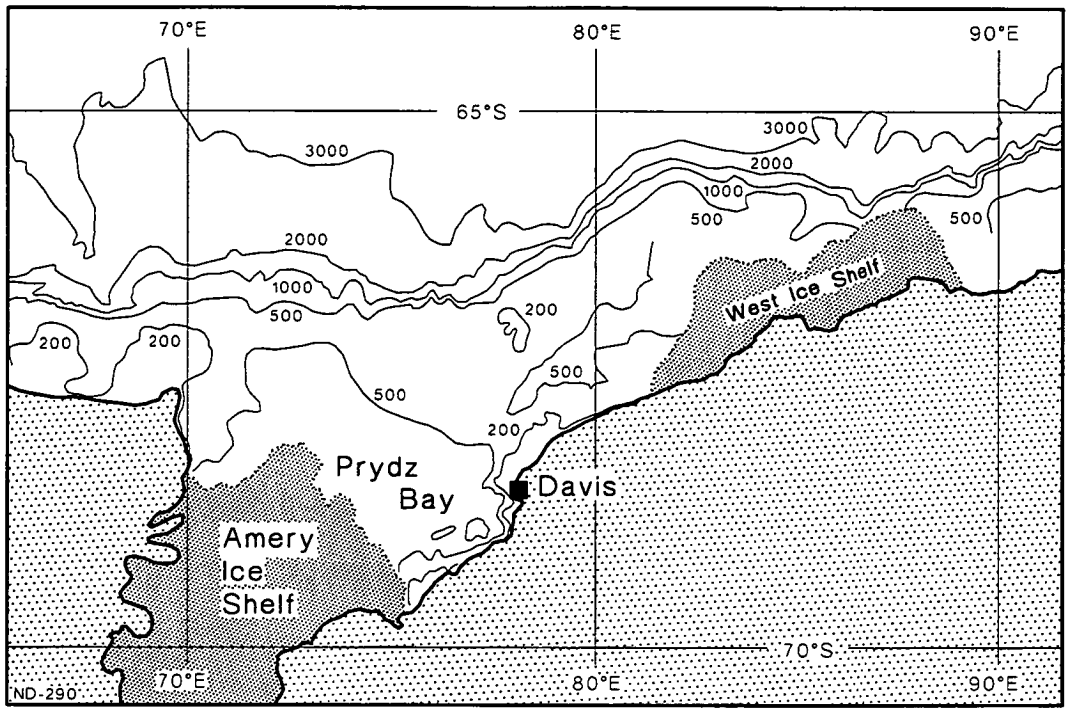

Figure 2.1. (c) A map of the Vestfold Hills region. The locations of Davis Station and Ellis Fjord are indicated.

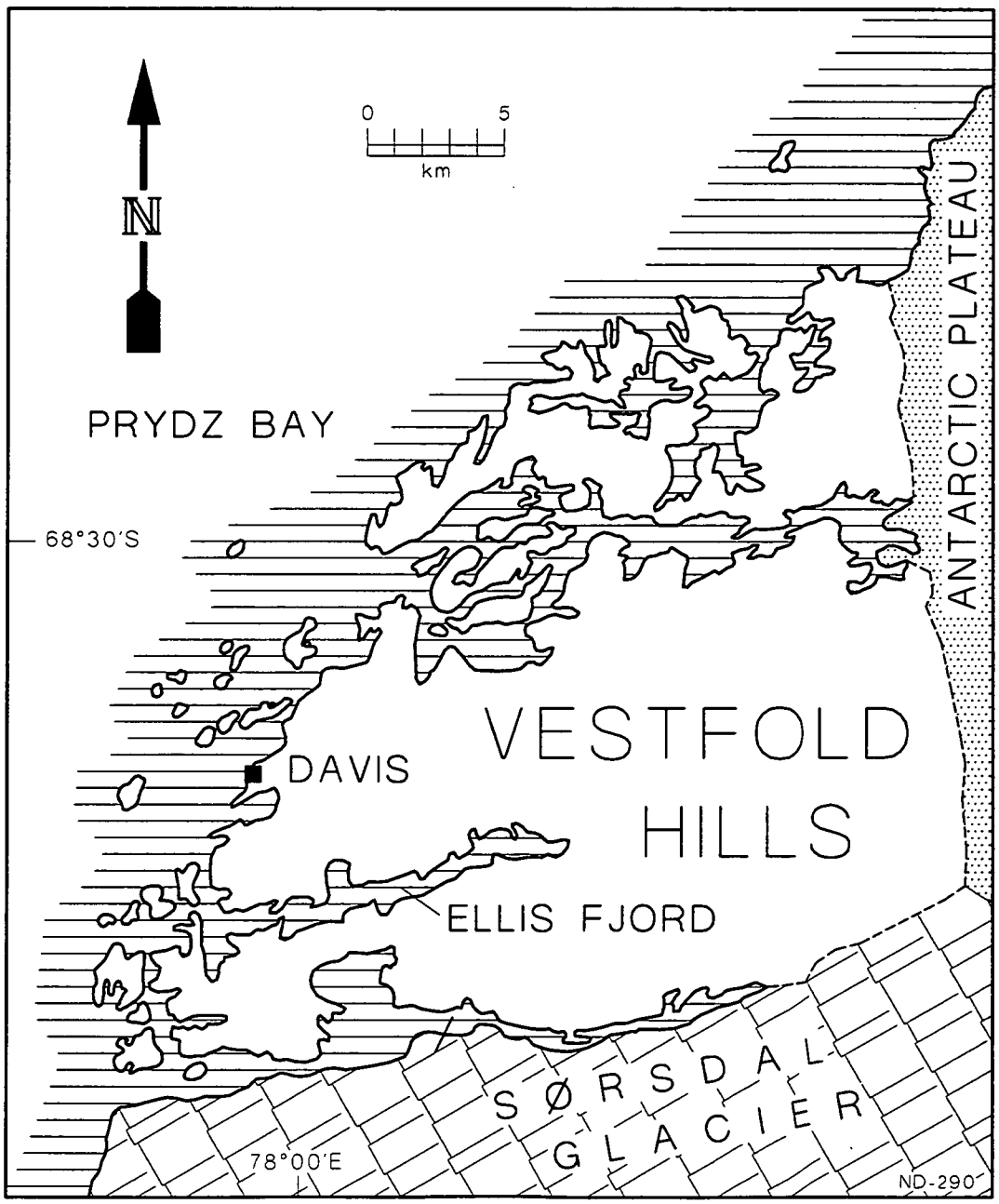

Figure 2.1. (d) A bathymetric map of the waters offshore from Davis Station showing the position of the O'Gorman Rocks site. The depth contours are again in metres.

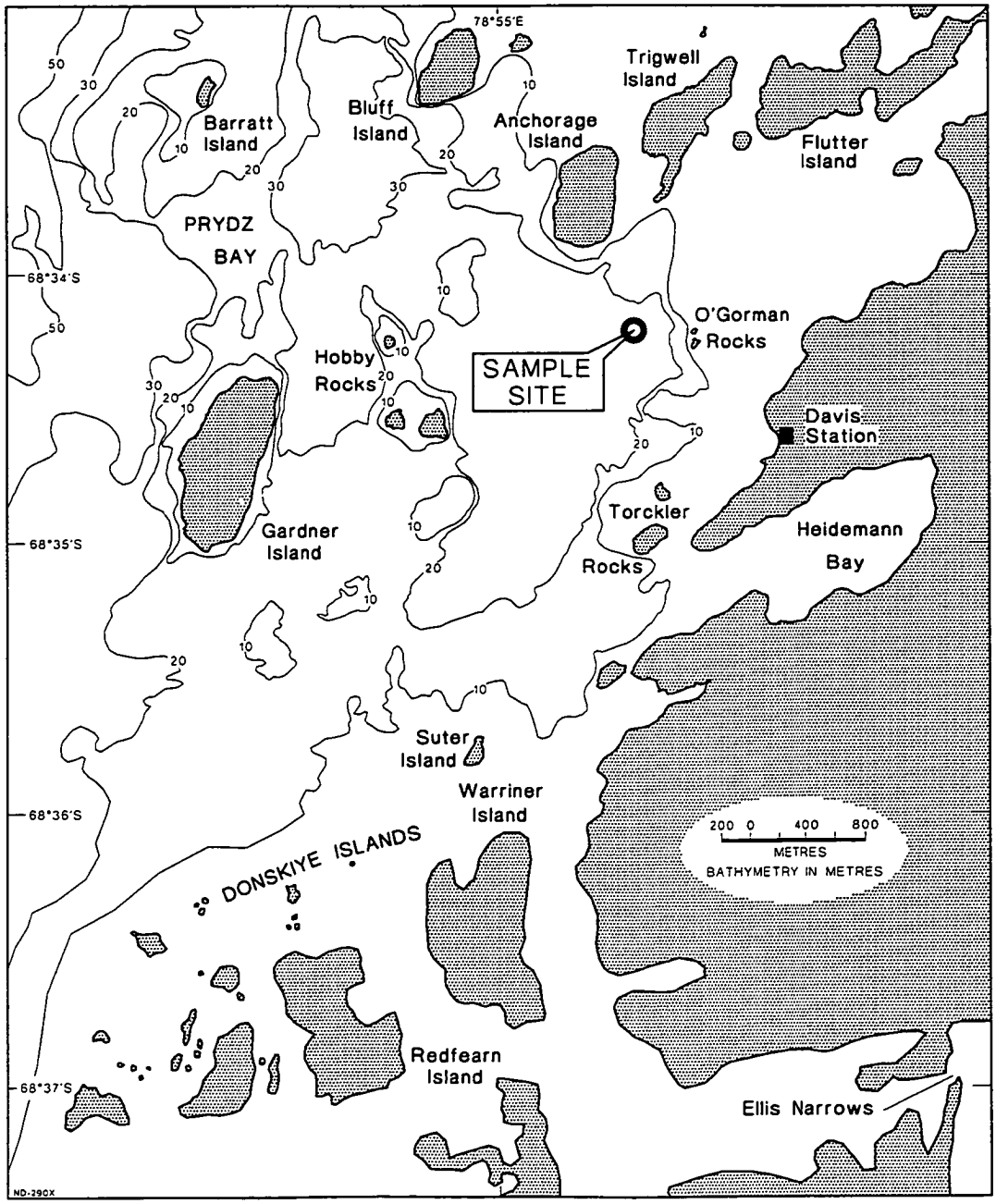

2.2 The Vestfold Hills

The Vestfold Hills (Figure 2.1) is an approximately triangular area of exposed rock 410 km^2 in area on the Antarctic coastline, and is bounded to the east by the Antarctic ice sheet, to the south by the Sørsdal Glacier, and to the north and west by the waters of Prydz Bay, a major embayment of the Antarctic coastline. The occurrence of the ice free area is probably due in part to relatively high topography, the nearby occurrence of a major outlet glacier and positive feedback effects from the low albedo, and therefore heating of the dark rocks of the hills (Pickard, 1986).

The Vestfold Hills were first discovered in 1935 (Mikkelsen, 1935), and Davis Station was established in 1957. The station has operated continually since then except for the period 1964-8, and now contains a modern scientific laboratory, in which much of the chemical and biological work described in this thesis was undertaken.

2.3 The Inshore Marine Environment of the Vestfold Hills

The coastline of the Vestfold Hills is aligned approximately north-east - south-west, and is fringed by small islands (Figure 2.1). The general current offshore from the Vestfold Hills parallels the coast from the north-east to the south-west. This current is part of the East Wind Drift (Foster, 1984), which flows around the coastline of Antarctica. In Prydz Bay, the East Wind Drift and the more northerly West Wind Drift interact to form the Prydz Bay Gyre, which is a cyclonic eddy similar to, but smaller than, the circulation in the Ross and Weddell Seas (Smith et al., 1984). The average velocity of water flow in the East Wind Drift is 13 - 20 cm s^{-1}, but considerably higher velocities (up to circa 60 cm s^{-1}) have been recorded in the waters offshore from the Vestfold Hills (Maksimov, 1958). Water flow through the inshore waters surrounding the sampling site has not been explicitly studied, but from casual observations of current direction it is probable that water enters the area from between Gardner and

Anchorage Islands and exits between Gardner Island and the Donskiye Group (Figure 2.1) (J. Gibson, unpublished observations).

A number of studies has investigated water mass distribution and movement within the Prydz Bay Gyre, and therefore the origin of the water which passes through the inshore area of the Vestfold Hills (Smith et al., 1984; Wong, 1994). These studies suggest that the main flow is along the coast from the direction of the West Ice Shelf (Figure 2.1), though transport of water in the gyre from the north-west could also occur. Water sourced from the vicinity of the West Ice Shelf has lower salinity than elsewhere in the region due to the input of fresh melt water from the shelf during summer (Smith et al., 1984). The water entering the inshore water near Davis is presumably near surface water (from depth < 30 m) which flows over the sill that connects Gardner and Anchorage Islands. The influence of the seasonal ice cover on this flow is uncertain, but it is likely that flow occurs more easily in the absence of ice. The average tidal range at Davis Station is approximately 1 m (Gallagher et al., 1989).

The strong currents which flow through the inshore water near Davis mean that even though the water depth at the site was only shallow, the water in the region cannot be considered in isolation, but rather must be considered to be representative of the wider Prydz Bay and the East Wind Drift, and, during winter, the Antarctic Winter Water layer.

The ice cover directly offshore from Davis Station begins to form in early March, and is sufficiently thick to support pedestrian traffic by the end of the month. The ice thickens rapidly at first, but then slows to reach a final thickness, depending on the severity of the winter, of 1.5 to 2 m. Ice break out occurs at any time from early December to late January, usually due to the occurrence of strong offshore winds and onshore swells.

The biology and chemistry of the inshore marine environment near Davis Station has been studied extensively over the last twenty years. Physical characteristics of the water column have been measured during a number of studies (e.g. Perrin et al., 1987; Davidson and Marchant, 1992a; McTaggart, 1994). Water temperature undergoes a general cycle of increase from the winter minimum of -1.85 to -1.90 °C to a summer maximum of 0 to 1 °C, followed by rapid cooling in autumn. Salinity exhibits a similar, but inverted, cycle, reaching a maximum of 34.2 to 34.5 practical salinity units (psu) at the end of winter before falling to *circa* 33 to 33.5 psu in summer as a result of freshwater input from the melting of the sea ice, icebergs and ice shelves.

The identity and abundance of bacteria and phytoplankton both in the water column and in the sea ice offshore from Davis have been studied (McConville et al., 1985; Perrin et al., 1987; McMeekin, 1988; Gibson et al., 1990a, 1990b; Davidson and Marchant, 1992a; Skerratt et al., 1995; Archer et al., 1996). Generally speaking, the communities present are similar to those found at other inshore Antarctic sites, both in species distribution and seasonal cycles (e.g Krebs, 1983; Holm-Hansen et al., 1989; Knox, 1990). Phytoplankton growth generally begins in spring in and at the base of the sea ice and spreads to the water column in late November - early December. The bloom in the water column continues until mid to late February. Species that appear to occur regularly in the area include diatoms of the genera *Entomoneis*, *Nitzschia*, *Fragilariopsis*, *Thalassiosira* and *Chaetoceros*, as well as the flagellates *Phaeocystis* and *Cryptomonas*. The intensity of the blooms in the inshore region, as indicated by the concentration of chlorophyll *a* (chl *a*), is often significantly greater than at sites further offshore (H. Marchant, personal communication). Bacterial abundance generally parallels the biomass of phytoplankton (Gibson et al., 1990b). Protozoan communities have been reported to contain a selection of heterotrophic dinoflagellates (Archer et al., 1996a), nanoflagellates (Leakey et al., in press), ciliates and choanoflagellates (Marchant and Perrin, 1990).

The biological activity during summer results in decreased concentrations of the nutrients nitrate, phosphate and silicate and increased pH (Perrin et al., 1987; McTaggart, 1994). As in other inshore Antarctic marine environments, the magnitude of the reduction of the concentrations of the nutrients is greater than generally found at deep water sites, with nitrate being reduced to near zero at the height of phytoplankton blooms (Perrin et al., 1987; McTaggart, 1994).

The zooplankton of the area is dominated by calanoid, cyclopoid and harpacticoid copepods (Tucker and Burton, 1988, 1990). Also prominent are amphipods, polychaete worms and appendicularians. The benthic fauna is both abundant and varied, though similar to that recorded at other Antarctic sites (Tucker, 1988; Tucker and Burton, 1988). A number of species of fish is found in the area (Williams, 1988), and higher predators include Weddell, Elephant and Leopard Seals and a number of species of birds, including Adelie Penguins, Cape Petrels, Snow Petrels and Wilson's Storm Petrels, which breed locally.

2.4 The Climate of the Vestfold Hills

Meteorological data for the Vestfold Hills are confined almost entirely to observations made at Davis Station since 1957 by staff of the Australian Bureau of Meteorology. The climate of the area is reasonably typical of similar areas of the Antarctic coastline, though the large expanses of exposed rock does introduce some distinctive local features (Streten, 1986). Meteorological data recorded between December 1993 and February 1995 are summarised in Appendix B.

The climate of the Vestfold Hills (Burton and Campbell, 1980; Streten, 1986) is dominated by the extreme seasonal variation in the amount of incoming solar radiation to the surface. Global radiation at the surface at Oasis Station in the Bunger Hills (at a similar latitude as the Vestfold Hills) has been reported to vary from 21 MJ m^{-2} $month^{-1}$

in June to 749 MJ m^{-2} $month^{-1}$ in December (Rusin, 1964, quoted in Streten, 1986). The range in radiation is reflected in the strong seasonal variation in average temperature, which at Davis ranges from -17.7 °C in July to +1.0 °C in January. Air temperatures below -40 °C occur occasionally during winter, though temperatures above freezing have been recorded during every month of the year. Summer temperatures in the Vestfold Hills, which occasionally exceed 10 °C, are slightly higher than at other Antarctic sites due to the absorption and re-radiation of incoming solar radiation by the dark rock of the hills (Streten, 1986). Cloud cover at Davis Station averages 5 - 6 8ths, and the percentage of totally overcast days (51 %) far outweighs totally cloud-free days (17 %) (Streten, 1986).

The Vestfold Hills are under the influence of the Antarctic trough, a permanent zone of low pressure which encircles Antarctica (Streten, 1986). At Davis Station the mean sea level barometric pressure averages *circa* 987 mb, and varies only slightly seasonally (Streten, 1986). However, major Southern Ocean depressions can approach the area at any time of the year, resulting in extended periods of strong winds and blizzard conditions. In contrast, periods of calm weather are recorded more often than at other Antarctic sites, and are more prevalent in spring and autumn (Streten, 1969; Streten, 1986). The prevailing wind direction in the Vestfold Hills is from the north-east, though onshore sea breezes from the south west often occur during summer, and to a lesser extent in spring and autumn (Streten, 1986). The average wind speed at Davis Station is circa 5 m s^{-1}, which is considerably lower than for many Antarctic coastal stations (Burton and Campbell, 1980; Streten, 1986).

Precipitation in the Vestfold Hills is dominated by snowfall. It is difficult to determine accurately the annual precipitation budget, as distinguishing between falling snow and wind blown drift is problematical (Burton and Campbell, 1980; Streten, 1986). Suffice it to say, the Vestfold Hills does not receive a great deal of snowfall, and the relative humidity of the air is typically very low (Streten, 1986). Wind-blown snow is

a more common occurrence in winter than in summer (Burton and Campbell, 1980), and leads to the development of large compacted snow banks in the lee of hills, rocks and buildings which usually melt in spring and summer, resulting in short melt water streams and soaks which debouch into lakes or into the sea.

2.5 Physical Oceanography at the O'Gorman Rocks Site, December 1993 - February 1995

2.5.1 Ice Cover

At the start of the study in December 1993 the O'Gorman Rocks site was covered by a layer of ice approximately 1.6 m thick. The ice broke out early in the morning of 23 December 1993 (the day after the first sampling trip), after which the site remained essentially ice free until the fast ice began to reform in early March (Figure 2.2). By

Figure 2.2. Ice and snow thickness (metres) at the O'Gorman Rocks site, March 1994 - January 1995.

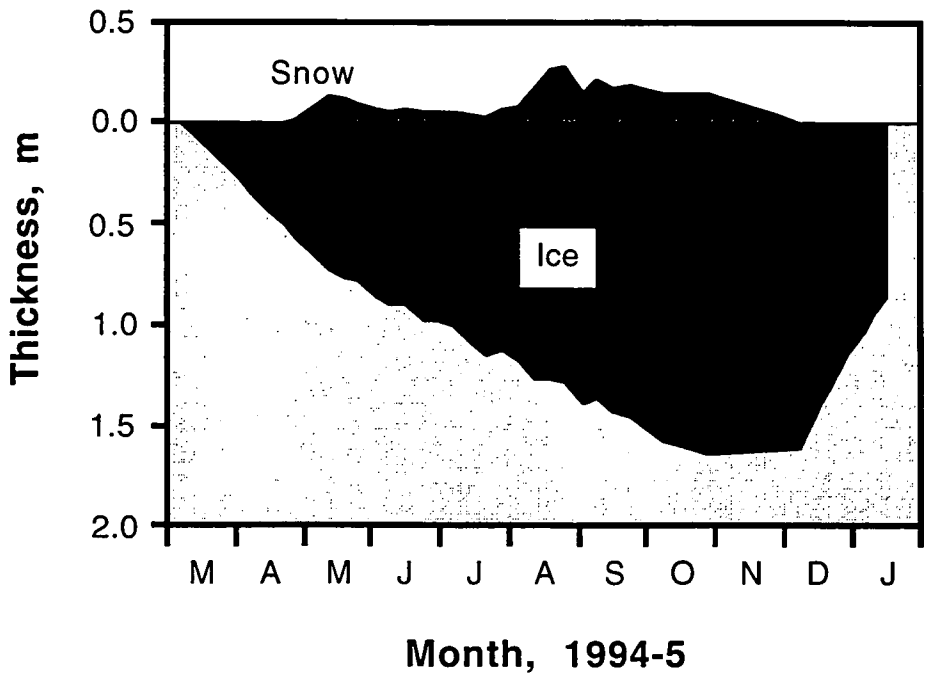

the end of the month it had reached a sufficient thickness to support pedestrian traffic, allowing access to the sampling site. The ice increased in thickness steadily to a maximum of 1.64 m in November (Figure 2.2), but by early December it had began to 'rot' (i.e. its structural strength was reduced by melting and the enlargement of internal brine channels), and it was blown out during a period of strong wind on 13 January 1995. After this, the site remained ice free for the rest of the study.

Snow cover on the surface of the ice during the year ranged from 0 to 280 mm (Figure 2.2). It should be noted, however, that the snow cover was very dynamic, as it depended on snowfalls and blizzards to deposit the snow, and blizzards and ablation to remove it. The presence of snow on successive sampling dates did not necessarily imply that snow was present at all times between the dates, and it is also likely that greater snow accumulation occurred at times between measurement dates.

2.5.2 Water Temperature

A contour plot of water temperature at the O'Gorman Rocks site from December 1993 to February 1995 is shown in Figure 2.3, while Figure 2.4 shows more clearly temperature changes at 10 m (temperature and salinity data are also presented in tables in Appendix D). Water temperature essentially underwent a simple cycle of warming due to input of solar radiation starting in November and continuing until January, and cooling during February and March. Between the end of March and early November the entire water column was essentially at its freezing point (at about -1.9 °C).

Solar heating in November initially occurred directly beneath the ice, but soon spread to the entire water column. Maximum recorded water temperatures were 0.04 °C and 1.39 °C during the 1993 - 4 and 1994 - 5 summers respectively. Higher temperatures were generally recorded when the sea ice was still present, as the ice insulated the water column against re-radiation of absorbed energy back to the atmosphere as long

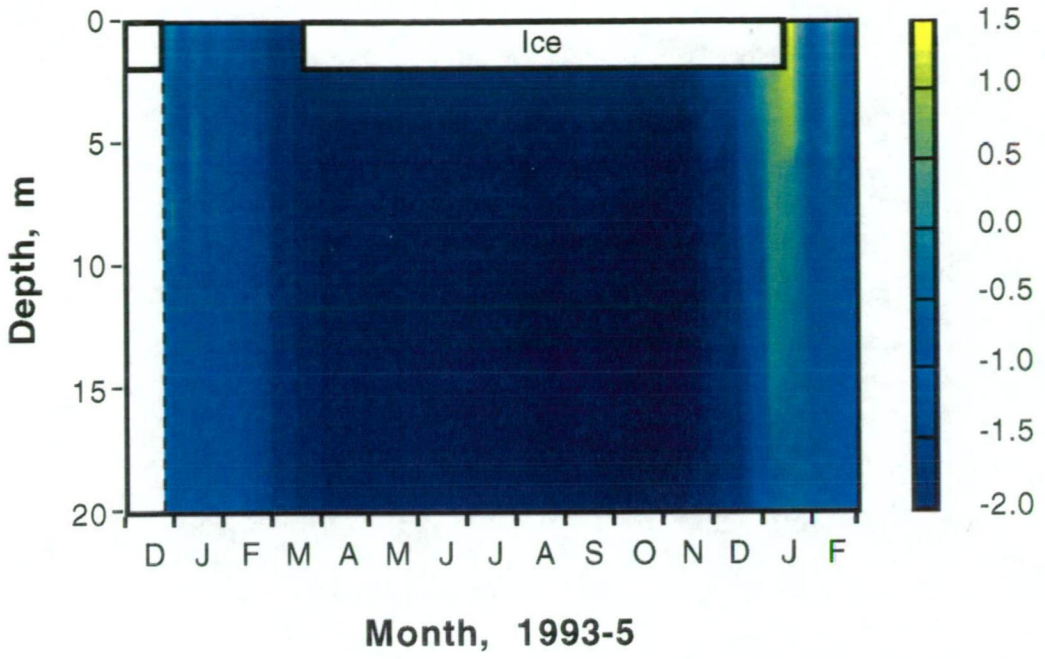

Figure 2.3. Water temperature (°C) at the O'Gorman Rocks site, December 1993 - February 1995. Temperature was recorded every metre.

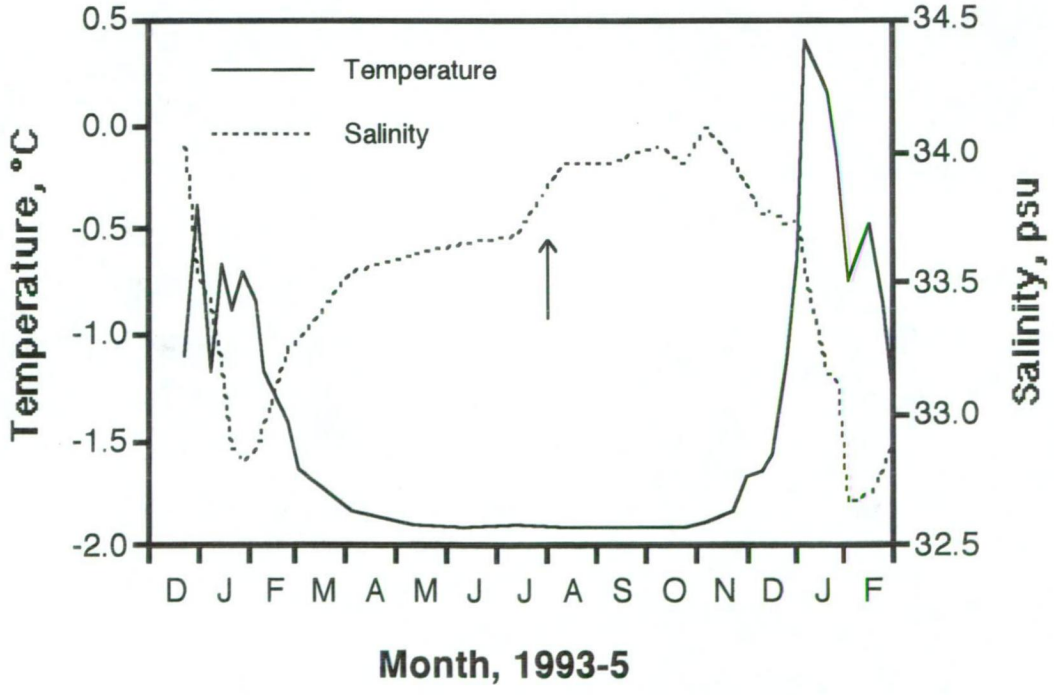

Figure 2.4. Temperature and salinity at 10 m at the O'Gorman Rocks site. The jump in salinity in winter discussed later in the chapter is arrowed.

wavelength radiation or sensible heat, and protected it from evaporative surface cooling. Warm periods after ice break out were the results of either warmer weather or advection of warmer water to the sampling site.

The water column was stratified during summer, with the temperature at the surface up to 1.5 °C warmer than at 20 m. Exceptions occurred directly after periods of high winds (e.g. early January 1994), when the water column was homogenous. The continued stratification of the water column indicated that water flow through the area itself was incapable of mixing the water. Soon after the ice cover began to reform in March 1994, stratification disappeared. This was presumably due to mixing from cooling of the surface water and the formation of denser brines resulting from the exclusion of salt from the rapidly forming ice not only at the site but also further out to sea. A single temperature and salinity profile recorded in July 1994 to a depth of 120 m further offshore indicated that the water column was mixed to at least this depth just after mid-winter.

The temperatures recorded during the study were similar to those measured previously from the area (Perrin et al., 1987; Davidson and Marchant, 1992a; McTaggart, 1994; Gibson et al., 1997).

2.5.3 Water Salinity

Water salinity at the O'Gorman Rocks site exhibited trends which mirrored those of the water temperature. As shown in Figures 2.4 and 2.5, salinity was lowest during summer, when fresh water from melting ice diluted the surface waters, and increased steadily during winter to a maximum in October as a result of brine exclusion during ice formation and entrainment into the winter mixed layer of more saline water.

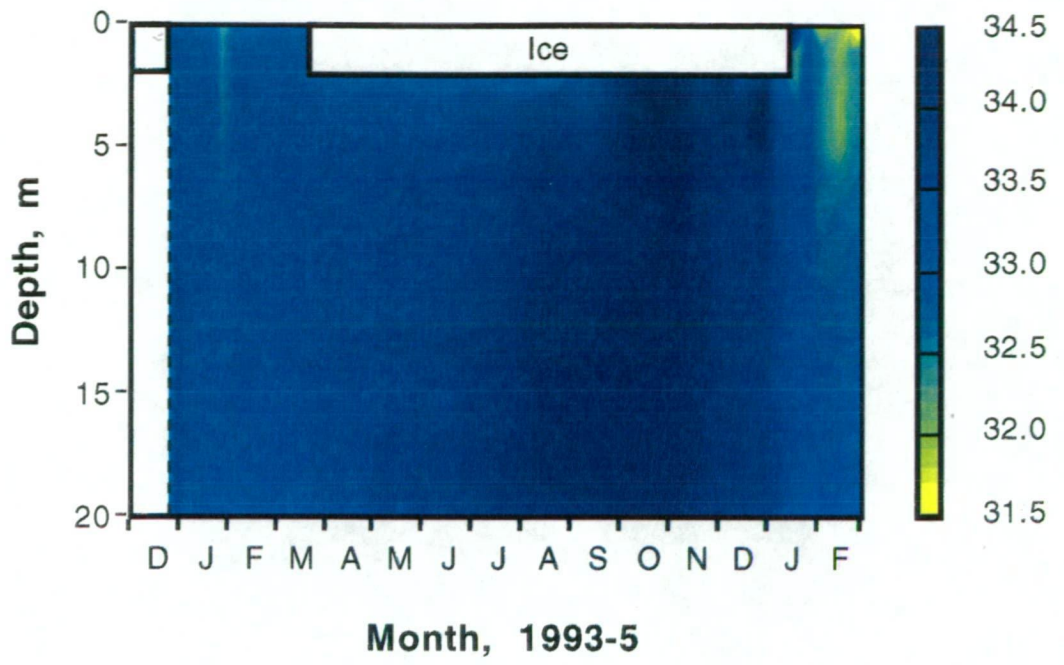

Figure 2.5. Water salinity (psu) at the O'Gorman Rocks site from December 1993 to February 1995. Salinity was recorded each metre.

Minimum salinities during both summers were recorded well after the break out of the fast ice, indicating that it was not only melting of the local sea ice but also of icebergs, ice shelves and the Antarctic plateau that was decreasing the salinity of the water. Figure 2.5 also indicates that the water column was stratified with respect to salinity throughout the ice free period except for some short periods after periods of strong winds. This was consistent with the stratification observed in temperature.

After the beginning of ice formation in March 1994 salinity increased steadily, reaching a maximum at the end of October, though a marked jump, discussed further below, occurred in late July - early August (Figure 2.4). The water column during much of winter retained some slight stratification, with less saline water near the surface. It is possible that this was an artefact of measurement, as the temperature profiles suggested that the water was well mixed. The maximum salinity, recorded in October, was 34.10 psu. The occurrence of more saline water just under the ice on occasions between October and December is difficult to explain, but may have been due to flow of hypersaline brine out of channels in the ice as it became rotten, possibly

exacerbated by the drilling of the ice hole through which the profiles were measured. Interestingly, Perrin et al. (1987) and Gallagher and Burton (1988) recorded the same phenomenon at the same time of the year in earlier studies.

Little data is available form the Davis area with which to compare the seasonal salinity cycle observed in this study. Perrin et al. (1987), in a more limited sampling regime, recorded a maximum winter salinity of 34.6 psu, and McTaggart (1994) reported a maximum of 34.45 psu. The maximum winter salinity recorded at the O'Gorman Rocks site in the present study was significantly lower than in these previous studies. The question must therefore be asked: Why were the salinities lower during the 1994 winter than in the other studies undertaken six and twelve years earlier?

The water that surrounds the Antarctic continent during winter is commonly called the winter water (abbreviated to WW) (Gordon and Huber, 1990). Remnants of this water can be observed in summer as a layer of minimum temperature between the sun-warmed water above and warmer Antarctic Intermediate Water below. WW is formed by development of convection cells due to the formation of denser water at the surface resulting from cooling as heat is lost to the atmosphere and from exclusion of salt during the development of sea ice. The convection cells deepen and the water becomes denser as the winter progresses largely due to an increase in salinity, reaching maximum depth and density at the time of maximum ice formation. The depth of penetration of the convection cell will depend on the pre-existing density profile and the amount of salt rejected from the forming sea ice.

WW in the Prydz Bay region has been studied by Smith et al. (1984), who reported a salinity range of 34.2 to 34.6 psu. As this study was undertaken during summer, these salinities would have been the maxima reached during the previous winter. Two distinct types of WW were identified, being characterised by high (>34.5 psu) and low (<34.25 psu) salinity. The low salinity water had its immediate source in the area of

the West Ice Shelf (Figure 2.1), where summer freshwater input reduced the salinity. Calculations of geostrophic flow by Smith et al. (1984), and Wong (1994) suggested that the low salinity water had its source in the westerly flowing littoral current, and that this water would continue to flow along the coastline from the ice shelf in the direction of Davis. It is likely that the water observed at Davis during the 1994 winter was from this source, though it was of slightly lower salinity than the minimum recorded by Smith et al. (1984). The higher salinities recorded by Perrin et al. (1987) and McTaggart (1994) were presumably a result of a greater influence of higher salinity WW from the anticyclonic Prydz Bay Gyre which could also supply water to the region offshore from the Vestfold Hills (Wong, 1994).

A number of lines of evidence, however, suggests that flow of water into the Vestfold Hills region during the 1994 winter was not of a single, homogenous water body. It is evident from the seasonal cycle of $\delta^{13}C$ and $\Delta^{14}C$ in the DIC ($\delta^{13}C_{DIC}$ and $\Delta^{14}C_{DIC}$) at the O'Gorman Rocks site (Figure 2.6) that significant changes in both parameters occurred during winter. $\delta^{13}C_{DIC}$ and $\Delta^{14}C_{DIC}$ decreased markedly in the August and September samples respectively, suggesting that a different water body or bodies with a greater deeper water character had been advected into the area ($\delta^{13}C_{DIC}$ and $\Delta^{14}C_{DIC}$ decrease beneath the winter mixed layer (Fairhall et al., 1971; Kroopnick, 1974; Schlosser et al., 1994)). This water body appeared, on evidence of $\Delta^{14}C_{DIC}$, to be present at the sampling site at least until January 1995. All $\Delta^{14}C_{DIC}$ values were in the range previously reported for Antarctic WW (Fairhall et al., 1971; Gordon and Harkness, 1992, Schlosser et al., 1994). Interestingly, $\delta^{13}C_{DIC}$ had recovered to typical Southern Ocean surface values (*circa* 0.8 - 1.0) (Kroopnick, 1974) by October, though $\Delta^{14}C_{DIC}$ remained at the lower level throughout the rest of the study. The subsequent increase in $\delta^{13}C_{DIC}$ during summer was largely attributable to biological activity (Chapter 5).

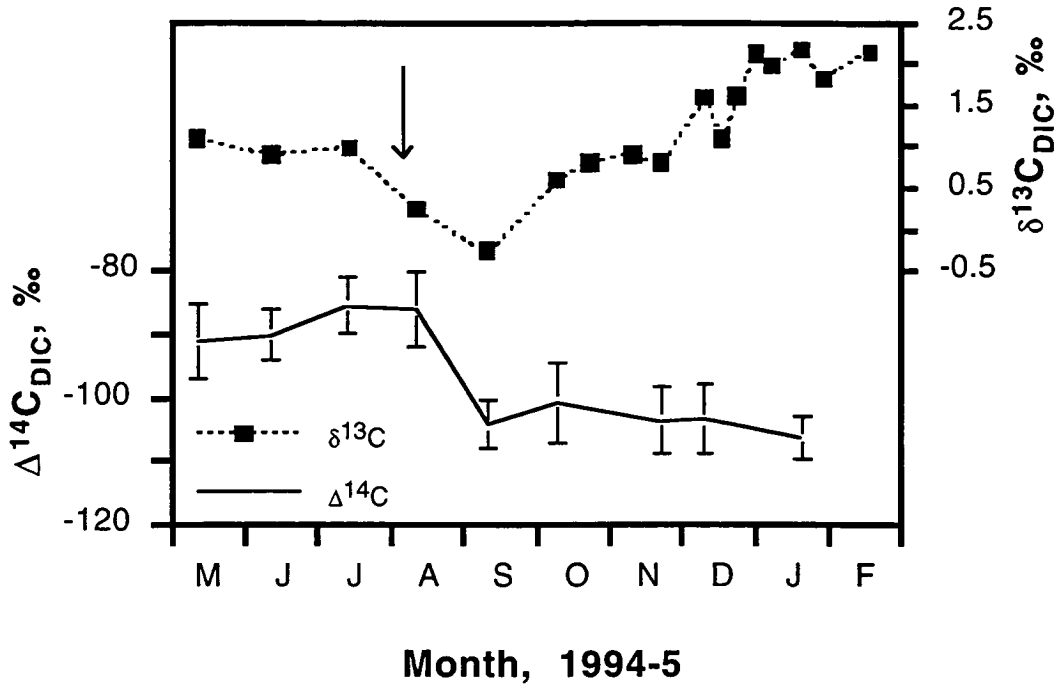

Figure 2.6. $\delta^{13}C_{DIC}$ and $\Delta^{14}C_{DIC}$ at 10 m at the O'Gorman Rocks site. Calculated error bars are shown for the $\Delta^{14}C_{DIC}$ data. Full details of the $\Delta^{14}C_{DIC}$ data are given in Appendix D. The arrow indicates the approximate timing of the salinity jump (Figure 2.4)

It is possible that the jump in salinity indicated in Figures 2.4 and 2.6 was related to the change in the water mass. This change in salinity appeared to occur as the same time as the initial drop in $\delta^{13}C$, but before the drop in $\Delta^{14}C$. The salinity jump could have been due to an increase in the depth of convective mixing (thus mixing a greater amount of deeper, more saline water into the WW), though it would be expected that if this process had occurred to any extent the maximum winter salinity would have been greater than the very low value observed (relative to previous studies). Perhaps it is more likely that salinity and isotope changes reflected the horizontal advection of a water mass or masses with different characteristics and history into the area offshore from the Vestfold Hills.

2.6 Conclusions

The water column at the O'Gorman Rocks site exhibited a simple cycle of temperature and salinity, being warmer and less saline in summer, and colder and more saline in winter. The water present at the O'Gorman Rocks site during winter was low salinity WW, which was part of a convection cell set up during ice formation in March. This water was at its freezing point, and had probably been transported to the area from the vicinity of the West Ice Shelf by coastal currents. The water column remained mixed until surface heating began in November, and summer saw dilution of the water and heating not only due to local processes, but also, as a result of advection, processes occurring elsewhere.

CHAPTER 3

PHYTOPLANKTON AT THE O'GORMAN ROCKS SITE: SEASONAL CYCLE AND INTERANNUAL VARIABILITY

3.1 Introduction

The conversion of inorganic to organic carbon in the ocean is the result of photosynthesis, in which algae and other photosynthetic organisms use radiant energy to fuel the conversion of CO_2 and water to simple organic chemicals and molecular oxygen. This process is also termed 'primary production', and forms the basis of nearly all food chains. The uptake of CO_2 by algae, its subsequent conversion to organic material and the sedimentation of this material out of the euphotic zone is often referred to as the 'biological pump', which, as discussed in Chapter 1, is an important mechanism for creating a DIC deficit in the water column, thus enhancing the uptake of CO_2 by the ocean from the atmosphere.

This chapter describes phytoplankton species composition and abundance recorded at the O'Gorman Rocks site between December 1993 and February 1995. The work was undertaken to provide a background for the more chemically-oriented studies of the uptake of DIC and nutrients from the water column during primary productivity (Chapter 4) and export of particulate organic carbon (POC) from the water column to the sediment (Chapter 5). The chapter also provides a comparison to earlier studies undertaken in the area, highlights the interannual variability of the phytoplankton community at the site, and discusses the effect of this variability on carbon export from the euphotic zone.

3.2 Results

All phytoplankton cell counts are tabulated in Appendix C.

3.2.1 Seasonal Phytoplankton Cycle

Phytoplankton species composition and abundance at the O'Gorman Rocks site was monitored from December 1993 to February 1995. Figure 3.1 shows the seasonal cycle of phytoplankton abundance recorded during the study. Six major species, or groups of species, are plotted in the figure: (i) an undescribed cryptomonad (termed cryptomonad A throughout the rest of this thesis); (ii) diatoms, which consisted of a wide range of species; (iii) *Phaeocystis* cf. *antarctica*; (iv) dinoflagellates, which also consisted of several species; (v) *Pyramimonas gelidicola* (McFadden); and (vi) and all other species plotted together. Figure 3.1b shows the same data expressed in terms of the percentage that each species or group of species made up of the total. The seasonal cycles of the first five of these species and groups are described in more detail below.

Total cell densities at the start of the study were *circa* 2 x 10^6 cells L^{-1}, but had decreased by the second sampling trip, suggesting that a peak in phytoplankton abundance might have occurred in early December 1993 prior to the commencement of sampling. A bloom of *Phaeocystis* cf. *antarctica* developed in late December and was at its peak at the end of the month, but was soon replaced by an community dominated by diatoms which peaked in late January 1994, but which disappeared abruptly in February. Phytoplankton numbers first rose above winter levels (*circa* 10^4 cells L^{-1}) in late October, and increased slowly throughout November before increasing sharply due to an intense bloom dominated by cryptomonad A present on 7 December 1994 (maximum total cell abundance 1.1 x 10^8 cells L^{-1} at 2m). This bloom faded away in the following weeks, to be replaced by a bloom of diatoms, which exhibited two peaks, one in early January and the second in early February.

Figure 3.1. Seasonal cycle of phytoplankton at 10 m, O'Gorman Rocks, December 1993 - March 1995: (a) Cell abundances of 5 species or species groups; (b) The same data expressed as percentages of total phytoplankton abundance.

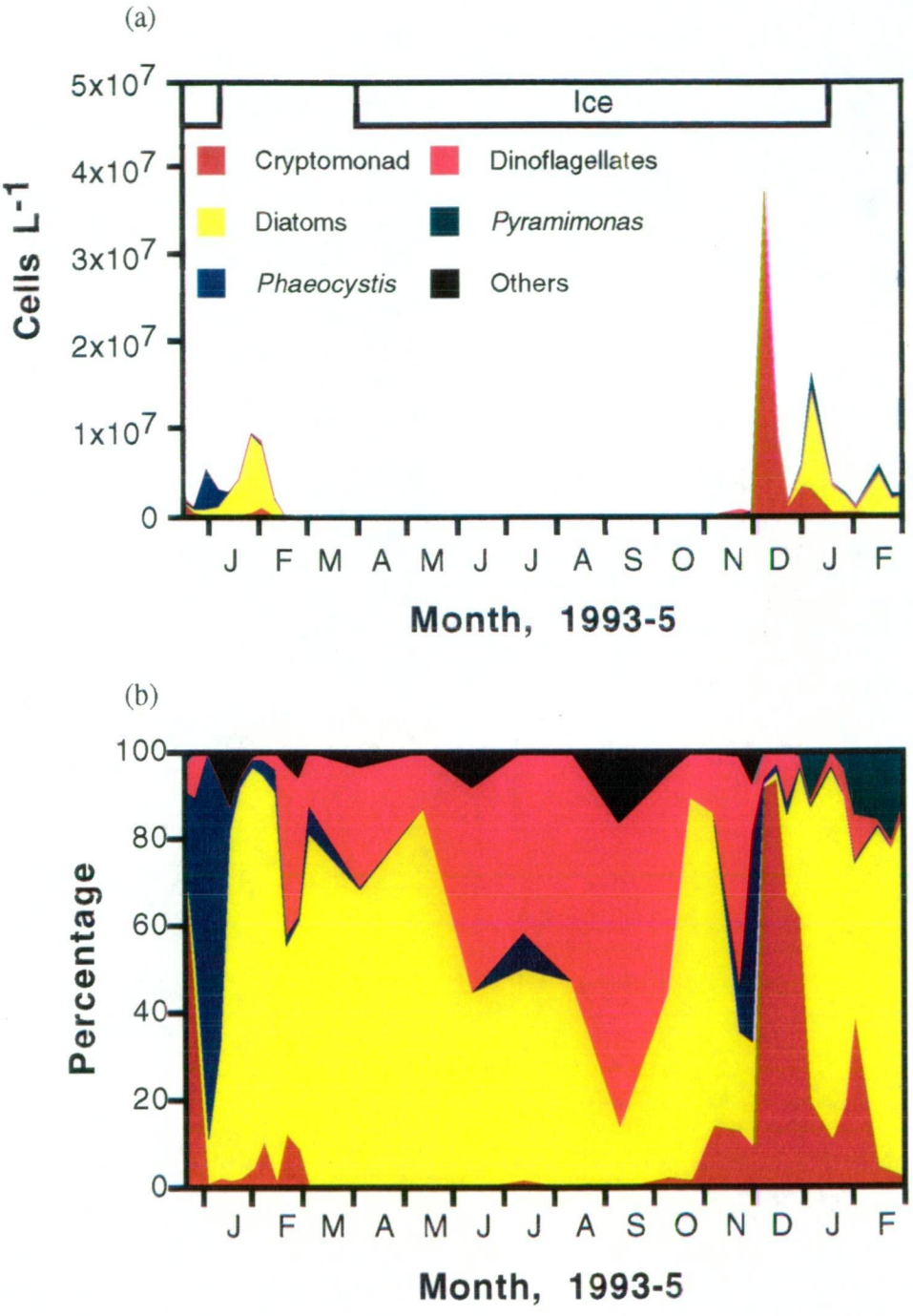

The end of the summer phytoplankton bloom in 1994 occurred in early to mid-February, but, in contrast, relatively high cell densities were still present on the last sampling date at the end of February 1995. Water clarity increased sharply in the week after the last sampling trip, indicating that the bloom had effectively ended.

When ice was present considerable stratification of the phytoplankton occurred, with much higher abundances in the water directly under the ice where irradiance was greater. In contrast, when the sampling site was ice free less stratification of the phytoplankton occurred, which reflected increased wind mixing in the water column as well as greater penetration of light.

3.2.1.1 Cryptomonad A

This small, undescribed flagellate (approximately 10 x 15 μm) was observed previously (but mis-identified as *Cryptomonas cryophila*) in a recent study in Ellis Fjord in the Vestfold Hills (McMinn and Hodgson, 1993), and could well occur elsewhere around the Antarctic continent, as cryptophytes have been recorded to be common in other Southern Ocean studies (Taylor and Lee, 1971, Jacques and Panouse 1991, Buma et al., 1992, Kopczynska, 1992). Another species of cryptophyte, *Geminigera cryophila* (Hill) (syn. *Cryptomonas cryophila* (Hill, 1991)) was observed on occasions during the present study, but was at no time numerically important.

The annual cycle of the abundance of cryptomonad A is shown in Figure 3.2. After the initial sampling date the abundance dropped as other species became dominant, though an increase in cell numbers occurred in late January 1994 at the time of peak phytoplankton productivity. Cryptomonad A was observed only occasionally throughout winter, but began to increase in abundance in late October. Cell numbers reached *circa* 10^5 cells L^{-1} by the end of November before the dramatic increase in abundance in early December, when cryptomonad A again became the dominant

Figure 3.2. Abundance of 5 species or groups of phytoplankton, O'Gorman Rocks, December 1993 - February 1995. The shaded area represents the range of cell abundances recorded. Note the logarithmic vertical scale.

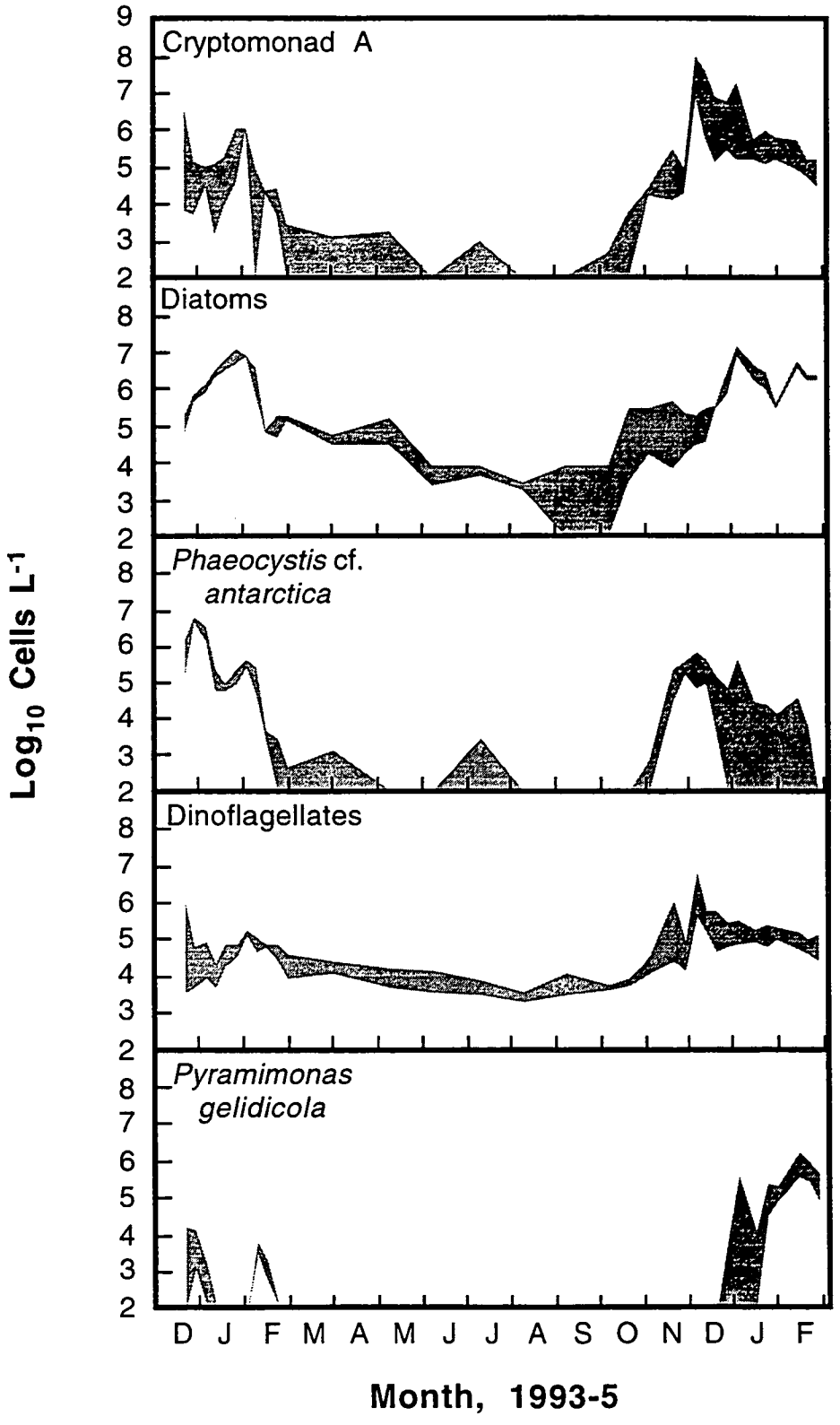

species. After this, the abundance of cryptomonad A dropped steadily for the rest of the summer, with the exception of a minor peak that occurred in late December - early January, again coincident with a maximum of phytoplankton abundance (Figure 3.1).

It is possible that the calculated cell numbers in the samples collected on 7 December 1994 did not reflect the true abundances of this species on this date. Cryptomonad A was observed in the laboratory to be highly phototactic, and it is possible that cells had migrated from nearby water into the shaft of light passing through the sampling hole between drilling of the hole and sample collection. The very high cell abundances recorded on this date must therefore treated with some caution. This point is further discussed in Chapter 4.

3.2.1.2 Diatoms

A wide variety of diatoms, ranging in length or diameter from smaller than 10 μm to over 300 μm, was observed during the study. Table 3.1 provides a list of the genera and species (with authorities) identified, though many more which were not positively identified were undoubtedly present. The range of species was similar to those recorded in other studies from the same area (Everitt and Thomas, 1986; Perrin et al., 1987; Davidson and Marchant, 1992a) as well as in other Antarctic studies (Krebs, 1983; Garrison et al., 1987; Kang and Fryxell, 1992).

The seasonal cycle of diatom abundance is shown in Figure 3.2. Abundances were relatively low initially, when cryptomonad A and then *Phaeocystis* cf. *antarctica* were dominant. The most common diatoms during this period were members of the genera *Fragilariopsis* and *Nitzschia.* In early January 1994, this consortium was replaced by the small (20 - 40 μm), centric species *Thalassiosira dichotomica*, which was the dominant diatom and phytoplankton species from mid-January 1994 until the end of the summer bloom in February (maximum abundance *circa* 10^7 cells L^{-1}).

Table 3.1. List of diatom species (with authorities) and genera observed during the study. Diatoms were identified after Priddle and Fryxell (1985) and Medlin and Priddle (1990).

Asteromphalus parvulus Karsten

Berkeleya rutilans (Trentephol) Cleve

Chaetoceros bulbosum (Ehrenberg) Heiden

Chaetoceros convolutum Castracane

Chaetoceros dichaeta Ehrenberg

Chaetoceros flexulosum Mangin

Chaetoceros neglectum Karsten

Chaetoceros neogracile van Landingham

Chaetoceros simplex Ostenfeld

Chaetoceros spp.

Cocconeis fasciolata (Ehrenberg) Brown

Corethron criophilum Castracane

Coscinodiscus bouvet Karsten

Dactyliosolen antarcticus Castracane

Dactyliosolen tenuijunctus Manguin

Entomoneis kjellmanii (Cleve) Thomas

Eucampia antarctica (Castracane) Mangin

Fragilariopsis cylindrus (Grun.) Krieger

Fragilariopsis curta Van Huerck

Fragilariopsis kerguelensis(O'Meara) Hustedt

Fragilariopsis spp.

Leptocylindrus sp.

Navicula glacei V.H.

Navicula spp.

Nitzschia angulata Hasle

Nitzschia lanceolata (Ehrenberg) Wm. Smith

Nitzschia seriata Cleve

Nitzschia spp.

Odontella weissflogii (Janisch) Grunow

Paralia sol (Ehrenberg) Crawford

Pleurosigma sp.

Porosira glacialis (Grunow) Jørgensen

Rhizosolenia alata Brightwell

Rhizosolenia hebetata (Hensen) Gran

Staurophora sp.

Thalassiosira antarctica Comber

Thalassiosira australis Peragallo

Thalassiosira dichotomica(Kozl.) Fryxell and Hasle

Thalassiosira gravida Cleve

Thalassiosira tumida (Janisch.) Hasle

Thalassiosira sp.

Thalassiothrix sp.

Trigonium arcticum (Brightwell) Cleve

During winter, a variety of species were present, though only at low densities. Diatom numbers began to rise in October 1994 with an increase in the abundance of *Entomoneis kjellmanii*, which peaked in late October and early November at *circa* 10^5 cells L^{-1}. From early December members of the *Fragilariopsis/Nitzschia* group were the dominant species, and were the most abundant phytoplankton group throughout January 1995. *Thalassiosira dichotomica* again became the dominant diatom and phytoplankton species in February, and remained so until the end of the study. The maximum cell abundance of this species in the 1994-5 summer was similar to that in the previous summer.

3.2.1.3 *Phaeocystis* cf. *antarctica*

Members of the genus *Phaeocystis* are characterised by involved life histories which include both single celled, motile, flagellated and non-motile colonial stages (Davidson and Marchant, 1992b). The latter stage consists of colonies of hundreds or thousands of cells, each 5 - 10 μm across, embedded in a matrix of polysaccharide up to 2 cm in diameter (Guillard and Hellebust, 1971; Janse et al., 1996). *Phaeocystis antarctica* (Medlin) was recently described from the Antarctic region (Medlin et al., 1994), where it commonly forms dense blooms (Bölter and Dawson, 1982; Garrison et al., 1987; Holm-Hansen et al., 1989; Davidson and Marchant 1992a). Previously, all occurrences of *Phaeocystis* in the Antarctic region, had been ascribed to the cosmopolitan species *Phaeocystis pouchetii* (Har.) Lager (Davidson and Marchant, 1992b), which is now considered to be confined to more northerly waters. The identity of the species observed in the present study could not be determined accurately, but is referred to in this thesis as *Phaeocystis* cf. *antarctica*, as it is likely that the species present was *Phaeocystis antarctica*.

Colonial stage *Phaeocystis* cf. *antarctica* was the numerically dominant phytoplankton species for a short period in late December 1993 - early January 1994, with cell

abundance peaking at nearly 10^7 cells L^{-1} (Figure 3.2). After the mid-January occasional large colonies were present, but more commonly individual, flagellated cells or small colonies of 4 to 8 cells were observed. Occasional flagellated cells were observed during winter, and, for a short period in November 1994, individual cells accounted for a significant percentage of the phytoplankton community (Figure 3.1b). Flagellated cells continued to be observed at intermediate abundances throughout December and the rest of the summer, but, in contrast to the previous summer, no colonies were observed. It is possible that a short bloom of the colonial phase of *Phaeocystis* cf. *antarctica* did occur which was missed by the sampling schedule, however no cells were observed in sediment trap samples (Chapter 5).

3.2.1.4 Dinoflagellates

A wide variety of dinoflagellates, including both heterotrophic and autotrophic species, was recorded. Genera represented included *Gymnodinium*, *Gyrodinium*, *Peridinium*, *Protoperidinium*, *Dinophysis* and *Amphidinium*. The sympagic gymnodimnoid dinoflagellate cyst described by Buck et al. (1992) was also observed regularly in the water column during the summers. In most cases, heterotrophic and autotrophic forms were not identified and counted separately in this study, and have been included as one group in this section. Heterotrophic dinoflagellates are not *sensu strictu* members of the phytoplankton community, but have been included here for the sake of simplicity.

Dinoflagellates were present throughout the year (Figure 3.2), and during winter made up a considerable percentage (up to 70 %) of the protists (Figure 3.1b). Cell abundance rose before other protists early in spring, probably as a response to the release of organic material from the ice (Chapter 5). Highest dinoflagellate abundance was recorded during the intense bloom of cryptomonad A on 7 December 1994, when a heterotrophic *Gymnodinium* species accounted for 6 - 8 % of the protists present. A similar consortium was observed during the 1992-3 summer (Gibson et al., 1997),

and again at the start of the present study in December 1993. Dinoflagellates were a minor but important members of the community throughout both summers.

3.2.1.5 *Pyramimonas gelidicola*

The prasinophyte *Pyramimonas gelidicola*, which is slightly larger than cryptomonad A., has been recorded in many studies from the Antarctic region as a reasonably significant member of the phytoplankton community (e.g. Davidson and Marchant, 1992a; McMinn and Hodgson, 1993; Kopczynska et al., 1995). This species was observed at low abundances throughout the 1993-4 summer (Figure 3.2), and was absent during the winter. Cell numbers were significantly higher from the end of December 1994 until the end of the study, when this species was a reasonably important member of the phytoplankton assemblage. Maximum cell counts (>1 x 10^6 cells L^{-1}) were recorded on the same dates as maxima in diatom abundance. *Pyramimonas gelidicola* was not present during the bloom of cryptomonad A early in the summer.

3.2.2 Chlorophyll *a*

The seasonal cycle of cell abundances shown in Figures 3.1 and 3.2 does not necessarily reflect the cycle in total phytoplankton biomass, as different species can have markedly dissimilar volumes and organic carbon contents. The concentration of the photosynthetic pigment chl *a* provides a measure of the intensity of phytoplankton blooms that is independent of the size and numbers of cells present. The seasonal cycle of integrated chl *a* (from the surface to the sediment at 23 m) is shown in Figure 3.3. The figure shows that during the 1993-4 summer, a single major peak in the concentration of chl *a* occurred in late January 1994, after which the concentration dropped rapidly to low winter levels (less than 5 mg m^{-2}). No major peak in chl *a* occurred in the month prior to the beginning of sampling in December 1993 (J. Grey,

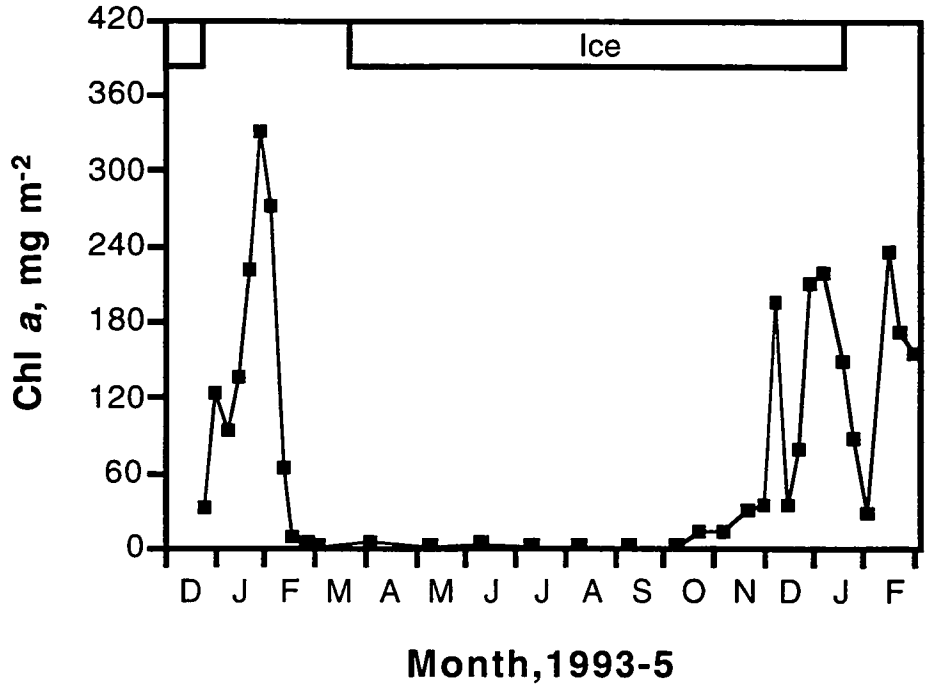

Figure 3.3. Integrated chl *a* (to 23 m), O'Gorman Rocks, December 1993 - February 1995.

personal communication). In contrast, three peaks of near equal intensity were observed during the 1994-5 summer, occurring in early in December and January and in mid-February, interspersed with periods of relatively low chl *a*. The peaks, however, were less intense that the single 1993-4 maximum.

3.3 Discussion

3.3.1 Comparison of the Seasonal Cycle to Previous Studies

The seasonal cycle of phytoplankton observed at O'Gorman Rocks has many similarities to those recorded in previous studies in the inshore waters of the Vestfold Hills. During the 1982-3 summer, *Entomoneis kjellmanii* was the dominant species in November, followed by *Phaeocystis* sp. in December (Perrin et al., 1987). The diatom *Nitzschia lanceolata* (syn. *Nitzschia closterium*) bloomed dramatically in January and February, reaching cell densities of 5.8 x 10^7 cells L^{-1}. Chl *a* was not measured at the

height of this bloom, but it probably approached or exceeded the maximum concentrations recorded in the present study. Limited data from the 1981-2 summer were also presented by Perrin et al. (1987), which indicated that *Nitzschia lanceolata* was numerically dominant in January 1982, but at only 2.5 % of the abundance recorded in January 1983. The frequency of sampling in this study was only once per month, and it is therefore likely that some peaks and other details of the phytoplankton cycle were missed.

Davidson and Marchant (1992a) investigated the phytoplankton during a more intensive study in the 1988-9 summer, and found a similar cycle, in which *Entomoneis kjellmanii* was again dominant in November, and was followed by colonial stage *Phaeocystis* sp., which peaked in abundance at *circa* 6 x 10^7 cells L^{-1} in late December. This bloom was succeeded by a variety of diatoms, mainly species of *Nitzschia*, in January.

From the results of these studies, Davidson and Marchant (1992a) concluded that the cycle of phytoplankton in the inshore waters of the Vestfold Hills was consistent and predictable. However, the results from the present study, as well as data from the 1992-3 summer (Gibson et al., 1997) indicate that greater interannual variation occurs than previously recognised.

Cryptomonad A was an important member of the phytoplankton community at the O'Gorman Rocks site during the 1993-4 and 1994-5 summers, being numerically dominant for long periods and always present at significant abundances. Remarkably, this species was not observed during the previous studies in the area (Perrin et al., 1987; Davidson and Marchant, 1992a; R. Perrin, A. Davidson, personal communications). Chemical evidence for the occurrence of cryptomonads was, however, recorded during the study of the lipid chemistry of particulate organic matter undertaken during summers between 1988 and 1993 (Skerratt et al., 1995). Why the

earlier studies failed to detect cryptomonads is uncertain, but the conclusion must be drawn that this species was absent, or present only at low abundance, in those summers.

The abundance of *Phaeocystis* cf. *antarctica* also exhibited considerable interannual variation. Colonies of *Phaeocystis* cf. *antarctica* were dominant for a short period at the end of December and early January during the 1993-4 summer and at similar times in earlier studies (Perrin et al., 1987; Gibson et al., 1990; Davidson and Marchant, 1992a), but were completely absent during the 1994-5 summer. Significant interannual variation in the intensity of the blooms of *Phaeocystis* was also reported by Skerratt et al. (1995), indicating that this species does not play an important role in the phytoplankton assemblage in all years.

The species of diatoms present also showed considerable contrasts between years and studies. The dominant diatom species during late summer in the present study was *Thalassiosira dichotomica*, which had not been recorded as abundant for any period of the earlier studies. The *Fragilariopsis/Nitzschia* community appeared irregularly; in 1982-3 it was dominant throughout January and February, but in 1988-9 only in January. At the O'Gorman Rock site the community appeared to be present at divers times, controlled in part by the presence of other major blooms. For example, in 1994-5 it bloomed during the period in early January when *Phaeocystis* dominated in previous years, but which in that summer was absent.

The biomass of phytoplankton, as reflected by the concentration of the proxy chl *a*, also differed significantly from year to year. The maximum integrated chl *a* concentration during the major peak of the 1993-4 summer was approximately 560 mg m^{-2}, which contrasted with 1994-5, when three major peaks, the highest of which was 390 mg m^{-2}, were observed. In contrast, the highest concentration of chl *a* at the same site during the 1992-3 summer was only 70 mg m^{-2} (Gibson et al., 1997). Although it

is difficult to compare this data directly with earlier figures (Perrin et al. 1987; McTaggart, 1993; F. Scott, personal communication), it appears that considerable variation in the maximum summer biomass occurs regularly at the site. Skerratt et al. (1995) came to the same conclusion in their study, as the amount of particulate lipids, another indicator of biomass, showed marked interannual variation.

3.3.2 Factors Contributing to Variation in the Phytoplankton Community

It is apparent from the results of this study, especially when compared to previous studies, that considerable interannual variations in both phytoplankton biomass and speciation occur in the inshore waters of the Vestfold Hills.

The phytoplankton biomass present will be a balance of primary production and processes which remove organic carbon from the water column, such as remineralisation by bacteria and heterotrophic protists, ingestion by metazoan zooplankton and higher animals, and sedimentation. Thus, no particular relationship between the amount of organic carbon production and measured phytoplankton biomass would be expected, and apparent variation in biomass could be more a change in the magnitude of the removal terms rather than in production. A better measure of net organic matter production can be derived from reductions in the concentrations of nutrients in the water column. For example, if organic matter production during the 1992-3 summer (when maximum integrated chl *a* was much lower than in 1993-4 and 1994-5) was considerably lower than in the subsequent summers, it would be expected that the concentrations of nutrients would have been significantly higher (assuming similar nutrient concentrations at the beginning of summer). In fact, the reductions in the concentrations for the three summers were similar (Chapter 4; Gibson et al., 1997), indicating that the low chl *a* in 1992-3 was more the result of increased removal of organic matter rather than low productivity. A true estimate of the

interannual variation in organic matter production in the inshore waters near the Vestfold Hills has yet to be obtained.

Variations in phytoplankton speciation stem to some extent from the life cycles of the species. For example, *Entomoneis kjellmanii* probably overwinters in the sea ice, as it appears regularly in spring and always in the same environment. Many other diatoms species also overwinter either in the ice or as cysts in the sediment, and presumably in summer provide relatively regular input into the phytoplankton community. *Phaeocystis* cf. *antarctica*, in contrast, is probably advected into the area from further north rather then being seeded from the ice or the sediment. This conclusion stems in part from its absence from the phytoplankton in much of Ellis Fjord (McMinn and Hodgson, 1993; Chapter 7), which in general is similar to that outside the fjord. *Phaeocystis* cf. *antarctica* occurs only near the entrance of the fjord, suggesting that cells of this species inside the fjord have to be first transported through the narrow entrance for a bloom to develop. Cryptomonad A forms strong blooms both inside and outside the fjord, and appears to be present throughout the year. Thus, the blooms that develop offshore from the Vestfold Hills will depend, in part, on the balance between local species, which probably tend to dominate early in summer, and advection of other species from elsewhere.

Advection of water masses with different chemical and biological characteristics plays an important role in controlling the ecosystem at O'Gorman Rocks. Although detailed studies of the currents in the area of the sampling site have not been carried out (Chapter 2), the normal situation appears to be either a near laminar flow of water of similar history along the coast, or effective entrapment of a body of water in the area with little import and export occurring. Periods of strong winds break up these patterns by disrupting the surface flows, and bring new water with different chemical and biological characteristics into the area from deeper in the water column or further offshore.

A particularly good example of the effects of advection was observed late in the study in January and February 1994. After ice break out in early January, the concentrations of chl *a* and dissolved oxygen (DO) dropped sharply (Chapter 4), indicating the collapse of the phytoplankton bloom and considerable remineralisation of organic material in the O'Gorman Rocks area. A period of strong winds occurred late in the month, and by the next sampling trip the situation had altered considerably. Chl *a* and DO had increased again, and the diatom *Thalassiosira dichotomica*, which had not previously been recorded during the summer, dominated the phytoplankton. That the water was different to that previously in the area was suggested by an increase in water temperature (Chapter 2) and by the relationship between silicate and nitrate (Figure 3.4), which shows that the water in February was much higher in silicate (relative to nitrate) than in January. It appeared that the strong winds resulted in the transport of a new water mass into the area, in which a diatom bloom was either already present or which subsequently developed.

Advection of new water to the O'Gorman Rocks area will be a stochastic event. Major wind events play an important role, and sea ice will also have an influence, as presence of ice will protect the water from the wind, and also induce drag and reduce current flow. Thus, the effect of advection on the speciation and biomass in the inshore region of the Vestfold Hills will differ from year to year, as the timing of periods of strong wind and sea ice break out are not consistent. The interannual variation evident in the abundance of *Phaeocystis* cf. *antarctica* probably reflects changes in the advection of this species into the inshore waters.

Finally, longer term environmental changes could also induce interannual variation especially in phytoplankton speciation . The level of UV-B radiation during spring has increased in recent years as a result of the Antarctic Ozone Hole (Lubin et al., 1989). Many reports have appeared detailing the effect of enhanced UV-B radiation on the phytoplankton species composition, and it has been shown recently that exposure to

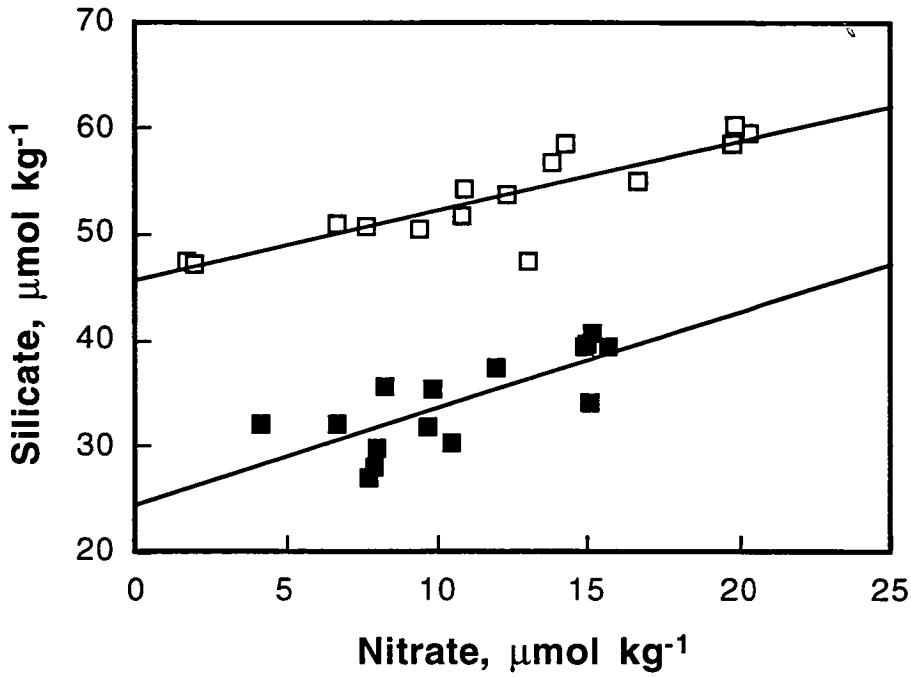

Figure 3.4. The relationship between nitrate and silicate concentrations (normalised to S = 35 psu) in January (closed symbols) and February (open symbols), 1995.

natural UV-B levels changes the species composition of Antarctic phytoplankton in mixed culture (Davidson et al. 1996). It is possible (though there is no supporting evidence) that the apparent increase in the abundance of cryptomonad A has been a response to the increase in UV-B, which could have increased its competitiveness relative to other species.

In summary, it appears that variation in phytoplankton biomass and speciation is the result of a complex suite of physical and biological factors. Many of the factors, such as the advection of new water masses into the area, rely on essentially random events, such as periods of strong winds and removal of the ice cover. Thus, it is unlikely that the succession of phytoplankton will be the same every summer, and, similarly, that some variation in phytoplankton biomass would be expected.

3.3.3 What Effect Could Phytoplankton Variability Have on Carbon Export?

From the above discussion it is evident that considerable interannual variation takes place in the phytoplankton assemblage that occurs in the inshore marine environment of the Vestfold Hills. The question then is: Will this variability have any effect on the production of organic carbon in inshore waters or the transport of carbon to the sediment or out of the euphotic zone?

The results discussed in the next chapter indicate that the species of phytoplankton present has little effect on the ratio of the uptake of DIC to phosphate and nitrate, as these nutrients were taken up by the phytoplankton community in an essentially constant ratio throughout the study. However, differences in the assimilation ratio between species undoubtedly occur. The most obvious case is that diatoms take up silicate to form their frustules, whereas flagellates, such as cryptomonads and *Phaeocystis*, do not have a silicate requirement.

The occurrence of intense blooms of *Phaeocystis* cf. *antarctica* could alter the relationship between DIC and the nutrients. All species of *Phaeocystis* excrete large amounts of organic material in the colonial stage which forms the matrix in which the individual cells of the colony are embedded. The C:N mole ratio in this material, which consists largely of polysaccharides (Guillard and Hellebust, 1971; Janse et al., 1996), has been found in some studies to be similar to that of other non-gelatinous phytoplankton (Verity et al., 1988), but in others to be much higher (Hickel, 1984; Billen and Fontigny, 1987). This variation possibly reflects the stage of colony formation; low nitrogen carbohydrate is thought to be produced in mature colonies as a carbon source for catabolism in the dark (Veldhuis et al., 1986). Therefore, during intense *Phaeocystis* blooms, especially during periods of near 24 hr light, carbon production could outstrip that predicted from the uptake of nitrogen and phosphate,

and could therefore lead to greater uptake of DIC than for other phytoplankton species for a given amount of nutrient.

Some evidence for this process was obtained by Davidson and Marchant (1992a), who reported very high organic carbon concentrations (greater than 100 mg L^{-1}, which is equivalent to over 8000 μmol kg^{-1}) during a *Phaeocystis* bloom near Davis Station. This concentration could not have been produced if the organic material had a C:N mole ratio close to the Redfield ratio (maximum predicted concentration of organic carbon: approximately 180 μmol kg^{-1}). If these organic carbon concentrations were in fact correct, decoupling of the uptake of DIC, and nitrate and phosphate must have occurred on a massive scale. Thus, if a shift in the phytoplankton speciation to *Phaeocystis* occurred, carbon uptake could be dramatically increased.

A second influence on the carbon cycle comes from propensity of cells to fall out of the euphotic zone or to the sediment. Sedimentation of particulate organic material (POM) will effectively remove carbon from the surface water, and will ultimately increase the concentrations of DIC and dissolved organic carbon (DOC) in deeper water, or if the POM reaches the sediment and is not remineralised, add to the carbon buried in this long term sink. Communities dominated by species with high sedimentation rates, either directly or indirectly in zooplankton faecal pellets, are often termed export communities, as carbon is exported out of the euphotic zone during sedimentation.

Diatoms and colonies of *Phaeocystis* are not motile, and cannot actively adjust their positions in the water column. Therefore, they are liable to sedimentation, transferring large amounts of organic carbon out of the water in which it was produced. Mass sedimentation of *Phaeocystis* colonies has been observed in the Barents Sea (Wassmann et al., 1991), and it has also been suggested that sedimentation of *Phaeocystis* was responsible for considerable transfer of organic carbon to deeper

water in the Greenland Sea (Smith et al., 1991; Smith, 1993). Mass sedimentation of *Phaeocystis* has not been reported in the Antarctic region, but considering the high cell densities that have been reported in some studies (e.g. Davidson and Marchant, 1992a), it would be expected to occur.

Diatoms blooms are also likely to undergo mass sedimentation, though another important mechanism - sedimentation in faecal pellets of copepods and other zooplankton - is probably more important. The importance of diatom sedimentation in the Southern Ocean is reflected by the diatomaceous ooze, made up essentially of siliceous diatom frustules, that covers much of the ocean floor in the Antarctic region (De Master, 1981; Ledford-Hoffmann et al., 1986).

If phytoplankton species not prone to sedimentation, such as the flagellate cryptomonad A, come to dominate carbon production, less carbon would be expected to be exported from the surface waters, as this species does not appear to actively undergo sedimentation (Chapter 5). The reduced rate of sedimentation reflects the ability of flagellates to maintain to some extent their position in the water column and the lower intrinsic sedimentation rates of small cells compared to larger diatoms (Stoke's Law). The carbon in flagellate cells is more likely to be released during grazing by zooplankton or senescence and remineralised in the upper water, resulting in a recycling-based community (though some carbon could still be lost from the surface in zooplankton faecal pellets). Development of such a community will probably lead to reduced transport of carbon to the sediment than for an export community for the same amount of primary production, though a recent study by Rivkin et al. (1996) suggested that the magnitude of export of OC could not be predicted solely from food web structure.

Thus a shift away from diatoms and *Phaeocystis* to non-colonial flagellates such as cryptomonads could lead to a reduction in the production of organic material per unit

nutrient, as well as a decrease in the amount of organic carbon transferred to the sediment or out of the euphotic zone. Further studies will have to be undertaken at the O'Gorman Rocks site to determine if the apparent shift in phytoplankton speciation observed in this study is (semi-)permanent, and also to determine the effect of this putative shift on the transport of carbon to deeper waters and to the sediment for burial.

3.4 Conclusions

The species making up the phytoplankton community at the O'Gorman Rocks site exhibited considerable variation between the two summers of the study, and the phytoplankton succession appeared to have few similarities with any previously recorded at the site. Of the important species, cryptomonad A was dominant for extended periods even though it had not been recorded at the site in studies during the 1980s. *Phaeocystis* cf. *antarctica* was absent during the second summer, and diatoms present showed little uniformity except for the regular bloom of *Entomoneis kjellmanii* in spring. The variation will have an affect on both the uptake of DIC and nutrients from the water column (Chapter 4), and sedimentation of POC out of the euphotic zone (Chapter 5).

The variation in the community can be ascribed to changes in the biological and chemical environment, particularly to the advection of new water masses into the area as a result of periods of strong winds and the presence of sea ice. Shifts in the dominant phytoplankton species could have some effect on the transport of carbon out of the euphotic zone, as particular species have different sedimentation rates. Formation of a flagellate based community could increase the recycling of nutrients and carbon at the expense of export to the sediment or to deep water.

CHAPTER 4

ORGANIC MATTER PRODUCTION AND ATMOSPHERIC CO_2 UPTAKE AT O'GORMAN ROCKS

4.1 Introduction

This chapter describes the seasonal cycles at of many parameters related to the photosynthetic production of organic material the O'Gorman Rocks site, including the concentrations of DIC, POC, DOC, chl *a*, nutrients (nitrate, phosphate and silicate) and DO, pH, alkalinity, fCO_2, and the $\delta^{13}C$ of various carbon pools. From these parameters the amount of OC production is calculated, as well as the uptake of CO_2 by the ocean that occurs in the area.

4.2 Results

All data for this chapter are presented in tables in Appendix C.

4.2.1 Dissolved Inorganic Carbon

Figure 4.1 shows plots of the concentration of DIC, which was typically in the range 2000 - 2250 μmol kg^{-1}. Concentrations at the lower end of the range were recorded between November and March. Extremely low DIC concentrations (less than 2000 μmol kg^{-1}, minimum 1300 μmol kg^{-1}) were measured in samples collected from directly under the sea ice on a few occasions during December in both 1993 and 1994. DIC concentrations when the sampling site was ice-free were nearly always above 2000 μmol kg^{-1}, and no very low concentrations were recorded. Figure 4.1b shows

the cycle of DIC concentration over a narrower concentration range, which highlights troughs in DIC concentration that occurred both under the sea ice, and, to a lesser extent, in late January 1994 and mid February 1995 during ice-free conditions.

4.2.2 Dissolved Organic Carbon

The concentration of DOC was not measured throughout the entire study period due to the unavailability of the required gases to run the DOC analyser for extended periods, and the failure of the muffle furnace in June 1994 which precluded thorough pre-cleaning of sample bottles until a replacement was shipped from Australia. The results

Figure 4.1. DIC (μmol kg^{-1}), O'Gorman Rocks site, December 1993 - February 1995: (a) all data; (b) the same data over a smaller concentration range. The symbols used in this and all similar plots in this chapter are: 0 or 2 m, □; 5 m, ◇; 10 m, ○; 15 m, △ and 20 m, ✣. The lighter shading shows the minimum value for the parameter on the sampling date, and the darker shading the range of the data. The periods during which ice covered the sampling site are also indicated.

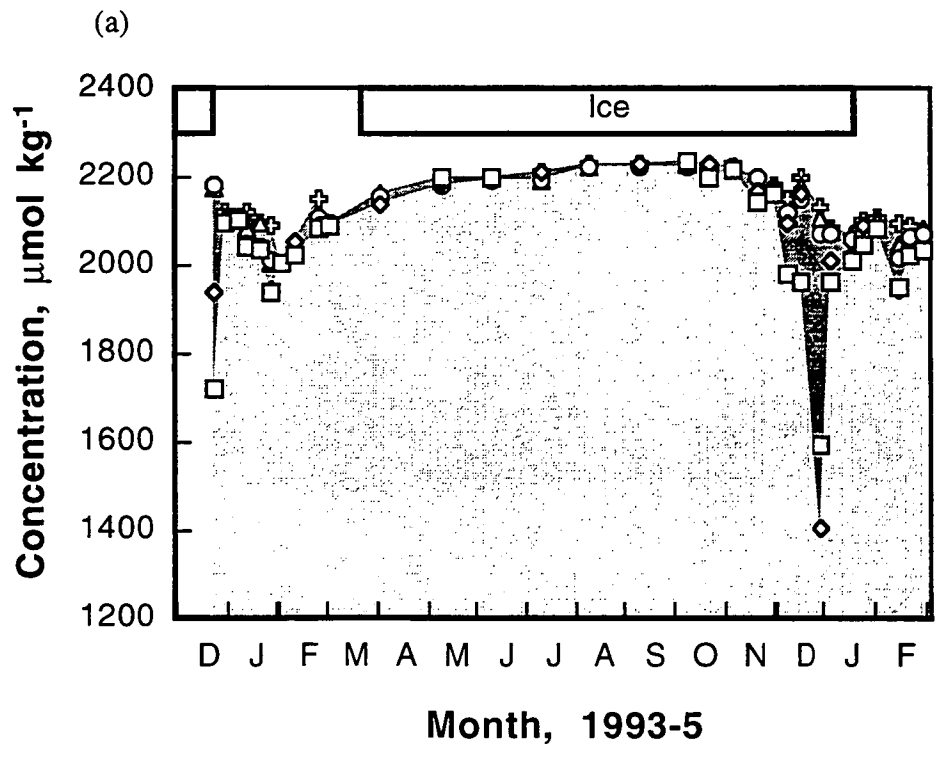

(b)

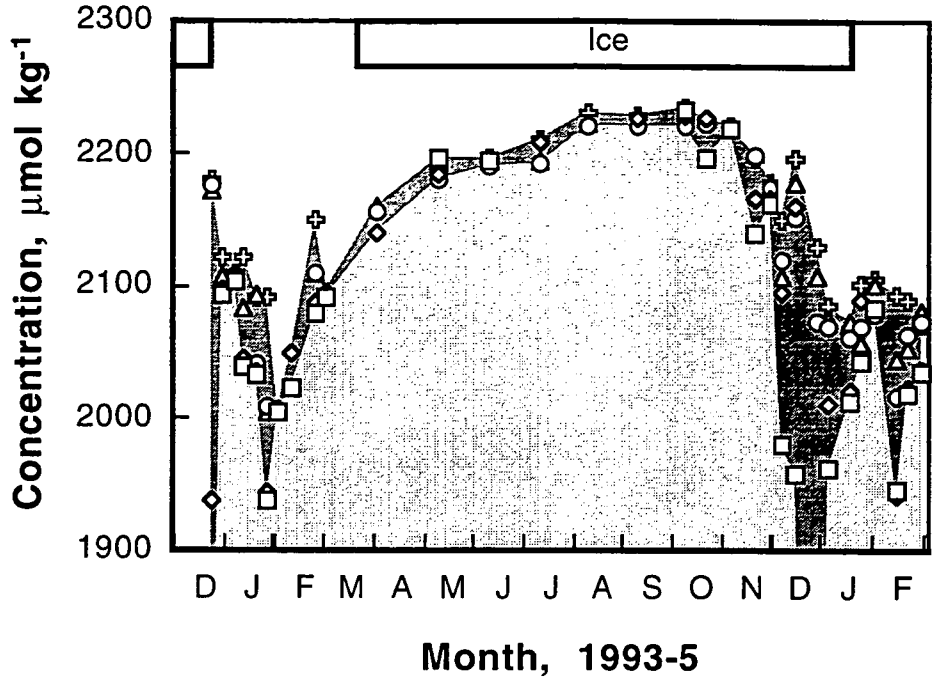

Figure 4.1. Continued.

from the period during which data were obtained is shown in Figure 4.2. The concentration of DOC ranged from a minimum of 53 µmol kg^{-1} early in November to 160 µmol kg^{-1} on 7 December 1994 during an intense phytoplankton bloom (Chapter 3).

4.2.3 Particulate Organic Carbon

Unlike DOC, the concentration of POC (Figure 4.3) was barely above the detection limit throughout November, when chl *a* concentrations were also very low. A large increase in POC occurred in samples collected on 7 December 1994, when concentrations of 560 µmol kg^{-1} at 2 m, 345 µmol kg^{-1} at 5 m and 160 µmol kg^{-1} at 10 m were recorded. These data have been plotted at the highest level (120 µmol kg^{-1}) in Figure 4.3 in order to make more detail apparent at lower concentrations. POC concentrations were generally lower than DOC concentrations throughout the study, with the exception of 7 December 1994.

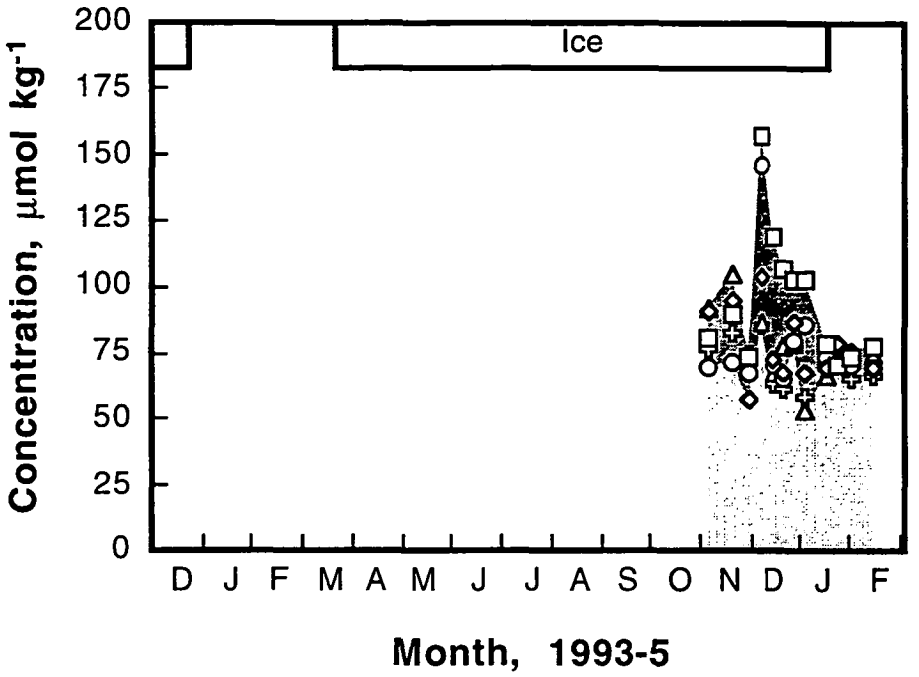

Figure 4.2. DOC (µmol kg^{-1}), O'Gorman Rocks site, November 1994 - February 1995.

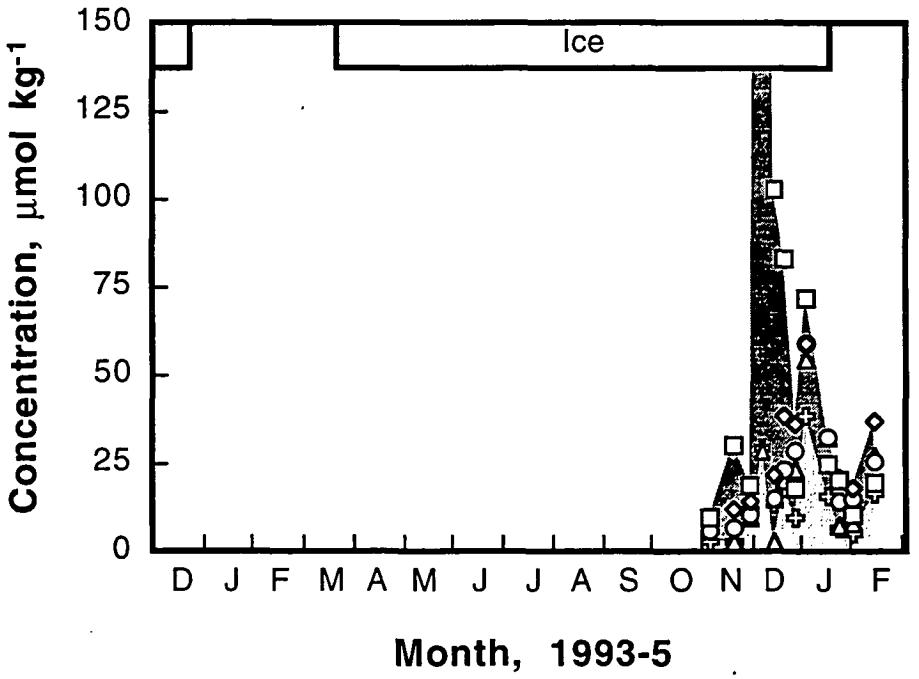

Figure 4.3. POC (µmol kg^{-1}), O'Gorman Rocks site, November 1994 - February 1995. Concentrations greater than 150 µmol kg^{-1} occurred in early December, and are detailed in the text.

4.2.4 Carbon Isotope Ratios

The seasonal cycle of $\delta^{13}C_{DIC}$ at 10 m is shown in Figure 4.4. Except for a period in August and September, $\delta^{13}C$ during winter was between 0.8 and 1.1 ‰, but began to rise above these levels in November. Maximum $\delta^{13}C_{DIC}$ was recorded between the end of December and February. The $\delta^{13}C$ of suspended particulate organic material was not measured, but the isotopic ratio of carbon in material caught in sediment traps at the site was between -24 ‰ and-20 ‰ for most of the year except for a short period in September - November, when much higher $\delta^{13}C$ (maximum -13 ‰) was recorded (this data is presented and discussed in more detail in Chapter 5).

4.2.5 pH

All pHs plotted and discussed in this thesis are on the 'free hydrogen' scale (pH_f). See

Figure 4.4. $\delta^{13}C_{DIC}$ (‰) at 10 m, O'Gorman Rocks site, March 1995 - February 1995.

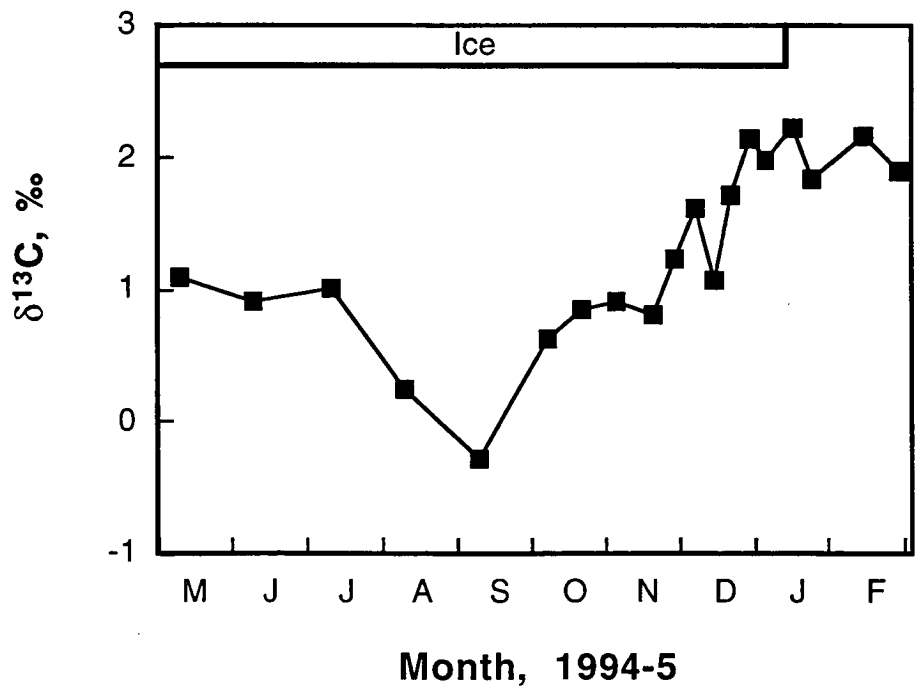

Appendix A for more discussion of pH measurement and scales. A contour plot of pH_f measured at 25 °C is shown in Figure 4.5. Throughout winter, when little biological activity was occurring, pH_f was between 7.6 and 7.7. Much higher values (>7.9) were recorded during the summer periods, with the highest pH_f, 8.29, being recorded in late December 1994 just prior to the break out of the fast ice. pH_f after ice break out was generally lower than when ice was present.

4.2.6 Chlorophyll *a*

Chl *a* concentrations (Figure 4.6) were above winter background levels (less than 0.15 mg m^{-3}) between the middle of November and the end of February. During the 1993-4 summer there was a single broad peak in chl *a*, which lasted from early January until the middle of February, and which was centred on late January (maximum concentration: 17.6 mg m^{-3}, 26 January 1994). During the 1994-5 summer, in contrast, three shorter but as intense peaks occurred (maxima: 23.7 mg m^{-3}, 7

Figure 4.5. pH, O'Gorman Rocks site, December 1993 - February 1995.

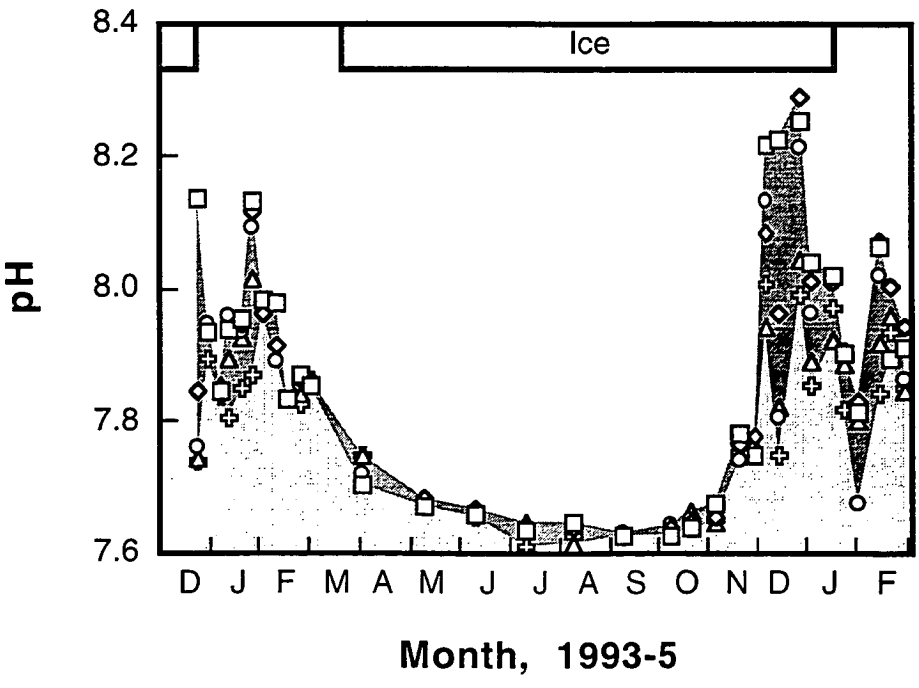

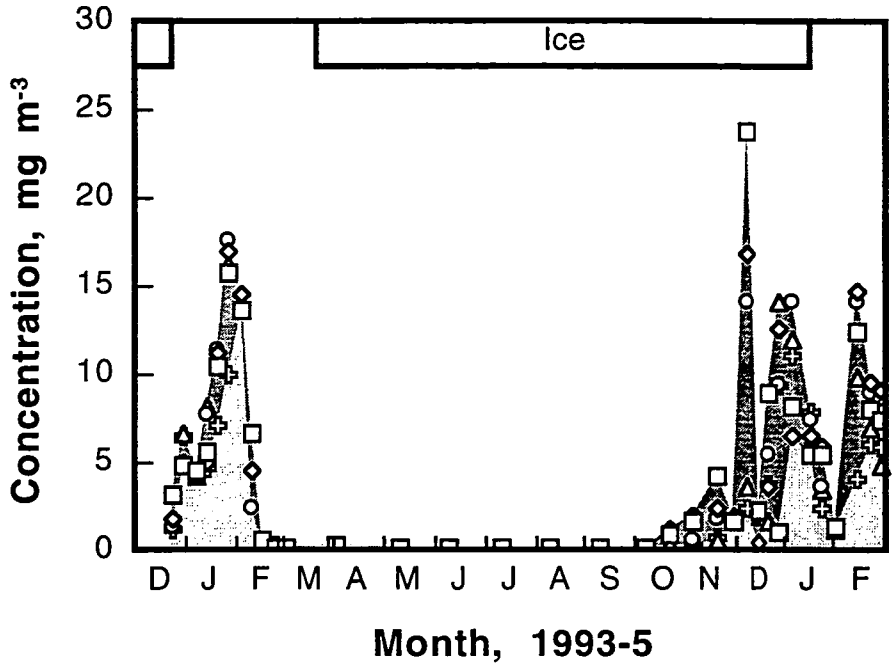

Figure 4.6. Chl *a* (mg m^{-3}), O'Gorman Rocks, December 1993 - February 1995.

December 1994; 14.1 mg m^{-3}, 4 January 1994; 14.7 mg m^{-3}, 13 February 1995), which were interspersed by periods of relatively low chl *a* (less than 3 mg m^{-3}). Integrated chl a (mg m^{-2}) at O'Gorman Rocks is shown in Figure 3.3.

4.2.7 Dissolved Oxygen

DO concentrations (Figure 4.7) were nearly constant from May to early November at *circa* 320 µmol kg^{-1}, except in September, when significantly lower concentrations (*circa* 300 µmol kg^{-1}) were measured. Oxygen concentrations were far higher during the summer periods, especially when the fast ice was still present. The highest concentrations (up to 540 µmol kg^{-1} under ice, and 465 µmol kg^{-1} during periods of open water) were recorded on the same dates as maximum chl *a* concentrations. The lowest concentrations of DO, less than 300 µmol kg^{-1}, were recorded in late February 1994 after the end of a phytoplankton bloom and before the reformation of an ice cover.

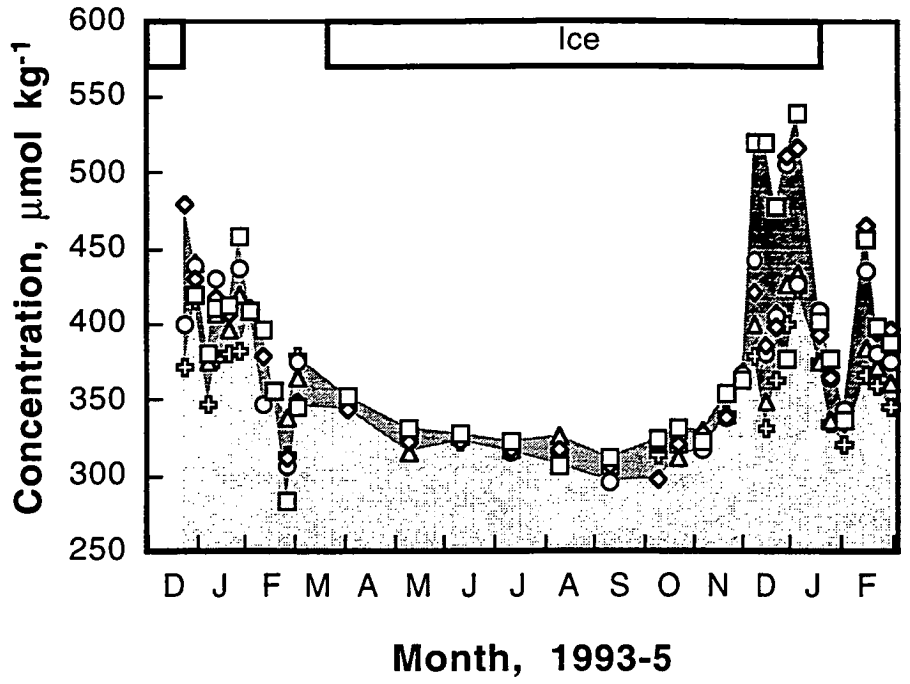

Figure 4.7. Dissolved oxygen (µmol kg^{-1}), O'Gorman Rocks site, December 1993 - February 1995.

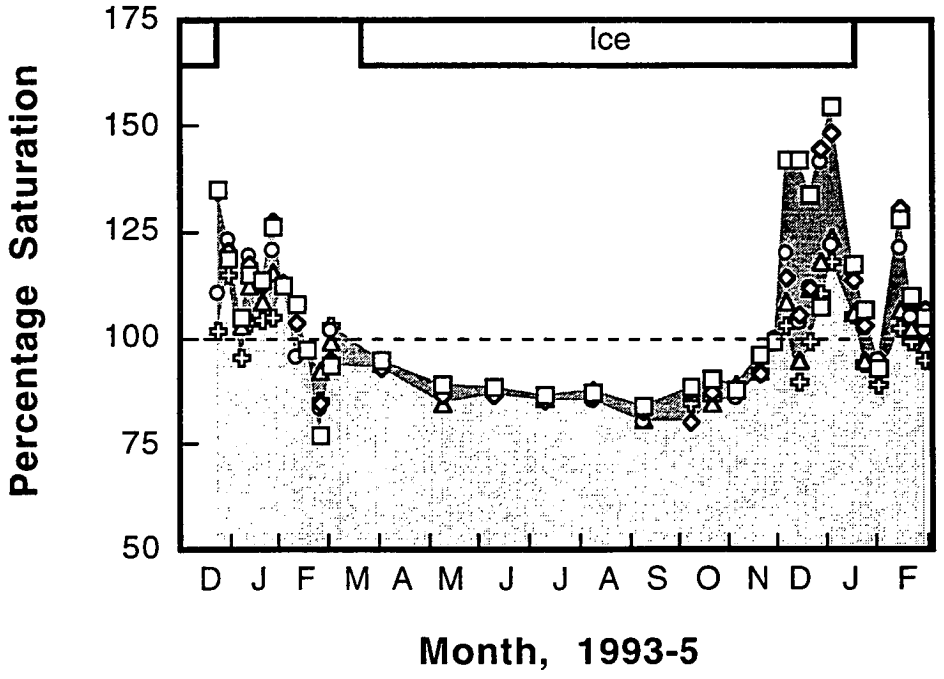

Figure 4.8. Dissolved oxygen saturation (%), O'Gorman Rocks site, December 1993 - February 1995. The dashed line indicates saturation .

The DO concentrations indicate that the gas was present at only 80 - 85 % saturation throughout the water column from April to November (Figure 4.8). During the summers, in contrast, oxygen saturation reached 150 % prior to the break out of the fast ice, and was consistently higher than 100 %.

4.2.8 Nutrients

Contour plots of the concentrations of the nutrients nitrate, phosphate and silicate are presented in Figures 4.9 to 4.11 respectively. 'Nitrate' here refers to the sum of the concentrations of nitrate and nitrite, as the method of analysis did not discriminate between these species (Appendix A).

The concentrations of the nutrients exhibited similar seasonal cycles throughout the study, generally increasing during winter to maxima in September - October and

Figure 4.9. Nitrate (μmol kg^{-1}), O'Gorman Rock site, December 1993 - February 1995.

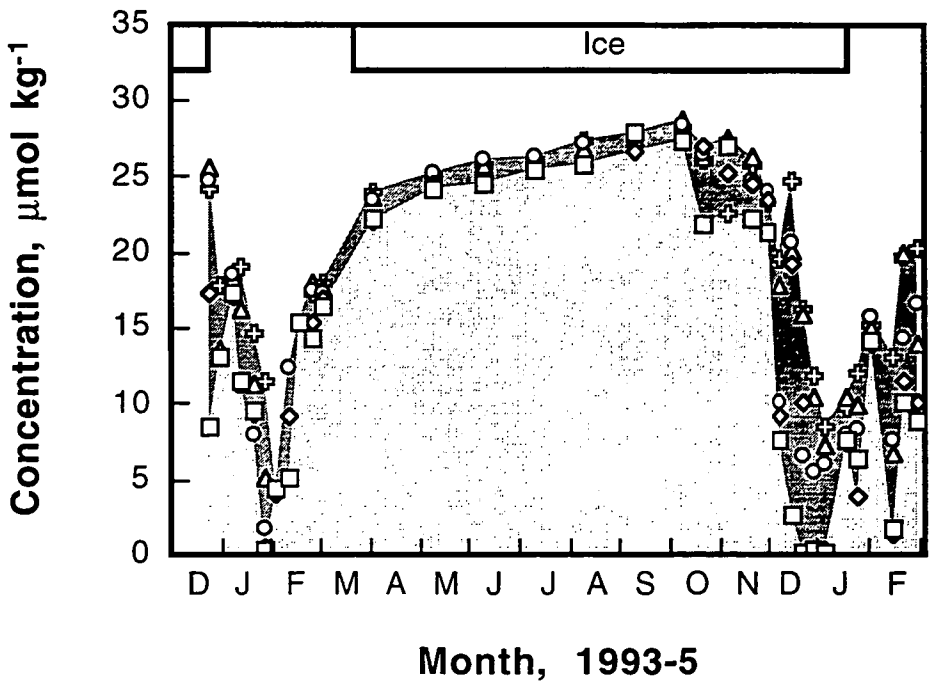

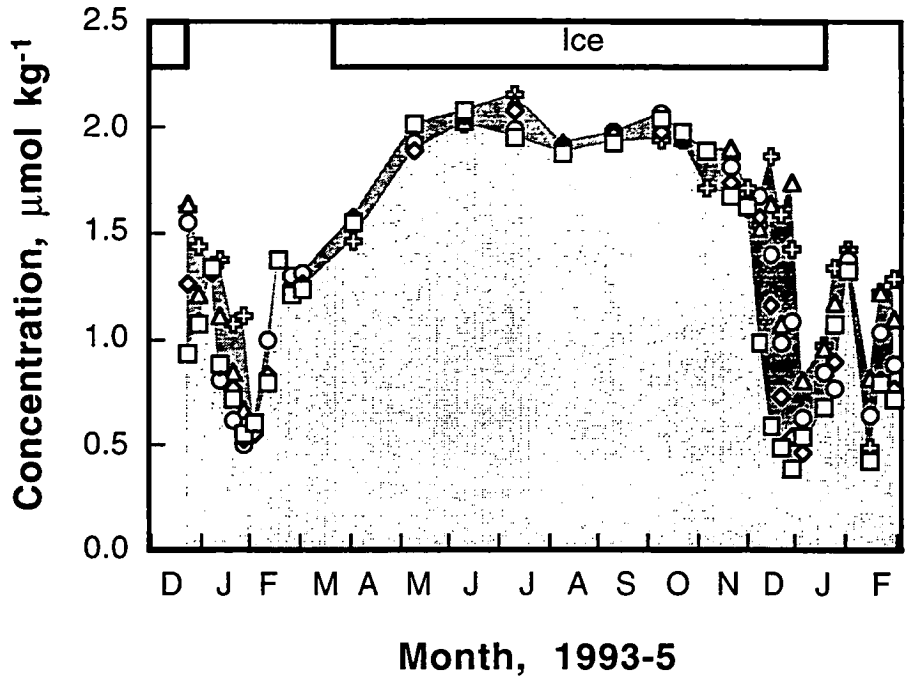

Figure 4.10. Phosphate (µmol kg^{-1}), O'Gorman Rocks site, December 1993 - February 1995.

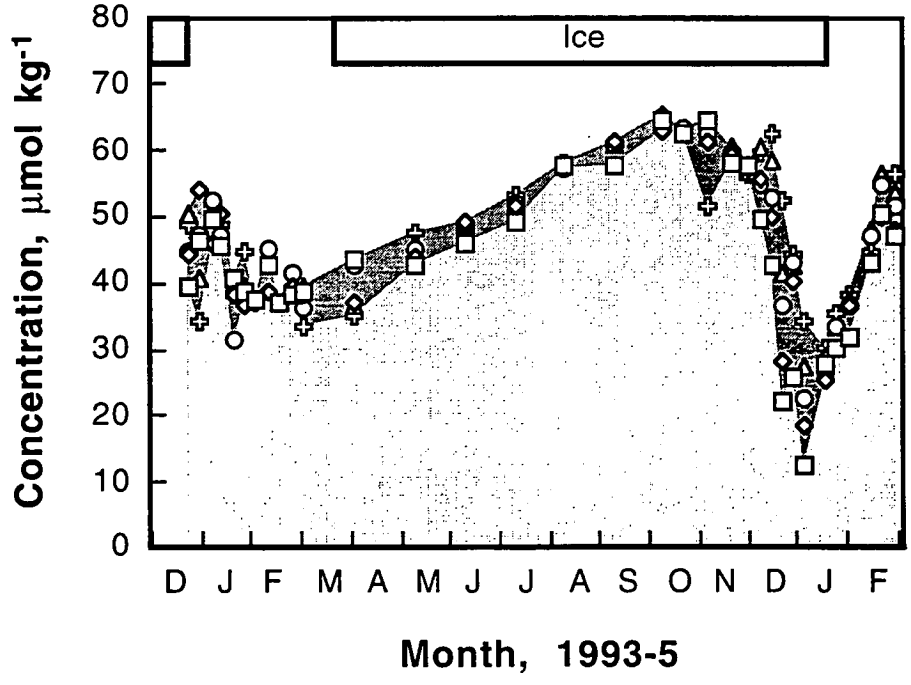

Figure 4.11. Silicate (µmol kg^{-1}), O'Gorman Rocks site, December 1993 - February 1995.

falling from November to minima in January. Closer inspection, however, revealed differences between the species. For example, at the end of the 1993-4 summer the concentration of silicate began to increase well after those of nitrate and phosphate. The concentration of phosphate, on the other hand, increased rapidly during the same period to a maximum in June and July before falling slightly in August. A second peak in the concentration of phosphate occurred in early October.

Lowest nutrient concentrations occurred in the summer months, usually during periods of maximum chl *a* and minimum DIC. Nitrate was reduced to the greatest extent relative to the late winter maxima, with concentrations only slightly above the detection limit (0.05 μmol kg^{-1}) present directly under the ice or at the surface on a number of occasions. The minimum summer concentrations of phosphate (0.4 μmol kg^{-1}) and silicate (12.3 μmol kg^{-1}) suggested that the availability of nitrate limited biological productivity.

The concentration of silicate was reduced to a far lesser extent during the 1993-4 summer than in 1994-5. The removal of silicate is dependant on the occurrence of diatoms and other silicon-containing species in the phytoplankton assemblage: if diatoms were abundant, uptake of silicate would be expected to be far greater than if the bulk of the phytoplankton comprised non-siliceous species which do not require silicon for growth. As discussed in Chapter 3, advection also appears to play a major role in controlling silicate concentrations.

4.2.9 Calculated Carbon Parameters

A suite of parameters, including total alkalinity (Alk_T) and the fugacity of carbon dioxide (fCO_2), were calculated as described in Appendix A from pH and the concentration of DIC. The calculated concentrations of $CO_{2(aq)}$ are not discussed here, but are also given in Appendix C.

4.2.9.1 Total Alkalinity

Alk_T, when normalised to a salinity of 35 psu, was reasonably constant throughout the study (Figure 4.12). Average Alk_T (for data collected between the formation of the fast ice and the beginning of the phytoplankton bloom) was 2410 μequiv kg^{-1} (standard deviation 30 μequiv kg^{-1}). Increases in Alk_T attributable to photosynthesis occurred in both summers, and significant decreases, presumably resulting from precipitation of carbonate containing minerals, were observed under the ice in December of both years. There appeared to be no discernible change in Alk_T associated with the advection of new water to the sampling site in winter (Chapter 2).

Figure 4.12. Calculated total alkalinity (μequiv kg^{-1}) O'Gorman Rocks site, December 1993 - February 1995. The data are normalised to a salinity of 35 psu.

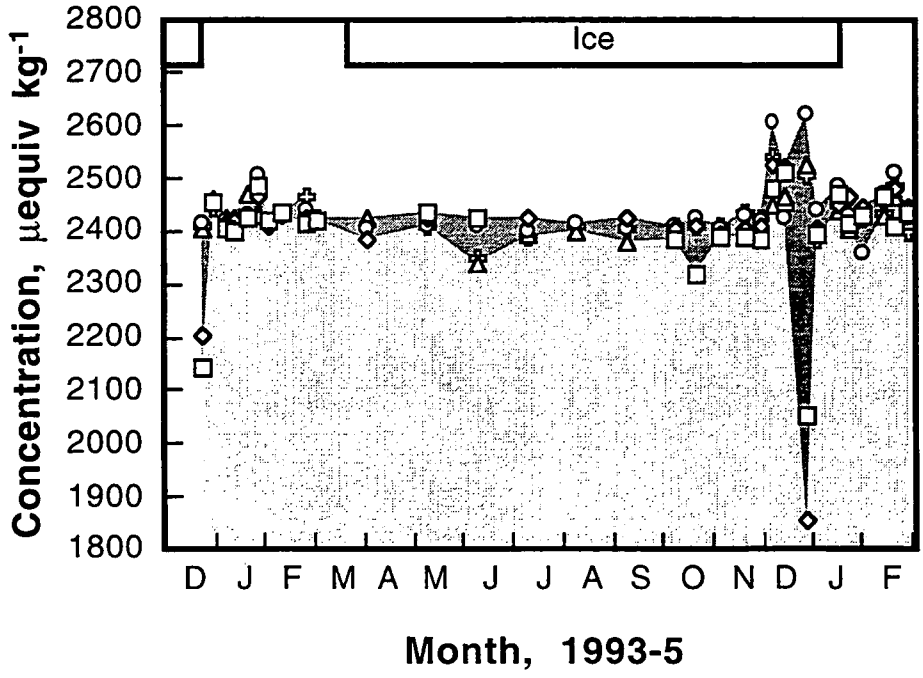

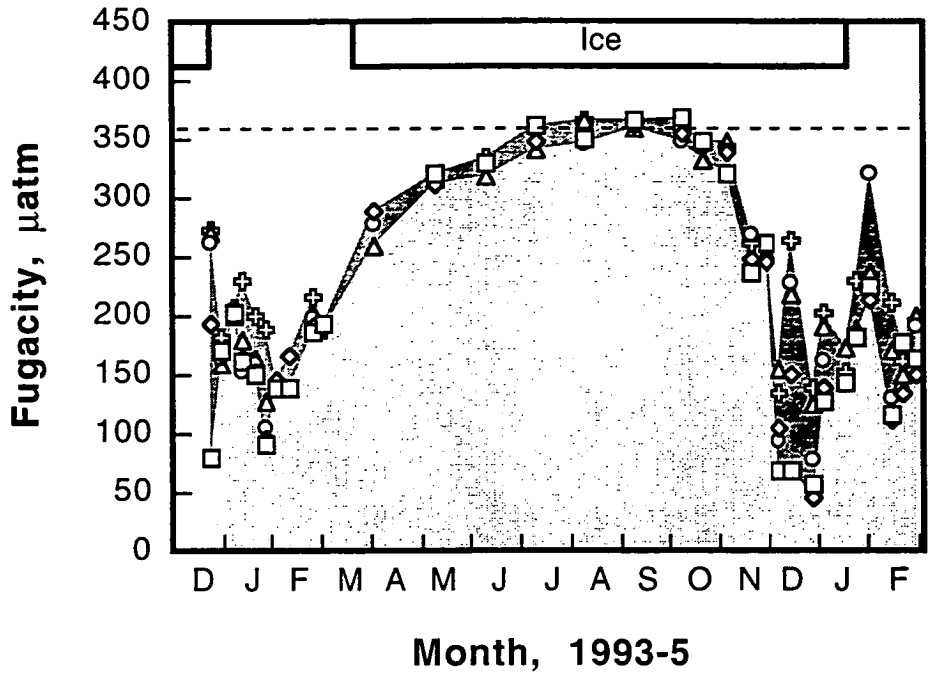

Figure 4.13. Calculated fCO_2 (µatm), O'Gorman Rocks site, December 1993 - February 1995. The approximate concentration of CO_2 in the atmosphere is indicated by the dashed line.

4.2.9.2 The Fugacity of CO_2

Calculated fCO_2 (Figure 4.13) ranged from a maximum of approximately 370 µatm in August and September, to a minimum under the fast ice in December 1994, when fCO_2 was as low as 45 µatm. fCO_2 during periods of open water, when uptake of CO_2 from the atmosphere could occur, was generally in the range 100 - 200 µatm.

4.2.10 Atmospheric Carbon Dioxide: Concentration and Isotopic Ratio.

The concentration of atmospheric CO_2 increased steadily from 356.4 µatm to 358.8 µatm between March and September 1994 (Figure 4.14). In contrast, the concentration varied within a much smaller range during the summer months. The $\delta^{13}C$ of the CO_2 (also shown in Figure 4.14) fell during winter, but, in a similar seasonal cycle to that of the concentration, remained within a small interval over summer. The trends in both the concentration and isotopic signature of the CO_2 were essentially identical to those

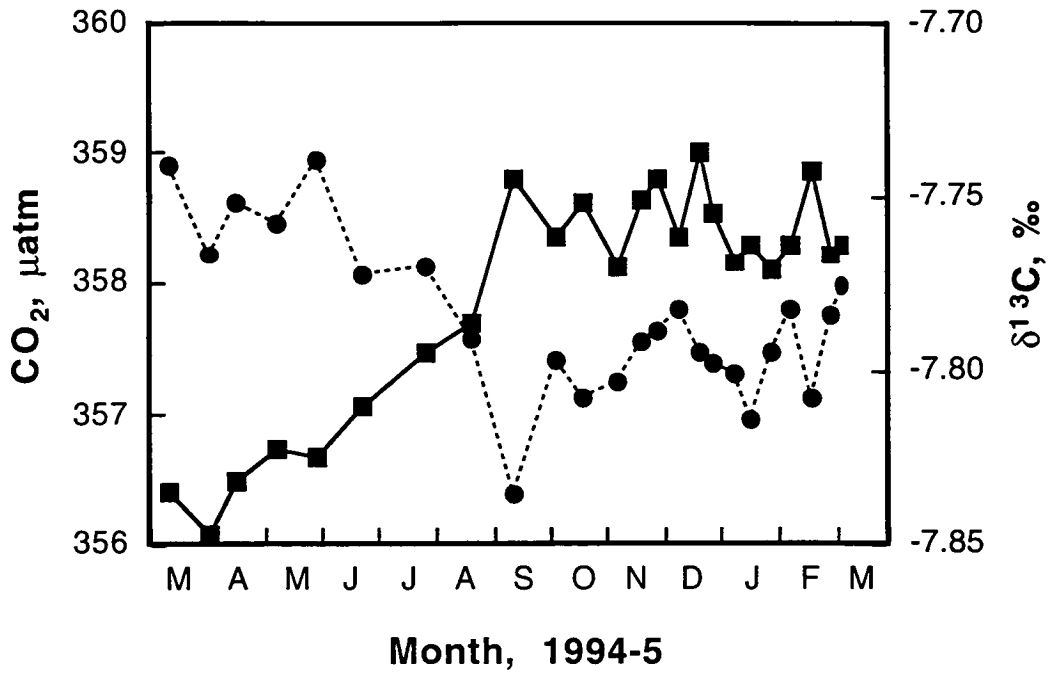

Figure 4.14. Concentration (µatm, squares) and $\delta^{13}C$ (‰, circles) of atmospheric CO_2, Davis Station, March 1994 - March 1995.

recorded at Cape Grim Baseline Air Pollution Station (40° 41'S 144° 41'E) at the same time (Allison et al., 1996; Steele et al., 1996).

4.3 Discussion

4.3.1 Seasonal Cycles of Primary Production and Related Parameters

4.3.1.1 The General Seasonal Cycle of Primary Productivity

Antarctic primary production is often thought to occur in a single summer pulse following the rapid spring increase in solar radiation and stratification of the upper water column (El-Sayed, 1988; Knox, 1990; Smith and Sakshaug, 1990). During this period DIC and nutrients decrease as they are taken up by growing organisms, while DO and chl *a* increase. Productivity largely ceases at the end of summer as a result of reduced irradiance and the onset of deep mixing, and remineralisation and upwelling of

deep water returns the nutrients, DIC and DO back to pre-bloom levels. Productivity at O'Gorman Rocks followed a qualitatively similar seasonal cycle.

The first evidence of significant photosynthetic activity in the water column at the end of the 1994 winter was a slight increase in chl *a* and reduction in nutrients in mid-October. Light levels had presumably become sufficiently high by this time to support some photosynthesis under the fast ice (and the snow cover on top of the ice), though the temperature and salinity profiles indicated that little stratification was present in the water column (Chapter 2). This activity was in part related to the presence of a bottom ice algal community, as the phytoplankton in the water column was dominated by the diatom *Entomoneis kjellmanii* (Chapter 3), a species usually associated with under ice communities (Garrison and Buck, 1989), but which is also capable of survival and growth in the water column (Davidson and Marchant, 1992a). Productivity in the water column increased only slowly during November, before rising dramatically in early to mid-December, as indicated by rapid increases in chl *a* and DO, and reductions in DIC and the nutrients.

The period of greatest photosynthetic activity was between early to mid-December and mid- to late February. The timing of chl *a* maxima and associated DIC and nutrient minima within this period differed between the two summers of the study. During the 1993-4 summer a single peak of chl *a* was observed in late January (no significant chl *a* peaks occurred at the site under the ice prior to the start of the study (J. Grey, personal communication)), while in the 1994-5 summer, three peaks of chl *a* and nutrient depletion occurred, two under the fast ice in early December and early January, and the third after ice break out in mid-February.

The end of the period of productivity at the completion of the summers was equally dramatic, with chl *a* falling rapidly during February 1994, and again in early March 1995 (after the end of the study, but ascertained from casual observations of water

clarity). Increased mixing associated with the formation of ice probably led to the end of productivity, though poor adaptation to much lower light levels by the phytoplankton might also have played a role. There was little evidence of a significant autumn bloom of phytoplankton in the water column, though chl *a* was slightly raised in April 1994 (compared to late February and March) and high chl *a* concentrations occurred in the sea ice (K. Swadling, personal communication). The post-summer decreases in DO and pH were less sharp than the fall in chl *a*, and increases in nutrients and DIC lagged similarly. These observations are discussed further below.

The seasonal cycle at O'Gorman Rocks was qualitatively similar to those observed in other year-long Antarctic studies of aspects of the carbon cycle (Bunt, 1960; Shabica et al., 1977; Krebs, 1983; Fukuchi et al., 1984; Perrin et al., 1987), as well as in equivalent studies in the northern hemisphere (Takahashi et al., 1993). The exact timing of the initiation of biological activity and the intensity and timing of peak activity during the summer phytoplankton bloom will differ between localities and years, but the general cycle is likely to be consistent throughout the Antarctic region.

4.3.1.2 DIC and Nutrients

The concentrations of DIC, nitrate, phosphate and silicate at the O'Gorman Rocks site were generally within the range expected for coastal Antarctic waters (e.g. Jennings et al., 1984; Fukuchi et al., 1985; Humphries, 1987; Perrin et al., 1987; Karl et al., 1991), though anomalously low DIC was measured on a number of occasions directly under the ice in the month prior to ice break out. These instances are discussed in more detail below in association with Alk_T.

Reduction in DIC and nutrients during primary production in summer was close to the theoretical maximum (calculated assuming constant C:N and N:P uptake ratios and the complete removal of all nitrate, the limiting nutrient (see below)), with approximately

85% of the nitrate in the water column being removed at the time of maximum chl *a*. The minimum DIC concentration expected (assuming total removal of inorganic nitrogen, dilution of the water from a salinity of 34 psu to 33 psu and a C:N assimilation ratio of 6) was slightly above 2000 μmol kg^{-1}, and DIC levels approaching this value were recorded during periods of high biological activity.

Previous summer studies in the Antarctic region have suggested that much less efficient use is made of nutrients (Holm-Hansen, 1985; El-Sayed, 1987; Nelson and Tréguer, 1992), and micronutrients, particularly iron, may limit production (Martin et al., 1990, 1991; de Baar et al., 1995). These results have led to a paradigm that nutrient concentrations are rarely depressed in the Southern Ocean. In contrast, water in the North Atlantic is often totally stripped of nutrients during the summer phytoplankton bloom (Takahashi et al., 1993). More recently, reports have appeared of substantial nutrient depression in the Antarctic region (Jennings et al., 1984; Fukui et al., 1986; Holm-Hansen et al., 1994; Perez et al., 1994; McMinn et al., 1995). Most of these studies, however, have been undertaken in inshore areas or near a receding ice edge, environments which are known to harbour greater biological activity than pelagic waters. The enhanced nutrient and DIC drawdown observed at O'Gorman Rocks and at other inshore Antarctic sites compared to the pelagic Southern Ocean possibly reflects the greater availability of micronutrients at these sites, resulting from aeolian input and sediment resuspension (Nolting et al., 1991), as well as strong surface water stratification associated with melting ice and shallower water depths.

The increase in DIC and nutrients at the end of summer was initially quite rapid (though not as rapid as the decrease in chl *a*), but then slowed during late autumn and winter, with maximum concentrations not being reached until October. Phosphate behaved slightly differently, reaching a maximum in July before falling slightly. The drop in phosphate was due to the arrival at the sample site of a new water mass (Chapter 2) with slightly lower phosphate concentration. The signature of this water

can also be discerned in DIC, where a slight jump in the concentration occurred at about the same time. The increase in silicate was considerably slower than the other nutrients and DIC, reflecting the different mechanism (dissolution c.f. bacterial remineralisation) which was responsible for regeneration, and consistent with the high silicate concentrations in Antarctic sediments (DeMaster, 1981, Ledford-Hoffmann et al., 1986).

DIC and nutrient increase during winter could have been the result of three different processes: remineralisation of organic matter near the surface; deep vertical convection; and mixing within the WW layer. Deep vertical convection can be ruled out as a regeneration mechanism, as this process would have resulted in sharp changes in the concentrations as high DIC and nutrient deep water was transported to the surface, after which little change would have occurred. Furthermore, the differing rates of increase in the nutrients indicate that it was not a single event which resulted in the increase.

If organic matter remineralisation were the only process responsible for the increase in DIC and nutrients, the concentrations of these species would fall from year to year, as a small percentage of the organic matter produced during photosynthesis is lost from the system to deep water or by burial in the sediment. The depth to which material must be transported to be lost from the surface water is effectively the maximum depth of the WW during winter, as any material remineralised above this depth will be mixed back into the surface water by convective mixing during winter. This process is shown schematically in Figure 4.15.

As DIC and nutrient concentrations in the WW are likely to be much the same at the end of each winter, there must be some mechanism that transports DIC and nutrients back into this water. DIC can come from uptake from the atmosphere during the ice-

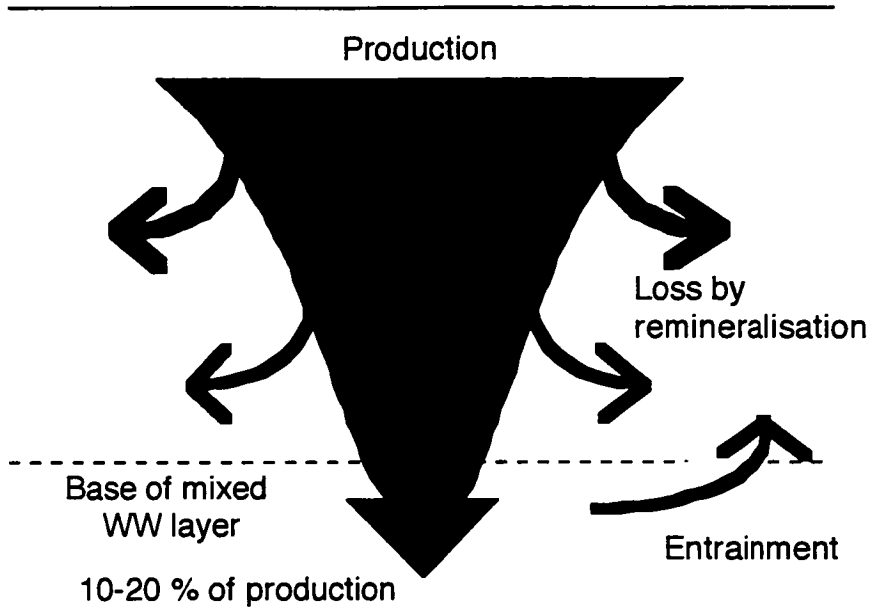

Figure 4.15. Schematic diagram of the sedimentation and remineralisation of organic material. Any nutrients and DIC formed by remineralisation above the maximum depth of mixed WW layer will be mixed evenly throughout the WW at the end of winter. Any carbon, nitrogen, phosphorus and silicate that is lost from the WW must be replaced by entrainment of deeper water into the WW for a long term balance to be maintained.

free summer or, along with nutrients, from entrainment of deep water into the base of the WW. Both of these mechanisms undoubtedly occur, though, from the small percentage of organic carbon that is either buried in inshore Antarctic sediments (Chapter 5) or reaches water beneath the WW (calculated to be approximately 10 - 20 % of organic production using the equation of Berger et al. (1988)) the majority of the winter recovery in the concentrations of DIC and nutrients would have come from organic matter remineralisation. Further evidence for this conclusion comes from the seasonal variation in $\delta^{13}C_{DIC}$. The end of winter $\delta^{13}C_{DIC}$ at O'Gorman Rocks was nearly identical to that in Ellis Fjord (Chapter 7), where deep water upwelling could not have occurred leaving remineralisation as the only major mechanism for nutrient renewal.

4.3.1.3 Dissolved Oxygen

DO was present at only *circa* 80 - 85 % saturation at the end of winter, which is typical for Antarctic surface water at this time of year (Shabica et al., 1977; Gordon et al., 1984; Jones et al., 1990). Gordon et al. (1984) suggested that entrainment of low oxygen deep water into the WW was responsible for this undersaturation. The supersaturation of oxygen resulting from photosynthesis during summer was also expected, as DO concentrations well above winter levels for this time of year have been reported in a number of other Antarctic studies (e.g. Shabica et al., 1977; Krebs, 1983; Bouquegneau et al., 1992).

The supersaturation of DO during the period of open water in summer suggests that a flux of oxygen from the ocean to the atmosphere could occur. The ice cover in winter would preclude any flux in the opposite direction resulting from undersaturation. Loss of oxygen to the atmosphere would exacerbate undersaturation during winter, as the amount of oxygen available for the remineralisation of organic material would be reduced. Evidence for loss of oxygen from the ocean in the present study is discussed below in Section 4.3.2.2.

4.3.1.4 pH

It is difficult to compare directly the pH data obtained in this study with that from many previous Antarctic studies due to problems with measurement techniques and pH scales. Shabica et al. (1977), Perrin et al. (1987) and Poisson and Chen (1987) reported similar but generally higher pHs during winter in coastal Antarctic environments. However, few details of the experimental methods or scales used are given in these papers. More recently, Bellerby et al. (1995) reported pH_f data measured spectrophotometrically from an early summer cruise in the Antarctic Peninsula region. pH varied between 7.65 and 7.75, which was consistent with the

late winter data from the present study prior to the onset of significant photosynthesis. The increases in pH observed at O'Gorman Rocks in summer were again similar to those recorded in earlier, year-long studies (Shabica et al., 1977; Perrin et al., 1987).

4.3.1.5 Total Alkalinity

Alk_T was near constant throughout winter at *circa* 2410 μequiv kg^{-1} (normalised to a salinity of 35 psu), which was slightly higher than expected for Antarctic surface waters (2390 μequiv kg^{-1}: Broecker and Peng, 1982; Poisson and Chen, 1987), and the difference could well have been due to a systematic error in measuring salinity, pH_f or DIC. The slight increases in alkalinity observed in summer were attributable to the reduction in the concentrations of nitrate and phosphate during the production of organic matter (Stumm and Morgan, 1991).

As mentioned previously, very low concentrations of DIC were recorded at times during the summers in samples collected from directly under the ice. The normalised alkalinities of these samples were also very low, which suggested that carbonate precipitation rather than photosynthesis or simple dilution was responsible for the reduction in DIC. That the low DIC concentrations and alkalinities were closely associated with the presence of sea ice indicated that the ice itself played an important role in their origin. As the sea ice begins to melt in December, brine channels form within the ice from the coalescence of enlarging brine pockets (Weeks and Ackley, 1982), and brine will drain into the underlying water. Concentrations of DIC in brine in melting first year sea ice have been reported to average 1500 μmol kg^{-1} (range 839 - 2055 μmol kg^{-1}, with salinities ranging from 21 to 41 psu) (Gleitz et al., 1995), indicating that this mechanism could indeed be the source of the low DIC water observed under the ice in the present study. The low DIC concentrations in the brine could be a result of biological processes within the ice (Gleitz et al., 1995), or the precipitation of $CaCO_3$ by sympagic organisms such as foraminifera (Dieckmann et

al., 1991) or during concentration and cooling of water in the brine pockets in winter (Nelson and Thompson, 1954; Jones and Coote, 1981). Carbonate precipitation, however, is the only mechanism that would also have produced the low alkalinities, and it is this process that most likely occurred.

4.3.1.6 fCO_2

The fugacity of carbon dioxide reached a maximum in late winter of approximately 360 - 370 µatm, which indicated that the water column at that time was slightly supersaturated with respect to the atmosphere, the concentration of CO_2 in which was in the range 356 - 359 µatm throughout the study. Little winter fCO_2 data is available for coastal Antarctic waters, though these observations were consistent with the data of Beggs (1995), who reported fCO_2 to be within 25 µatm of saturation over wide areas of the pack ice zone in Prydz Bay in October and November. It is interesting to note, however, that the water became saturated with respect to atmospheric CO_2 only in August and September. For most of the period of ice cover, the water was undersaturated. Formation of brine flows prior to saturation may have resulted in the transport of low fCO_2 (and DIC) water to the deep ocean, which would reduce the efficiency of this mechanism for CO_2 transport to bottom waters.

During summer, reduction of fCO_2 resulting from removal of DIC by biological activity outweighed the effect of the slight increase in temperature, which would have increased fCO_2 by approximately 20 µatm if the concentration of DIC remained constant. The minimum fugacities recorded, which were less than 100 µatm, have Antarctic precedents in the Bransfield Strait (Karl et al., 1991) and near the Amery Ice Shelf in Prydz Bay (Beggs, 1995). Many other studies from the Antarctic region have reported fCO_2 in the range 150 - 300 µatm during summer (e.g. Takahashi and Chipman, 1982; Takahashi et al., 1993; Robertson and Watson, 1995), and similar

fugacities have been recorded in the Bering Sea in the Northern Hemisphere polar region by Codispoti et al. (1982, 1986).

The return of fCO_2 to near saturation by the end of winter indicates that the WW was essentially in equilibrium with the atmosphere at this time. The summer reduction in fCO_2 is counteracted by the uptake of CO_2 from the atmosphere, the remineralisation of organic material and the entrainment of DIC-rich water from deeper in the water column. The late winter fugacity suggests that the concentration of CO_2 in the WW has responded to the increase in atmospheric CO_2 over the last 200 years. If the WW had not responded, the late winter fCO_2 would be expected to be closer to pre-industrial atmospheric concentration of the gas, circa 280 μatm. Conversely, it may be that late winter fCO_2 in the WW has been near constant or has not varied in concert with the concentration of CO_2 in the atmosphere, and that this water is in the process of going from being a source area of CO_2 to an atmospheric sink, ice notwithstanding. Further study during winter is required to determine if the WW is in fact in longer term equilibrium with the atmosphere.

4.3.2 Correlations: DIC, Nutrients and Dissolved Oxygen

4.3.2.1 Correlation of DIC and the Nutrients

Strong correlations occurred between DIC (ignoring the anomalously low under ice data recorded in the month prior to ice break out), nitrate, and phosphate throughout the study (all normalised to a salinity of 35 psu: Figure 4.16), though correlations with silicate were far less significant. Table 4.1 gives details of all the regressions.

On average, the C:N:P molar assimilation ratio (i.e. the ratio in which DIC and nutrients were removed from the water during primary production, and in this case the

Table 4.1. Details of regressions between the concentrations of DIC, nutrients and DO (all normalised to a salinity of 35 psu). Anomalously low concentrations of DIC and DO during the ice free periods were excluded from the calculations (see text). The standard errors for the regressions are given.

Regression	Slope	Slope error	Intercept	Intercept error	r^2
DIC - N	6.08	0.22	2113	4	0.85
DIC - P	97.8	3.7	2079	6	0.84
DIC - Si	2.76	0.34	2083	17	0.34
DIC - DO	-0.83	0.04	2554	14	0.89
N - P	15.0	0.5	-4.06	0.74	0.86
Si - N	0.97	0.08	32.0	1.5	0.48
Si - P	14.6	1.4	28.0	2.0	0.43
DO - N	-7.16	0.37	514	8	0.81
DO - P	-109.3	7.6	557	13	0.72
DO - Si	-2.43	0.35	506	17	0.24

opposite processes during respiration) was 97.8 (± 3.7):15.0 (± 0.5):1. Silica exhibited no fixed assimilation ratios.

The average C:N assimilation ratio, 6.08 (± 0.22), was slightly lower than the Redfield Ratio (6.6: the average molar ratio of C to N in marine organic material (Redfield et al., 1963)). In contrast, much higher assimilation ratios (10.1-12.2) were recorded in the Bransfield Strait region near the Antarctic Peninsula by Karl et al. (1991), who suggested that this was the result of the seasonal accumulation of dissolved organic matter (DOM) of very high C:N ratio. The C:N mole ratio of suspended POM was not measured in samples from O'Gorman Rocks during the study, but the ratio in material caught in sediment traps was determined, and was *circa* 6.5 during the period of maximum organic matter sedimentation in December 1994 (Chapter 5). This ratio was consistent with that calculated from the concentrations of DIC and nitrate, and was similar to the ratios determined for POC in other Antarctic studies (Copin-Montégut and Copin-Montégut, 1978, 1983; Nelson and Smith, 1986; Nelson et al., 1987; Tréguer et al., 1988; Perez et al., 1994).

The C:P molar assimilation ratio (97.8 ± 3.7) was again slightly lower than the Redfield Ratio (105; Redfield et al., 1963). C:P ratios reported in other Antarctic studies show considerable variation, with Karl et al. (1991) calculating very high assimilation ratios (*circa* 160), while Copin-Montégut and Copin-Montégut (1978, 1983) reported much lower ratios (39 to 84) in particulate material. The N:P molar assimilation ratio in the present study (15 ± 0.5) was similar to that recorded in the Bransfield Strait (14.3) (Karl et al., 1991) and the Princess Elizabeth Trough (T. Trull, personal communication), but was higher than ratios in the Weddell Sea (Weiss et al., 1979) and the Indian sector of the Southern Ocean (Simon, 1986). Copin-Montégut and Copin-Montégut (1978, 1983) found N:P ratios in particulate material in

Figure 4.16. Normalised nutrient correlation plots: (a) DIC and nitrate; (b) DIC and phosphate; and (c) nitrate and phosphate. Data obtained when the site was ice covered are represented by closed squares, and during periods of open water by open squares. Anomalously low DIC concentrations have been excluded from the plots (see text).

(a)

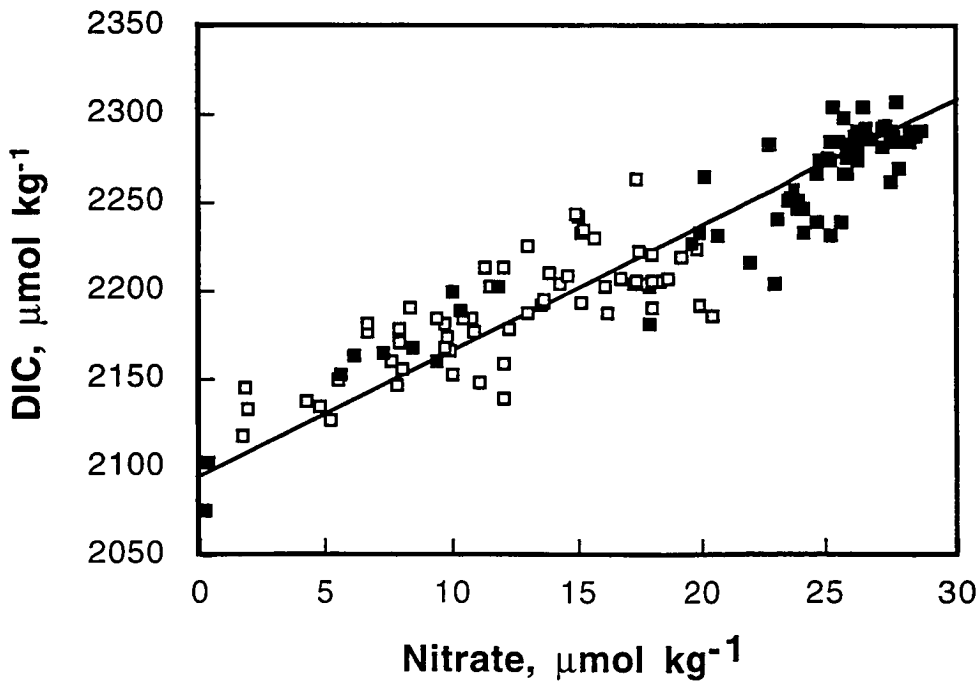

(b)

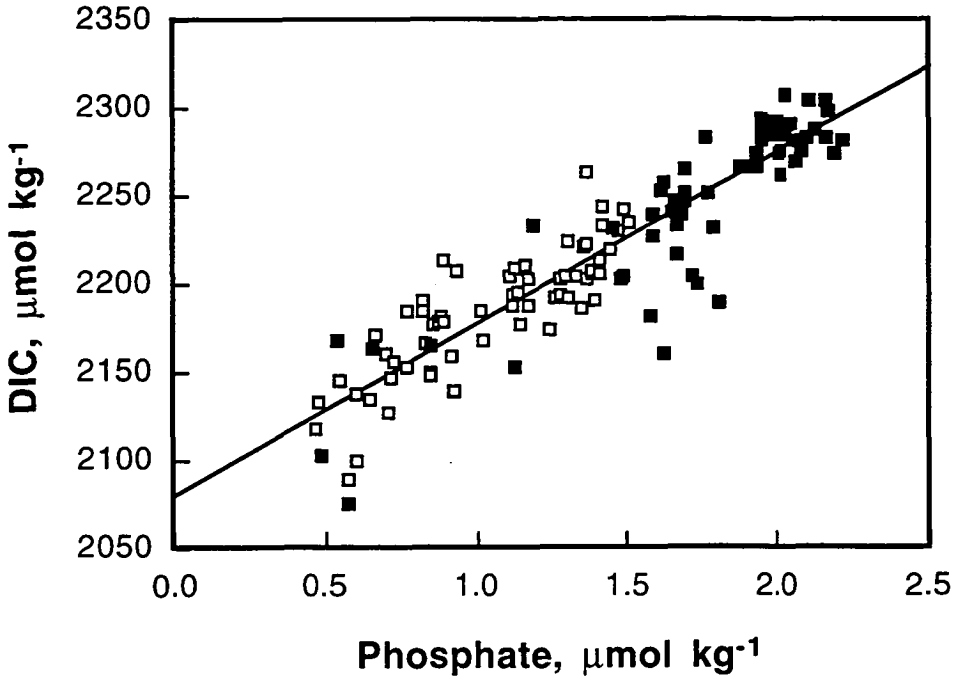

(c)

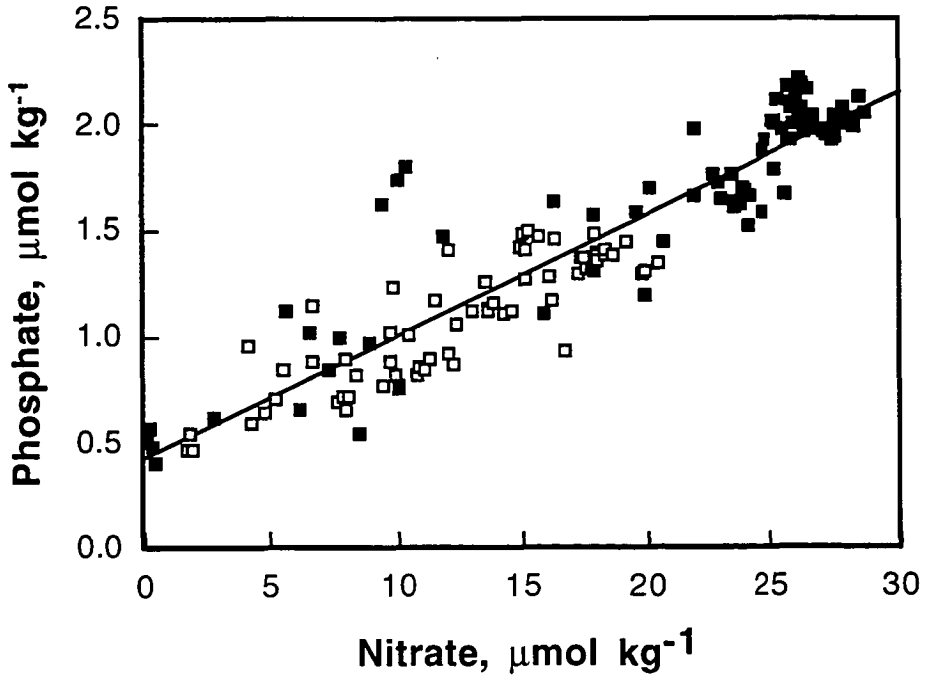

Figure 4.16. Continued

the range 5.9 -14.3, with the low ratios being associated with the very low C:N ratios mentioned above.

The C:N:P molar assimilation ratios calculated in the present study appear to be quite unremarkable, as they are in fact closer to the Redfield Ratio than those determined in many other studies undertaken in the Antarctic region. Published ratios range from 183:15:1 (Karl et al., 1991) to 62:11:1 (Copin-Montégut and Copin-Montégut, 1983; Jennings et al., 1984). Perez et al.(1994), however, reported a similar ratio (111:15:1) to that found in the present study in the Weddell Sea.

The poor correlations observed between the concentration of silicate and the other parameters (Table 4.1) reflect variations in the phytoplankton communities present during the summers of the study (Chapter 3) and the advection to the site of water with markedly different ratios of silicate and the other nutrients (Figure 3.4). Silicate uptake would be considerably lower during periods when the community was dominated by non-siliceous phytoplankton than when diatoms were prevalent.

Figure 4.16c suggests that nitrate was the limiting nutrient during summer in this study (assuming that production did not continue in the absence of nitrate). As removal of nutrients to the extent that one of the nutrients becomes limiting has been reported only rarely from the Southern Ocean, there is little data regarding which nutrient limits primary production in the Antarctic region. Nitrate also appeared to limit productivity in two studies in Ellis Fjord (McMinn et al., 1995; Chapter 7).

4.3.2.2 Correlations of Dissolved Oxygen with DIC and the Nutrients

The correlation of DO and DIC was significantly stronger during the periods of ice cover than when the sampling site was ice free (Figure 4.17), which was also true for correlations of DO with nitrate and phosphate. During periods of open water, DO

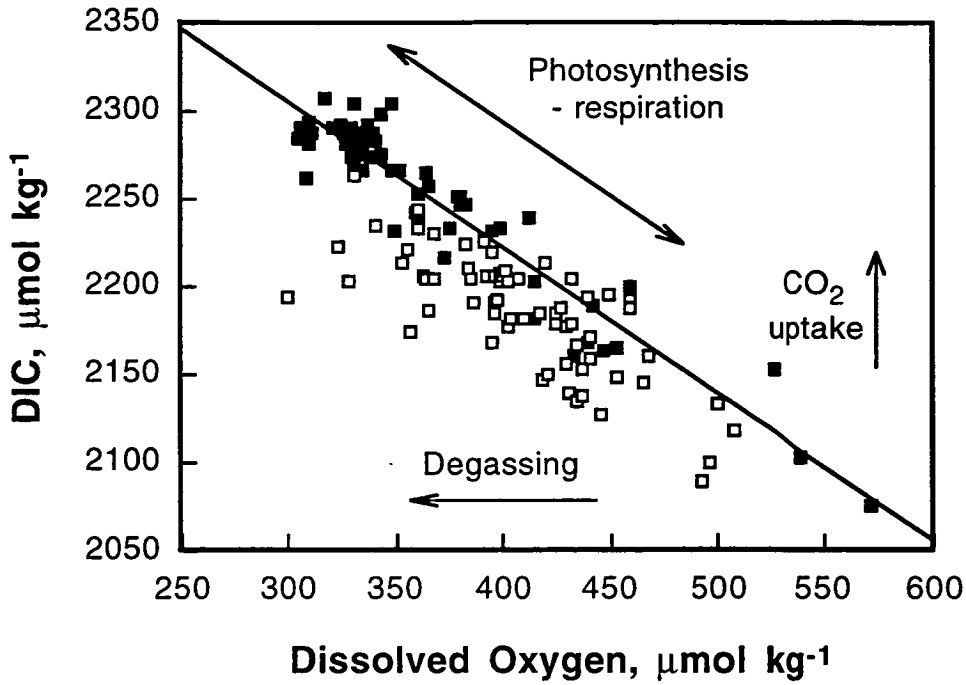

Figure 4.17. Correlation plot of the concentrations of DIC and dissolved oxygen. All concentrations have been normalised to S = 35 psu. Data obtained when site was ice covered are represented by closed squares, and during periods of open water by open squares. Anomalously low DIC concentrations have been excluded from the plots (see text). The regression line shown is for data points from when the sampling site was ice covered Also shown are the trends resulting from photosynthesis, respiration, DO degassing and CO_2 uptake.

levels fell consistently below the regression line from the period of ice cover. Of the six data points from the periods of open that lie above the regression line, five were from a sampling date immediately after ice break out. The simplest interpretation of the dependence on ice cover is that loss of oxygen to the atmosphere occurred during periods of open water. Loss of CO_2 to the atmosphere resulting in a decrease in DIC during this period is not an alternative explanation because the surface waters were undersaturated and the correlations between DIC and the nutrients indicated no ice cover dependence.

Another possible explanation of the lowered DO in open water conditions is a decrease in the ratio of O_2 production to DIC uptake during photosynthesis. This ratio is

dependent on the type of organic material being synthesised, and can range from 1.0 (production of hexoses) to 1.4 (production of lipids) to 1.6 (production of proteins from nitrate). The ratio under ice at O'Gorman Rocks was 1.20. It is possible that the variations in the O_2:DIC relationship after ice break out are due to changes in this parameter, possibly as a response by the phytoplankton to much higher light conditions. Gleitz et al. (1996a), however, reported a transfer to lipid production by phytoplankton held in a high light environment in crack pools between ice floes, which would have resulted in a shift in DO relative to DIC in the opposite direction to that observed.

Assuming degassing dominated the variations, a rough estimate of the amount of oxygen lost can be made by comparison of the predicted concentrations of DO (calculated from the concentrations of nitrate and the relationship between DO and nitrate during the period of ice cover) with the measured concentrations. The results of the calculations are shown in Figure 4.18.

The apparent degassing of oxygen amounted to a maximum of over 20 $\mu mol\ kg^{-1}$. It is apparent from Figure 4.18 that loss of oxygen generally occurred during periods both when oxygen in the water was supersaturated, providing the driving force for gas loss, and when the sampling site was ice free, allowing gas exchange. The importance of the ice cover is highlighted by the correlation between measured and calculated DO under the ice cover during December 1994 when DO was supersaturated, compared to the large deficits which appeared immediately after the break out of the ice in early January 1995. The average oxygen deficit during the ice free period was approximately 30 % of the difference between the saturation concentration and the oxygen concentration calculated from the concentration of nitrate.

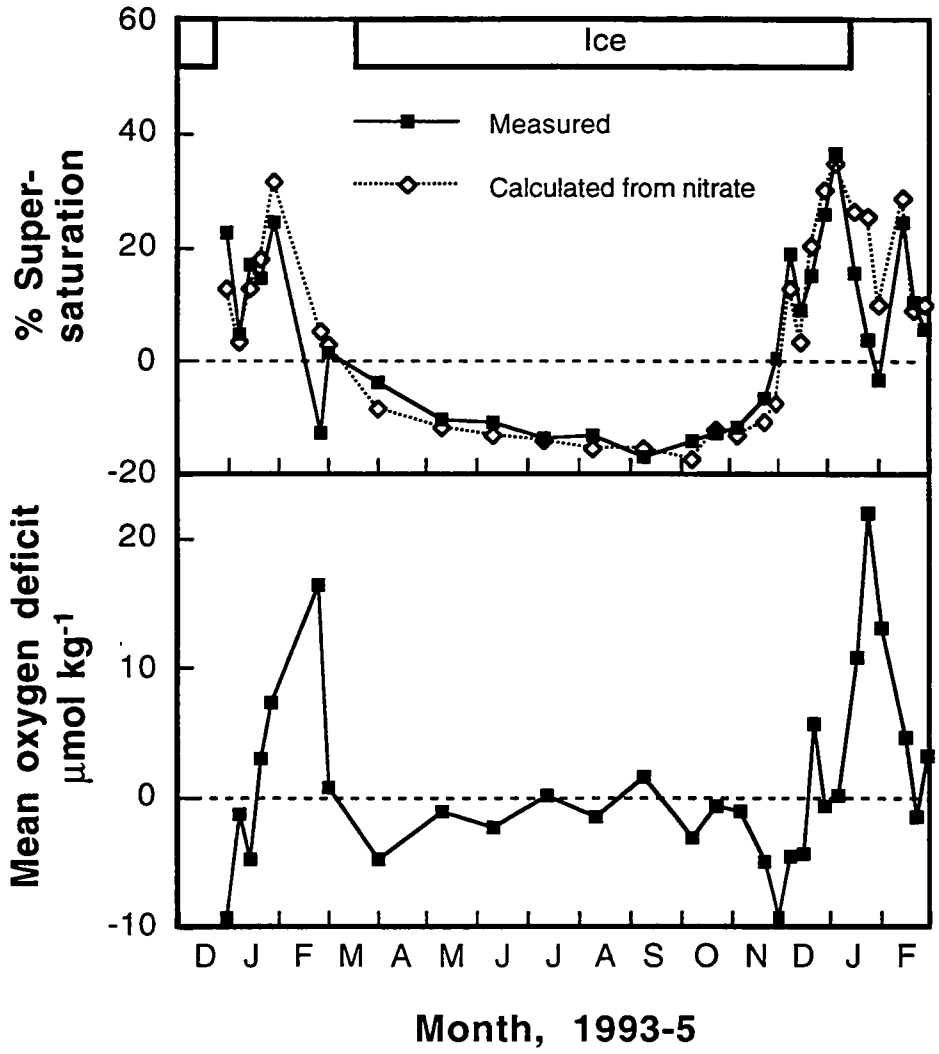

Figure 4.18. Oxygen degassing. The upper panel shows the average measured oxygen supersaturation along with that calculated from the concentration of nitrate. The lower panel shows the mean oxygen deficit per kg of seawater.

Excess DO was present in December 1993 and, to a lesser extent, in November and December 1994. These data suggest that the ratio of DO production to nitrate uptake altered during these periods, possibly by the formation of material with high C:N ratio.

It is probable that both biological and physical mechanisms operated to some extent in creating the oxygen deficit. Oxygen lost from the ocean as a result of physical processes could not be replaced by transfer from the atmosphere later in the year due to the impermeable ice cover when oxygen saturation returned to negative. This 'lost'

oxygen would therefore not be available for remineralisation of organic matter, and thus a net deficit of oxygen would continue, which provides another mechanism, along with upwelling of low oxygen deep water, for the winter undersaturation observed in the WW.

4.3.3 Carbon Budget Calculations and Correlation of Measured and Calculated Organic Carbon

4.3.3.1 Carbon Budget Calculations

The magnitude of the seasonal depletions in the nutrient and DIC concentrations can be used to estimate the amount of OC produced prior to sampling. Note that this calculation does not require the OC still to be present in the water at the time of sampling. Net OC production was calculated using the following equation, which assumes that all decreases in the concentrations of DIC and nutrients from the end of winter maxima were the result of organic matter production during photosynthesis and dilution of the water by melting ice, and assumes that any increase in nutrient concentrations was the result of remineralisation rather than arrival of new nutrients:

$$P = F\left(\frac{C_0 S_S}{S_0} - C_S\right) \qquad (4.1)$$

where P is the net theoretical production of organic carbon (ignoring sedimentation), C is the concentration of DIC, nitrate or phosphate, S is the salinity and F is the molar assimilation ratio for nitrate or phosphate given in Table 4.1 (if the concentration of DIC is used to calculate P, F equals 1). The subscript '0' refers to the values of the parameters at the end of winter, which are given in Table 4.2, and 'S' refers to the values for the sample of interest. DO was not used to calculate OC concentrations due to the variable relationship observed between DIC and DO discussed above.

Parameter	Value
Salinity	34.10 psu
DIC	2230 μmol kg^{-1}
Nitrate	27.5 μmol kg^{-1}
Phosphate	2.00 μmol kg^{-1}

Table 4.2. Estimated end of winter values for the parameters used in the calculation of OC production.

The net OC production calculated from the reduction in DIC (ignoring the samples with anomalously low DIC) agreed reasonably well with those calculated from nitrate and phosphate (Figure 4.19). Variations away from the 1:1 equivalence line (shown in the figure) could be due to a number of factors, including localised differences in the uptake of DIC, nitrate and phosphate during the production of organic material,

Figure 4.19. The net OC production (μmol kg^{-1}) calculated from the concentrations of nitrate and phosphate plotted against net OC production calculated from the concentration of DIC. The 1:1 equivalence line is also shown.

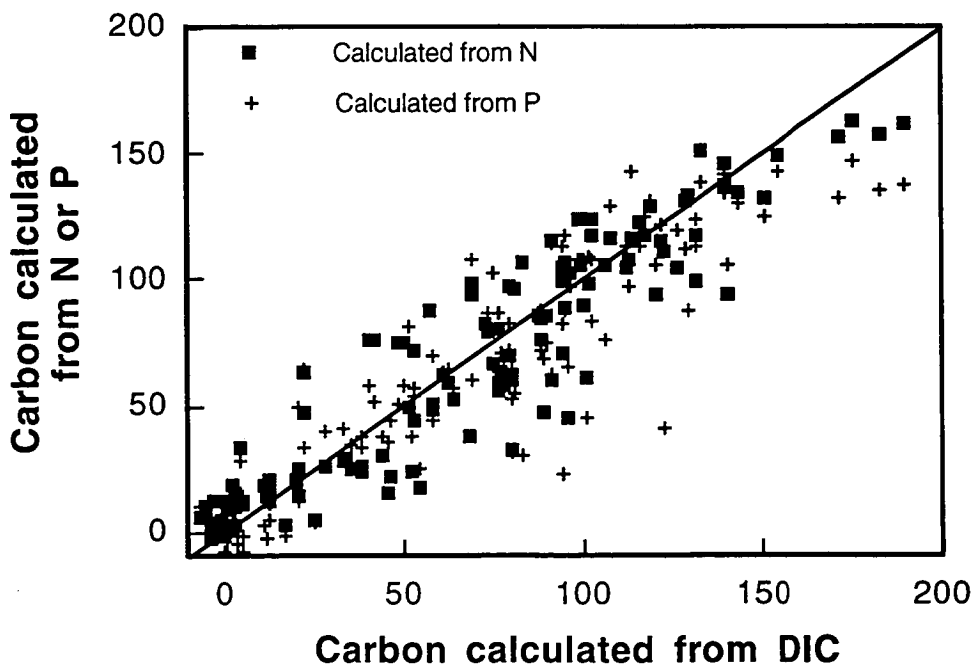

decoupled regeneration of the organic material (i.e. relatively more carbon is returned to the water column than nitrate or phosphate or *vice versa*), incorrect choice or non-universality of the initial concentrations, CO_2 uptake from the atmosphere, or precipitation of calcium carbonate.

An estimate of the net OC production which had occurred for each depth from the end of winter to the sampling day was determined by averaging the figures calculated using the various parameters. These data are shown in Figure 4.20, which also shows the net OC production for the entire water column determined by integrating the calculated concentrations of OC from the surface to the sediment at 23 m. As expected, the greatest calculated net OC production occurred during summer when chl *a* was high and greatest nutrient depletion occurred.

Figure 4.20. Calculated net OC production (μmol kg^{-1}) for each sampling date and depth (crosses) and integrated calculated OC (g m^{-2}, line).

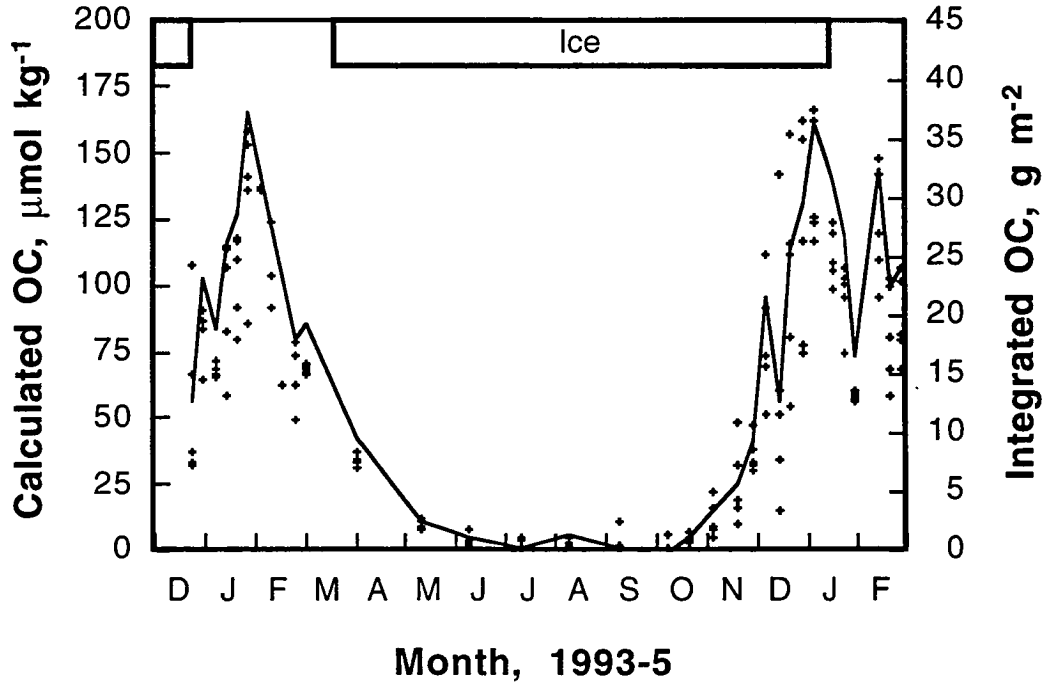

The theoretical maximum net OC production possible (if all of the limiting nutrient, nitrate, was removed from the water, no dilution with nutrient poor melt water occurred, and the C:N molar uptake ratio was 6:1) was 168 μmol kg^{-1}, which was approached in the surface waters on a number of occasions in both summers. The theoretical maximum net OC production integrated from the surface to the sediment was *circa* 47 g m^{-2}. Integrated OC did not reach this figure during the study due to the stratification of the water column, with lower net production occurring at depth.

The net rate of OC production was calculated by dividing the difference between the integrated net OC production on successive sampling dates by the number of days between the dates, and are shown in Figure 4.21. These rates were 'net', as they were in fact the balance of OC production and remineralisation, rather than being production alone.

Figure 4.21. Calculated rates of OC production at the O'Gorman Rocks site.

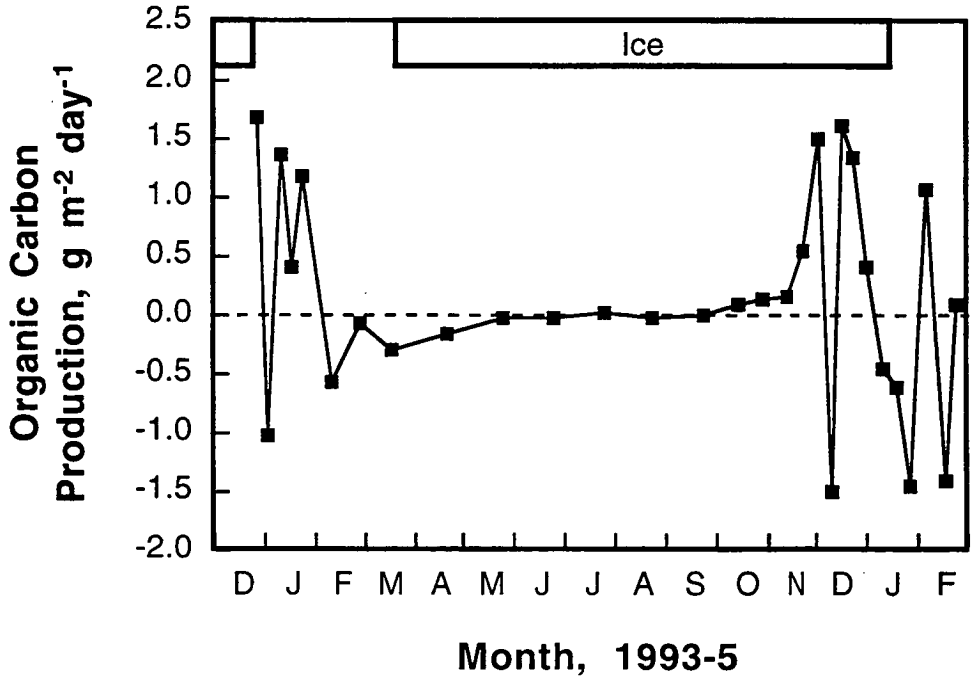

The maximum net rate of OC production was near 1.6 g m^{-2} day^{-1} in both summers (equivalent to an average of approximately 70 mg m^{-3} day^{-1} or 6 µmol kg^{-1} day^{-1} for the entire water column), with the average rate from the beginning of December to the time of maximum calculated OC near 0.8 g m^{-2} day^{-1}. These rates are comparable to the observations of Karl et al. (1991), who calculated a production rate of OC of 1.6 g m^{-2} day^{-1} to a depth of 50 m in the Bransfield Strait by an equivalent method, in the Weddell Sea, where productivity during summer has been reported to range from 100-700 mg m^{-2} day^{-1} (El-Sayed and Taguchi, 1981, Jennings et al. 1984; von Bröckel, 1985; von Bodungen et al., 1988), and in the Ross Sea, where rates of 0.4 - 2.0 g m^{-2} day^{-1} have been recorded (Wilson et al., 1986; Barry, 1988; Smith and Nelson, 1990). Thus, the rates of primary productivity calculated in the present study are comparable to other summer data from the coastal Antarctic region.

^{14}C based productivity measurements made in surface water at the O'Gorman Rocks site during December 1994 and February 1995 (Swadling et al., in press) ranged from 110 to 220 mg C m^{-3} day^{-1}. These data are consistent with the calculated rates given above, especially considering that these data were for surface samples, where productivity would have been greater than in deeper water, and that nutrient based calculations smooth out periods of higher and lower productivity. Similar agreement between calculated and measured rates of organic production was recorded in the Bransfield Strait by Karl et al. (1991).

It must be pointed out, however, that the apparent rates of OC production at the O'Gorman Rocks site could be artefacts of advection of water with differing nutrient and DIC characteristics to the area. Thus, periods of OC remineralisation, represented by negative OC production rates in Figure 4.21, might not have been due to breakdown of organic matter at the site, but rather to the transport into the area of higher nutrient water in which organic production had never reached the extent of that

in the water it replaced. A similar proviso applies also to periods of apparent OC production.

4.3.3.2 Correlation of Calculated and Measured Organic Carbon

The concentrations of DOC and POC were measured during the 1994-5 summer, allowing a comparison to be made between the calculated and measured concentrations of OC (Figure 4.22). It is evident from the figure that considerable scatter occurred in the data, even though many data points appeared to fall close to a linear relationship . If the very high carbon results from 7 December 1994 (on which date the massive phytoplankton bloom may have resulted in unusually high carbon concentrations) and

Figure 4.22. Plot of measured total OC against calculated OC for discrete depths: (a) All data; (b) The same plot with an expanded vertical axis. Shown are the 1:1 line (dashed) and the regression line discussed in the text. The data not considered in calculation of the regression line are shown as crosses.

(a)

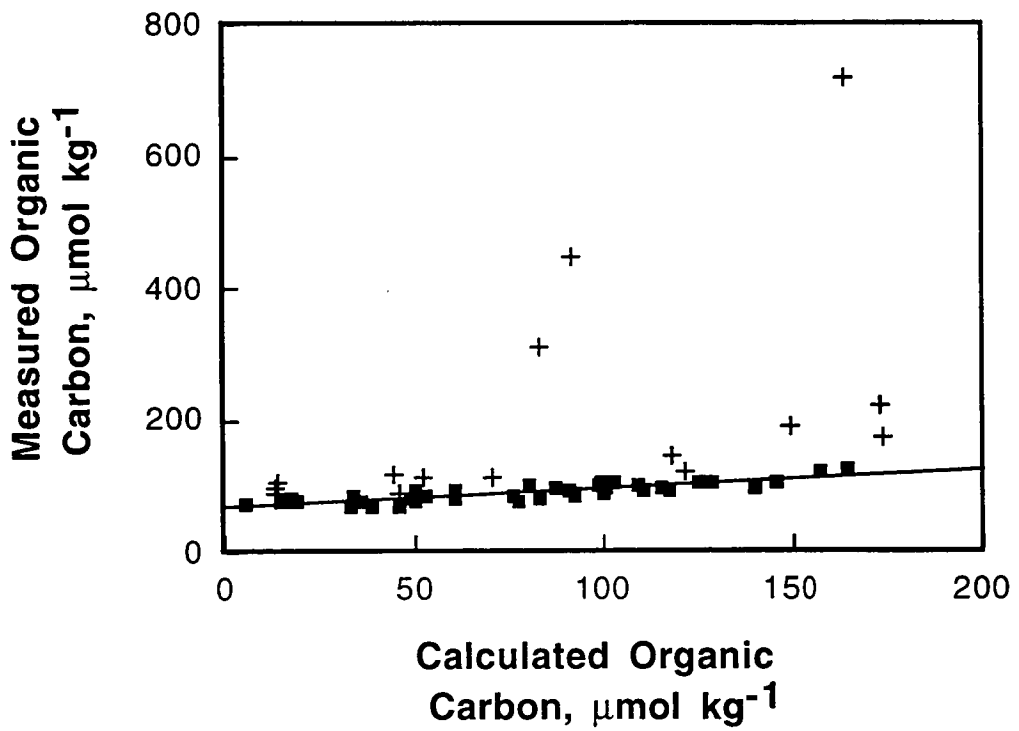

(b)

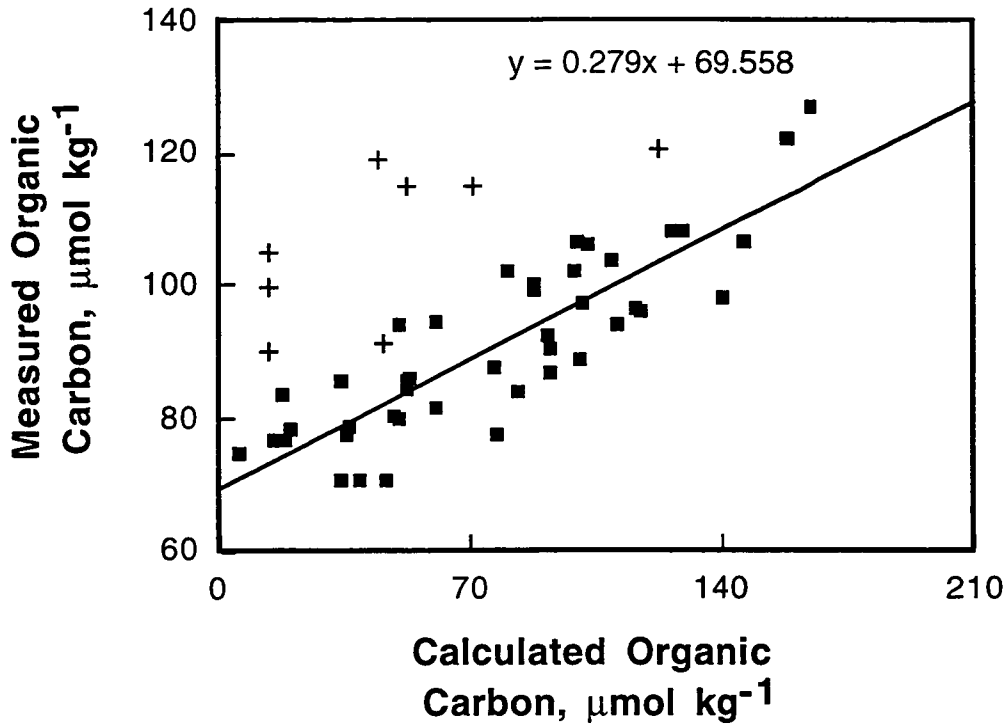

Figure 4.22. Continued.

data from immediately under the ice (where bottom ice algae may have resulted in increased POC) are removed, a reasonable correlation (shown in Figure 4.22b), was observed between the calculated and measured concentrations.

Two important points can be established from the regression shown in Figure 4.22b. Firstly, the intercept of the regression line implies that the concentration of DOC during winter was *circa* 60 - 70 µmol kg^{-1}, which was higher than that measured in other Southern Ocean studies (45 - 55 µmol kg^{-1}: Cadée 1992; T. Trull, personal communication). The higher background concentration measured in this study might have resulted from an increased instrument blank (Appendix A), but could also reflect incomplete remineralisation of OC from the previous summer prior to the onset of production in the 1994-5 summer.

Secondly, the slope of the regression line is only 0.28, which indicates that over 70 % of OC produced was not present in the DOC or POC fractions. This loss could either be due to transfer of carbon to metazoan zooplankton and larger animals, by sedimentation of POC to the sea floor or by advection away from the sample site. A similar result was reported by Perez et al. (1994), who estimated that in the Weddell Sea approximately 65 % of organic production was exported out of the euphotic zone by sinking, or was grazed, and by Karl et al., (1991). Sedimentation of OC at O'Gorman Rocks was near 10 g m^{-2} on an annual basis (Chapter 5), or approximately 20 - 30 % of the annual OC production of circa 25 - 35 g m^{-2} (Figure 4.20).The remaining 'missing' OC was presumably grazed and recycled, or sedimented elsewhere.

The data from 7 December 1994 are difficult to interpret. On this date, a massive phytoplankton bloom was present at the sampling site, and the sum of POC and DOC, which was as high as 720 µmol kg^{-1}, was far greater than the calculated level of organic production from DIC and nutrient removal (100 µmol kg^{-1}). It is possible that the analytical techniques overestimated the amount of organic carbon by including some carbon in both fractions due to rupture of cells on the glass fibre filters during filtration, but this explanation alone cannot reconcile the differences. The dominant species in this bloom, cryptomonad A (Chapter 3), was observed in the laboratory to be highly motile and phototactic. Therefore it is possible that the phytoplankton had removed nutrients and DIC at a location away from the sampling site, but had congregated at the site possibly in response to light from the ice hole through which samples were collected, resulting in higher POC concentrations.

In summary, the uptake of the DIC and nutrients balanced reasonably well and allowed the calculation of the magnitude and rate of OC production. However, the measured amount of OC in the water column did not match that calculated from DIC and the nutrients. This disparity has been noted in previous Antarctic studies, and was

presumably due to the loss of OC by sedimentation or transferral to metazoan zooplankton and higher trophic levels.

4.3.4 Is the Ocean at O'Gorman Rocks a Sink of CO_2 for the Atmosphere?

From the fCO_2 values calculated for the O'Gorman Rocks site it is apparent that the area will be a sink for CO_2 throughout the year, except for the possibility of the short period of near-equilibrium in September - October. Gas transfer to the water will, of course, be hindered by the cover of ice that is present for all but 6 - 10 weeks of the year. The low fCO_2 recorded during the periods of open water should lead to the uptake of CO_2 by the ocean. In this section, the theoretical uptake of CO_2 at the O'Gorman Rocks site is calculated, and evidence from a number of sources is used to determine whether this uptake did in fact occur.

4.3.4.1 Calculation of the Amount of CO_2 Taken up by the Ocean

A number of equations has been developed that allow the calculation of the flux of CO_2 into or out of the ocean (e.g. Smethie et al., 1985; Liss and Merlivat, 1986; Wanninkhof, 1992). These equations are functions *inter alia* of wind speed and the difference in fCO_2 between the atmosphere and the ocean. The equation of Wanninkhof (1992) is used here to calculate the theoretical flux:

$$F = 0.0936\sigma_m W^2 (Sc/660)^{-0.5} (\Delta fCO_2) \qquad (4.2)$$

where F is the flux of CO_2 in grams of carbon per square metre per day, σ_m is the solubility of CO_2 (which in turn is a function of temperature and salinity, and was calculated using the equation of Weiss (1974)), W is the long term average wind speed in metres per second, Sc is the Schmidt number (which is a function of the viscosity of

the seawater and the diffusivity of gaseous CO_2, and which was calculated using the equation given in Wanninkhof (1992)), and ΔfCO_2 is the difference in fCO_2 between the atmosphere and the surface water. The atmospheric fCO_2 was assumed to be 358 µatm, and the constant included a term to convert to the units of gas transfer velocity to m day^{-1}.

The flux was calculated for the periods of open water during both the 1993-4 and 1994-5 summers. Wind speed was assumed to be the average monthly speeds recorded at Davis Station (Appendix B), water temperature 0 °C, surface water salinity 33.5 psu, and that fCO_2 varied linearly between sample dates. The calculations suggest an invasion of CO_2 into the ocean during the ice free period of 2.0 mol m^{-2} (equivalent to uptake of 87 µmol kg^{-1} throughout the water column) and 1.1 mol m^{-2} (equivalent to 50 µmol kg^{-1}) for the first and second summer respectively. These fluxes represent a small but significant percentage of the DIC inventory at the O'Gorman Rocks site, which, before the onset of phytoplankton activity, was approximately 51 mol m^{-2}. The calculated fluxes would replace 20 to 40 % of the maximum amount of CO_2 removed by biological activity during the periods of open water.

4.3.4.2 Evidence for CO_2 Uptake

As noted above, the calculated uptake of CO_2 from the atmosphere is equivalent to an increase in DIC by 50 - 90 µmol kg^{-1} throughout the water column. If this uptake occurred it should be identifiable in the DIC - nutrient plots (Figure 4.16), in which a shift to higher DIC would be expected during the ice free period. These plots, however, show no apparent change in the DIC-nutrient relationships before and after ice break out. However, any shift might not be identifiable due to the scatter of the data around the regression line.

The C:N molar uptake ratio calculated from these plots, 6.08 (considerably lower than the Redfield Ratio, 6.6 (Redfield et al., 1963)), provided indirect evidence for the uptake of CO_2 from the atmosphere. CO_2 uptake would result in an apparent decrease in this ratio, as it would appear that less DIC had been removed from the water than actually occurred. The C:N mole ratio of organic material caught in sediment traps during January 1995 was actually slightly higher than the Redfield Ratio (Chapter 5), which suggests CO_2 uptake from the atmosphere was occurring. Furthermore, the C:N assimilation ratio in Ellis Fjord, which remained ice covered throughout the study described in Chapter 7, was close to 7, also consistent with uptake of CO_2 from the atmosphere at O'Gorman Rocks.

The degassing of oxygen, which was supersaturated in the ocean during the ice free period, from the ocean (Section 4.3.2.2) provided further indirect evidence that a flux of CO_2 would occur from the gaseous to the aqueous phase, as CO_2 in the surface water was undersaturated with respect to the atmosphere. Approximately 30 % of the excess DO above saturation concentration was lost during the ice free period (Figure 4.23). Considering that the gas exchange rates for oxygen and CO_2 are quite similar (Broecker and Peng, 1982), it is expected that CO_2 uptake would occur to a similar extent.

Assuming that the C:N assimilation ratio during the ice free period from January 1995 was actually 6.6 rather than 6.08, an estimate of the CO_2 uptake can be developed. Plotting the DIC surfeit (calculated by subtracting the measured DIC concentrations from those calculated from nitrate concentrations) against the calculated oxygen deficit (Figure 4.23) suggests that the rate of CO_2 uptake was (very) approximately 25 % of oxygen degassing (it is recognised, however, that the regression is rather poor). This translates to DIC uptake of 5 $\mu mol\ kg^{-1}$ in mid-January, lower than the uptake calculated from Equation 8.3 above. The present approach does not allow integration of uptake over the ice free period, and direct comparisons between the two methods

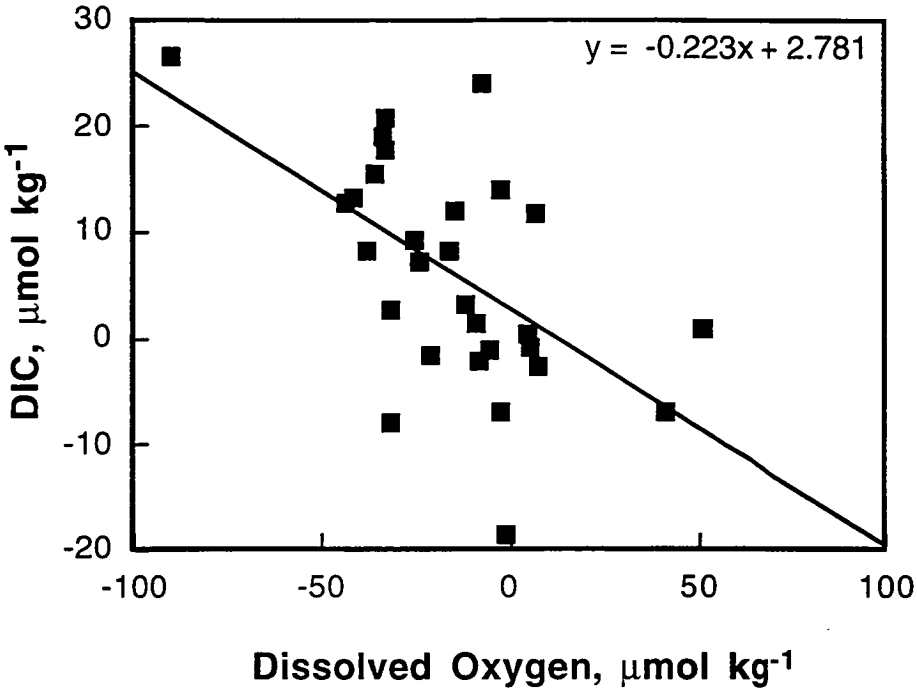

Figure 4.23. A plot of the calculated DIC surplus (assuming a C:N assimilation ratio of 6.6) against calculated dissolved oxygen deficit for the ice free period from 16 January 1995 until the end of the study.

are difficult. If the uptake of CO_2 from the atmosphere was only of the order of 5 µmol kg^{-1} it is unlikely that it would be evident in the DIC - nutrient plots.

Seasonal changes in the concentration of ^{13}C in the DIC also provide an insight into the extent of atmospheric CO_2 uptake by the ocean. As shown in Figure 4.4, $\delta^{13}C_{DIC}$ increased from 0.8 ‰ in early November 1994 to a summer maximum of 2.3 ‰. This increase could conceivably be due to uptake of CO_2 from the atmosphere or biological production.

The $\delta^{13}C$ of atmospheric CO_2 at Davis Station was in the range -7.80 ± 0.02 ‰ during the period from the beginning of November 1994 to the end of February 1995 (Figure 4.14). Seawater in equilibrium with atmospheric CO_2 of this isotopic ratio would not have the same $\delta^{13}C$ as atmospheric CO_2. The expected $\delta^{13}C$ of the DIC can be

calculated using the equation of Zhang et al. (1995). Assuming a water temperature of 0 °C, the predicted equilibrium seawater $\delta^{13}C_{DIC}$ would be in the range 2.7 - 2.8 ‰. Thus, the increase in $\delta^{13}C_{DIC}$ during summer could be the result of uptake of atmospheric CO_2 by the ocean, but would require the gaseous and aqueous phases to come close to equilibrium. It is clear, however, from Figure 4.4 that $\delta^{13}C_{DIC}$ began to increase from near constant late winter values in early December, well before the area became ice free. After ice break out, when uptake of CO_2 and therefore increase of $\delta^{13}C_{DIC}$ would have been expected, there was little consistent variation. These observations, as well as the limited apparent invasion of CO_2 from the atmosphere discussed above suggest that the system had not come to equilibrium, and that physical processes alone do not explain the seasonal variation in $\delta^{13}C_{DIC}$.

The variations in $\delta^{13}C_{DIC}$ are more consistent with biological activity. During photosynthesis, fractionation of the carbon isotopes occurs, as plants and algae preferentially take up the lighter isotope ^{12}C. In the marine system, the extent of the fractionation is a complex function of a number of factors, including the species of phytoplankton present, concentration of dissolved CO_2 (as distinct from carbonate and bicarbonate), temperature and phytoplankton growth rate (Mook et al., 1974; Wong and Sackett, 1978; Rau et al. 1989, 1991a, 1991c, 1992; Descolas-Gros and Fontugne, 1990; Falkowski, 1991; Kopczynska et al., 1995; Laws et al., 1995).

The average isotopic fractionation during organic matter production can be determined from a plot of DIC against $\delta^{13}C_{DIC}$ (Kroopnick, 1974); a plot of these parameters is shown in Figure 4.24, and the linear regression line indicated. All DIC lost from the water can be assumed to be converted to organic matter, and, using a mass balance equation, the $\delta^{13}C$ of the OC can be calculated from the slope of the regression line:

$$[DIC]_1\ \delta^{13}C_{DIC1} = [DIC]_2\ \delta^{13}C_{DIC2} + ([DIC]_2 - [DIC]_1)\ \delta^{13}C_{OC} \quad (4.3)$$

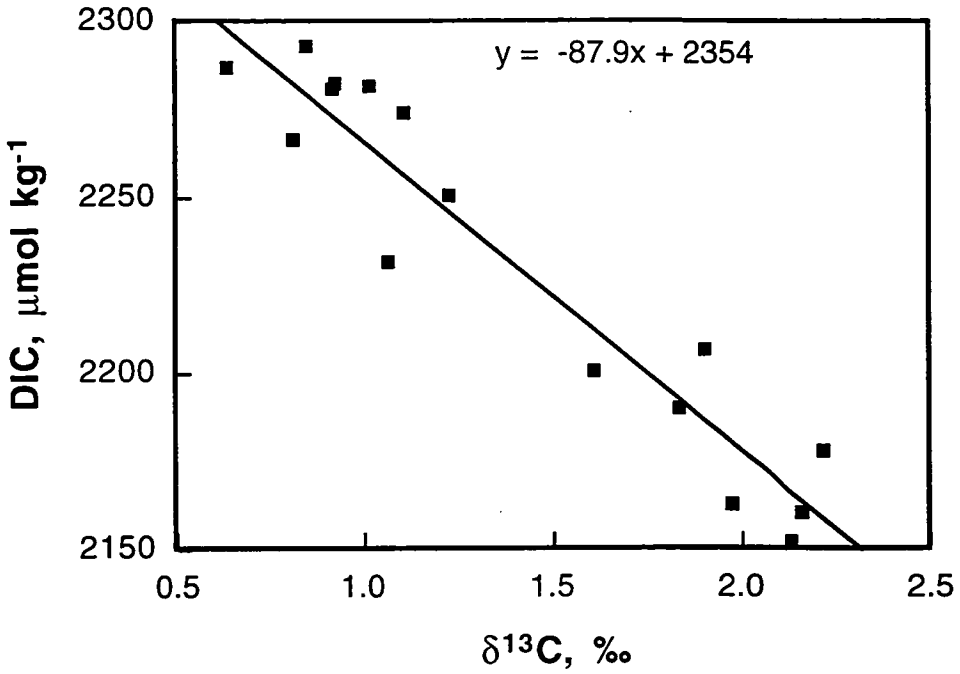

Figure 4.24. A plot of DIC (normalised to S = 35 psu) against $\delta^{13}C_{DIC}$. The low $\delta^{13}C_{DIC}$ data from August and September have not been plotted.

where [DIC] is the concentration of DIC, $\delta^{13}C_{DIC}$ is the $\delta^{13}C$ of the DIC, $\delta^{13}C_{OC}$ is the $\delta^{13}C$ of the OC produced and the subscripts '1' and '2' refer to any 2 points along the regression line.

Substituting values from the line of best fit in Figure 4.24 into Equation 4.3 yields an average $\delta^{13}C$ for the organic carbon of -23.8 ‰, consistent with the $\delta^{13}C$ of POC caught in sediment traps at the site (Chapter 5), which for most of the year was near -22 ‰. Therefore, the variation of $\delta^{13}C_{DIC}$ was consistent with biological production as well as uptake of CO_2 from the atmosphere. It must again be pointed out that the scatter of the data points in Figure 4.24 could hide the effect of DIC uptake. However, the scatter could also be a reflection in variation in the fractionation associated with organic carbon production.

It is also possible that uptake of CO_2 (and isotopic fractionation) continued after the water had left the sampling site. If the greater part of the biological production

occurred when the water was in shallow regions close to the coast (i.e. when the water was at or near O'Gorman Rocks), there may have been insufficient time for gas exchange to take place prior to sampling. Instead, uptake occurred after the water had left the area. This would also explain the lack of ice cover dependence of the correlations between DIC and the nutrients.

4.4 Conclusions

The results of the study described in this chapter provide insight into biogeochemical processes occurring in coastal waters adjoining the Antarctic continent. The seasonal cycle of primary production at the O'Gorman Rocks site was similar to that observed in other inshore Antarctic studies. However, considerable variation occurred between the two summers of the study both in the timing and number of the peaks of biomass. This reflects the influence of physical processes such as the persistence of the ice cover and advection of low biomass, high nutrient water into the inshore waters during summer. The development and timing of coastal phytoplankton blooms will be strongly influenced by these processes, and there is unlikely to be an entirely 'typical' summer in which the processes occur in a completely predictable fashion.

The autumn recovery of the concentrations of nutrients and DIC did not occur rapidly, but rather continued until September and October, immediately prior to the commencement of water column primary productivity in the subsequent summer. This observation was consistent with most of the biomass produced being remineralised within the incipient WW layer, which returned nutrients to the surface waters by convective mixing. The slow increase reflected deeper mixing of the WW as winter progressed. Entrainment of deep water into the WW replaced nutrients transported by sedimentation of organic material to beneath the base of the WW. Deep convection did not play a major role in the recovery of the DIC and nutrient concentrations in winter.

The uptake ratios of DIC and the nutrients during organic matter production were reasonably consistent throughout the study, and it would be expected that the concentration of DO, produced during photosynthesis, would also be closely related to these parameters. However, some evidence was observed to suggest that oxygen was lost to the atmosphere during the ice free summer period when the gas was supersaturated in the surface waters. This loss would exacerbate the undersaturation of DO observed in the WW layer.

When the amount of DIC lost from the water column was compared to measured concentrations of organic carbon, it was apparent that a lot of OC was missing, indicating that sedimentation or grazing of OC were important loss terms. Even though primary productivity resulted in CO_2 in the water column being undersaturated with respect to the atmosphere throughout the period of open water in summer, only limited evidence for the transport of CO_2 into the ocean was observed, though the flux might have occurred in the water after it had left the sampling site, especially if much of the decrease in fCO_2 had occurred in inshore waters.

CHAPTER 5

ORGANIC MATTER SEDIMENTATION AND BURIAL AT O'GORMAN ROCKS

5.1 Introduction

The uptake of CO_2 by phytoplankton during photosynthesis, which results in a seasonal CO_2 deficit in ocean surface waters, is the first step in the transfer of carbon from the atmosphere to long term sinks. The second step is the transport of this POM to deep water or the ocean floor, and the final step is its burial and long term preservation of this material in the sediment. This chapter discusses sedimentation of POM from the water column to the sediment and its subsequent burial at the O'Gorman Rocks site, and compliments the data presented and discussed in Chapter 4.

5.2 Results

All experimental data discussed in this chapter are given in tabular format in Appendix E.

5.2.1 Total Sedimentation

The seasonal cycle of the total sedimentation rate (i.e. including organic and non-organic fractions) at the O'Gorman Rocks site is shown in Figure 5.1. Little variation was observed between the sedimentation rates at the different trap depths (5, 10, 15 and 20 m), and the graph shows the average of data from all traps deployments (Appendix A), excluding the 20 m trap from April to October and again from ice break out to the end of the study (discussed further below). Estimates of the total and OC

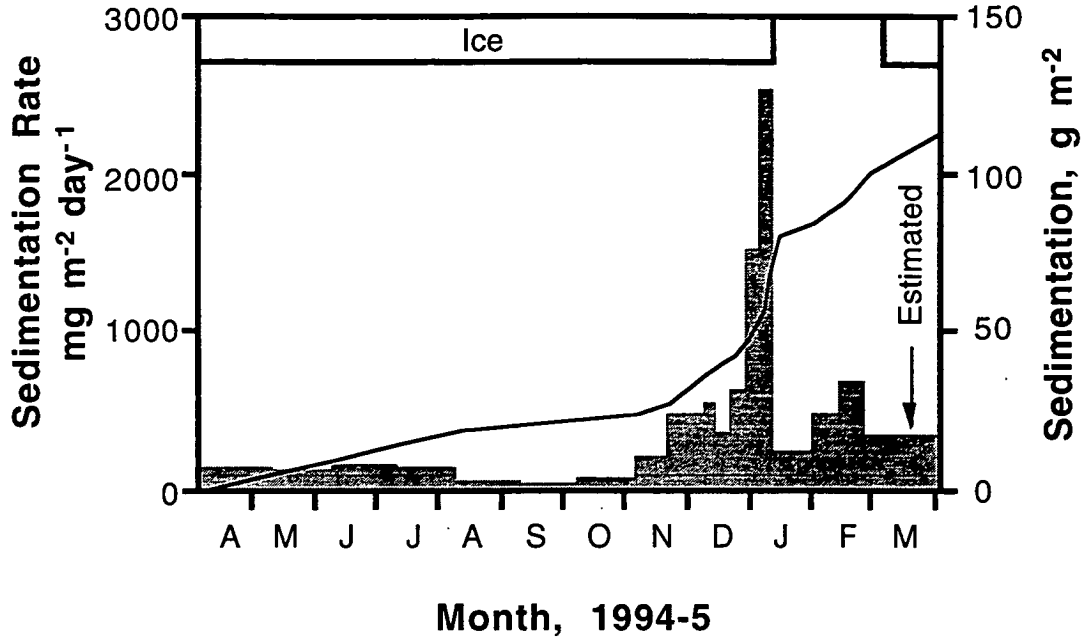

Figure 5.1. Total sedimentation rates (columns, left hand axis) and cumulative sedimentation (line, right hand axis) at the O'Gorman Rocks site between April 1994 and April 1995.

sedimentation rates from 27 February to 4 April 1995 were made using the method described in Appendix A.

Total sedimentation rates early in the study (April - July) were relatively uniform, averaging 146 mg m^{-2} day^{-1}. The rate dropped in August to approximately 60 mg m^{-2} day^{-1}, and remained near this level until October. A rapid increase in sedimentation occurred during November to an initial maximum of 560 mg m^{-2} day^{-1} in early December, before another, sharp, increase late in the month and in early January resulted in a peak rate of 2560 mg m^{-2} day^{-1}. The rate dropped dramatically after the fast ice broke out in early January, and then rose to another minor peak associated with a diatom bloom during February (Chapter 3).

Also shown in Figure 5.1 is the cumulative sum of total sedimentation, which amounted to 113.3 g m^{-2} yr^{-1}, equivalent to an average daily flux of 310 mg m^{-2} day^{-1}.

5.2.2 Organic Carbon Sedimentation

The rate of OC sedimentation, shown in Figure 5.2, followed a similar cycle to the rate of total sedimentation, being lowest (2 - 5 mg m^{-2} day^{-1}) between August and October, and highest (161 mg m^{-2} day^{-1}) in early January before a marked decrease associated with the break out of the fast ice. The minor peaks between mid-November and early December, and in February were relatively more important for carbon than total sedimentation. The comments made above in Section 5.2.1 regarding the use of data from the 20 m trap in the calculation of sedimentation rates during winter and after ice break out also apply to OC sedimentation.

Figure 5.2 also shows the cumulative sum of OC sedimentation, which totalled 9.8 g m^{-2} for the year (equivalent to an average daily OC flux of 27 mg m^{-2}). OC caught in

Figure 5.2. Sedimentation rate of OC (columns, left hand axis) and cumulative OC sedimentation (line, right hand axis) at the O'Gorman Rocks site between April 1994 and April 1995.

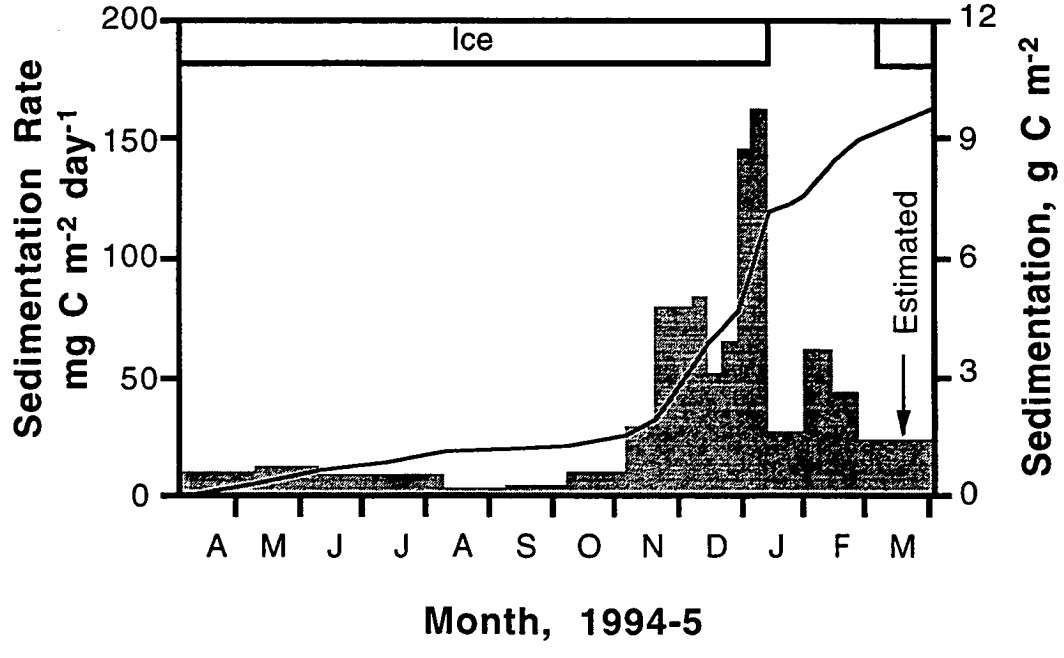

the sediment traps during the non-summer months accounted for approximately 25 % of the annual total.

No estimate was made of the sedimentation rate of inorganic carbon. However, very few carbonate-containing organisms such as coccolithophorids, foraminifera or pteropods were noted in the water column or sea ice (K. Swadling, personal communication) or in the sediment traps. No evidence for the formation of authigenic calcium carbonate was observed, and thus the role of inorganic carbon in total carbon sedimentation from the water column was probably of little consequence.

The percentage that OC made up of the total sedimenting material varied considerably during the study (Figure 5.3), dropping slightly during winter from the initial percentage of 6 % before rising steadily in spring and early summer. The maximum

Figure 5.3. The percentage of OC in the sedimenting material. The symbols used in this and all similar figures in this chapter are: 5m, ◇; 10 m, ○; 15 m, △; and 20 m, ✣. The line is the average of the data. Superimposed on the graphs are the rates of OC sedimentation from Figure 5.2.

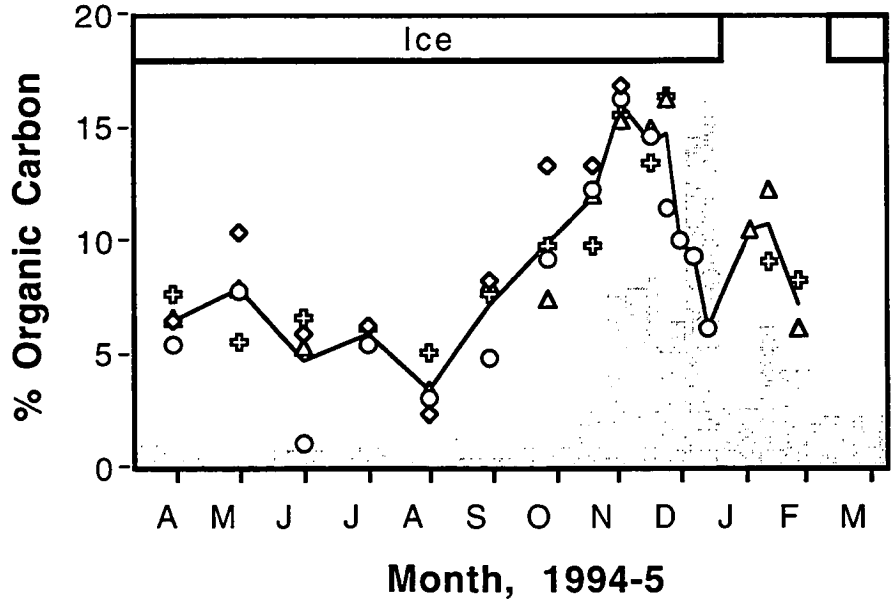

percentage, which was over 15 %, was reached in late November and early December (coincident with the initial peak in OC sedimentation), and was followed by a sharp drop back to 6 %. The percentage increased again during the February phytoplankton bloom, but by the end of the month had returned to near that recorded at the beginning of the study.

5.2.3 The Problem of Resuspension

Trapping of material resuspended from the sediment surface by wave action and current flow will lead to erroneously high estimates of the sedimentation rate. This process will be a greater problem for sediment traps close to the sediment-water interface, as the effect of resuspension should be inversely related to the distance that a trap is above the bottom of the water column (Håkanson et al., 1989; Overnell and Young, 1995). Resuspension will be lower in quiescent water where turbulence is suppressed or absent. The consistently higher total and organic sedimentation rates recorded from the 20 m trap (which was only 3 m above the sediment surface) during the winter months compared to those in the upper waters (Appendix E), suggested that some resuspension did in fact occur. From the start of the study until the end of October, total sedimentation recorded at 20 m averaged 60 mg m^{-2} day^{-1} greater than the average of the rates recorded in the shallower traps (n = 7, standard deviation = 24 mg m^{-2} day^{-1}). OC at 20 m during the same period was similarly higher, with the average increase being 4.6 mg m^{-2} day^{-1} (n = 7, standard deviation = 3.4 mg m^{-2} day^{-1}). Assuming that the rate of trapping of resuspended material over time was constant, this source appeared to account for 30 - 60 % of carbon collected in the 20 m traps from the start of the study to the end of October, but a lower percentage of the material in the other traps. Due to the increase in the apparent sedimentation flux resulting from resuspension in the trap at 20 m, the data from this period were not included in the calculations of both total and carbon fluxes.

The rates of trapping of resuspended material, which would be expected to remain at approximately the same levels until the break out of the fast ice in January, were insignificant compared to the far higher total and organic sedimentation rates recorded during November, December and early January, and thus could be ignored for this period.

After ice break out, when waves and swells would not have been damped by the presence of the ice cover, turbulence at the water-sediment interface would have increased, and resuspension could have been considerably higher. Between 30 January and 13 February, total sedimentation at 20 m was greater than at 15 m (though organic sedimentation at the two depths was nearly identical (Appendix E)). In the subsequent trap deployment, the differences were even greater in both total and carbon sedimentation. These results reflected in part the relatively uniform distribution of phytoplankton in the water column (Chapter 3), but this alone cannot account for the increased rates recorded at 20 m. Little microscopic evidence for resuspension in the trapped material was observed during this period. However, the more conservative estimates of total and carbon sedimentation from the trap at 15 m are shown in Figures 5.1 and 5.2 and were used in calculating the annual sedimentation rates.

5.2.4 Carbon to Nitrogen Mole Ratio of the Sedimenting Material

The carbon to nitrogen mole ratio of the material caught in the sediment traps (Figure 5.4) was initially slightly above the Redfield Ratio (6.6: Redfield et al., 1963). The ratio rose steadily until September (coinciding with the period of minimum sedimentation) before decreasing to near the Redfield Ratio in December. A short lived increase after the break out of the ice was followed by a return to the initial ratio by the end of the study. The C:N mole ratio was essentially the same at all trap depths on any particular recovery date except for a time during the period of lowest sedimentation, when much greater variation occurred. The mass weighted average C:N mole ratio

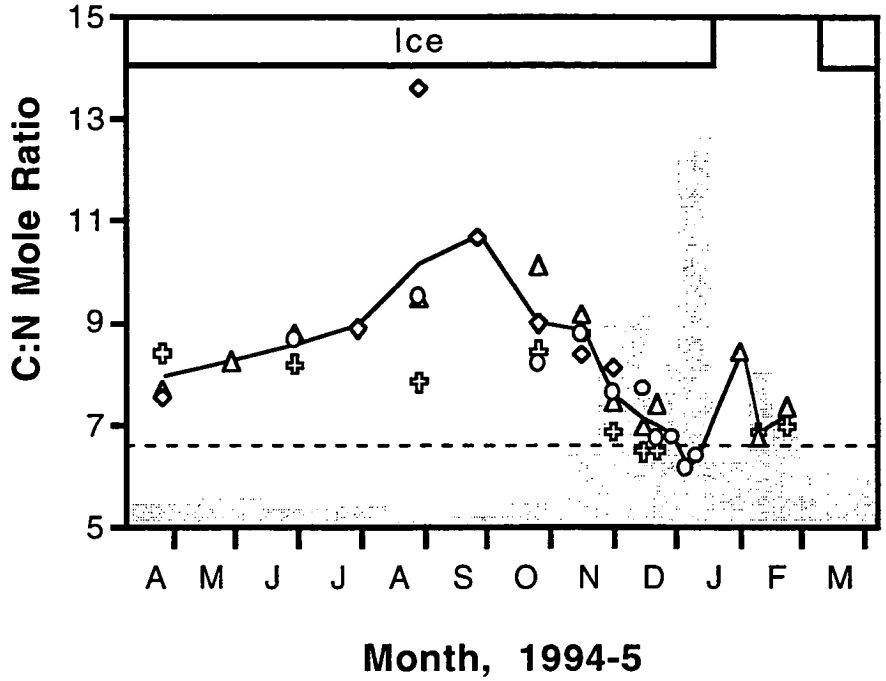

Figure 5.4. The carbon to nitrogen mole ratio of the sedimenting material. The dashed line represents the Redfield Ratio. See Figure 5.3 for an explanation of the plot symbols and background.

(taking into account the varying rates of sedimentation) was 7.6, inferring an annual sedimentation rate of organic nitrogen of *circa* 1.5 g m^{-2}.

5.2.5 The $\delta^{13}C$ of the Sedimenting Organic Carbon

The $\delta^{13}C_{OC}$ of the material caught in the sediment traps (Figure 5.5), was close to -20 ‰ at the start of the study, and dropped to -24 ‰ in September during the period of lowest sedimentation rate. A dramatic increase in $\delta^{13}C_{OC}$ began during October, with a peak close to -13 ‰ occurring in November. This was followed by a minimum in mid-December, whereafter $\delta^{13}C_{OC}$ rose slightly for the rest of the study. The $\delta^{13}C_{OC}$ in the final samples collected were only marginally higher than at the start of the study. There was little inter-depth variation in $\delta^{13}C_{OC}$ except for during October and November, the period of most rapid change in the isotope shift. The mass weighted average $\delta^{13}C_{OC}$ over the entire study was -18.8 ‰.

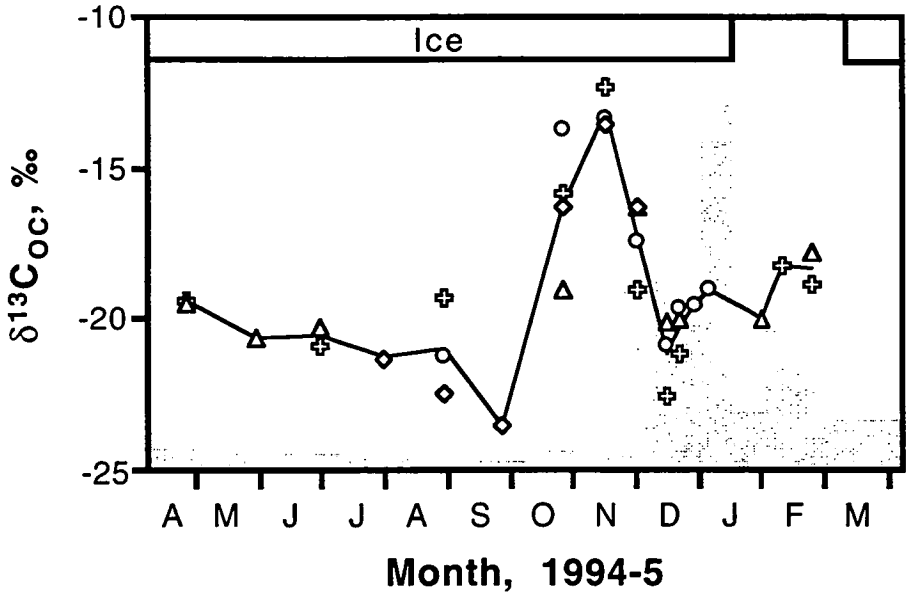

Figure 5.5. Seasonal trend in the $\delta^{13}C$ of organic carbon in the sedimenting material. See Figure 5.3 for an explanation of the plot symbols and background.

5.2.6 Characteristics of the Sedimenting Material

The material caught in the sediment traps during the first deployment period of the study was dominated by diatoms, including members of the genera *Eucampia* (including many heavily silicified overwintering cysts), *Chaetoceros* (also including heavily silicified forms), *Nitzschia, Fragilariopsis, Corethron* and *Thalassiothrix*. A small number of zooplankton faecal pellets, mostly cigar shaped with approximate dimensions 200 x 40 µm, was also present. These pellets contained complete and broken diatom frustules and organic material enclosed within an organic periotrophic membrane. The source of these faecal pellets was not entirely certain, but was possibly the amphipod *Paramoera walkeri* Stebbing which was associated with the undersurface of the sea ice at the O'Gorman Rocks site throughout winter (K. Swadling, personal communication). A similar selection of diatoms was present in the traps at the end of the second deployment, though faecal pellets were far more predominant than in material recovered in May.

The cigar shaped faecal pellets made up the majority of the organic fraction of the trap material from June until early November, when chains of the diatom *Entomoneis kjellmanii* appeared in the traps in large numbers. The abundance of this species peaked in mid-November, and it was replaced in December by other diatom genera, including most of those observed early in the study, as well as *Odontella, Coscinodiscus* and chain-forming *Thalassiosira* species. A similar suite of diatoms, along with smaller numbers of faecal pellets, was observed in the sediment traps throughout the rest of December and January, though *Fragilariopsis* spp. became more dominant as the summer progressed. Considerable numbers of copepod eggs, most likely of the species *Paralabidocera antarctica* (I.C. Thompson) (K. Swadling, personal communication), were trapped in late December. Somewhat surprisingly, the diatom *Thalassiosira dichotomica* (Kozl.) Fryxell, which was the dominant phytoplankton species in the water column late in the study (Chapter 3), did not appear in significant numbers in the sediment traps. Very few individual cells of the flagellate cryptomonad A, which was dominant in the water column in early December (Chapter 3), were observed in the traps, and large colonies of *Phaeocystis* cf. *antarctica* were entirely absent, which was consistent with absence of such colonies from the phytoplankton community during this summer.

The non-biogenic fraction of the sedimenting material consisted of clastic material, which ranged in size from fine silt to coarse sand, with occasional pieces of gravel up to 3 mm across. This material was an important component of the total flux during December and early January, but did not constitute a significant proportion of the sedimenting material either during winter and spring or after the break out of the fast ice.

5.2.7 Carbon in the Sediment

A short sediment core collected from the site of the trap deployment consisted to a large extent of fine silt and diatomaceous material, with occasional larger pieces of sand and gravel. The colour of the core material when wet was green-brown, and, after drying, tan-brown. In the top 5 cm of the core little macroscopic biological carbonate was evident, but deeper in the core large pieces of shell, probably of the bivalve *Laternula elliptica* (King and Broderip), a common filter feeder in the infauna of sediments of the inshore environment (Everitt et al., 1980; Tucker, 1988), were common. The water content of the core was above 80 % at the water-sediment interface, dropping to about 65 % at 10 cm (Figure 5.6). No evidence of anoxic conditions in the core (colour, smell) was observed.

Figure 5.6. Chemical characteristics of the short sediment core obtained from the O'Gorman Rocks site. The C:N mole ratio and the $\delta^{13}C_{oc}$ are for the organic fraction of the core.

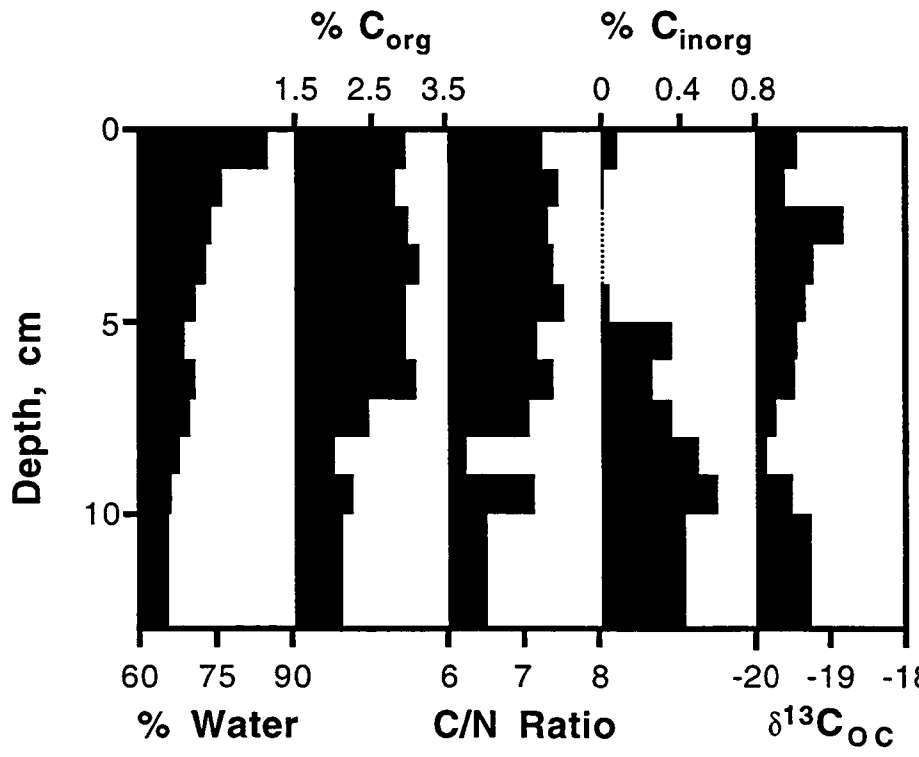

The percentage by weight of total carbon in dried core sections decreased from 3.1 % at the surface to 2.6 % at 10 cm. OC made up the greater part of total carbon in the top 5 cm, but beneath this depth, inorganic carbon became relatively more significant (Figure 5.6). Between 8 cm and the bottom of the core, the percentage of OC was near 2.1 %, with 0.5 % inorganic carbon. The carbon to nitrogen mole ratio in the organic fraction of the core material was essentially constant in the top 8 cm (range 7.1 - 7.5, Figure 5.6), but was lower at the bottom of the core. Organic nitrogen accounted for between 0.3 and 0.4 % of the dried core material.

Also shown in Figure 5.6 is the variation of the $\delta^{13}C_{OC}$ in the sediment core, which ranged from -18.8 ‰ to -19.9 ‰. The dry mass weighted average $\delta^{13}C_{OC}$, -19.4 ‰, was only slightly lower than the average for OC caught in the sediment traps (-18.8 ‰). The $\delta^{13}C$ of large pieces of shell material from beneath 7 cm averaged 1.39 ‰ (range: 1.28 - 1.46 ‰, n = 3).

5.3 Discussion

5.3.1 Sediment Trap Design

Blomqvist and Håkanson (1981) and Håkanson et al. (1989) suggested that the following considerations be taken into account when choosing sediment traps:

- traps should be simple cylinders
- narrow necked traps should be avoided, as they overtrap sediment
- funnels should be avoided, as they undertrap sediment
- cylinders should have height to diameter ratios greater than 3
- cylinders should have a diameter greater than 4 cm.

The characteristics of the sediment traps used in the present study were not optimal, as the height to diameter ratio, 2.2 (Figure A.2), was less than recommended. Blomqvist and Kofoed (1981) reported that in most cases traps of this ratio collected the same amount of material as traps with a ratio greater than 3, but that such traps would be expected to perform less efficiently in turbulent conditions, when resuspension of material in the traps could occur. Fortunately, turbulence at the O'Gorman Rocks site would have been damped due to the presence of the ice, and thus it is probable that the traps used were able to collect and retain sedimenting particles efficiently. Some underestimation of the true sedimentation rates probably occurred during periods of open water as a result of loss of material from the traps.

The use of poisons such as mercuric chloride, formaldehyde or iodine to reduce heterotrophy in the traps was not recommended by Håkanson et al. (1989), who felt that they cause more problems than they solve for the chemistry of the trapped material and the naturally occurring biological community structure. The absence of poison, however, means that remineralisation processes of the trapped material continues. Bloesch and Burns (1980) have shown that loss of OC and nitrogen can be as high as 10 % over a period of 14 days in unpoisoned traps. No poisons were used in the traps in the present study. Thus, the data presented in this chapter and in Chapter 8 are likely to underestimate the true sedimentation rates. The design of the sediment traps and difficulties encountered with deploying them through the small hole drilled through the ice, which inevitably contained an icy mush, also meant that use of a poison was impracticable.

5.3.2 The Cycle of Sedimentation

The general features of the seasonal cycle of sedimentation at the O'Gorman Rocks site were very similar to those reported from other year-long studies in the Antarctic region (Platt, 1979; Matsuda et al., 1987b; Fischer et al., 1988; Wefer et al., 1988; Dunbar et

al., 1989; Wefer and Fischer, 1991; Nedwell et al., 1993). All these studies recorded great seasonal variation in the rate of sedimentation, being described by Wefer et al. (1988) as being 'on for two months, off for ten months'. The data from the present study indicate that although this is a reasonable description, sedimentation during spring and autumn (i.e. outside the period December - February) was also significant, accounting for up to 30% of the annual OC flux. However, it should be remembered that resuspension of surface sediment material could have contributed to this percentage (even when discounting the data from the traps at 20m in the calculations).

The cycles of total and organic sedimentation recorded during this study reflected variations in the strength of the three main sediment sources: diatoms, faecal pellets and clastic material. Early in the study (April - May), the sedimenting material was dominated by viable diatoms from a wide variety of genera. As has been observed in a number of previous Antarctic sediment trap studies (von Bodungen et al., 1986; Leventer, 1991), heavily silicified resting cysts of a number of species, including *Eucampia antarctica* and *Chaetoceros bulbosum* were included amongst this material. These species survive winter in this state before reforming vegetative cells in spring. The diatoms observed early in this study were either from the tail end of the summer phytoplankton bloom or from an autumn bloom associated with newly forming sea ice.

During winter, when sedimentation rates were lowest, trapped material was dominated by faecal pellets that were probably produced by amphipods that fed on diatoms growing in association with the undersurface of the sea ice. This material was characterised by low percentage of OC and relatively high C:N molar ratios, which was indicative of the removal of carbon, and, to a relatively greater extent, nitrogen during passage through the gut of the zooplankton (Matsuda et al., 1986). Biggs et al. (1989) recorded similarly high C:N molar ratios in faecal pellets caught in sediment traps at offshore sites in Prydz Bay.

The increase in the sedimentation rates during October and November was largely due to increased abundance in the traps of the diatom species *Entomoneis kjellmanii*. This species grows in association with the base of the sea ice (Perrin et al., 1987; Garrison and Buck, 1989; McMinn, 1996), and is regularly the first species to attain significant biomass both directly under the ice and throughout the water column in the Vestfold Hills region at the start of summer (Perrin et al., 1987; Davidson and Marchant, 1992a; McMinn and Hodgson, 1993; Chapter 3). The increase in the direct sedimentation of algal material led to an increase in the percentage of OC in the trapped matter, as well as a decrease in the C:N mole ratio. During early December, when living (or at least not significantly decomposed) diatom cells of a variety of species made up the bulk of the sedimenting material, the percentage OC was the highest recorded and the C:N mole ratios were close to the Redfield Ratio.

After mid-December the percentage OC dropped steeply, though the C:N mole ratio was little changed. Sedimentation during this period became increasingly dominated by inorganic clastic material, significant amounts of which had been blown onto the ice from the Vestfold Hills during blizzards in winter (J. Gibson and D. Franklin, unpublished data), had become trapped in the ice, and was now being released to the water underneath as the ice melted. The highest total sedimentation rates measured during the study were recorded in late December - early January just prior to the break out of the sea ice when the ice was structurally least sound. The constant C:N mole ratio of the organic material was consistent with biogenic fraction of the sedimenting material continuing to consist mainly of intact diatom cells. That the ice did not melt *in situ*, but rather drifted away from the trap site with wind and currents, probably resulted in more material in the ice, both inorganic and biogenic, being released to the water column (and thus the sediment) further offshore rather than at the site. This material would have been missed by the anchored sediment traps at O'Gorman Rocks.

Sedimentation after ice break out was again dominated by biogenic material. The percentage OC increased once more as the sedimentation of clastic material became unimportant, and the C:N mole ratio generally remained close to the Redfield Ratio.

The nature of the sedimenting material highlighted the fact that not all OC produced by phytoplankton sedimented at the same rates or by the same routes. The phytoplankton in the traps was dominated by diatoms, and the zooplankton faecal pellets also appeared to contain remains of diatoms. The carbon in the cells of flagellates was not transferred directly to the sediment, but rather must have been either rapidly remineralised on cell lysis and death within the water column, or was included in zooplankton faecal pellets. Both cell lysis of the flagellates and 'sloppy feeding' by zooplankton would result in transfer of intracellular material to the DOC pool, which would not sediment through the water column.

No evidence for the sedimentation of inorganic carbon was observed in the trap material. The lack of carbonate precipitation was consistent with the observations of Sambrotto et al. (1993), who recorded little carbonate flux from the surface waters of Gerlache Strait (near Bransfield Strait in the Antarctic Peninsula region; Figure 2.1), and Fischer et al. (1988), who reported that carbonate made up only 3 % of the total carbon flux in their year long study in the Weddell Sea.

It is surprising that the OC sedimentation rates calculated for the traps at 10, 15 and 20 m were similar, especially during early summer when the highest rates of sedimentation were recorded. If the distribution of the sedimenting material was uniform, it would be expected that the measured rate would increase with depth, as each trap is essentially integrating sedimentation from the entire water column above it. That sedimentation was uniform suggests that the major source of the sedimenting material was above the top trap, i.e. that most organic production was occurring directly under the ice. As this area would have had the highest light levels before ice

break out, this conclusion seems reasonable. After ice break out, sedimentation increased significantly with depth, and though this could be interpreted as being a result of increased resuspension, it might also reflect sedimentation from a more uniform phytoplankton source.

The efficiency of the traps used in the study is uncertain. A number of the problems were alluded to above: trap design was not optimal and the lack of poisons could have allowed losses of organic carbon by the action of heterotrophic organisms. Another factor was the heterogeneity of the bottom ice algal mat. Photographs of the bottom ice community near Davis Station in McConville and Wetherbee (1983) indicate that the mat community was not spatially homogeneous, and that large sections of the mat can detach randomly from the ice (forming 'marine snow') and fall to the sediment, especially during December. There was little evidence for such large detachments of mats in the trap material, possibly due to the presence of the trap array altering flow for large pieces of marine snow. Therefore, the flux data presented here may be in error, and it is entirely possible that the true organic flux to the sediment was greater than recorded.

5.3.3 Sedimentation Inventories and Rates: Comparison to Other Antarctic Studies

The rates of total and OC sedimentation determined in this study were remarkably similar to those reported in the only other comparable study in inshore waters of Eastern Antarctica undertaken near Syowa Station (Figure 2.1) (Matsuda et al., 1987b). In the Japanese study a maximum OC flux of 136 mg m^{-2} day^{-1} was measured (compared to the maximum flux of 161 mg m^{-2} day^{-1} at the O'Gorman Rocks site), and while Matsuda et al. (1987b) did not estimate an annual flux of OC, inspection of their data suggests it would be similar to that recorded in the present study.

Many of the other studies in the Antarctic region that have measured the annual flux of sedimenting OC were undertaken in deeper water further offshore. The traps in these studies were usually placed well below the base of the euphotic zone, and thus the data are not directly comparable to that obtained in the present study, as remineralisation of OC will occur as the particulate material falls through the water column, resulting in lower apparent carbon sedimentation rates. Measurements of OC production at the surface and sedimentation rates at depth have allowed the derivation of the following equation, which allows the calculation of primary productivity in the euphotic zone from trap data (Berger et al., 1988; Jahnke, 1996):

$$P = \frac{J}{\left(\frac{9}{z} + \frac{0.7}{\sqrt{z}}\right)} \qquad (5.1)$$

where P is primary production at the surface (grams per unit area per unit time), and J is the carbon flux (measured in the same units) at depth z metres. Annual carbon fluxes measured at depth in year-long Antarctic studies as well as the corresponding surface fluxes calculated using Equation 5.1 are given in Table 5.1.

The annual rates of sedimentation in Table 5.1 vary over nearly 4 orders of magnitude. It is likely that terrestrial input adds to sedimentation at Signy Island and South Georgia, but the variation in the remaining coastal and offshore sites is still surprising. The calculated amount of surface primary production will essentially be the amount of carbon exported from the euphotic zone, and organic production remineralised in this zone or transferred to higher trophic levels will not be included in this amount. Therefore, the apparently high productivity in the Bransfield Strait and the Ross Sea might be the result of inefficient remineralisation and grazing of phytoplankton near the surface, whereas the extremely low calculated productivity in the Weddell Sea

Location	Period of Collection	Depth of Deployment metres	Measured Flux g m^{-2} yr^{-1}	Calculated Surface Flux g m^{-2} yr^{-1}	Reference
South Georgia	4/75-3/76	Surface	60	60	Platt, 1979
Ross Sea	83-84	225	3.2	37	Dunbar, 1984
Bransfield Strait	12/83-11/84	494	7.0	140	Wefer et al., 1988
Bransfield Strait	12/83-11/84	1588	3.0	130	Wefer et al., 1988
Weddell Sea	1/85-3/86	863	0.024	0.58	Fischer et al., 1988
Signy Island	9/89-8/90	Surface	395	395	Nedwell et al., 1993
Signy Island	9/90-8/91	Surface	200	200	Nedwell et al., 1993
Ross Sea	1/90-2/92	250	5.5	69	DeMaster et al., 1992
Ross Sea	1/90-2/92	250	9.0	112	DeMaster et al., 1992
Prydz Bay	4/94-4/95	Surface	9.8	9.8	This study

Table 5.1. OC fluxes in year long studies of sedimentation in the Antarctic region. The surface fluxes were calculated using Equation 5.1.

suggests that a far greater percentage of primary production in this region is remineralised above the trap depth.

Sedimentation rates of OC during short term trap deployments in the Antarctic region during summer (tabulated in Karl et al., 1991) have been recorded to be as high as 1400 mg m^{-2} day^{-1} at a depth of 100 m (von Bodungen, 1986), which is nominally

equivalent to an OC flux at the surface of 8750 mg m^{-2} day^{-1}. Typical calculated surface OC fluxes, however, appear to be in the range 50 - 500 mg C m^{-2} day^{-1}. The data from the present study, and from that of Matsuda et al. (1987b), fall within this range, but towards the lower end. The variations in these fluxes could be due to a number of factors. Firstly, it should be recognised that trapping of material in sediment traps does not necessarily reflect the true flux (Buesseler, 1991), so that all these figures could be considerable under- or overestimations. If the measured rates are correct, very large variations in the rate of primary production would appear to occur: intense blooms of diatoms or other species liable to sedimentation could lead to mass sedimentation and thus the high rates observed. A third consideration is the role that zooplankton, especially krill (*Euphausia superba*), play in sedimentation. In many Antarctic studies it is reported that krill faecal pellets are the major source of sedimenting material throughout the periods of trap deployment (e.g. Dunbar, 1984; Fischer et al., 1988; Wefer et al., 1988; Biggs et al., 1989). Zooplankton dynamics and behaviour therefore will play an important role in determining the sedimentation rates. For example, zooplankton are able to focus sedimentation by swarming, and are also able to transport organic material from deep water back into the upper waters, which can then be re-sedimented, during diurnal vertical migration.

The variations in the sedimentation rates recorded in the Antarctic region make it difficult to draw any general conclusions apart from the extreme seasonality of the flux. The rates, both daily and annual, recorded at the O'Gorman Rocks site appear to be within the range observed in other Antarctic studies, and must therefore be considered not in any way unusual. However, that the rates in this study were similar to those recorded by Matsuda et al. (1987b) does suggest that sedimentation in inshore Antarctic water, where the effect of krill is negligible, could be quite uniform.

5.3.4 The $\delta^{13}C$ of the Sedimenting Organic Carbon

From April to early October, and again from the end of December until the end of the study, the $\delta^{13}C$ of the material caught in the sediment traps was in the range -23 to -19 ‰ (Figure 5.5). These values were significantly higher than recorded for particulate organic matter in many other Antarctic studies, in which shifts in the range -25 to -30 ‰ have been recorded (Sackett et al., 1965; Sackett et al., 1974; Bathmann et al., 1991; Rau et al., 1991a, 1991c; Dunbar and Leventer, 1992; Rogers and Dunbar, 1993; Kennedy and Robertson, 1995). The isotopic fractionation during the production of organic material at the O'Gorman Rocks site was calculated from the concentrations of DIC and the $\delta^{13}C_{DIC}$ to average -23.8 ‰ (Figure 5.24). Organic material produced in the water column would be therefore be predicted to have $\delta^{13}C$ in the range -24.2 ‰ to -21.5 ‰, as $\delta^{13}C_{DIC}$ ranged from -0.4 ‰ to 2.3 ‰ (Figure 5.4). Considering the scatter in the data in Figure 5.24, as well as interspecific variations in the isotope fractionation during photosynthesis and DIC uptake by phytoplankton and possible further fractionation resulting from passage through grazing and excretion by zooplankton (which increases $\delta^{13}C_{OC}$ by up to 3 ‰ (Wada et al., 1987; Bathmann et al., 1991; Fischer, 1991)), the $\delta^{13}C_{OC}$ measured in the sedimenting organic material at O'Gorman Rocks was altogether consistent with the water column chemistry.

Another factor which would have played a considerable role in determining $\delta^{13}C_{OC}$ during winter was resuspension of material from the sediment. Organic carbon in the surface sediment exhibited a $\delta^{13}C_{OC}$ of *circa* -19 ‰, which was higher than measured for the sediment trap material. Therefore, increased sediment resuspension would also result in higher $\delta^{13}C_{OC}$, obscuring the isotopic characteristics of the non-resuspended OC. Some evidence for an increase of $\delta^{13}C_{OC}$ with depth (resulting from increased trapping of resuspended material closer to the sediment) is apparent in the data, especially from August, but missing data make it difficult to draw conclusions for the entire non-productive period. From the $\delta^{13}C_{OC}$ recorded from the upper traps, it

appears that the isotopic ratio of non-resuspended material dropped during winter, possibly to a minimum of -24 to -25 ‰ in September.

In late October and November, $\delta^{13}C_{OC}$ of the trapped material increased dramatically to a maximum of -13 ‰. Production of material with this $\delta^{13}C_{OC}$ appears to be unprecedented in studies of Antarctic sediment trap or water column samples. The increase in $\delta^{13}C_{OC}$ was coincident with the appearance of large numbers of the diatom *Entomoneis kjellmanii* in the sediment traps. Rau et al. (1991a) and Dunbar and Leventer (1992) reported that the $\delta^{13}C$ of algae that had grown in sea ice was considerably higher than that of the water column, reaching -8.3 ‰. The enrichment in ^{13}C has been attributed to a number of factors (Descolas-Gros and Fontugne, 1990), but is most likely to be due to primary production drastically reducing the concentration of DIC in the brine channels of the sea ice, which increases competition for the lighter carbon isotope and thus increases $\delta^{13}C$. *Entomoneis kjellmanii* grows largely in mats at the base of the sea ice rather than within the fabric of the ice. However, it is likely that reduced concentrations of DIC also occur within such mats, as the water exchange with the rest of the water column will be limited both by the mat itself and boundary layer effects, and that increased competition for the lighter carbon isotope will occur.

The results from this study highlight the importance of organic material produced in close association with the ice in sedimentation of organic carbon in the inshore Antarctic environment. Assuming that organic material produced in the water column had on average $\delta^{13}C_{OC}$ of -20 ‰, sea ice (or under ice mat) diatoms -13 ‰, and that the average $\delta^{13}C_{OC}$ for the entire study was -18.75 ‰, it can be calculated that the percentage of sea ice material was approximately 20 % of the total OC flux. Comparison of the magnitude of the measured fluxes (Figure 5.2) during the period of maximum $\delta^{13}C$ to those later in the study, however, suggest that this percentage was actually considerably lower than suggested by this calculation. Horner and Schrader

(1982) reported that 65 % of sedimenting material came from the ice during a study in the Beaufort Sea, though water column chl *a* concentrations were significantly lower during summer in this study than at the O'Gorman Rocks site. The percentage that sedimentation from the sea ice will make up of the total will obviously vary from year to year in response to productivity and remineralisation in both the ice and water column environments as well as export from both environments, but will always be significant.

The $\delta^{13}C_{OC}$ throughout the sediment core was very similar to the annual average $\delta^{13}C$ recorded from the water column (-18.75 ‰). Some fractionation would be expected during remineralisation processes in the sediment, but this action would be unlikely (Fischer, 1991) to alter the $\delta^{13}C$ from values -25 to -30 ‰, expected if sedimentation at the site had 'typical' Antarctic values, to -19 ‰. The $\delta^{13}C_{OC}$ in other modern marine sediment cores from the Antarctic region have been found generally to range from -25 ‰ to -28 ‰ (Sackett, 1986a, 1986b). Wada et al. (1987) did, however, record $\delta^{13}C_{OC}$ at the top of deep sea sediment core of -20.2 ‰, and concluded that the phytoplankton cells which made up the organic fraction of the core must have grown under low DIC conditions. These data indicate that the core from the O'Gorman Rocks site had anomalously high $\delta^{13}C$ in comparison to other Antarctic cores, and that sedimentation of high $\delta^{13}C_{OC}$ material had occurred over an extended period. Marine sections of sediment cores obtained from marine-derived lakes in the Vestfold Hills and dated by radiocarbon techniques (Bird et al., 1991) show similar $\delta^{13}C_{OC}$ to the core from O'Gorman Rocks, suggesting that the sedimentation of high $\delta^{13}C_{OC}$ material from either sea ice or water of low DIC concentration resulting from high productivity in the inshore region has been occurring in this area for many thousands of years.

5.3.5 Factors Influencing $\delta^{13}C$ of the Sediment Trap Material

A number of models has been suggested to explain variations observed in the $\delta^{13}C_{OC}$ of POM throughout the ocean. The variation in the fractionation will depend on the physical and chemical environment in which the organic matter is formed and the mechanism by which carbon is transferred between carbon reservoirs. In the case of the production of organic material by phytoplankton during photosynthesis, the fractionation was originally thought to have been controlled by temperature (Sackett et al., 1965; Eadie and Jeffrey, 1973; Fontugne and Duplessy, 1981), and more recently to be a function of $[CO_{2(aq)}]$, (as distinct from the carbonate and bicarbonate ions) (Rau et al., 1989, 1991c, 1992). Laws et al. (1995), however, demonstrated recently in a laboratory study that the isotopic fractionation was inversely proportional to $[CO_{2(aq)}]$ but proportional to the growth rate of the phytoplankton. It is unlikely that these variables are the only influences on isotope fractionation in the formation of organic carbon, as other factors, such as phytoplankton species composition, have also been shown to effect the fractionation (e.g. Falkowski, 1991; Hinga et al., 1994; Fry, 1996).

The relationships between $\delta^{13}C_{OC}$, water temperature and $[CO_{2(aq)}]$ are of particular interest, as they in theory allow reconstruction of the surface water environment at the time of organic carbon formation from $\delta^{13}C_{OC}$ in sediment cores and marine-derived rocks. For example, if $\delta^{13}C_{OC}$ is in reality closely correlated to water temperature, information about ocean surface water temperature and therefore global climate can be ascertained, and, if the relationship with $[CO_{2(aq)}]$ holds true, atmospheric CO_2 concentrations can be estimated (e.g. Arthur et al., 1985; Popp et al., 1989; Rau et al., 1989; 1991b). In this section, the data from the present study are considered in terms of each of the three models mentioned above, and the utility of the models discussed.

The sediment trap $\delta^{13}C_{OC}$ data are plotted against water temperature (at the depth of the trap on the date of recovery) in Figure 5.7, along with the empirical $\delta^{13}C_{OC}$ - temperature relationship determined by Rau et al. (1991c) on a cruise across the Drake Passage between the Antarctic Peninsula and South America:

$$\delta^{13}C_{OC} = -29.13 + 0.62\ T \qquad (5.2)$$

where T is the temperature in °C. Figure 5.7 indicates that the data from the present study did not fall near the curve given by Equation 5.2. The temperature at the trap depth, however, might not reflect that at the depth at which the OC was produced, but the temperature calculated from Equation 5.2 for the production of OC with $\delta^{13}C_{OC}$ of 13 ‰, approximately 26 °C, is unlikely to be reached in the Antarctic marine environment. It is probable that temperature plays some direct role in the determination

Figure 5.7. The $\delta^{13}C_{OC}$ of the sedimenting material plotted against the water temperature at the trap depth on the day of recovery. Also shown is the relationship (Equation 5.2) found by Rau et al. (1991c) to relate $\delta^{13}C_{OC}$ and water temperature in another Antarctic study.

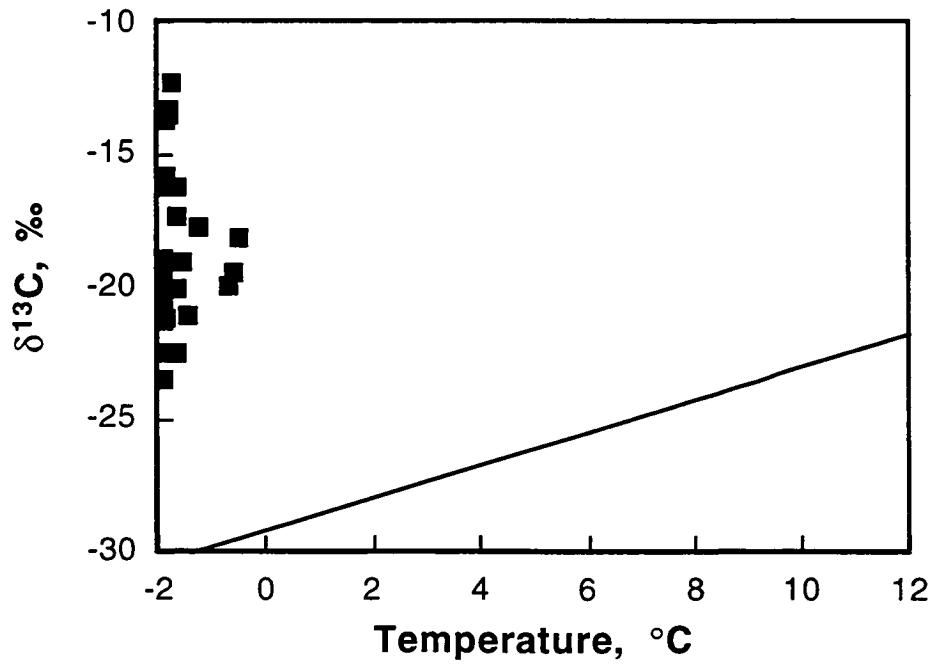

of the $\delta^{13}C$ of phytoplankton, but the data from the present study suggest that this role is small. These results, however, support the conclusion that results from one section of the Antarctic region -in this case the Drake Passage - cannot be directly applied to others.

The second model suggests that there is a linear relationship between $\delta^{13}C_{OC}$ and $[CO_{2(aq)}]$. Rau et al (1991c) found the following equation described the relationship between these parameters during their study in the Drake Passage:

$$\delta^{13}C_{OC} = -9.40 - 0.90[CO_{2(aq)}] \quad (5.3)$$

A similar empirical relationship has been recorded for samples from the North Atlantic Ocean (Rau, 1992).

The relationship between $\delta^{13}C_{OC}$ of sediment trap material and $[CO_{2(aq)}]$ (Appendix E) is shown in Figure 5.8. Also shown is the line defined by Equation 5.3. The data are separated into three groups, and are represented by different plot symbols in the figure: (i) from the start of the study until 7 October, represented by squares; (ii) from 4 and 19 November (diamonds); and (iii) from 7 December until the end of the study (crosses).

The only group of data points to fall anywhere near the line defined by Equation 5.3 were for the samples collected late in the study, though even this relationship was poor. This data was for the period when production of POC occurred in the water column (i.e. not associated with the sea ice), and was therefore more or less equivalent to the conditions for which Rau et al (1991c) determined Equation 5.3. The scatter in the data in the present study could be in part a result of the $[CO_{2(aq)}]$ used in the plot being those for the recovery date and depth of the trap rather than in the water in which the organic material was produced. It is probably ingenuous to expect a single

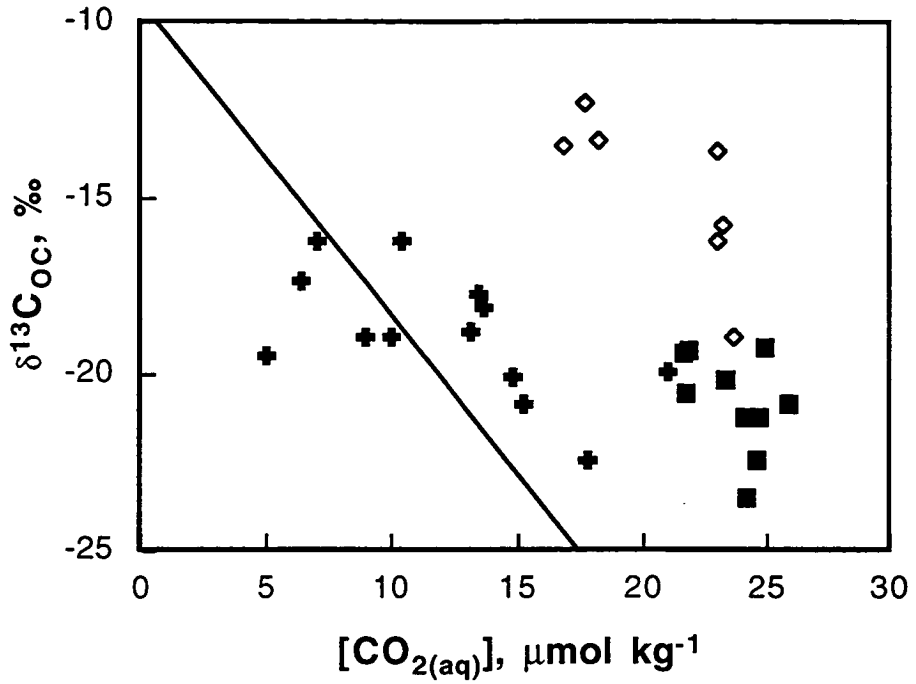

Figure 5.8. The $\delta^{13}C_{OC}$ of the sedimenting material plotted against the calculated $[CO_{2(aq)}]$ on the date of trap recovery. Also shown is the lines defined by Equation 5.3 The various plot symbols are described in the text.

relationship to occur in a complex system. The $\delta^{13}C_{OC}$ of different species of phytoplankton is not constant, even when grown under the same physical and chemical conditions (Descolas-Gros and Fontugne, 1990; Falkowski, 1991; Fry and Wainwright, 1991; Fry, 1996), and shifts in the dominant phytoplankton species (i.e. those species competing more intensely for CO_2) or the species actually sedimenting could also have been the reason for the poor relationship. The effects on $\delta^{13}C_{OC}$ of the processing of OC by pro- and eucaryotic heterotrophs, which is poorly known, could also be important.

The data from November plotted on the high $[CO_{2(aq)}]$ side of the line, which suggested that the particulate organic matter collected during this period was formed in an environment with much lower $[CO_{2(aq)}]$ than that in which it was trapped. This was consistent with the formation of this material either in brine channels in the ice or in a mat directly under the ice in which enhanced competition for CO_2 (and therefore

reduced fractionation) would occur as a result of the reduction in the concentration of DIC. The material was then trapped in water of much higher [$CO_{2(aq)}$] after becoming detached from the ice.

The data from winter also plotted on the high [$CO_{2(aq)}$] side of the line, but at lower $\delta^{13}C_{OC}$ than the material in the second group. There was little, if any, water column primary productivity during this period, and therefore it is not surprising that Equation 5.3 did not hold. There could be two reasons for the data plotting where it does. Firstly, some of this material might have been produced during an autumn ice bloom, and therefore in an environment with lower [$CO_{2(aq)}$] than in the water column. Secondly, the shift away from the line could reflect the relatively large input of resuspended material into the traps during this period. $\delta^{13}C_{OC}$ at the sediment surface was circa -19.5 ‰, and inclusion of significant amounts of this material would affect the value for the trap material. As mentioned above, resuspension appeared to be a greater problem for the trap at 20 m than for those closer to the surface. $\delta^{13}C_{OC}$ data is only available from limited recovery dates for traps from this depth, but the average for these traps was -19.8 ‰ (c.f. an average of -21.2 ‰ for traps at other depths), close to the $\delta^{13}C_{OC}$ of the sediment surface and supporting the role of resuspension.

The third model suggests that fractionation of ^{13}C during photosynthesis (i.e. the difference between $\delta^{13}C_{DIC}$ and $\delta^{13}C_{OC}$) is a function of the growth rate of the phytoplankton and is inversely proportional to [$CO_{2(aq)}$] (Laws et al., 1995):

$$\varepsilon = k - k'\mu/[CO_{2(aq)}] \qquad (5.4)$$

where ε is the fractionation, μ is the growth rate, and k and k' are constants. Thus a plot of ε against $\mu/[CO_{2(aq)}]$ should be yield a straight line with slope of k'.

Unfortunately, this equation contains three unknowns, and therefore cannot be investigated as such for the data available here.

From the present study, it would appear that neither of the first two models adequately describes the variation in $\delta^{13}C_{OC}$ caught in the sediment traps. It is possible that the third could yield more information, but without field estimates of growth rates it is of little utility. The relationship between $\delta^{13}C_{OC}$ and temperature given by Rau et al (1991c) is most likely the result of autocorrelation in their study between temperature and $[CO_{2(aq)}]$, and thus $\delta^{13}C_{OC}$ is not a useful proxy for temperature. The relationship between $\delta^{13}C_{OC}$ and $[CO_{2(aq)}]$ in the present study provides some, albeit limited, support for the equation of Rau et al. (1991c), especially considering that the OC trapped was not necessarily produced in water with the same $[CO_{2(aq)}]$ as that at the trap depth on the date of recovery. In order to clarify the relationship in the area of this study, samples of POC should be collected at the same time as water for the determination of $[CO_{2(aq)}]$.

The sedimentation and burial of organic carbon with high $\delta^{13}C$ produced in close association with the sea ice provides a confounding factor to the use of $\delta^{13}C_{OC}$ in ancient sediment samples as a proxy for $[CO_{2(aq)}]$ in the surface ocean water at the time. If the input of such material to the sediment is high, $\delta^{13}C$ in the sediment will increase and lower $[CO_{2(aq)}]$ will be calculated. Care therefore must be used in interpreting data from cores from polar regions, especially if the sediment was originally formed in areas close to the shore, where the effect of ice algal sedimentation might be higher.

5.3.6 Carbon in the Sediment

Sedimenting POC can have two fates: it can be remineralised in the water column or in the first few centimetres of the sediment (and the resulting inorganic carbon returned to the water column), or it can be buried in the sediment and thus removed for extended

periods from the atmospheric and oceanic carbon pools. Advection, however, will decouple the formation of POC and the carbon to the sediment at a particular site. Thus, accumulation of carbon in the sediment does not necessarily reflect local OC production, though the effect of advection is expected to be lowest where the water column is shallow, resulting in short water column residence times for the POC. The sediment core obtained at the O'Gorman Rocks site allowed an examination of the processes of OC burial and remineralisation in the sediment.

OC made up between 2 and 3 % (dry weight) of the sediment core (Figure 5.6), typical of the few inshore marine cores collected in the Antarctic region. A core recovered from Granite Harbour in the Ross Sea (Dunbar et al., 1989) contained 1.8 % OC, while cores from inshore sites at Signy Island (Nedwell et al., 1993) and South Georgia (Platt, 1979) contained from 1.2 to 3.8 % and 1.2 to 3.4 % OC respectively. Cores recovered from deeper Antarctic sites have much lower OC levels of up to 0.5 % (Sackett et al., 1974; Sackett, 1986a, 1986b; DeMaster et al., 1992), with the percentage OC (at least in the Ross Sea) approximately inversely proportional to the distance from the coast (DeMaster et al., 1992).

That the carbon to nitrogen mole ratio in the organic fraction was between 6 and 8 for the entire core indicated that sedimentation of intact phytoplankton was perennially a more important source of organic material at this site than sedimentation of faecal pellets, which would have higher C:N mole ratios due to the preferential removal of nitrogen. It would appear that remineralisation by the benthic community did not increase the C:N mole ratio, and, if anything, preferentially removed carbon from the sediment.

The percentage of inorganic carbon in the core was very low near the sediment surface, consistent with the absence of calcareous organisms or authigenic calcium carbonate in the sediment traps. The far higher inorganic carbon concentrations

towards the base of the core were the result of the presence of shell fragments of benthic organisms. The $\delta^{13}C$ of this material was close to that of DIC in the water column between November and February (Chapter 4), which was consistent with the limited fractionation of the carbon isotopes that occurs during the production of marine carbonates (Rao, 1996) and confirms the surface-benthic coupling of seasonal productivity.

Figure 5.6 shows that the sediment core could be readily divided into two sections. Sediment above a depth of 5 - 8 cm had higher OC, higher C:N mole ratio and negligible inorganic carbon than deeper in the core. This demarcation was related to the depth of bioturbation, the process in which infauna within the sediment, such as the bivalve *Laternula elliptica*, mix the upper layer of the sediment both by ingestion of sediment material and their movement within the sediment. The sharp increase in inorganic carbon at 6 - 7 cm was coincident with the appearance of large amounts of shell material of this species. It therefore appeared that *Laternula elliptica* lived and fed in at least the top 5 cm of the sediment. OC and C:N mole ratio decreased at a slightly greater depth, suggesting that there was a zone from 5 to 8 cm where either both live and dead *Laternula elliptica* occurred or other species, for example polychaete worms, were responsible for the bioturbation. The bioturbation depth is similar to that observed in the deep sea (Nozaki et al., 1977; Peng et al., 1977), and recorded in the fjords of the Vestfold Hills (D. Franklin, personal communication).

5.3.7 A Model of Carbon Remineralisation and Burial

A simple model of the sedimentation, remineralisation and burial of organic and inorganic carbon at the O'Gorman Rocks site was developed from a consideration of the mass balance of OC and the total burial mass flux at the site. Figure 5.9 shows the model schematically and Table 5.2 gives the definitions of the parameters used in the model. All parameters in the model except for f_r (the fraction of sedimenting OC

subsequently remineralised in the sediment) were determined experimentally either from the sediment trap data or the sediment core.

The mass balance for OC can be written simply as:

$$R_b f_b = R_s f_s - R_s f_r \tag{5.5}$$

This equation assumes that no OC is removed by any process other than remineralisation or diffusion out of the sediment as small organic molecules, and that any sediment winnowing and resuspension does not fractionate OC from the total sediment.

Figure 5.9. A schematic representation of the model used to calculate the magnitude of carbon burial and remineralisation. The abbreviations and subscripts used are defined in Table 5.2. Also shown are the OC sedimentation and burial fluxes measured or calculated using the model.

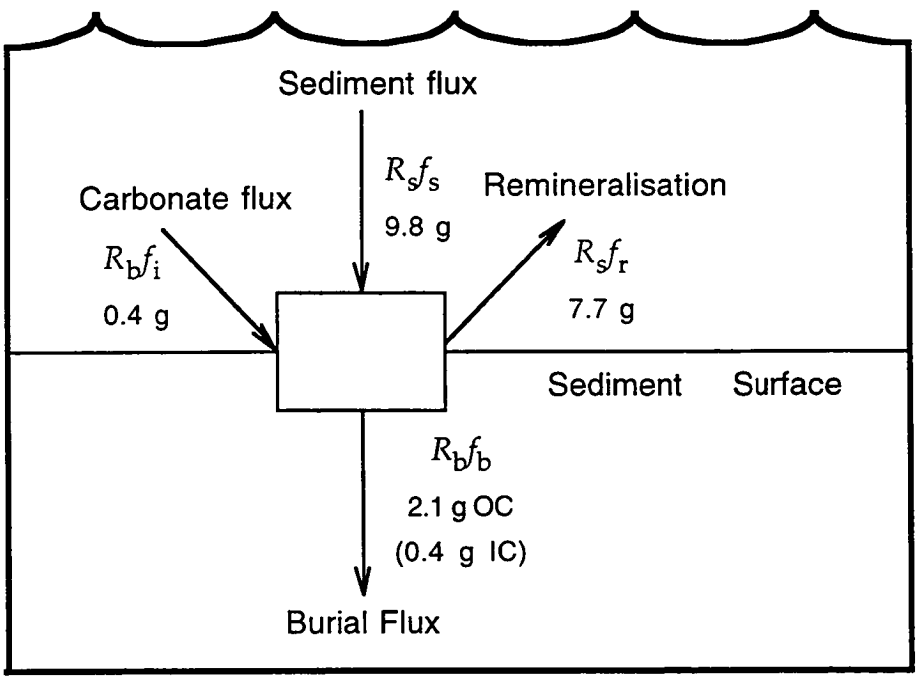

Abbreviation	Model Component
R_s	Total sedimenting flux (g m^2 yr^{-1})
R_b	Total burial flux (g m^2 yr^{-1})
f_s	Organic carbon fraction in sedimenting flux (g C per g sediment, $0 \leq f_s \leq 1$)
f_b	Organic carbon fraction in buried sediment (g C per g sediment, $0 \leq f_b \leq 1$)
f_r	Fraction of sedimenting organic carbon remineralised in the sediment (g C per g C, $0 \leq f_r \leq 1$)
f_i	Fraction of inorganic carbon in the burial flux (g C per g sediment, $0 \leq f_i \leq 1$)

Table 5.2. Components of the model of carbon sedimentation and burial.

The total burial mass flux can be equated to:

$$R_b = R_s - R_s f_r + R_b f_i \tag{5.6}$$

where $R_s f_r$ is the amount of carbon remineralised and $R_b f_i$ is the flux of inorganic carbon buried in the sediment. Rearranging Equation 5.6 and substituting into Equation 5.5 yields:

$$R_s f_b - R_s f_b f_r = R_s f_s - R_s f_r - R_s f f_i + R_s f f_i \tag{5.7}$$

Cancelling out R_s and rearranging this equation to solve for the unknown f_r yields:

$$f_r = \frac{\left(f_s(1-f_i) - f_b\right)}{\left(1 - f_i - f_b\right)} \tag{5.8}$$

Values of f_s, f_i and f_b can be estimated from the results from the sediment traps and the core given above. f_s in the sedimenting material was, on an annual basis, 0.086, f_i was 0.0033 at the base of the core, and f_b was *circa* 0.020 also at the base of the core. Substituting these values into Equation 5.8 yields a value for f_r of 0.068. Multiplying this fraction by the total sediment flux, R_s, indicates that 7.7 g m^{-2} yr^{-1} of the sedimenting organic carbon is remineralised within the sediment with the resulting carbonate transferred to the water column.

If f_s were to increase, the fraction of the carbon remineralised would also have to be greater, and similarly, if the proportion of clastic material increased, remineralisation would have to be reduced in order to produce the observed characteristics of the core. The other parameters, f_b and f_i, can be constrained reasonably well from the sediment core data. The value of f_b would be expected to reach a near steady state value somewhere beneath the base of the sediment core. Estimating this value is difficult from the short core, but, considering that most of the heterotrophic remineralisation activity is likely to occur in the bioturbated region (Gaillard et al., 1989), an estimate of 0.02 is probably reasonable. If the final f_b is 0.015, f_r increases to 0.073. f_r, however, is quite insensitive to changes in f_i.

The ratio of OC remineralisation to burial indicated that 22 % of the OC reaching the sediment at the O'Gorman Rocks site was preserved within the sediment (calculated for f_b = 0.020. If f_b = 0.015, the percentage preservation drops to 16 %). DeMaster et al. (1992) found values of OC preservation ranging from 77 % at an inshore site to 13 % and only 2 % at offshore, deeper water sites. The preservation of organic material will be a function of the efficiency of the heterotrophic community in the benthos. It would be anticipated that greatest efficiency will occur in areas of low flux, and least where the flux is high.

Assuming that the sedimenting carbon flux was derived from the entire water column, the measured flux of 9.8 g m^{-2} $year^{-1}$ was equivalent to a drop in the concentration of DIC throughout the water column by 35.5 μmol kg^{-1}. Remineralisation returned 28.0 μmol kg^{-1} of this to the water column, resulting in a net decrease of 7.5 μmol kg^{-1}. Inorganic carbon burial removed another 1.3 μmol kg^{-1}. Thus it would be expected that, if winter mixing did not introduce DIC rich water back into the surface water or that CO_2 uptake from the atmosphere did not occur, the concentration of DIC would drop as a result of carbon burial by approximately 9 μmol kg^{-1} $year^{-1}$. However, it must be remembered that these reductions in the concentrations were calculated for a water column of 23 m and that OC production and preservation might not have been as high further offshore, both of which would reduce this apparent DIC deficit.

5.4 Conclusions

The study described in this chapter highlighted a number of important features of the sedimentation in the Antarctic region. The sedimentation flux was highly seasonal, with a high percentage of OC sedimentation occurring between mid-November and the end of February. The flux was generally related to organic production in the water column (Chapter 4) or, during October and November, from production associated with the base of the sea ice. The phytoplankton species observed in the sediment traps, however, did not necessarily match those present in the water column, reflecting interspecific differences in the tendency of the cells to sediment and the palatability to zooplankton grazers. No evidence of the sedimentation of colonies of *Phaeocystis* was observed and indeed such colonies were absent from the site during the study.

There were, however, a number of interesting difference between the results from the this and previous Antarctic studies. The $\delta^{13}C$ of the sedimenting OC was for most of the study between -18 and -22 ‰, which was significantly higher than generally observed in the region, and which was consistent with organic matter production at

low DIC concentrations. Furthermore, $\delta^{13}C_{oc}$ in November, when the sedimenting material was dominated by the diatom *Entomoneis kjellmanii*, a species which grows in close association with the sea ice, increased to near -13 ‰, which was higher than previously recorded for Antarctic sediment trap material. Increased input of high $\delta^{13}C$ material to the sediment from shallow, ice covered areas will have important implications for any conclusions regarding the concentration of atmospheric CO_2 and water temperatures drawn from the $\delta^{13}C$ of organic material in sediments or rocks.

Burial and preservation in the sediment was a relatively minor sink for organic material reaching the sediment, though preservation was considerably greater than at deeper water sites. Most of the carbon was remineralised, or transferred by secondary production to benthic organisms near the sediment - water interface. If the amount of carbon buried in the sediment of inshore waters is to be increased then enhanced primary production is only the first step in the process, and careful attention must be made to the fate of the organic material in the water column and the sediment.

CHAPTER 6

ELLIS FJORD SITE: LOCATION, PREVIOUS STUDIES AND PHYSICAL OCEANOGRAPHY

6.1 Introduction

The sampling site in Ellis Fjord was located at 68° 36.2'S 77° 08.0'E (Figure 6.1). This site was chosen to be as far as possible from the entrance of the fjord (thus reducing the possibility of exchange of water at the sampling site with the open ocean) without the water column being permanently stratified and anoxic at depth, as occurs in the basins closer to the head of the fjord (Gallagher and Burton, 1988). The depth at the sampling site was 75 m, which indicated that the site was close to the deepest point of Middle Basin, which has a maximum depth of 85 m.

This chapter gives a brief description of Ellis Fjord and reviews previous physical, chemical, biological and sedimentological studies. The chapter is concluded with a description of the physical oceanography recorded at the sampling site between May 1994 and February 1995.

6.2 Ellis Fjord

Ellis Fjord is a narrow embayment (Figure 6.1) with an entrance approximately 5 km south of Davis Station (Figure 2.1). The fjord lies in a deep, linear valley that parallels boundaries between geological units in the Vestfold Hills, and the occurrence and position of the valley undoubtedly reflect a zone of weakness where two units meet (Collerson and Sheraton, 1986). The valley can be traced past the end of the fjord through a number of lakes to the ice sheet.

Figure 6.1. Ellis Fjord (a) A bathymetric map of the fjord showing the location of the sampling site. (b) A cross-sectional view of the fjord, highlighting the presence of a series of shallow sills.

(a)

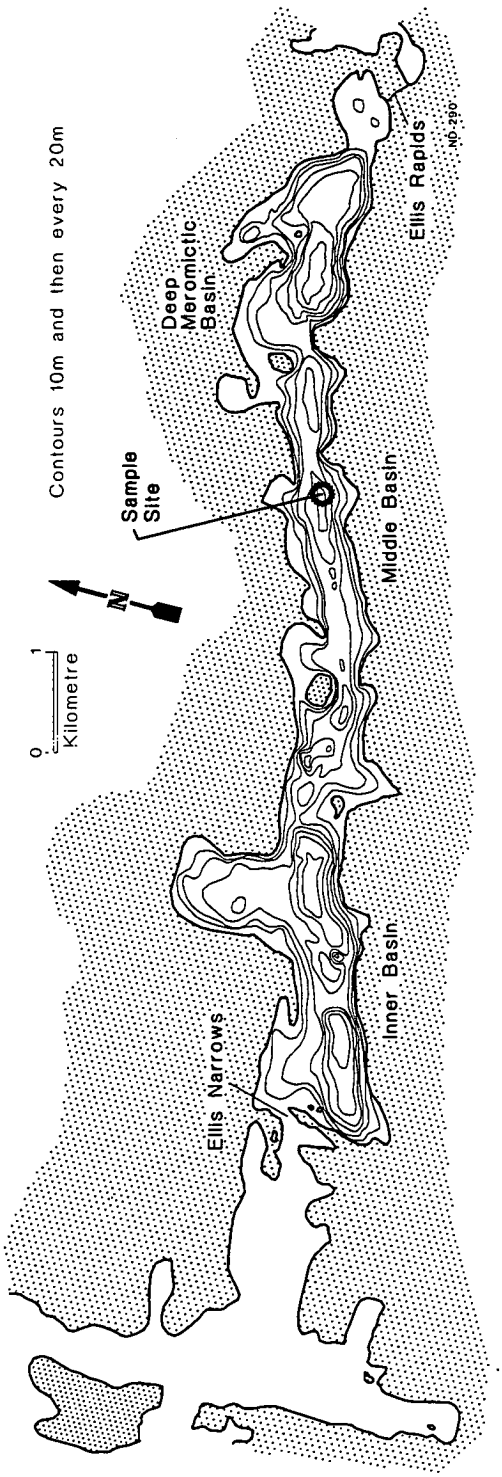

Figure 6.1. (b) A cross-sectional view of the fjord, highlighting the presence of a series of shallow sills

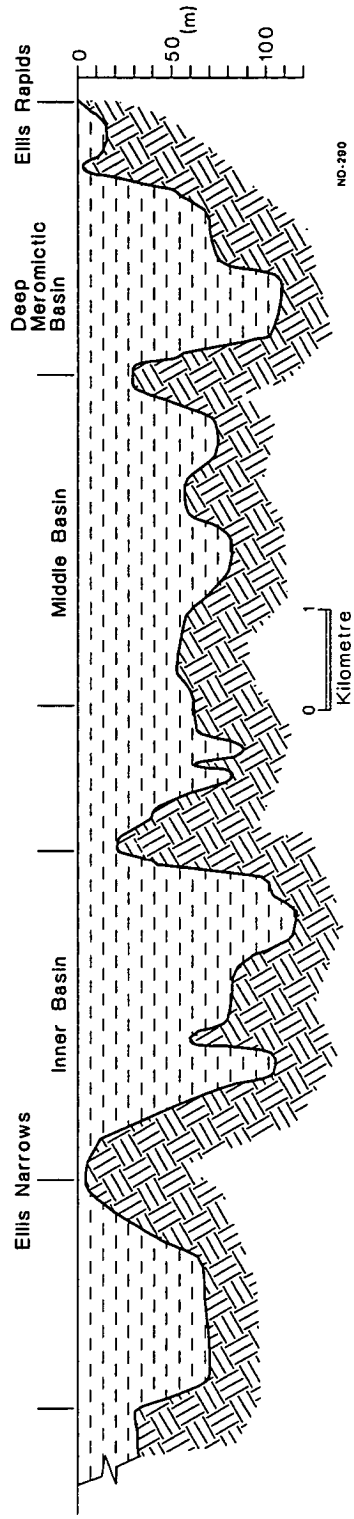

The fjord is 10 km long from its entrance at Ellis Narrows to the end of Watts Basin (Figure 6.1). It is generally *circa* 1 km wide, but in places is much narrower. The bathymetry of the fjord was determined by Gallagher and Burton (1988), who found it to be divided into 5 major basins separated by sills of depths ranging from 1 m to 40 m. (Figure 6.1b). The sill at the entrance to the fjord is only 3 m deep and 160 m across (Kirkwood, 1993), though the basin immediately inside the narrows reaches a depth of 109 m. The maximum recorded depth in the fjord, which occurs in Inner Basin, is 117 m, though at least five other basins with depths of greater than 80 m are present.

The narrow and shallow entrance to the fjord and the sills restrict the mixing of water both within the fjord, and between the fjord and the open ocean (Gallagher and Burton, 1988). The tidal range within the fjord is reduced by Ellis Narrows to approximately 0.1 m during winter (compared to *circa* 1.0 m at Davis Station), though it increases to *circa* 0.3 m in summer when less ice is present to restrict flow at and outside the narrows (Kirkwood, 1993). Tidal range decreases in the fjord with distance from the entrance (Kirkwood, 1993), and thus mixing and influence of the ocean are reduced further away from the entrance of the fjord. This has resulted in the two landward basins becoming permanently stratified (meromictic) beneath 40 m (Deep Meromictic Basin) and 5 m (Watts Basin).

Freshwater input into the fjord is limited to flow through Ellis Rapids (Figure 6.1), which drains a 60 km^2 area of the Vestfold Hills and the surrounding ice sheet (Tierney, 1975; Adamson and Pickard, 1986b), and summer melt from local snow banks. Flow of freshwater through Ellis Rapids occurs in January and February (Colbeck, 1977; Gallagher and Burton, 1988; Kirkwood, 1993), though the magnitude of the flow varies markedly between years (Kirkwood, 1993; J. Gibson, unpublished observations) due to the extent of melt on the ice sheet and the need to fill lakes between the ice sheet and Ellis Rapids before flow begins. Freshwater flow into

the fjord in summer forms a thin, fresh layer at the top of the water column in the landward basins (Gallagher and Burton, 1988; Kirkwood, 1993). Due to the absence of any significant terrestrial vegetation in the Vestfold Hills, input of plant-derived organic material *via* Ellis Rapids is negligible. The lake system that drains through the rapids, however, does contain a sparse flora and fauna, some of which enters the fjord (Kirkwood, 1993).

The ice cover in Ellis Fjord varies both within the fjord and from year to year. The cover is generally at a minimum in January. In some years open water appears only near Ellis Narrows and in Watts Basin, while in other summers the fjord becomes essentially ice free (Kirkwood, 1993; McMinn, 1994; J. Gibson, unpublished observations). McMinn (1994) correlated changes in the summer ice cover to air temperatures at Davis Station; in warmer years, greater melting and break out of the ice occurred. Ellis Narrows remains ice free long after the rest of the fjord has frozen as the flow through the entrance reduces the likelihood of ice formation. However, even this portion of the fjord freezes in late winter, presumably during periods of low tidal range.

Seasonal variations in water temperature and salinity in the fjord during the 1985 winter were discussed by Gallagher and Burton (1988). In the oxygenated section of the fjord water temperatures dropped to a minimum of -1.89 °C by August 1985, and rose again in the summer to near 0 °C as result of the input of solar radiation and warmer water from outside the fjord. Salinity in the fjord was slightly higher than outside the entrance. The water column was stratified until June, with each basin having a unique salinity profile. As winter progressed, ice formation and brine rejection increased the salinity and mixed the water column throughout the oxygenated sections of the fjord.

Various components of the ecosystem of Ellis Fjord have been investigated. The phytoplankton community during summer consists of a variety of diatom and flagellate species (McMinn and Hodgson, 1993). A thick mat of diatoms occurs at the bottom surface of the sea ice, especially during spring, and this mat and sympagic species probably play a role in seeding subsequent phytoplankton blooms in the water column (McMinn, 1996). Little information regarding the bacterial community in the fjord is available, though the protozoan community appears to be similar to those in other Antarctic marine environments, with the occurrence of a number of species of heliozoa (Croome et al., 1987) and choanoflagellates (Marchant et al., 1987) noted.

The zooplankton community in the fjord consists largely of cyclopoid, calanoid and harpacticoid copepods, hydromedusae, ctenophores, appendicularia and polychaete worms (Kirkwood and Burton, 1987; Kirkwood, 1993). The larvae of meroplanktonic organisms are also seasonally abundant. The overall density of zooplankton was found to be quite variable, ranging from 90 to 16000 individuals m^{-3}, equivalent to dry biomasses from 0.7 to 130 mg m^{-3}. A well developed macrobenthic community occurs in the fjord (Kirkwood and Burton, 1988), and contains a wide variety of species which included a greater percentage of filter feeders (as distinct from raptorial species) than at offshore sites near the Vestfold Hills. One of the more important species was the tube worm *Serpula narcoensis* Baird, which forms extensive reefs on the sides of the fjord to a depth of at least 30 m. Other common taxa included sponges, sea urchins, starfish and crustacea. The benthic communities at the bottom of the deeper depressions of the fjord have not been. Four species of fish have been recorded from the fjord, all of which are likely to be resident (Kirkwood and Burton, 1988; Williams, 1988). The only other large animal that has been observed in the fjord are Weddell Seals, which enter the fjord at times during summer to feed and haul out on the ice, but which are not permanent residents (J. Gibson, unpublished observation).

The sediments within Ellis Fjord have been characterised by Bloxham (1993) to consist of three distinct types: a littoral facies associated with massive bioturbation; a glaciogenic facies; and a diatomaceous mud facies. The littoral facies was present largely around the edge of the fjord, while the second was common in deep water from the near the centre of Middle Basin to the entrance of the fjord. The third facies was generally predominant at depth in the eastern half of the fjord. Bird et al. (1991) described a core recovered from the anoxic zone of Deep Meromictic Basin, and suggested a sedimentation rate derived from ^{14}C dating of *circa* 2 mm yr^{-1}.

6.3 Physical Characteristics of the Ellis Fjord Site, May 1994 - February 1995

6.3.1 Ice Cover

Before the beginning of the study, the Ellis Fjord site had been continually covered by ice since at least the 1991 winter, three years before sampling started (McMinn, 1994; J. Gibson, unpublished observations). Ice thickness was near 1.9 m in May 1994, and increased slowly to just over 2 m by December. Slight thinning occurred in January, when the ice became very soft, but by late February 1995, the ice had again become hard and was thickening slowly. Snow cover in Ellis Fjord was much less than at the O'Gorman Rocks site due to the regular occurrence of strong katabatic winds which were channelled along the main axis of the fjord. On most sampling dates no snow cover was present.

6.3.2 Water Temperature

A contour plot of water temperature at the sampling site in Ellis Fjord is shown in Figure 6.2, and Figure 6.3 shows the cycle of temperature (and salinity) at 10 m. The first temperature profile, recorded in May 1994 (Figure 6.4), was particularly

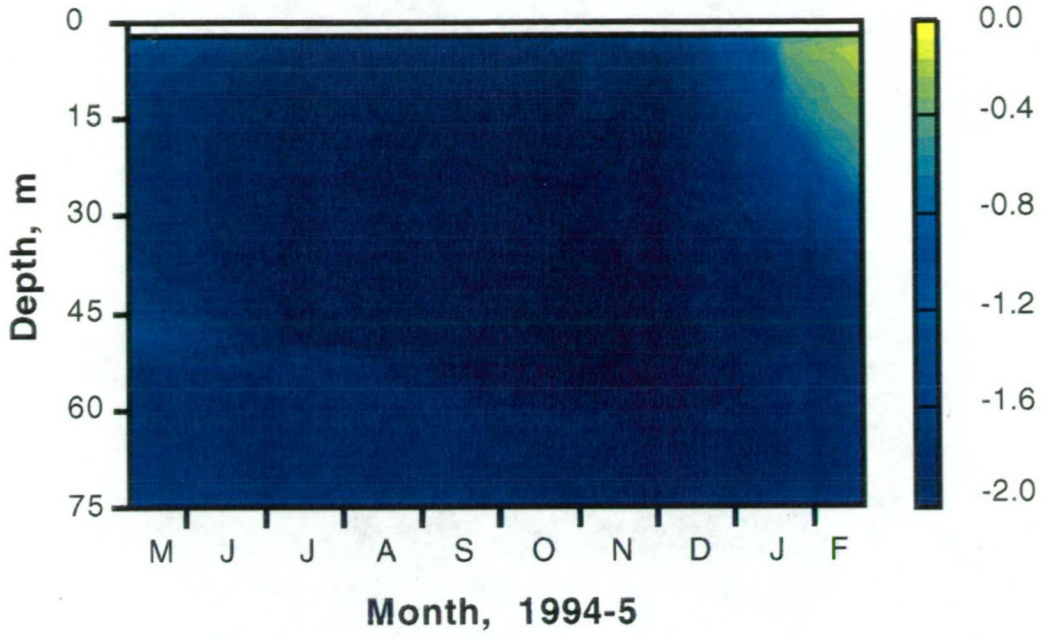

Figure 6.2. Water temperature (°C), Ellis Fjord site, May 1994 - February 1995. The ice cover in this and all similar plots of data from Ellis Fjord is represented by the thin white area at the top of the plot.

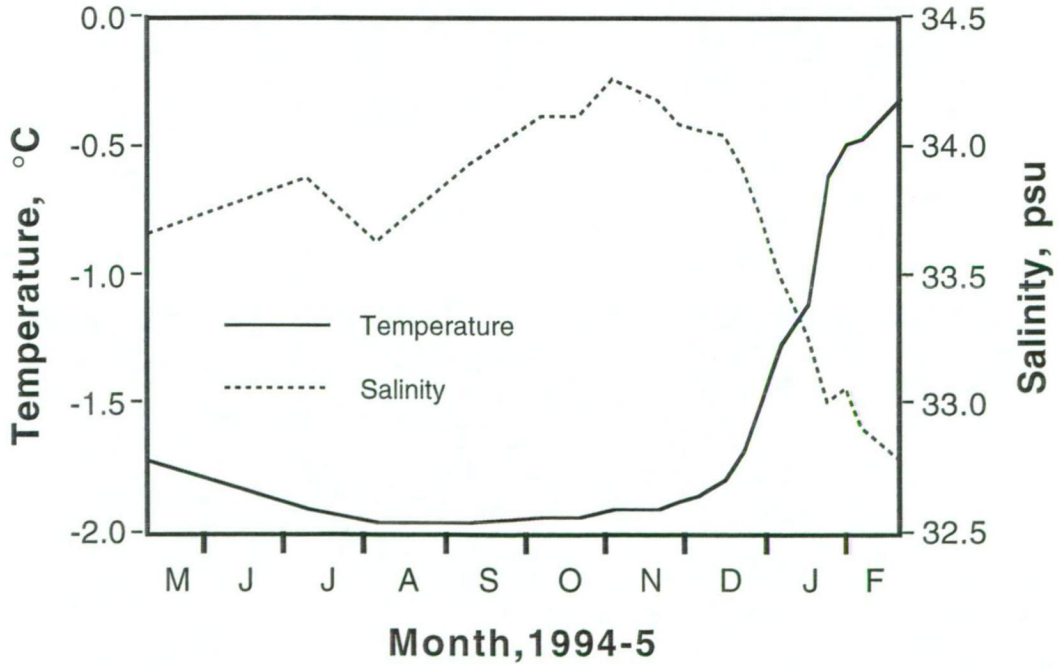

Figure 6.3. Temperature and salinity at 10 m at the Ellis Fjord site.

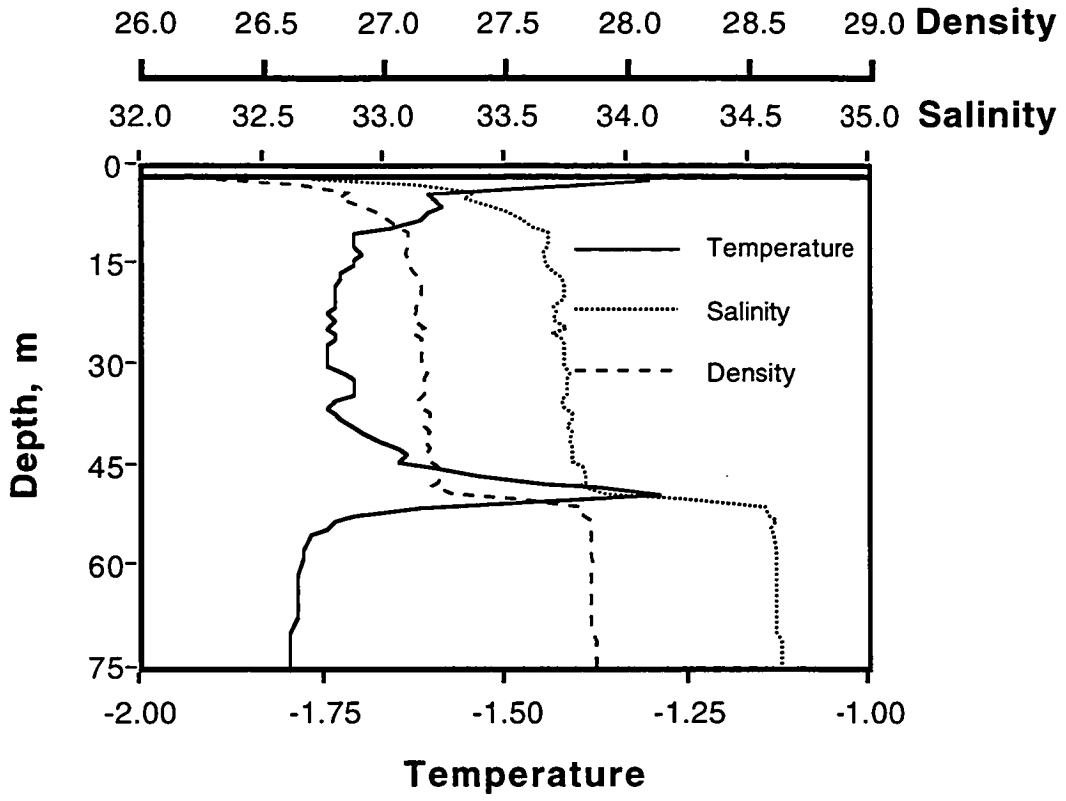

Figure 6.4. Temperature (°C), salinity (psu) and *in situ* density (kg m^{-3} - 1000) profiles, Ellis Fjord, 7 May 1994.

interesting, as it revealed a number of surprising characteristics which provided insight into the processes occurring in the fjord. The temperature (and salinity) profiles indicated the presence of a deep warm layer just above the coldest, most saline layer (which extended from 50 m to the bottom), as well as several other less pronounced warm layers (for example just beneath 30 m) and a fresh, warm, highly stratified zone near the surface. The processes that resulted in these profiles are discussed below.

The water above 50 m had become essentially isothermal by July at a temperature of *circa* -1.9 °C. and remained so until early November. The isolated bottom water (initially beneath 50 m) remained at near a constant temperature throughout the study, though the interface between the cooler (in winter) and warmer water deepened slowly, and, though not evident in Figure 6.2, was near 70 m by the end of the study. The first evidence of summer warming was observed just under the ice in November,

but significant warming deeper in the water column did not occur until December. The upper 35 m increased in temperature between December and the end of the study, and the maximum temperature recorded was 0.20 °C at 5 m on the last sampling date.

6.3.3 Water Salinity

A contour plot of water salinity at the Ellis Fjord site is presented in Figure 6.5. Figure 6.3 shows changes in salinity at 10 m and Figure 6.4 shows the salinity profile recorded on the initial sampling date in May 1994.

The salinity in the top 50 m generally increased throughout winter, though at no time did the water column appear to be truly isohaline. Maximum salinity was reached in late October - early November, and salinity remained near this level until December, except in a thin layer directly under the ice where significantly less saline water was present. Towards the end of December water under this layer began to become less

Figure 6.5. Water salinity (psu) at the Ellis Fjord site, May 1994 - February 1995.

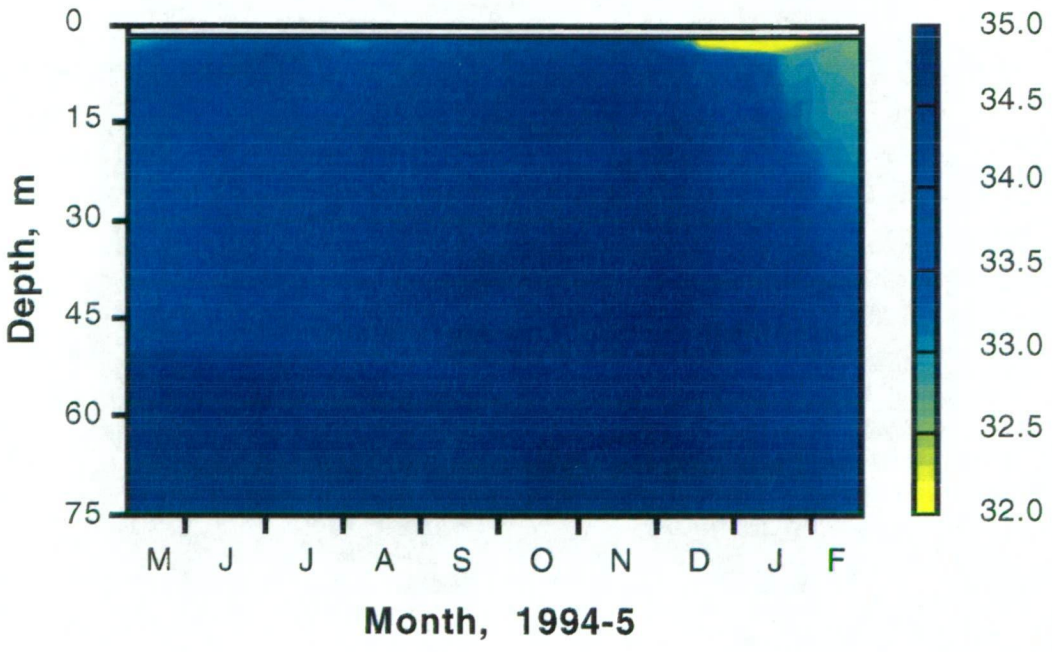

saline, and this process continued until the end of the study and probably beyond, also reaching a depth of 35 m.

Water salinity in the isolated bottom water decreased throughout the study, but remained higher than in the upper water. By the end of the study the differential in salinity between the water bodies was only slight.

6.3.4 Mixing and Water Body Sources in Ellis Fjord

6.3.4.1 Winter Cooling

The strong temperature and salinity stratification in the top 15 m in May 1994 (Figure 6.4) suggested that brine rejection had not provided a sufficiently strong force to mix the water column by this time. This was in part a response to the maintenance of the ice cover during the previous summer: if rapid freezing of new ice had occurred at the site, it would be expected that a zone of isopycnal water at its freezing point would form at the top of the water column (Kantha, 1979; Gibson and Burton, 1996). However, even though air temperatures were very cold in May (Appendix B), little new ice was forming at the sampling site due to the insulating capacity of the ice reducing heat loss to the atmosphere.

Water salinity and temperature in May were nearly constant from 15 to 50 m, but were not entirely uniform as would be expected if the zone were mixed. This water could not have been the result of brine freeze out during the formation of ice (at least at the sampling site), as the water was not at its freezing point and less saline and warmer water was still present at the surface. The most probable source of this water was mixing of low salinity, warm summer water (as was observed to occur at these depths during the 1994-5 summer) with cold, saline water that had its source near shallow terraces at the edge of the fjord (shown schematically in Figure 6.6). In these areas, ice

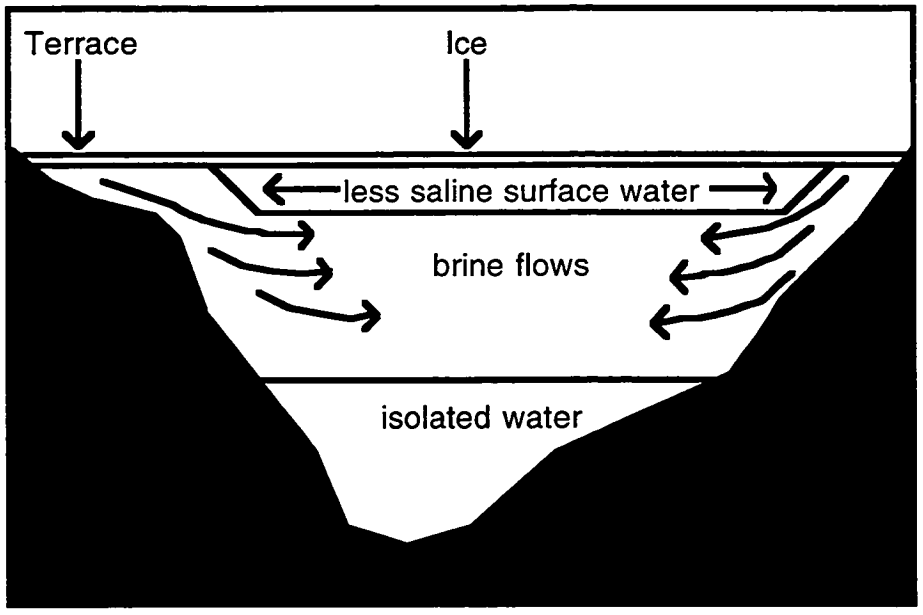

Figure 6.6. A schematic diagram of the formation of brine as the result of ice formation near the edge of Ellis Fjord, and the mixing of the brine flows into the mid-depth water.

melt during summer would have occurred to a greater extent (a moat of open water is typically formed around the edge of the fjord during summer even if the ice in the centre of the fjord remains relatively intact), and brine formation during refreezing of the moat would have produced dense, saline water at its freezing point (Gallagher and Burton, 1988; Gallagher et al., 1989). This water would then flow down the side of the fjord, eventually coalescing with water of the same density. The efficient horizontal mixing that occurs in isolated stratified Antarctic water bodies (Shirtcliffe, 1964; Gallagher and Burton, 1988; Gibson et al., 1989) would then transport this water into the centre of the fjord, where it would mix with the warmer water and result in the observed profile. The nearly, but not quite, isopycnal water between 15 and 50 m suggests that a number of episodes of saline water formation and mixing into the water column had occurred.

The water temperature maximum near 50 m was obviously a remnant of the warm summer layer from the 1993-4 summer which must have extended to this depth. Brine

flows occurring before May did not penetrate to this depth, and the temperature maximum was maintained. (Note the slight salinity and density increases that occurred in concert with the temperature maximum (Figure 6.4).) However, its disappearance later in winter indicated that the input of flows eventually mixed into and cooled this water.

It is also possible that the colder and saltier subsurface water was the result of input from outside the fjord, and that salt was imported into the fjord. However, the water inside the fjord was typically slightly more saline than at the O'Gorman Rocks site, and the nutrient and DIC concentrations showed significant differences between the two site (Chapters 4 and 7), suggesting that the influence of extra-fjord water, at least at the sampling site during winter, was limited.

6.3.4.2 The Isolated Bottom Water

That the water above 50 m did not appear at any stage of the winter to become truly isohaline indicated that brine formation at the edges of the fjord rather than strong convection at the centre of the fjord was the major mixing process throughout winter. As more brine was formed, the less dense surface water layer would have thinned and been transported towards the edges of the fjord and eventually been subsumed into forming brine (Figure 6.6). The increase in salt content of the upper 50 m between May and November was near 18 g m^{-2}. Approximately half a metre of new ice would need to be formed over the entire fjord if brine rejection were the sole mechanism for the observed salinity increase. Only *circa* 10 cm of ice was formed during this period at the sampling site in the centre of the fjord, suggesting that the bulk of ice formation occurred closer to the shore from the refreezing of the summer moat.

The water beneath 50 m was quite distinct in May from that above, being both colder and denser. This water remained isolated throughout the study, though the interface

between the upper and lower water bodies deepened slowly and the lower layer became less saline, even though the temperature remained essentially constant.

The isolation of the lower body probably occurred during the 1993 - 4 summer as a result of freshening of the surface water. The depth to which higher temperatures occurred during the 1993-4 summer (as shown by the mid-water maximum in Figure 6.4) and to which significant water freshening occurred (by comparison to the 1994 - 5 summer) was essentially at the top of the isolated water, which supports this contention. Ice formation during the 1994 winter was insufficient to mix the entire water column either by brine flows or a general increase in salinity.

By the end of the study the interface between the layers had become far less sharp and was close to the bottom of the basin, suggesting that within a short period after the end of sampling the isolated water would have been totally entrained into the upper water, and that during the 1995 winter, no isolated water would be present unless, again, production of more saline water during this winter was unable to mix through the pycnocline at the base of the fresh layer which developed during the 1994-5 summer.

6.3.4.3 Summer Warming and Salinity Decrease

Summer warming of the water beneath the 5 m began in December, and was still occurring at the end of the study. Warming was initially the result of the absorption of solar radiation, but the temperature increase from December to February was far higher than expected solely from this mechanism. Simple calculations using summer insolation of 2000 MJ m^{-2} (Chapter 2), an albedo for old, dirty ice and snow of 50 % (Gallagher and Burton, 1988), an extinction coefficient of the ice and snow of 98 %, and a specific heat capacity for seawater of 4 kJ kg^{-1} $°C^{-1}$ suggested that temperature would increase by *circa* 0.2 °C to a depth of 30 m if all incoming radiation was converted to heat in the water column. This increase was considerably less than that

observed (average: 1.4 °C). Furthermore, the presence of a lens of fresh, warm water just under the ice in November (Figures 6.2 and 6.5), which undoubtedly resulted from solar heating, indicates that the affects of such heating were likely to be limited to the top few metres of the water column.

From December to the end of the study, water temperature and salinity to 50 m (except at 2 m directly under the ice) were strongly negatively correlated (Figure 6.7), which suggested that the input of warmer, less saline water into the basin rather than solar heating was the primary cause of the summer warming. This less saline water could have come from three sources: input of freshwater resulting from the melting of ice and snow either *via* Ellis Rapids or locally from snow banks built up during winter; melting of the ice cover of the fjord; or transport of low salinity water to the site from elsewhere in the fjord or through Ellis Narrows.

Figure 6.7. A plot of temperature versus salinity at the Ellis Fjord site from 12 December 1994 to the end of the study, indicating the close correlation between these parameters. Data from 2 m is not included in this plot.

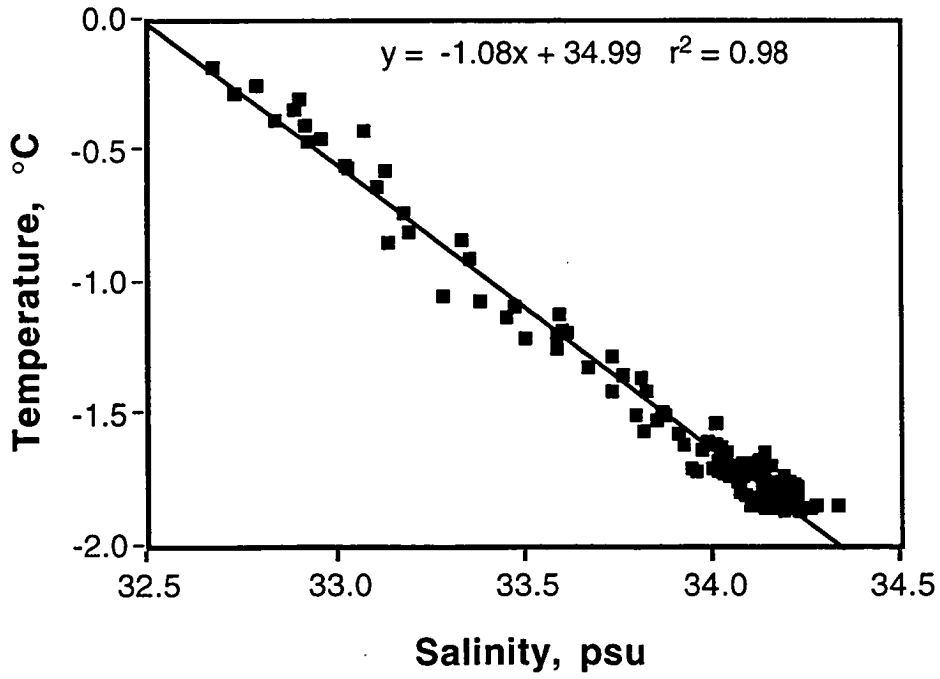

Input of freshwater was unlikely for two reasons. Firstly, flow through Ellis Rapids, the major freshwater input into the fjord, was near zero during the study (though it was not monitored explicitly). Secondly, extrapolating the line of best fit in Figure 6.7 suggests that the temperature of the freshwater input into the fjord would have been near 35 °C, which is not realistic. The ice cover did not melt significantly during this summer, and was therefore unlikely to be the source of the water (even though a thin layer of less saline water from this source was present at the site from November). Furthermore it is unlikely that melting of the ice would have produced the linear relationship observed.

Gallagher and Burton (1988) suggested that strong tidal jets (Stucchi, 1979) passing through Ellis Narrows during periods of high tides in late November were sufficient to mix Inner Basin (Figure 6.1) to the bottom, resulting in a decrease in salinity and increase in temperature in this basin. It is likely that a similar process occurred during 1994, and was responsible for the sudden appearance of warm, less saline water at the sampling site. Transport of water from the mixed Inner Basin along the fjord by tidal action and other mixing forces resulted in it reaching Middle Basin by early December. The water input into Middle Basin need not have had constant temperature and salinity, but the characteristics of water reaching the sampling site and/or mixing with the water in the basin must have fallen somewhere on the regression line shown in Figure 6.7, with at least some the water having a temperature of greater than -0.2 °C and salinity less than 32.6 psu.

Plots of temperature increase between sampling dates against water depth (Figure 6.8) indicates that the input of the warmer, less saline water (for which temperature is a proxy) did not occur smoothly or regularly. Increases in temperature tended to be greater in the upper 20 m until mid-January, but, later in the study, water input had a greater effect deeper in the water column. Decreases in salinity followed similar trends. The interleaving of warmer, less saline water deeper in the water column indicates that

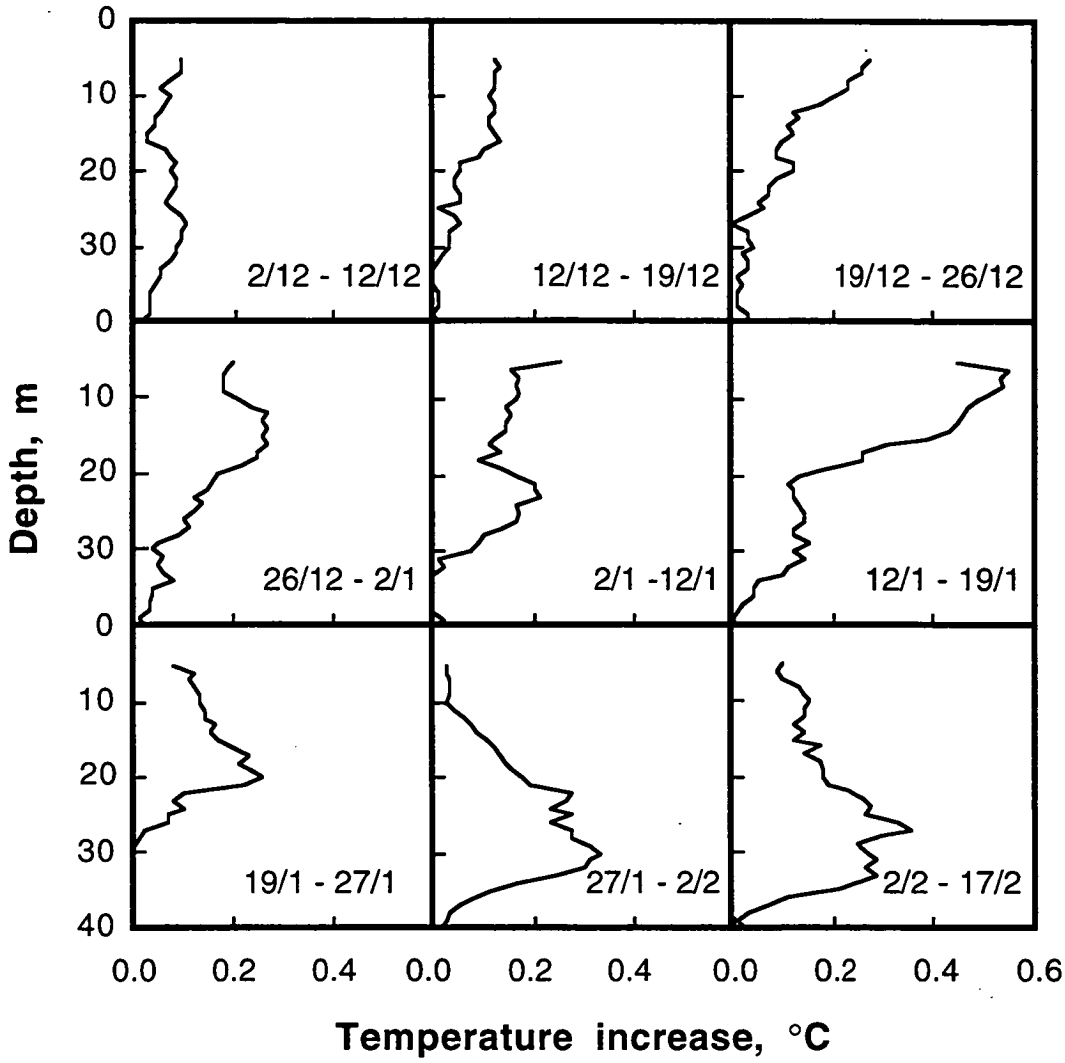

Figure 6.8. Temperature increase between sampling dates as a function of water depth between 5 and 40 m at the Ellis Fjord site from December 1994 to February 1995.

the density of this water was greater than that at the surface, where the initial input occurred. Figure 6.8 provides further evidence that solar heating was not the cause of warming at the sampling site.

It appears that a similar process occurred during the 1993-4 summer, but extended deeper in the water column, as increased water temperature occurred to a depth of 50 m at the start of the present study. The apparently greater penetration of water from this source during into Middle Basin during the 1993-4 summer reflects the interannual variability in such mixing processes.

6.4 Conclusions

In contrast to the O'Gorman Rocks site, the water in Ellis Fjord did not cool as rapidly, remaining significantly warmer than freezing and stratified in May. Due to the maintenance of the ice cover over the centre of the fjord through the previous summer, strong convective mixing resulting from rapid ice formation did not occur. The main processes of water mixing in the fjord appeared to be brine flows resulting from ice formation near the edges of the fjord, and mixing was not sufficiently intense to completely homogenise the water column, with an isolated water mass being retained at the bottom of the water column throughout the study. Warming and dilution in summer was to a large extent the result of input of water from outside the basin.

CHAPTER 7

ORGANIC MATTER PRODUCTION AND PHYTOPLANKTON IN ELLIS FJORD

7.1 Introduction

This chapter describes the chemistry and biology of photosynthetic OC production in Ellis Fjord from May 1994 to February 1995. The study was undertaken to complement that at the O'Gorman Rocks site, as the fjord is a marine system with restricted water movement and is less influenced by currents than offshore. The fjord also remained covered by ice throughout the study, and thus removed variable ice cover as a determining factor in OC production and gas transfer. The sampling site in Ellis Fjord also differed in being significantly deeper than the offshore site.

7.2 Results

All data described in this chapter are presented in tables in Appendix E. As discussed in Chapter 6, the water column at the Ellis Fjord sampling site remained stratified throughout the study, with two major water masses separated by an interface at 50 - 70 m. The results from the lower water mass (sampling depth: 70 m) are generally treated separately from the shallower sampling depths (2, 5, 10, 20 and 40 m).

7.2.1 Dissolved Inorganic Carbon

Figure 7.1a shows a plot of the concentrations of DIC measured at the Ellis Fjord site. The same data is shown in Figure 7.1b over a reduced concentration range to highlight

Figure 7.1. DIC (μmol kg^{-1}), Ellis Fjord site, May, 1994 - February 1995: (a) all data; (b) the same data over a smaller concentration range. The symbols used in these and all similar plots in this section are: 2 m, □; 5 m, ◇; 10 m, ○; 20 m, △ and 40 m, ✣. The lighter shading shows the minimum value (0 - 40 m) for the parameter on the sampling date, and the darker shading the range of the data. Data from 70 m is represented by inverted triangles joined by a line.

(a)

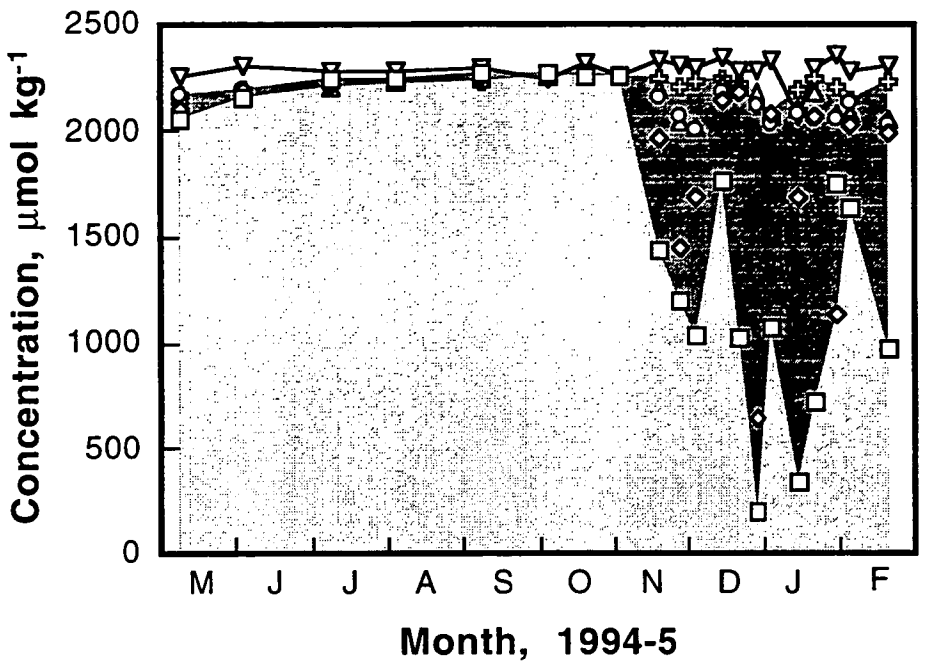

(b)

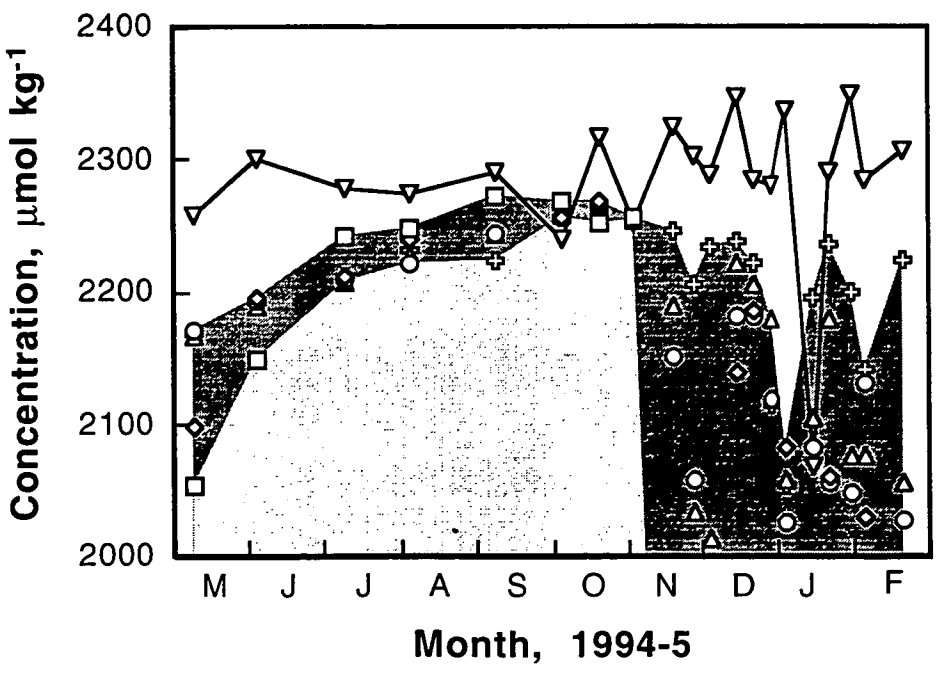

subtle changes. At the beginning of the study in May, DIC in the upper 40 m were still comparatively low (2050 -2170 μmol kg^{-1}), and increased with depth. The concentrations increased by June, and then rose steadily until October, when DIC was essentially constant throughout the upper 40 m at *circa* 2260 μmol kg^{-1}. DIC had dropped sharply near the surface by mid-November, and at all depths to 40 m by the end of the month. From November until the end of the study, DIC at 2 m, and on many occasions at 5 m, was very low (< 2000 μmol kg^{-1}, Figure 7.1a). The minimum concentration measured at 2 m was 197 μmol kg^{-1} on 26 December 1994, and many other occurrences of DIC less than 1000 μmol kg^{-1} were recorded.

The concentration of DIC at 70 m was initially near 2260 μmol kg^{-1}, and generally increased during the rest of the study to a maximum of 2350 μmol kg^{-1}, though a significantly lower concentration was recorded on one occasion during January. This occurrence was most probably due to a leak in the water sampling bottle.

7.2.2 Dissolved Organic Carbon

A plot of the concentrations of DOC, which were measured from the end of October until early February, is shown in Figure 7.2. Highest of DOC was recorded at 2 m, with the maximum being 184 μmol kg^{-1} in early December. DOC generally decreased with depth, with the minimum concentration being 58 μmol kg^{-1} at 40 m in early January, though similar concentrations were recorded regularly at this depth. The concentrations of DOC at 70 m were comparable to those in the upper water, but dropped steadily throughout the period of measurement.

7.2.3 Particulate Organic Carbon

The concentrations of POC (Figure 7.3) were always highest at 2 and 5 m, reaching a maximum of 132 μmol kg^{-1} in late January. However, in mid-December POC at the

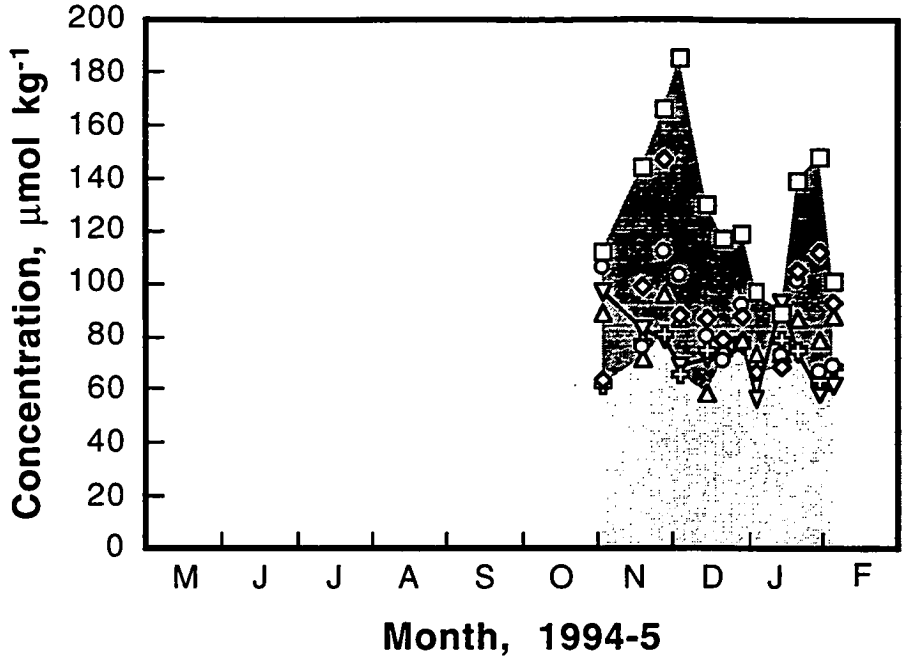

Figure 7.2. DOC (µmol kg^{-1}), Ellis Fjord site, May 1994 - February 1995.

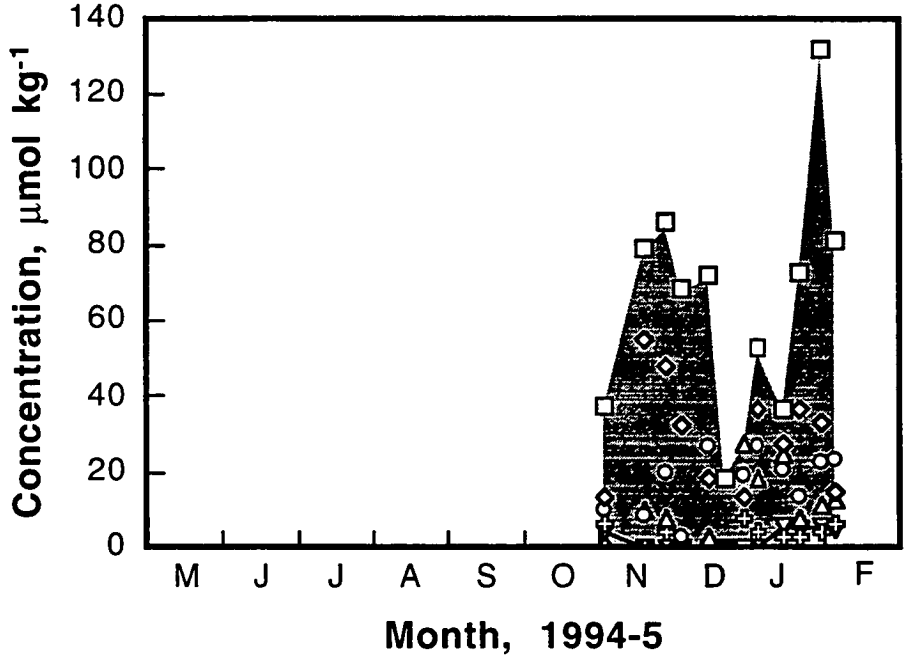

Figure 7.3. POC (µmol kg^{-1}), Ellis Fjord site, May 1994 - February 1995.

surface was much lower, and was beneath 10 μmol kg^{-1} throughout much of the water column. Several pulses in the concentration of POC occurred, but these were not always aligned with peaks in DOC. The concentration of POC at 70 m was very low throughout the study. As at the O'Gorman Rocks site, POC concentrations were generally lower than DOC concentrations throughout the study.

7.2.4 The $\delta^{13}C$ of Inorganic and Organic Carbon

$\delta^{13}C_{DIC}$ at 10 m was initially above 1 ‰, but then slowly dropped to *circa* 0.80 - 0.85 ‰, where it remained from August to early November (Figure 7.4). $\delta^{13}C_{DIC}$ then rose steadily throughout the rest of the study to a final value of 1.79 ‰ in late January. The $\delta^{13}C$ of suspended POM was not measured, but $\delta^{13}C_{OC}$ in material caught in sediment traps was between -22 ‰ and -18 ‰ for most of the year except for a period in

Figure 7.4. $\delta^{13}C_{DIC}$ in water at 10 m, Ellis Fjord site, June 1994 - January 1995.

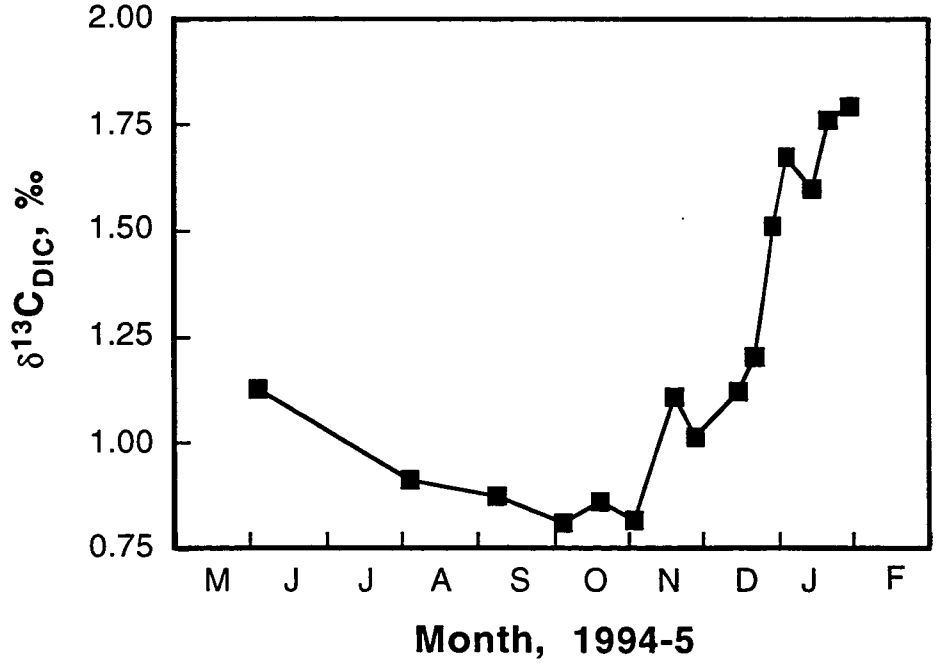

November and December, when much higher $\delta^{13}C_{OC}$ (maximum -14.2 ‰) was recorded (this data is presented and discussed in more detail in Chapter 8).

7.2.5 pH

pH_f at 25 °C (Figure 7.5) in May was 8.15 at 2 m and *circa* 7.95 between 10 m and 40 m, and after this first sampling date dropped steadily until the middle of October, when the lowest values, 7.77, were recorded. For most of the winter pH_f was essentially constant throughout the water column to a depth of 40 m. In early November a sharp increase to 8.70 occurred at 2m, and pH_f remained high (> 8.3) at this depth for the rest of the study. In deeper water, pH_f was lower than in the surface water, but still regularly reached values as high as 8.1.

The pH_f at 70 m was similar to that of the overlying water during winter, but then decreased as the study progressed. The minimum pH_f recorded at 70 m was 7.55.

Figure 7.5. pH_f, Ellis Fjord site, May 1994 - February 1995.

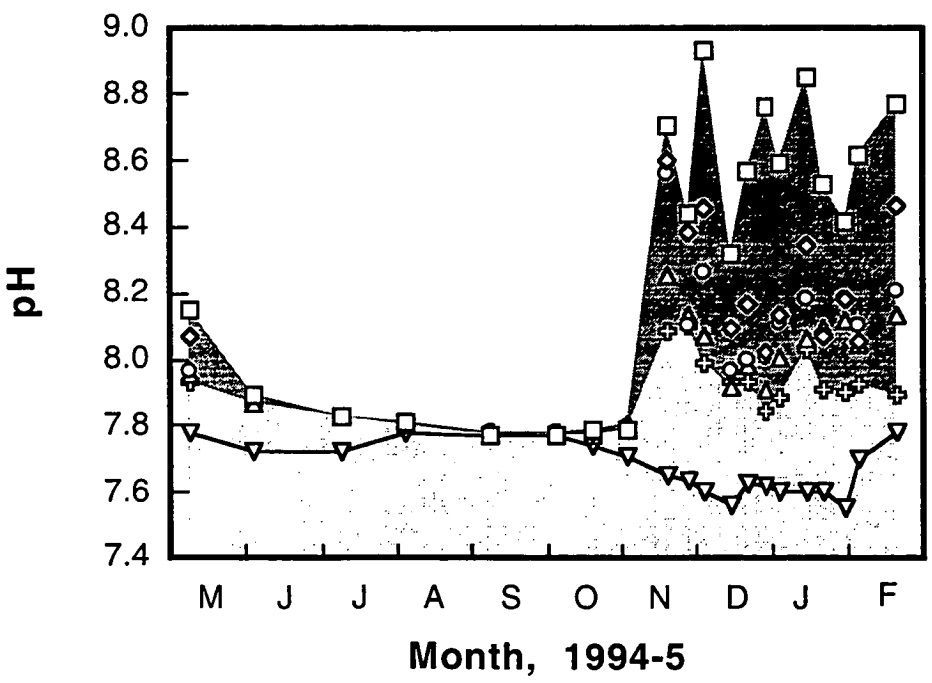

7.2.6 Chlorophyll

A contour plot of the concentration of chl *a* is shown in Figure 7.6, which highlights the depths at which chl *a* maxima occurred from October to the end of the study. For the sake of clarity, the maximum concentration plotted is 15 mg m^{-3}. The measured concentration exceeded this level on a number of occasions in October and November (Appendix F), and these instances are mentioned specifically in the text below.

The concentration of chl *a* in water collected from 2 m on the first sampling trip was 1.2 mg m^{-3}, and was greater than 0.2 mg m^{-3} throughout the rest of the water column to 40 m. From June until the mid-October chl *a* was generally below 0.15 mg m^{-3}, indicating that the winter background level was similar to that at the O'Gorman Rocks site. Chl *a* increased significantly between the middle and the end of October, when a concentration of 22.6 mg m^{-3} was recorded at 2m. The concentration dropped in early November before rising again later in the month and early December to a maximum of

Figure 7.6. A contour plot of the concentration of chl *a* (mg m^{-3}), Ellis Fjord site, May 1994 - February 1995.

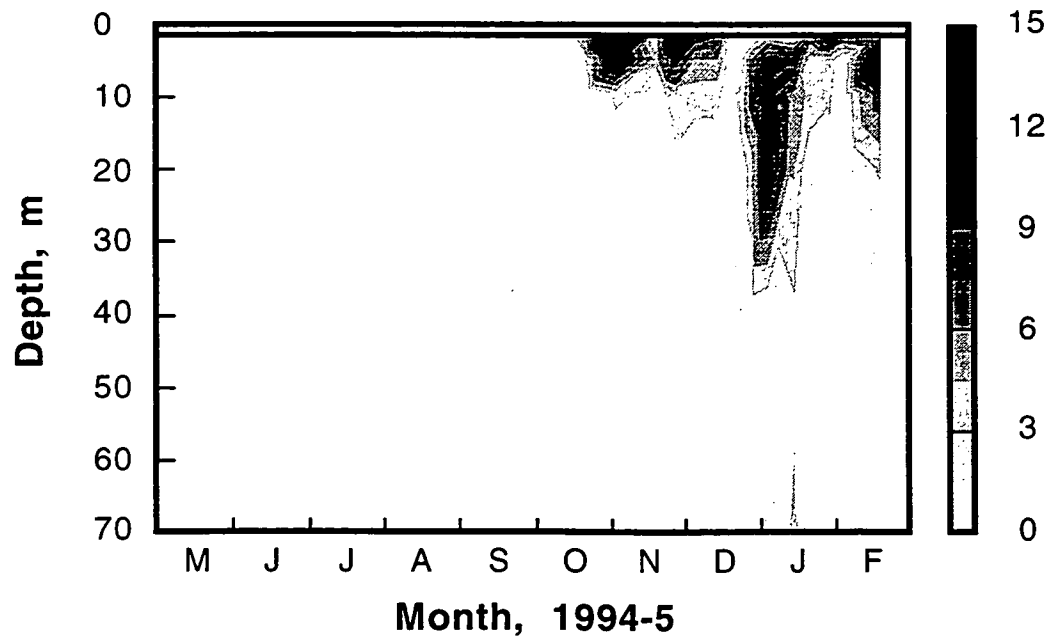

20.6 mg m^{-3} again at a depth of 2 m. Throughout October and November chl *a* decreased rapidly beneath 2 m to less than 1 mg m^{-3} at 40 m. After a period in mid-December when the concentration was low, another peak in chl *a* occurred late in the month and in early January (maximum concentration: 10.0 mg m^{-3} at 5 m on 2 January)), but in this case, the depths at which maximum chl *a* occurred was between 5 and 20 m. Chl *a* dropped away again in late January, but had increased once more in the upper 10 - 20 m by the last sampling date (maximum concentration: 14.2 mg m^{-3} at 5 m).

The concentration of chl *a* at 70 m was generally low during winter, but increased to significant levels in November and January, reflecting the sedimentation of phytoplankton out of the surface waters. It is unlikely that primary production occurred at 70 m.

Significant levels of chlorophyll *b* (chl *b*) were recorded in samples from 2 m between late January and the end of the study, reaching 10.0 mg m^{-3} on 17 February. Concentrations at other times and depths were much lower.

7.2.7 Dissolved Oxygen

DO was considerably higher near the surface in May (maximum 445 µmol kg^{-1}) than in the rest of the water column (Figure 7.7). This stratification had largely disappeared in early June when the concentration had dropped to circa 320 µmol kg^{-1} throughout the water column. DO continued to decrease until early October, when a minimum concentration in the top 40 m of *circa* 275 µmol kg^{-1} was recorded. The concentration then increased slowly throughout the rest of the month, before a sharp jump in early

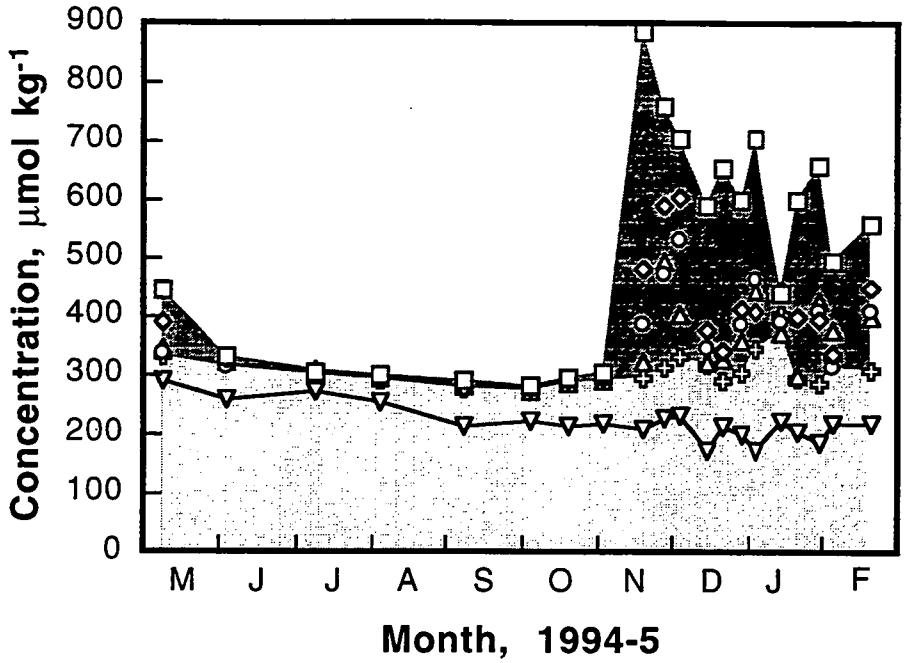

Figure 7.7. Dissolved oxygen (µmol kg^{-1}), Ellis Fjord site, May 1994 - February 1995.

November. The maximum concentration, 885 µmol kg^{-1}, was recorded at 2 m, but the increase lower in the water column was less dramatic. DO remained high (>400 µmol kg^{-1}) at 2 m throughout the rest of the study, while at other depths in the water column oxygen exhibited a number of pulses of increased concentration which extended to 40 m. DO at 70 m was initially 288 µmol kg^{-1}, and generally decreased throughout the rest of the study.

The concentrations of DO during winter represent a marked undersaturation of the water column (Figure 7.8). Oxygen saturation dropped to *circa* 75 % by early October but then rose, at least at 2 m, to over 240 % in November. Oxygen saturation was greater than 100 % for most of the summer to a depth of at least 20 m, but the water at 70 m remained undersaturated throughout the study.

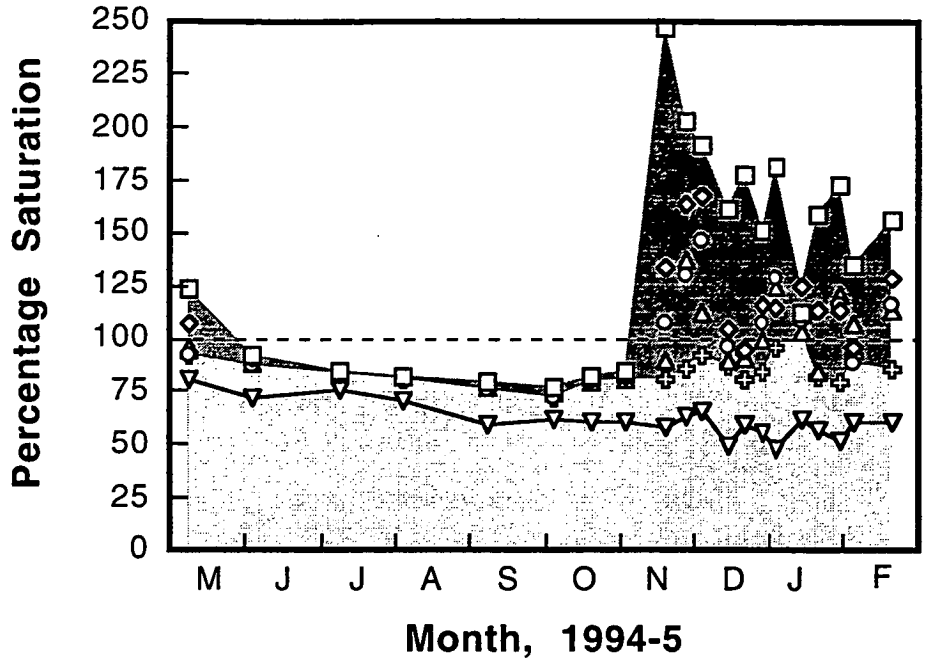

Figure 7.8. Percentage saturation of dissolved oxygen, Ellis Fjord site, May 1994 - February 1995.

7.2.8 Nutrients

Plots of the concentrations of the nutrients nitrate, phosphate and silicate are presented in Figures 7.9 to 7.11 respectively. The nutrients exhibited similar cycles throughout the study. They were considerably lower throughout the water column in May than in June, but from June until early October rose steadily to winter maxima of *circa* 24.1 μmol kg^{-1} (nitrate), 2.18 μmol kg^{-1} (phosphate) and 61.6 μmol kg^{-1} (silicate) throughout the water column to 40 m.

The concentrations of the nutrients began to drop in early November, initially in the surface water, but by the end of November to 40 m. Throughout the rest of the study nutrient concentrations were reduced below winter levels, but, as for many of the other chemical parameters, there were periods of lower concentrations followed by increased levels. The concentration of nitrate was near the detection level (0.05 μmol kg^{-1}) in water from 2 m during most of the summer, while the concentrations of phosphate and silicate were reduced to a lesser extent. The nutrients increased in concentration with

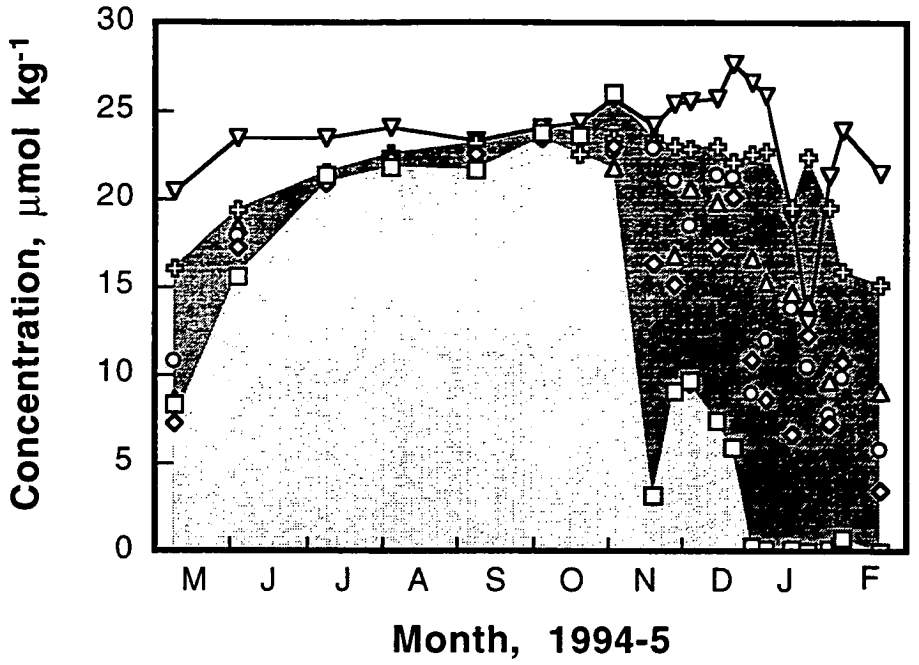

Figure 7.9. Nitrate (µmol kg^{-1}), Ellis Fjord site, May 1994 - February 1995.

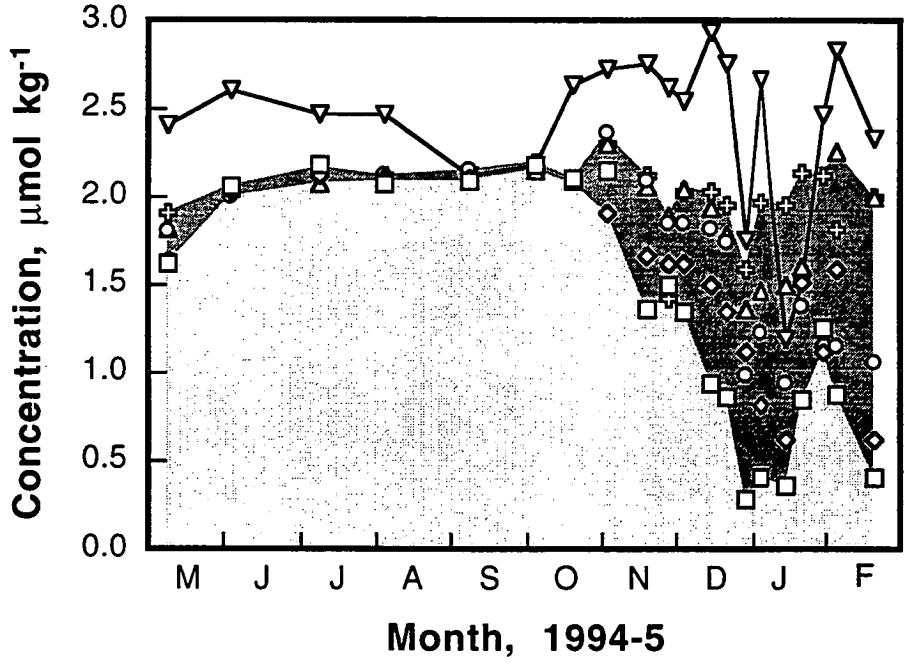

Figure 7.10. Phosphate (µmol kg^{-1}), Ellis Fjord site, May 1994 - February 1995.

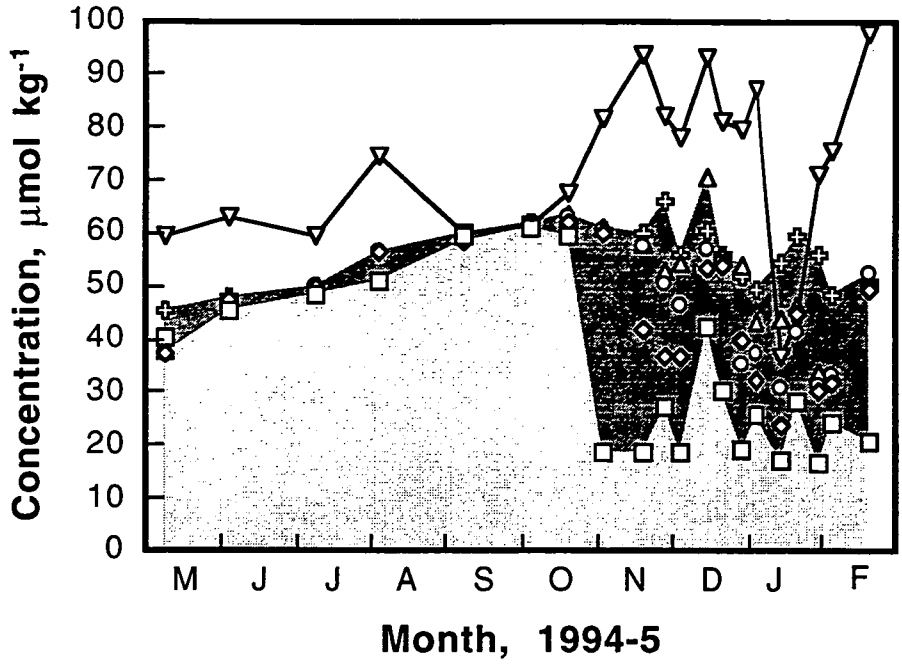

Figure 7.11. Silicate (µmol kg^{-1}), Ellis Fjord site, May 1994 - February 1995.

depth, and at 40 m they remained from October to February at 70 % or more of the end of winter values.

The concentrations of the nutrients at 70 m were generally higher than at 40 m and above, and increased steadily throughout the study. Reductions in the nutrients in December could again have been the result of a leaky sampling bottle

7.2.9 Calculated Carbon Parameters

7.2.9.1 Total Alkalinity

Alk_T, when normalised to a salinity of 35 psu, was reasonably constant throughout winter (Figure 7.12) at 2490 µequiv kg^{-1}. Significant decreases in Alk_T occurred at 2 m and 5 m from November until the end of the study. Occasional higher values were also recorded during summer. Alk_T at 70 m was very close to that of the upper water.

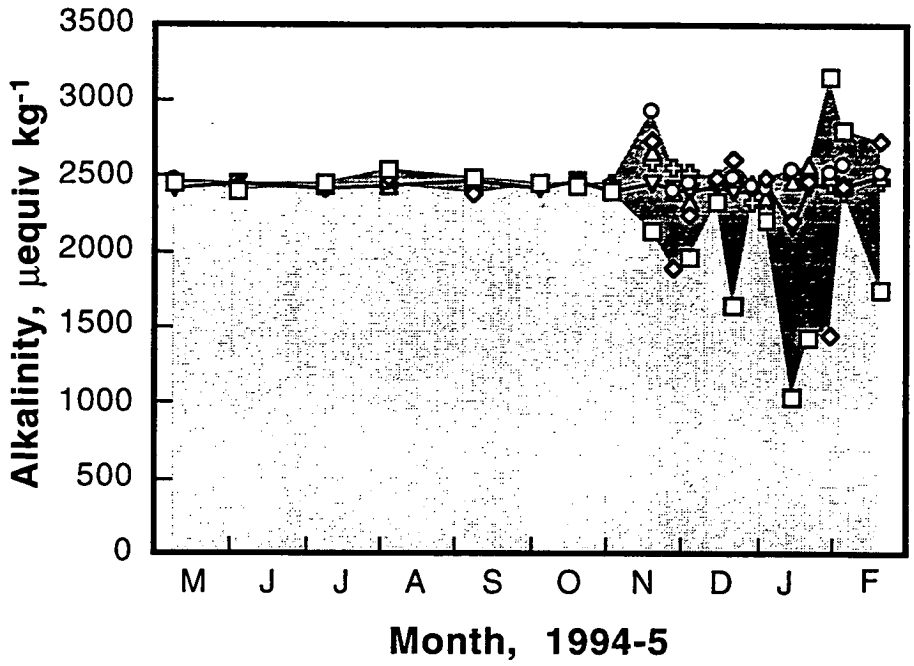

Figure 7.13. Total alkalinity (µequiv kg^{-1}) normalised to S = 35 psu, Ellis Fjord site, May 1994 - February 1995.

7.2.9.2 fCO_2

Calculated fCO_2 (Figure 7.13), reached a winter maximum (in the upper 40 m) of between 340 - 345 µatm in the middle of October. The fugacity decreased rapidly in November, especially at 2 m, where it fell to 17 µatm in mid-November and to even lower values in January and February. fCO_2 increased with depth, though from October until the end of the study it was significantly lower at 40 m than at the end of winter maximum. At 70 m fCO_2 rose from 345 µatm in May to a maximum of 654 µatm late in January.

7.2.10 Phytoplankton

The phytoplankton community at the Ellis Fjord site was not monitored as closely as at the O'Gorman Rocks site (Chapter 3). The dominant species were noted for all water samples, but cell counts were made only on selected samples during periods of particular interest. The general cycle of phytoplankton is shown schematically in

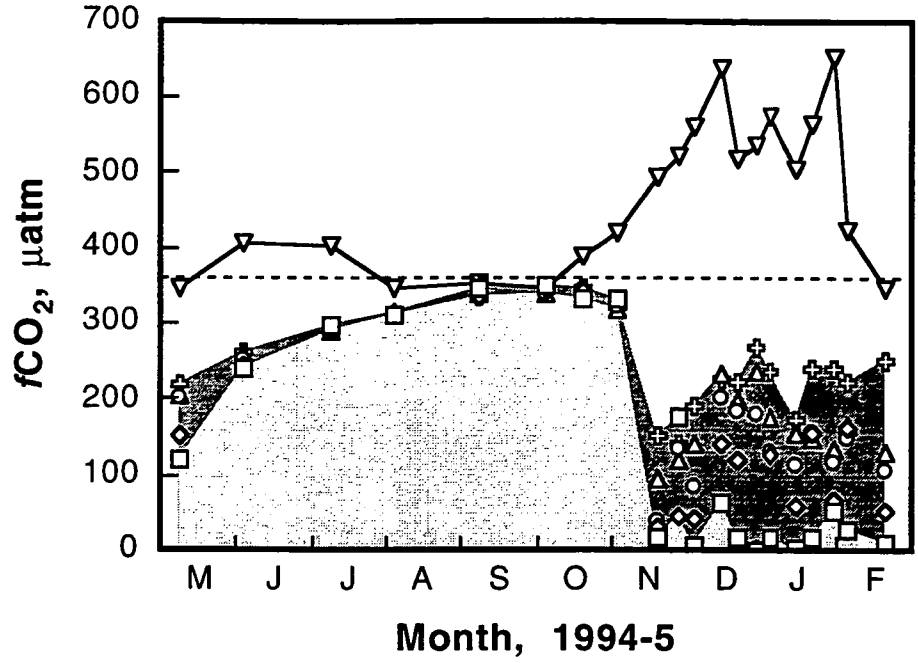

Figure 7.13. fCO_2 (µatm), Ellis Fjord site, May 1994 - February 1995. The dashed line indicates the concentration of CO_2 in the atmosphere.

Figure 7.14. Water samples from 70 m typically contained few apparently live cells and a great deal of detritus.

The phytoplankton community in May was dominated by the small diatom *Fragilariopsis curta.* This species was still present, but at lower densities, just under the ice in June, while heterotrophic dinoflagellates (not strictly members of the 'phytoplankton') were more common at greater depth. Dinoflagellates remained the dominant protists at all depths throughout winter, but were only present at low abundances (*circa* 5 x 10^4 cells L^{-1}). The range of genera of dinoflagellates present was similar to that at the O'Gorman Rocks site (Chapter 3).

The abundance of diatoms first began to increase in the water directly under the ice in early October, when the species *Nitzschia lecontei* was dominant at 2 m. By the mid-October, this species had been joined by *Entomoneis kjellmanii* and *Thalassiosira australis.* These two species were present at highest abundance at the end of October along with *Thalassiosira antarctica*, but by mid-November the diatoms had been

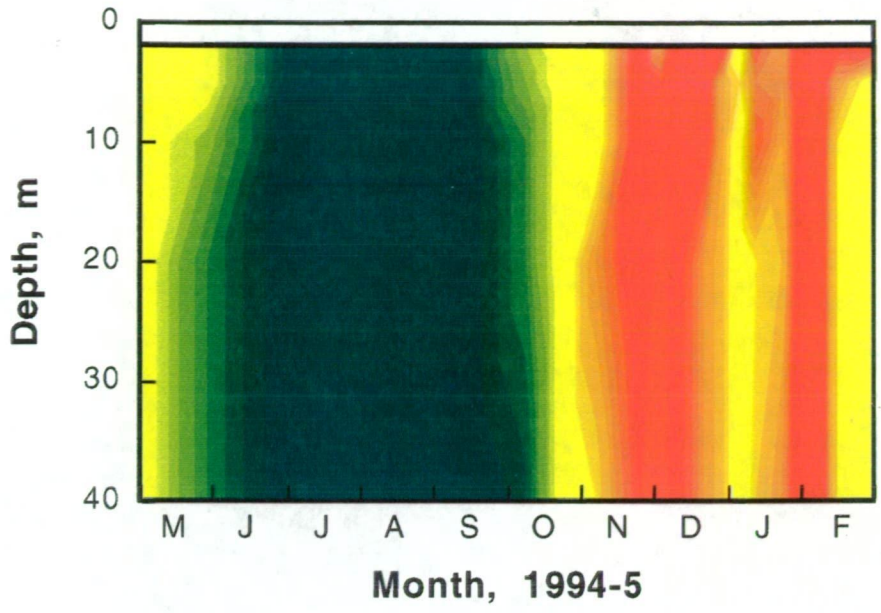

Figure 7.14. General cycle of dominant phytoplankton at the Ellis Fjord site. Green represents dominance by dinoflagellates, yellow diatoms, and red the flagellates cryptomonad A and/or *Pyramimonas gelidicola*. Orange essentially reflects mixed communities of diatoms and flagellates. Few viable phytoplankton were observed in samples from 70 m.

replaced by cryptomonad A (Chapter 3). From November till the end of the study, the dominant phytoplankton species alternated between cryptomonad A and various diatoms. At the end of November, the diatoms included *Berkeleya rutilans* and *Thalassiosira australis*, and in late December and early January *Porosira socialis* and *Fragilariopsis* spp. During the final period of domination by diatoms in February, *Thalassiosira dichotomica* was the most abundant species, though *Fragilariopsis curta* was also present. Many other species of diatoms, most of which were also present at the O'Gorman Rocks site (Table 3.1), were observed at lower abundances.

Cryptomonad A abundance peaked at over 1 x 10^7 cells L^{-1} in early December, and during other periods of dominance was between 1 x 10^6 and 1 x 10^7 cells L^{-1}. The prasinophyte *Pyramimonas gelidicola* was an important species just under the ice in late January, and was the dominant species at 2 m during February. Motile cells of

Phaeocystis cf. *antarctica* were observed at low abundances, and only very few colonies of this species were observed in sediment trap samples during late December.

7.3 Discussion

7.3.1 Seasonal Cycles of Primary Production and Related Parameters

7.3.1.1 The General Cycle of Productivity

The seasonal cycle of productivity in Ellis Fjord exhibited similar characteristics to that at the O'Gorman Rocks site. In particular, the winter increases in the concentrations of the nutrients and decreases in pH and DO were not coupled to the concentration of chl *a* and phytoplankton abundance. A number of important differences, however, occurred between the cycles. The first indication of phytoplankton growth in Ellis Fjord at the end of winter, evidenced by increasing concentrations of chl *a*, was observed in early October, and by the mid-October chl *a* at 2 m was very high (>20 mg m^{-3}), with concentrations significantly above winter levels occurring at all depths to 40 m. In contrast, the concentration of chl *a* in the water column offshore did not rise significantly until late November or early December.

The period during which primary productivity occurred in Ellis Fjord extended at least until the last sampling date in the middle of February, and probably considerably longer, as the samples collected in early May (at the beginning of the study) contained significant abundances of phytoplankton, above background chl *a* and markedly reduced nutrient concentrations (compared to later winter values and also to O'Gorman Rocks at the same time). Primary production therefore possibly extended over a seven month period between October and May, which was considerably longer than at O'Gorman Rocks (Chapter 4) and other Antarctic sites (Bunt, 1960; Krebs, 1983; Fukuchi et al., 1984; Perrin et al., 1987).

The extended period of primary production was in part a result of reduced tidal action and the persistent ice cover, which resulted in a reduction in the formation of new ice and mixing resulting from brine exclusion (Gade et al., 1974; Kantha, 1979; Gallagher and Burton, 1988) during winter. Thus, summer density stratification due to surface heating and partial ice melt was more easily maintained, and phytoplankton remained near the surface rather than deeper in the water column beneath the critical depth. In contrast to the situation in the fjord, the water column at the O'Gorman Rocks site was mixed by ice formation, brine freeze out and tidal action by early April, and nearly all phytoplankton activity had ceased.

The limited mixing would also have assisted in the initiation of the spring phytoplankton bloom in the fjord in mid-October. This bloom was at first restricted to the very top of the water column, and the algae were probably present as a mat of diatoms growing at the bottom of the sea ice (McConville and Wetherbee, 1983; McMinn, 1996). Even though high concentrations of chl *a* were recorded in the water column at this time, there was little reduction in DIC or nutrients (or increase in DO) from the winter values, especially when compared to the changes in the concentrations observed in November. Thus, the chl *a* in the water column was probably the result of detachment of mat material from the base of the ice. The nutrients and DIC required for the formation of this material were presumably derived from close to the ice-water interface and within brine channels in the ice.

7.3.1.2 Seasonal Cycle of Phytoplankton

The phytoplankton community throughout most of the water column was dominated from October to the end of the study by either a selection of diatoms or the undescribed species cryptomonad A, which was also observed at the O'Gorman Rocks site (Chapter 3). After the initial diatom 'bloom' recorded in October that appeared to be material dislodged from the mat community at the base of the ice, growth of

phytoplankton (largely diatoms) within the water column was occurring by early November, as evidenced by reduction in DIC and the nutrients. These diatoms were in turn replaced by cryptomonad A by the middle of the month, but at the end of November diatoms were again more numerous. This alternation of dominant species continued throughout the rest of the summer. Peaks in the abundance of cryptomonad A were generally associated with periods of lower chl *a*, suggesting that this species was most abundant in periods between diatom blooms and peaks of primary productivity. The prasinophyte *Pyramimonas gelidicola* was present at 2 m in late January and February, which accounted for the increased concentration of chl *b* observed in these samples.

This cycle was generally similar to that reported from an earlier study of the fjord (McMinn and Hodgson, 1993). These authors documented a November diatom bloom in Deep Meromictic Basin (Figure 6.1) consisting of the same species recorded in the present study, which was followed by a peak in abundance of cryptomonad A in mid-December. Another diatom bloom followed, and then a period when diatoms and cryptomonad A and diatoms were nearly co-dominant.

The phytoplankton succession recorded at the Ellis Fjord sampling site could be divided into two periods related to the mixing processes occurring in the fjord: Spring, when little mixing or input of external waters was occurring; and summer, when ingress of water from outside the basin increased. As discussed in Chapter 6, prior to mid-December there appeared to be little input of water to Middle Basin (and the sampling site) from other parts of the fjord or from outside the entrance to the fjord. Warmer, less saline water which had entered Middle Basin from Inner Basin (Figure 6.1) was first recorded on 12 December and the continued throughout the rest of the summer (see Figure 6.8).

Early in spring (before the onset of water advection) the phytoplankton community at the sampling site was free of external influences. The species of phytoplankton present, which included *Nitzschia lecontei*, *Thalassiosira australis* and *Entomoneis kjellmanii*, must have been derived from a local source, most likely the ice cover, or from cysts which had overwintered in the sediment (Leventer, 1991; McMinn, 1996). The initial bloom in October was replaced by cryptomonad A, which indicated that this species was also present in Middle Basin throughout the year. This situation continued through November and early December, with locally derived diatom species or cryptomonad A dominating the phytoplankton.

On 19 December the situation had changed considerably. Cryptomonad A was dominant, few diatoms were present, the concentration of chl *a* was lower than at any time since mid-October, and the concentration of the nutrients were greater than early in the month. This change was coincident with the first major ingress of water from Inner Basin (Chapter 6), and suggested that either cryptomonad A was transported into Middle Basin with the low chl a and high nutrient water.

The diatom blooms that were present in summer exhibited a number of differences to those present in spring. Firstly, the bloom was centred at greater depth, with maximum chl *a* occurring between 5 and 20 m. Secondly, the species making up the bloom had changed, with *Porosira socialis*, *Fragilariopsis* spp. and later on *Thalassiosira dichotomica* dominant. These species could well have been introduced into Middle Basin with the water input, and subsequently developed into a bloom. Another period of relatively low chl *a* occurred in mid-January coincident with the second period of increased water input. Cryptomonad A was again common at this time, but the diatom had became dominant by the end of the month.

In summer the phytoplankton in the water at 2m was quite different to that deeper in the water column. For example, the prasinophyte *Pyramimonas gelidicola* was

common at this depth in January and February, but was not present at other depths. The generally strong correlation between temperature and salinity did not hold at 2 m (Chapter 6), indicating that this water was less affected by external water inputs. Therefore, the phytoplankton community at this depth could develop separately from that deeper in the water column.

The existence of intense phytoplankton blooms in Ellis Fjord throughout summer indicates that such blooms can develop under a cover of ice. The diatom communities present in spring undoubtedly developed under ice, though the situation after the influx of water from Inner Basin was less clear-cut. It is possible that the phytoplankton blooms observed at the sampling site after this time had in fact developed in ice free conditions close to the entrance of the fjord (where a small area of open water developed late in December) or outside the fjord. However, a number of points suggest that most growth occurred after advection of the water to the Inner Basin. Firstly, chl *a* and POC concentrations immediately after major periods of advection were generally low, indicating that the incoming water contained low numbers of phytoplankton. Secondly, the phytoplankton species dominant after the inputs of water, cryptomonad A, was replaced by diatoms during subsequent periods of higher chl *a*. From these observations it can be concluded that phytoplankton blooms observed at the sampling site after mid-December had developed in Middle Basin under ice.

The development of phytoplankton blooms under the ice suggests that the species involved were adapted to growth in low light conditions. A profile of light transmission at wavelengths from 400 to 750 nm was recorded at the Ellis Fjord site on 12 December (K. Michael, personal communication). The profile indicated that the 1.2 % of the surface irradiance was transmitted through the ice, with the 1 % isolume falling at *circa* 2.5 m. The light level at 16 m (the depth of the profile) was 0.2 % of the surface irradiance. Given a maximum summer surface irradiance of *circa* 1500 μE

m^{-2} s^{-1} (Burch, 1988), the percent transmissions equate to *in situ* irradiances from 18 μE m^{-2} s^{-1} at the under surface of the ice and 3 μE m^{-2} s^{-1} at 20 m. Development of a diatom bloom at less than 1 % of surface irradiation has been reported from McMurdo Sound (Palmisano and Sullivan, 1983), which indicates that Antarctic phytoplankton can adapt to very low light levels, as do photosynthesis - irradiance relationships determined for Antarctic sea ice microalgae. Maximum growth rates at irradiances as low as 5 μE m^{-2} s^{-1} have been reported (Palmisano et al., 1985). Even though photosynthesis - irradiance relationships are not available for bottom ice algae and phytoplankton from Ellis Fjord, it was clear that they were adapted to low light conditions, and thus were able to develop into blooms both in the bottom ice community and to a considerable depth in the water column.

Many previous workers have assumed that major phytoplankton blooms do not occur in the under ice environment (e.g. Smith and Sakshaug, 1990; Bouquegneau et al., 1992) and that any blooms in this environment have been advected from open water (e.g. Knox, 1990). Marginal ice zones are recognised as highly productive areas in the Southern Ocean (Sullivan et al., 1988), but the generally accepted paradigm suggests that no water column bloom occurs under the ice prior to ice melt and development of stratification. The results from Ellis Fjord indicate that this is not necessarily the case, and that significant phytoplankton blooms can develop in the spring prior to break up of the ice cover.

7.3.1.3 Seasonal Cycle of DIC, Nutrient and Oxygen Concentrations

The concentrations of DIC and the nutrients rose steadily from June to October, while DO decreased. The major process leading to the increase in these concentrations was remineralisation of organic material that had been produced by photosynthesis, as upwelling of DIC and nutrient rich water was not possible in Ellis Fjord, and there was no evidence in the salinity, temperature and nutrient data for winter introduction of

water from outside the basin. Remineralisation occurred either at the sediment-water interface, or within the water column from resuspended organic material (Chapter 8). Entrainment of the relatively nutrient rich waters in the isolated water initially beneath 50 m occurred, as shown the deepening of the interface between the water bodies (Chapter 6), but this process had only a minimal effect on upper water nutrients.

The concentrations of DIC and the nutrients generally dropped from early October until the end of the study. The concentrations recorded during this period were the balance of uptake by phytoplankton, release by remineralisation within the water column and by the benthic community and import or export resulting from tides. A significant increase in the concentrations of the nutrients that occurred in early December was attributable to import associated with transport of water from Inner to Middle Basin. A further increase was recorded in January again probably due to the import of high(er) nutrient water.

7.3.1.4 Alkalinity

Alk_T in Ellis Fjord was considerably higher than at the O'Gorman Rocks site. The only process that could have led to this increase was the dissolution of carbonate minerals. Ellis Fjord has significant populations of calcareous benthic organisms such as serpulid tube worms (Kirkwood and Burton, 1988), and dissolution of old tubes and other calcareous material must have occurred after the water entered fjord. The consistently higher alkalinity is an indication of the effective isolation of the fjord from the influence of outside waters.

Anomalously low DIC concentrations recorded regularly at depths of 2 and 5 m throughout the summer (Figure 7.1) were associated with low total alkalinities (Figure 7.15). Also shown in the figure are arbitrary trend lines which indicate the expected change in alkalinity if carbonate precipitation or photosynthesis/respiration were the

only mechanisms by which DIC was removed. The figure suggests that the low DIC concentrations were to some extent the result of the precipitation of carbonate, but also that removal during photosynthesis occurred, as the data fall to the low DIC side of the carbonate precipitation line.

The very low values of DIC and alkalinity recorded on many occasions at 2 and 5 m during the summer were generally associated with high DO concentrations, confirming that they were in part the result of photosynthesis. These extreme concentrations often occurred during blooms of the diatoms *Entomoneis kjellmanii* and, especially, *Thalassiosira australis*, indicating that rapid growth of these species was responsible

Figure 7.15. Total alkalinity (μequiv kg^{-1}) plotted against DIC (μmol kg^{-1}) for the Ellis Fjord site. All data have been normalised to S = 35 psu. Also shown is the relationship between these parameters expected (assuming an initial alkalinity of 2490 μequiv kg^{-1} and DIC of 2320 μmol kg^{-1}) if carbonate precipitation occurred. The dashed lines indicate the joint effect of carbonate precipitation and the production of organic material with C:N mole ratios ranging from 7.4 to 30.

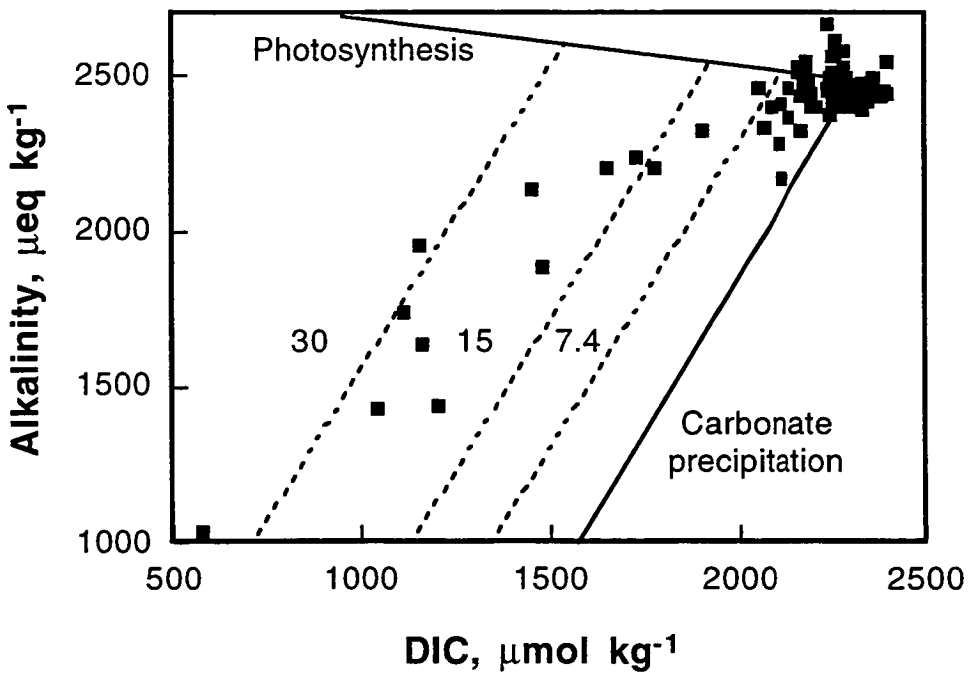

for the decrease of DIC to low concentration. Even taking into account the precipitation of carbonate, the reduction in DIC in these instances was far greater than the maximum predicted from the concentration of nitrate and the average C:N molar uptake ratio (7.4: see below). Therefore it appears that these phytoplankton species, especially when growing immediately under the ice, were capable of production of OC (and DO) even after the exhaustion of nitrate. As the concentration of phosphate was not reduced to zero in these cases, the OC produced after exhaustion of nitrate must have been essentially nutrient free, and thus would have had a high C:N and C:P mole ratio. The dashed lines in Figure 7.15 indicate that a C:N mole ratio of 30 was needed to explain some of the data points.

Sediment trap data from Ellis Fjord (Chapter 8) confirmed the formation of low nitrogen organic material in the present study, especially during the spring and early summer when the diatom species mentioned above were dominant. C:N mole ratios between 10 and 14 were recorded regularly in the trap material. These conclusions parallel those from a study of crack pools in rotting sea ice (Gleitz et al., 1996a). In this case, the overconsumption of carbon relative to the nutrients occurred during rapid photosynthesis in a high chl *a*, high light environment, with the result that the POC produced had C:N ratios of up to 15. The diatom community in the crack pools were dominated by *Thalassiosira antarctica*, a species that was sub-dominant Ellis Fjord, and closely related to *Thalassiosira australis*. The environment directly under the ice in the present study must have been sufficiently stable, and the light intensity high enough, for similar overconsumption to occur. Cota and Sullivan (1990) recorded C:N mole ratios in bottom ice mat organic material of *circa* 14, confirming that low nitrogen organic material can be produced under ice.

7.3.1.5 The Fugacity of CO_2

As at O'Gorman Rocks, fCO_2 in the upper 40 m increased to a maximum late in winter. The fugacity reached, however, was slightly lower than offshore, and the surface water remained undersaturated with respect to the atmosphere throughout the study. This was probably the result of a reduction in the concentration of DIC in the surface water due to the sedimentation of OC to the isolated water beneath 50 m, in which fCO_2 increased to very high levels as a result of the remineralisation of OC, and the sediment. The return of DIC to the surface water after OC remineralisation was not as efficient in the fjord as offshore, where convection in the WW layer provided a strong mixing force.

As at the O'Gorman Rocks site, primary production reduced fCO_2 during the summer. The fugacity was typically lowest at 2m, at which depth values of less than 10 µatm were recorded on occasions, but increased with depth. These low fugacities reflected the high pHs and low concentrations of DIC recorded at the top of the water column during the summer.

7.3.1.6 Nutrients, DIC and Dissolved Oxygen at 70m

The concentrations of DIC and the nutrients continued to increase (and DO decrease) at 70 m during summer as a result of remineralisation of organic material sedimenting from the upper waters. The DIC and nutrients produced during remineralisation were not returned to the upper water layer due to the pycnocline separating the two water bodies. Likewise, DO could not be replenished. The concentrations of DIC and the nutrients began to rise soon after the initiation of the phytoplankton bloom, indicating that OC from near the surface began to reach the isolated water soon after primary production began. The concentration of silicate rose by a greater relative amount than the other nutrients, suggesting that sedimentation of diatoms was important in the

transfer of organic material from the surface to this region. The decreases in DIC and nutrients at 70 m observed late in the study reflected mixing of upper water with lower DIC and nutrient concentrations to this depth (as evidenced by the progressive decrease in salinity at 70 m (Chapter 6)).

Alk_T in the isolated water was virtually identical to that in the upper water, indicating that the increases in DIC (and the nutrients) was due solely to remineralisation of organic matter rather than carbonate dissolution.

The rates at which the nutrients increased at 70 m during winter can be used to estimate when this water became isolated from the surface water by extrapolating back to end of winter levels, which suggested that the lower water body became isolated sometime during the 1993-4 summer. This was consistent with the input of low salinity and density water into Middle Basin during that summer. Evidence from the temperature and salinity profiles in May 1994 (Chapter 6) indicated that surface warming and freshening occurred to 50 m during the 1993-4 summer, coincident with the top of the isolated water body. The same process occurred during the 1994-5 summer, and the water beneath about 35 m would have remained isolated for at least part of the 1995 winter before mixing into the rest of the water column.

7.3.2 Correlations: DIC, Nutrients and Dissolved Oxygen

The concentrations of DIC (ignoring the anomalously low under ice values during summer), the nutrients (including silicate) and DO (also ignoring very high concentrations observed on occasions at 2 and 5 m) in samples from all depths to 40 m from Ellis Fjord were quite strongly intercorrelated. Figure 7.16 shows a number of the correlation plots, and Table 7.1 gives full details of all the regressions.

The correlations between the parameters were generally less strong than in samples from the O'Gorman Rocks site (Chapter 4). This could have been a result of reduced mixing in the fjord, which would not have smoothed out any local or short term heterogeneities in the concentrations in the water column, due, for example, to phytoplankton during a particular bloom having different nutrient uptake ratios to those present at other times (Section 7.3.3.1). The advection of water to the sampling site in December and January did not appear to affect the relationships, but could also have been a source of scatter.

Silicate was more strongly correlated to the other parameters in Ellis Fjord than at the offshore site. This, paradoxically, is probably again a reflection of the lack of mixing in Ellis Fjord. At the O'Gorman Rocks site, the advection of water with quite different silicate concentrations into the area (Chapter 3) probably decreased the strength of the

Table 7.1. Details of regressions between the concentrations of DIC, nitrate (N), phosphate (P), silicate (Si) and DO (all normalised to S = 35 psu). The errors given are the standard errors for the regressions. All regressions were significant at the 1 % level.

Regression	Slope	Slope error	Intercept	Intercept error	r^2
DIC - N	7.40	0.66	2118	13	0.65
DIC - P	101	10	2067	20	0.58
DIC - Si	3.85	0.51	2052	27	0.46
DIC - DO	-0.92	0.06	2569	20	0.77
N - P	12.9	0.8	-5.92	1.42	0.74
Si - N	1.34	0.08	27.1	1.6	0.72
Si - P	17.6	1.6	18.3	2.9	0.55
DO - N	-7.30	0.58	477	11	0.69
DO - P	-95.6	10.0	520	19	0.57
DO - Si	-3.44	0.51	523	27	0.41

Figure 7.16. Correlation plots of the concentrations (normalised to S = 35 psu) of (a) DIC and nitrate; (b) DIC and phosphate; (c) DIC and silicate; (d) DIC and dissolved oxygen; (e) nitrate and phosphate and (f) nitrate and silicate. Low concentrations of DIC and high concentrations of dissolved oxygen have not been included (see text).

(a)

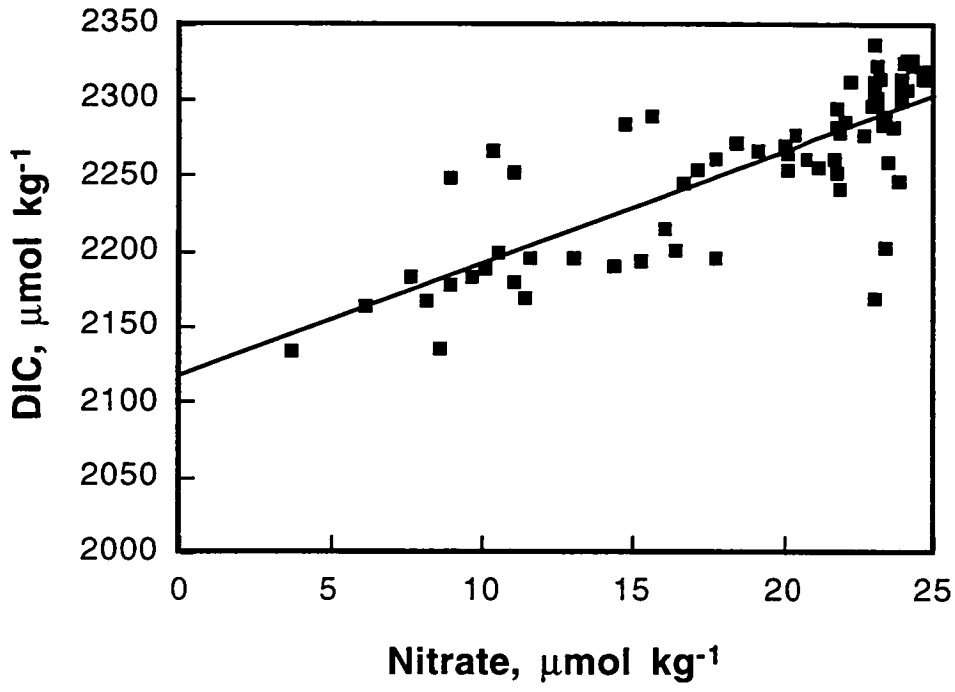

(b)

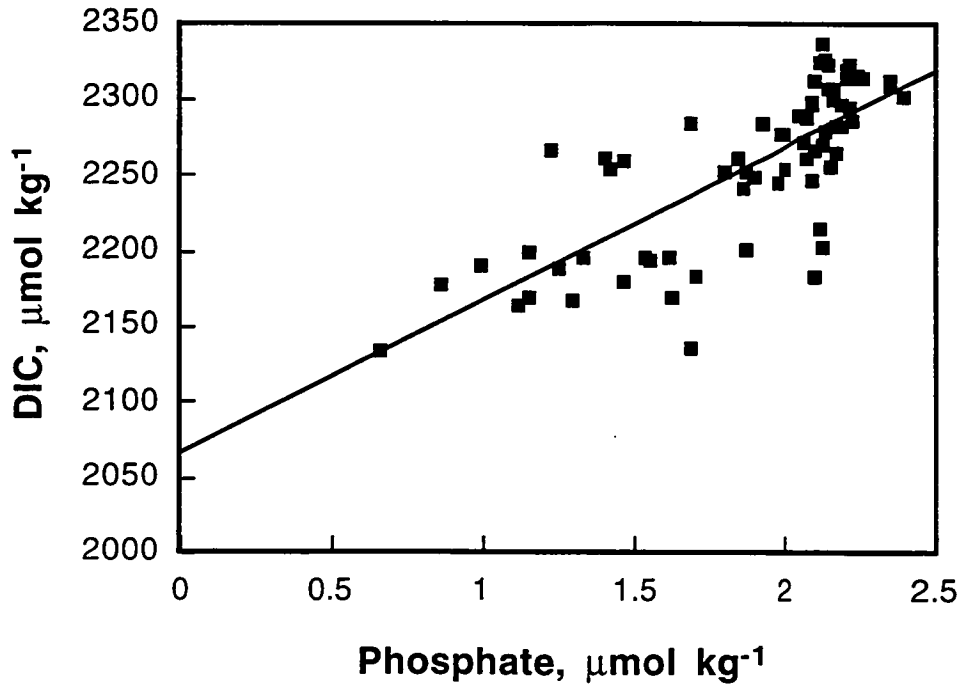

Figure 7.16. Continued

(c)

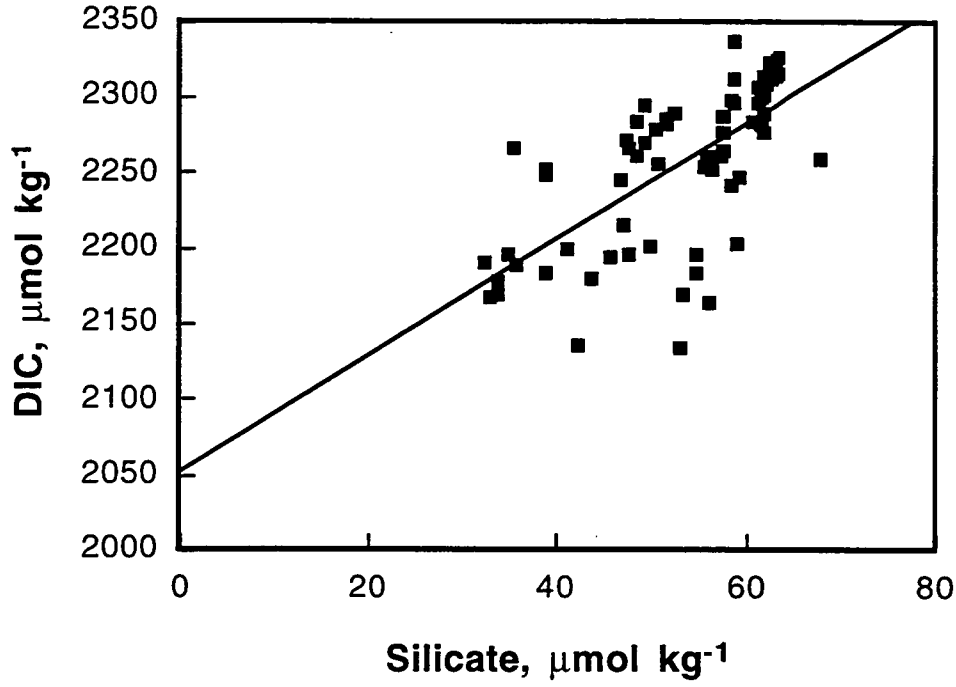

(d)

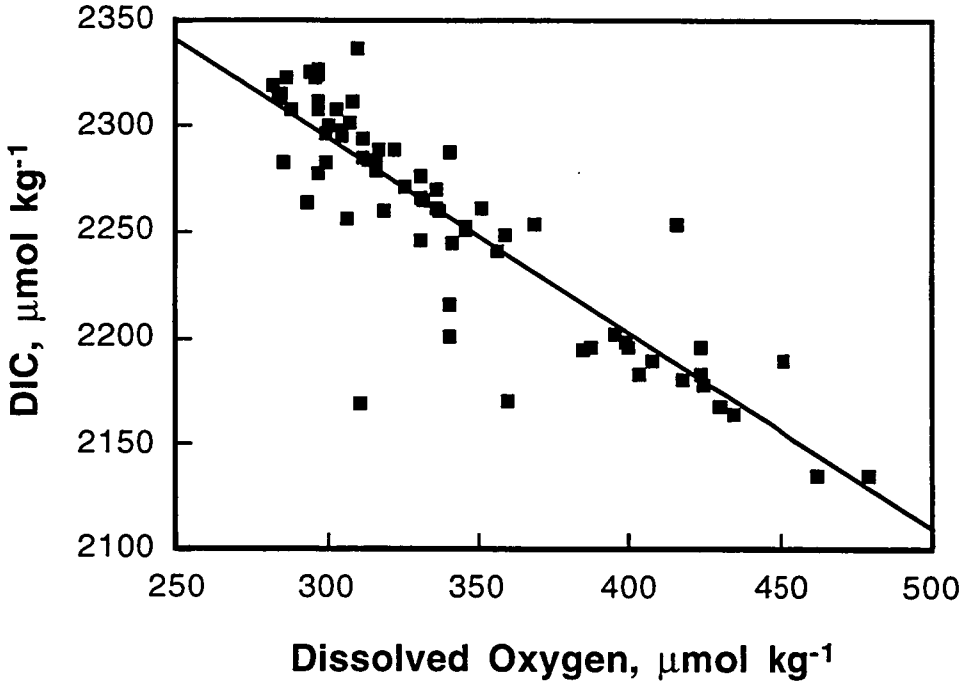

Figure 7.16. Continued

(e)

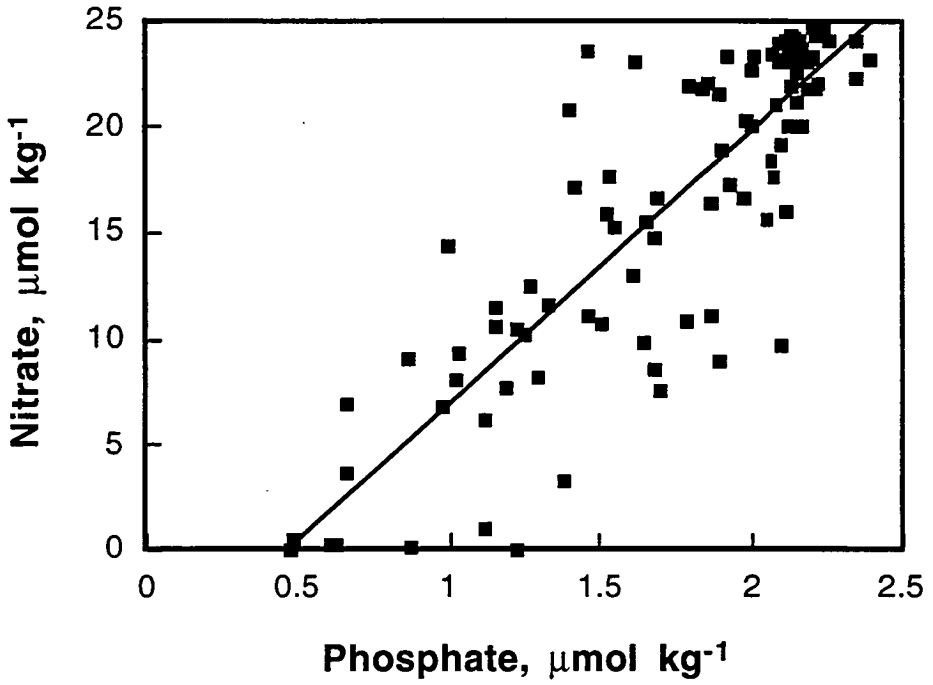

(f)

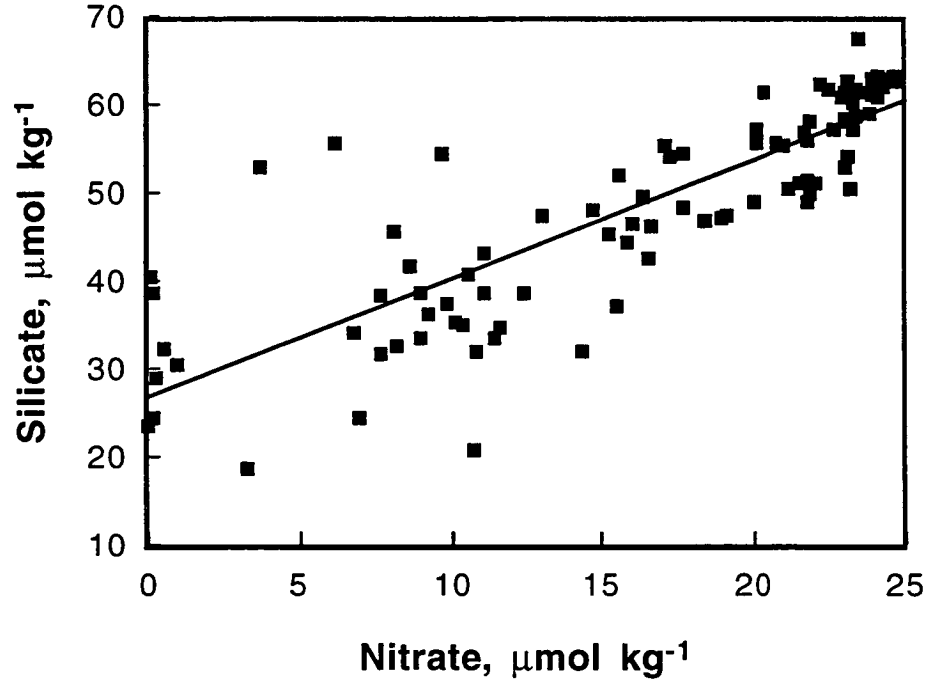

correlations, whereas advection in Ellis Fjord did not introduce water of markedly different nutrient ratios.

The average C:N:P molar uptake ratio for Ellis Fjord was 101:12.9:1. This ratio was quite similar to that determined at the O'Gorman Rocks site (97.8:15.0:1), with the main differences being that slightly more OC was produced in Ellis Fjord per mole phosphate, and that less nitrate was taken up in the process. As for the O'Gorman Rocks site, the C:N:P molar uptake ratio was quite close to the Redfield Ratio (Redfield et al., 1963), and unremarkable. McMinn et al. (1995) found a similar N:P ratio (13.8:1) in the only other study of nutrients in Ellis Fjord. The O_2:C ratio in the fjord, -1.09, was of slightly lower absolute magnitude than at O'Gorman Rocks during the period of ice cover, -1.20.

The Si:N molar uptake ratio in Ellis Fjord, 1.34:1, was lower than the ratio calculated for the fjord in the study of McMinn et al. (1995) (1.85:1), and much lower than ratios recorded during Antarctic ice edge blooms (up to 2.9) (Jennings et al., 1984). Brzezinski (1985) reported Si:N uptake ratios between 0.8:1 and 1.2:1 for cultures of diatoms growing in nutrient replete conditions, with the former ratio being typical of small species (<20 μm) and the latter for larger species. Brzezinski (1985) further noted that light, photoperiod, temperature, nutrient limitation and diatom species composition produced 2 to 3 fold variations in the Si:N uptake ratios. Furthermore, the relative importance in the fjord of flagellate phytoplankton species which do not have a requirement for Si would also have influenced the ratio.

Figure 7.16e suggests that nitrate was the limiting nutrient in Ellis Fjord during the study, as it was at the O'Gorman Rocks site. It is interesting to note that the uptake of silicate and nitrate became decoupled in some of the samples with very low nitrate concentration (Figure 7.16f), with uptake of silicate being less than predicted from the regression line. This decoupling reflects the dominance of flagellates such as

cryptomonad A and *Pyramimonas gelidicola* (which do not have a requirement for silicate) in these samples, which were all collected from directly under the ice in January and February. The concentrations of silicate in these samples could have been close to the minimum required for the growth of diatoms, which is species specific and in the range 5 - 20 μmol kg^{-1} for the small, lightly silicified species present at the time (Jacques 1983; Sommer, 1986; Nelson and Tréguer, 1992), thus favouring the growth of flagellates.

7.3.3 Organic Carbon Production and Budgets

7.3.3.1 Estimates of Net Organic Carbon Production

The amount of OC produced by primary productivity in Ellis Fjord was estimated by calculating the loss of DIC and nutrients (or increase in the concentration of DO) from the end of winter values for these parameters, correcting for dilution and then scaling to carbon using the slopes of the regression lines given above and the approach outlined in Chapter 4 (specifically Eqaution 4.1). The end of winter values used in the calculations are given in Table 7.2, and the calculated amounts of net OC production integrated from 2 to 40 m are shown in Fig 7.17.

Table 7.2. Estimated end of winter values for the parameters used in the calculation of net OC production.

Parameter	Value
Salinity	34.17 psu
DIC	2263 μmol kg^{-1}
Oxygen	276 μmol kg^{-1}
Nitrate	24.1 μmol kg^{-1}
Phosphate	2.17 μmol kg^{-1}

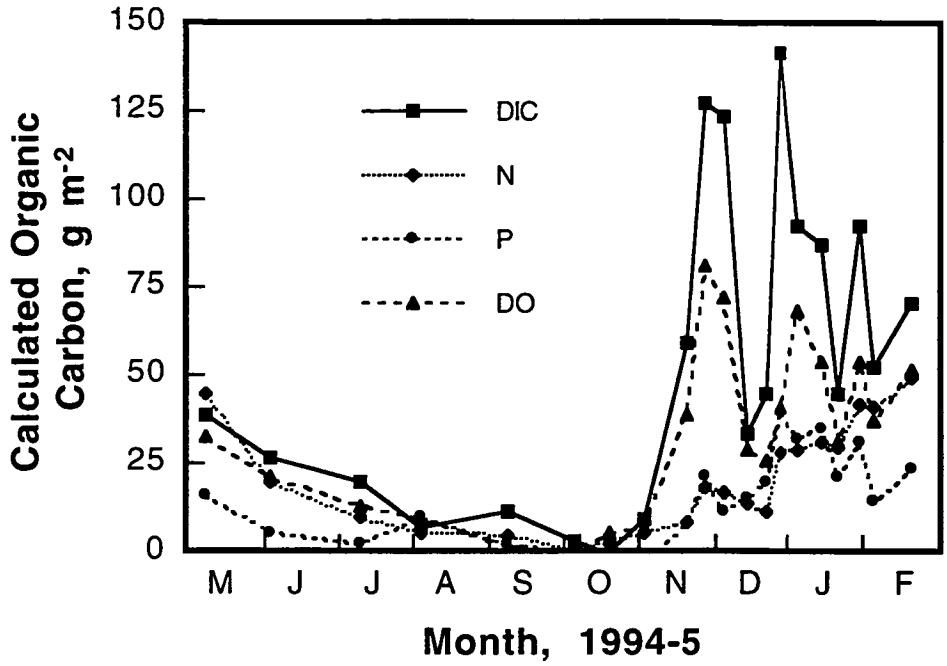

Figure 7.17. Net organic carbon production (g m^{-2}) calculated from the concentrations of DIC, nitrate (N), phosphate (P) and dissolved oxygen (O).

In contrast to the O'Gorman Rocks site, considerable variation occurred in the calculated net OC production depending on the parameter used for the calculation. Throughout the summer OC calculated from the concentrations of DIC were significantly higher than those calculated from the other parameters. Net OC production calculated from the concentrations of DO parallelled those from DIC quite closely, but were always lower. This disparity was largely due to the increases in the concentrations of DO being insufficient to match the very low DIC concentrations recorded at 2 and 5 m on many occasions throughout the summer, which was presumably the result of precipitation of inorganic carbonate from the water. The concentration of DO is therefore likely to provide the best estimate of net OC production.

The net OC production calculated from the other parameters (nitrate and phosphate) were much lower than calculated from DIC and DO (Figure 7.17). These data were consistent with the formation of organic matter during periods of high productivity which had higher C:N and C:P ratios than 'standard' organic material, as discussed

above and confirmed to some extent by the higher C:N ratio of material caught in sediment traps at this time (Chapter 8). Maxima in organic matter standing stock, along with decoupling of the C:N and C:P ratios, were associated with the presence of diatom blooms. In between these blooms, when the flagellate cryptomonad A was the dominant species, net OC production calculated from the four parameters was much more consistent, supporting the contention that the ability to produce OC without the incorporation of nutrients was a characteristic of at least some species of diatoms and not of cryptomonad A.

7.3.3.2 The Magnitude of Organic Carbon Production

For the reasons discussed above, the net OC production calculated from the concentrations of DO will be used unless otherwise stated in this discussion. It should be noted, however, that these calculations of OC production assume a constant O_2:C ratio, which may not be the case during periods of intense productivity.

The highest calculated net OC production, *circa* 80 g m^{-2}, was recorded in late November (Figure 7.17), with average values during summer of approximately 30 g m^{-2}. Calculation of the net summer OC production at the Ellis Fjord site is difficult, as OC varied dramatically and rapidly throughout the summer, indicating that a very active balance between OC production, grazing, import and export was occurring. However, it is worth noting that the net OC produciton in May, prior to winter mixing and cessation of photosynthesis, was near 40 g m^{-2} (equivalent to 220 mg m^{-2} day^{-1} from the beginning of November), similar to the annual net production in eastern McMurdo Sound, 55.7 g m^{-2} (Knox, 1990).

The rates of organic matter production were again determined by dividing the difference between the calculated net OC production on successive sampling dates by the number of days between the dates. The calculated rates, shown in Figure 7.18, are

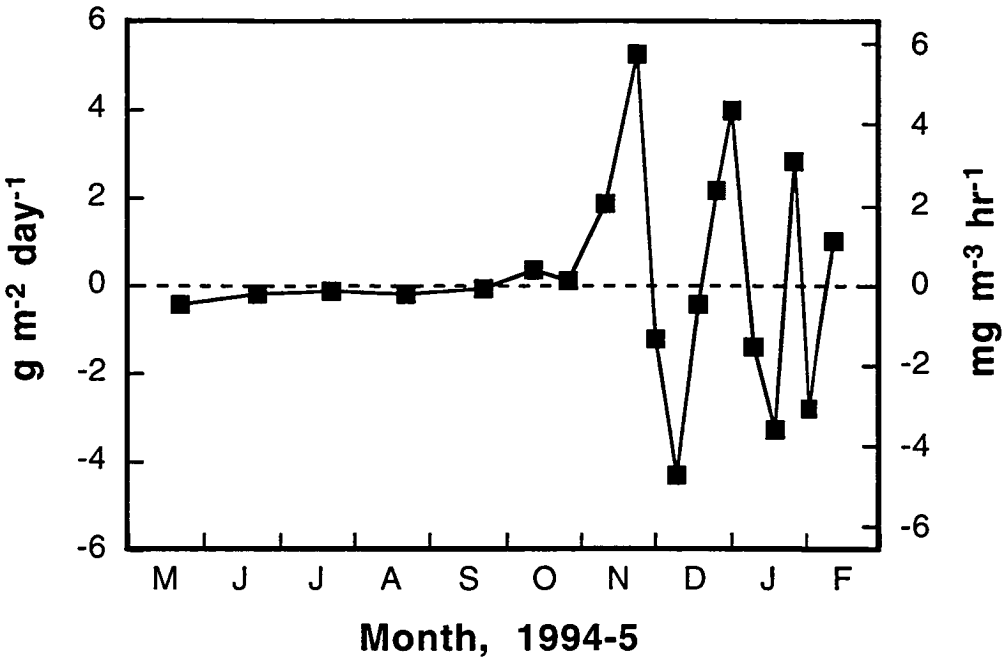

Figure 7.18. Calculated rate of organic matter production (or remineralisation) for the entire water column to 40 m.

averages for the water column to 40 m, and are at the high end of the range of rates measured in the Antarctic region. Smith and Sakshaug (1990) stated that highest rate of primary productivity for the entire water column recorded in the Antarctic region was 3.62 g C m^{-2} day at an inshore site near Deception Island (Burkholder and Mandelli, 1965), considerably lower than the maximum rates recorded here. However, production rates of 12 g C m^{-2} day^{-1} were measured in the Chukchi Sea during a period when chl *a* reached 40 mg m^{-3} (Smith and Sakshaug, 1990)), which were similar to chl *a* concentrations measured in Ellis Fjord. Gleitz et al. (1996a) recorded rates of primary productivity of up to 30 mg C m^{-3} h^{-1} in slush filled crack pools between ice flows, and the rate of primary productivity in the under ice water in Ellis Fjord might have reached this rate, as that given for the fjord is the water column average. Thus, the rates of primary productivity calculated in the present study are very high, but not without precedent in polar regions.

The net average rate of primary productivity from October to the end of the study in Ellis Fjord, 510 mg C m^{-2} day^{-1}, was similar to seasonal productivity during spring in

ice edge environments in the Weddell Sea (562 mg C m^{-2} day^{-1}; Smith and Nelson, 1990) and in the Ross Sea (962 mg C m^{-2} day^{-1}; Wilson et al., 1986). These ice edge environments are considered to be particularly productive due to the formation of shallow stratification due to ice melt which allows the phytoplankton to remain near the surface and in a high light environment. Ellis Fjord is a similar environment, in that stratification of the water column was present during the period of phytoplankton blooms, but had the added advantage of the absence of wave and swell action that would tend to destroy the stratification and, indirectly, reduce productivity.

The apparent OC remineralisation that occurred during the summer could have resulted from major influxes of nutrient rich(er) water into Middle Basin, and therefore a proportion of the apparent remineralisation did not occur at the site, but rather was the result of the import of low OC water (or at least high nutrient water). Export of OC from the site not replaced by import in the water arriving at the site indicates that the actual net rate of productivity at the site was greater than calculated. Some remineralisation undoubtedly occurred in the water column at the sampling site, however. Even if export and import were the major causes for the rapid variations observed in the concentration of OC, the net summer productivity and rate estimates, which compared the concentrations of DIC and the nutrients at the start of summer and at the end of the study, remain meaningful numbers.

7.3.3.3 Correlation of Calculated and Measured Organic Carbon

Figure 7.19 shows a plot of the concentration of OC calculated from the increase in concentration of DO and that measured experimentally (the sum of DOC and POC) for the period from early October to the end of the study. A background DOC concentration of approximately 70 μmol kg^{-1}, slightly higher but similar to that at the O'Gorman Rocks site (Chapter 4), is suggested by the regression line. The ratio between measured and calculated OC is also similar to that at the offshore site,

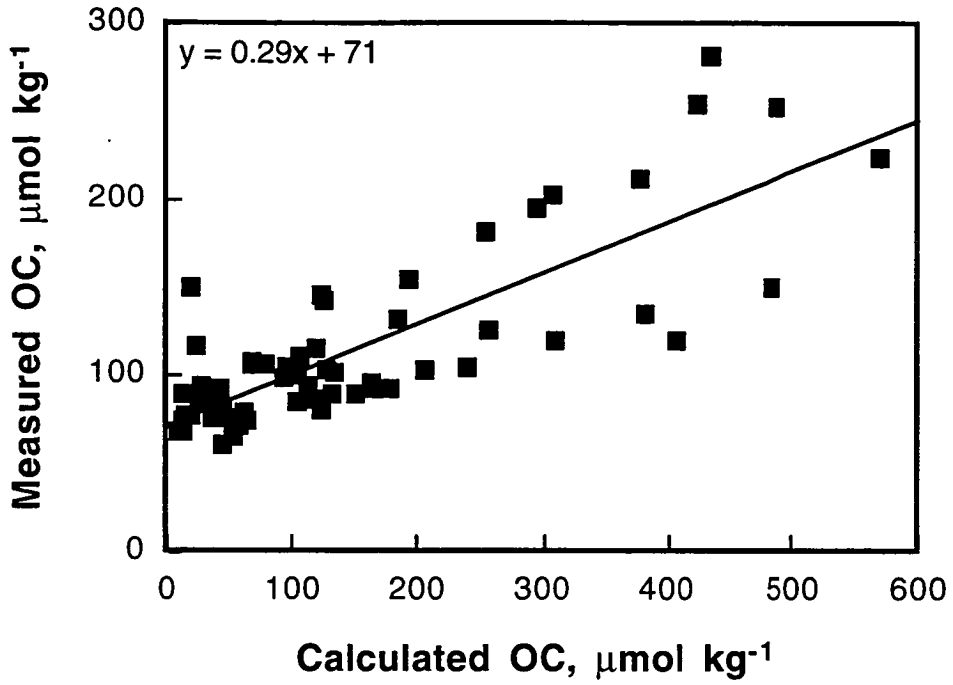

Figure 7.19. Plot of the calculated and measured concentrations of organic carbon in Ellis Fjord.

indicating that a large percentage of the OC produced has been removed from the water column by sedimentation or transfer to zooplankton and high trophic levels. The apparent percentage loss of OC was nearly identical at the two sites.

7.3.4 Carbon Isotope Chemistry: Nutrient Correlations and the Effects of Primary Production

The seasonal cycle of the $\delta^{13}C_{DIC}$ at 10 m was very similar to that at the O'Gorman Rocks site, with the exception that $\delta^{13}C_{DIC}$ was essentially constant throughout winter in Ellis Fjord while offshore a sharp but temporary drop was recorded near midwinter. Due to the permanent sea ice cover in the fjord (at least during the study), there could have been no uptake of CO_2 from the atmosphere, and therefore any variation in the $\delta^{13}C$ of the DIC must have been due to fractionation during the transport of CO_2 into the cell and photosynthesis.

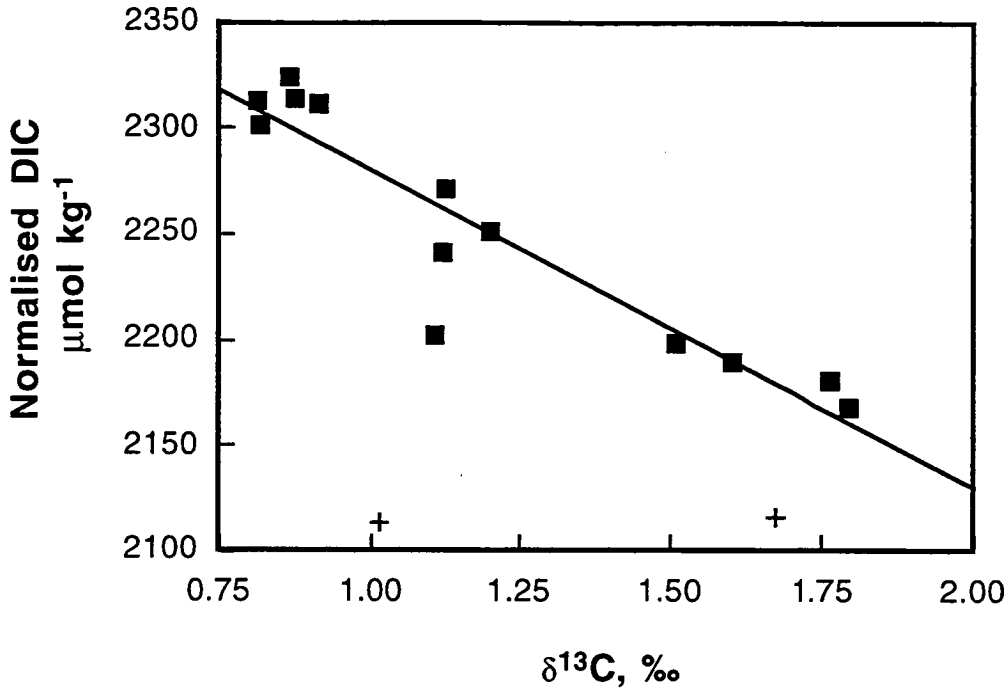

Figure 7.20. The correlation between DIC (normalised to S = 35 psu) and $\delta^{13}C_{DIC}$ for samples from 10 m. The data represented by crosses were not included in the calculation of the regression line.

Figure 7.20 shows a pot of $\delta^{13}C_{DIC}$ against the concentration of DIC (normalised to constant salinity) at 10 m for Ellis Fjord. The slope of the regression line relating these parameters can be used to calculate the average isotope fractionation during organic matter production (see Chapter 4 for discussion of the calculations). Two data points in Figure 7.20 (shown by crosses) were excluded from the calculation of the regression line in the figure. These points were from sampling dates when carbonate precipitation, which would remove DIC but would not influence $\delta^{13}C_{DIC}$, was presumed to reduce the concentration of DIC. The calculated fractionation of $\delta^{13}C$ during the production of organic matter was -14.2 ± 2.2 ‰, which was significantly lower than for the offshore site. This result, however, was consistent with the generally higher $\delta^{13}C$ recorded in sediment trap material from Ellis Fjord.

Similar graphs can be drawn using the concentrations of DIC calculated from the nutrients rather than measured DIC, which would remove problems with carbonate

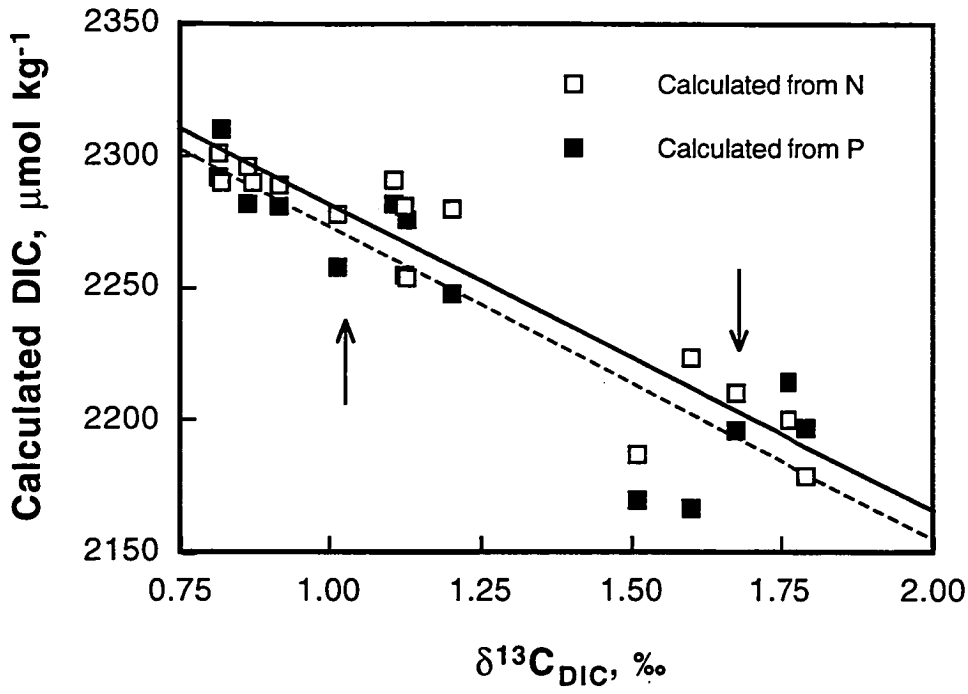

Figure 7.21. A plot of $\delta^{13}C_{DIC}$ against DIC calculated from the concentrations of phosphate and nitrate (normalised to S = 35 psu) and the relationships given in Table 7.1. The slope of the regression line was used to calculate the isotopic fractionation of carbon during organic matter production. The data points equivalent to those shown by crosses in Figure 7.20 are arrowed.

Nutrient	Fractionation, ‰
DIC	-14.2 ± 2.2
Nitrate	-18.8 ± 2.2
Phosphate	-18.3 ± 2.9
Silicate	-19.2 ± 2.9
DO	-16.8 ± 2.5

Table 7.3. Calculated isotopic fractionation during the production of organic matter calculated as described in the text.

precipitation and/or variations in the carbon to nutrient ratio in the organic matter formed. Figure 7.21 shows two such plots, and the calculated fractionations are given in Table 7.3.

The fractionations calculated from plots involving the nutrients and DO (Table 7.3) are all of greater magnitude than that calculated from DIC, but still remain lower than typical expected for Antarctic studies. However, the fractionations calculated from nitrate, phosphate and silicate were in good agreement with the $\delta^{13}C_{OC}$ of material captured in sediment traps placed in the fjord (Chapter 8). The variation between the calculated fractionations was probably the result of the limited data used in the regressions (shown by the large estimated errors in the calculated fractionation) and/or subtle differences in the uptake ratios of the nutrients during rapid production of organic matter.

The two data points discarded from the regression in Figure 7.20 (those with normalised concentration of DIC of *circa* 2120 μmol kg^{-1}) were associated with occasions of anomalously low DIC and periods of rapid phytoplankton growth. The same isotope data fell close to the regression lines in Figure 7.21, suggesting that the process which resulted in the increased uptake of DIC above that expected from the concentration of the nutrients did not involve fractionation of the carbon isotopes. This was consistent with precipitation of inorganic carbonate, but could also be due to the use of bicarbonate, as distinct from dissolved CO_2, as the carbon source by the rapidly growing phytoplankton (Riebesell et al., 1993). Some species of diatoms associated with sea ice from the antarctic region have been shown to be capable of the use of bicarbonate in growth (Mitchell and Beardall, 1996), and if fractionation during rapid uptake of carbon by phytoplankton from this large carbon pool was minimal, the observed low $\delta^{13}C$ values are understandable.

7.4 Conclusions

Primary production in the protected waters of ice covered Ellis Fjord extended for a considerably longer period than at the offshore site due to the maintenance of water column stratification well after it had been broken down at the O'Gorman Rocks site,

and the redevelopment of stratification earlier in spring. The rates of primary productivity in the fjord, calculated from decreases in the concentrations of the nutrients, were extremely high, indicating that the phytoplankton present, especially a number of diatom species, were highly adapted to the low light levels.

Marked overconsumption of DIC (compared to the nutrients) occurred throughout spring and summer in the water directly under the ice, and probably resulted in the formation of particulate and/or dissolved organic material of particularly high C:N mole ratio and $\delta^{13}C$. Similar observations in crack pools (Gleitz et al., 1996a) and in under ice diatom mats (Cota and Sullivan, 1990) indicate that this process could be widespread throughout the Antarctic region, and sedimentation of the material formed during this process could have a significant effect on the chemistry and isotopic signature of OC reaching and preserved in the sediment.

CHAPTER 8

ORGANIC CARBON SEDIMENTATION AND BURIAL IN ELLIS FJORD

8.1 Introduction

This chapter describes the sediment trap portion of the study in Ellis Fjord. Sedimentation in the fjord differed from the offshore O'Gorman Rocks site offshore in that lateral advection of organic material both to and away from the site, was far less significant, as exchange of water between the fjord and the open ocean was limited by the narrow, shallow sill at the entrance to the fjord and reduced wind mixing because of the permanent ice cover. Nonetheless, some advection of water to the sampling site occurred in December and January (Chapter 6). The greater depth of the fjord also meant that a better understanding of remineralisation of organic matter in the top 70 m of the water column could be obtained.

8.2 Results

The sediment traps were initially deployed at 5 depths (5, 10, 20, 40 and 70 m) in June 1994, and were recovered regularly from July 1994 until early March 1995. They were deployed for a further 3 months before being retrieved by members of the 1995 overwintering ANARE group from Davis Station. The total length of the study was slightly over a year. Throughout this chapter, sedimentation rates given as 'per year' are for the entire study.

All data obtained in this study are presented in tables in Appendix G.

8.2.1 Total Sedimentation

Total sedimentation rates varied greatly among the 5 trap deployment depths (Figure 8.1). This was in contrast to the O'Gorman Rocks site, where, except for some evidence of resuspension in the traps closest to the sediment, total sedimentation rates were essentially independent of trap depth. Thus, averaging the results from different trap depths was not a viable proposition for the Ellis Fjord Site.

Figure 8.1 shows that the sedimentation rate recorded in the traps at 10, 20 and 40 m was low and reasonably uniform during winter and spring until the beginning of biological productivity in October. The rate of sedimentation then rose to a peak during mid-January, before falling again to the winter rates. The situation for the trap at 5 m was slightly different, in that a broader maximum was recorded in November and December, with no mid-January peak. The rate of sedimentation at 70 m was much lower in summer than in the upper traps, and exhibited no discernible trends.

The relationship between trap depth and sedimentation rate showed a number of different patterns during the study (Figure 8.2). In winter, the sedimentation rate was lowest at the surface and increased steadily with depth. This behaviour began to alter in October, and by December the situation had reversed, with maximum sedimentation recorded in the traps closer to the surface. In January the situation changed again, with mid-water sedimentation rates greatest. In the final, extended trap deployment, the trend returned to that observed during the 1994 winter.

The increase in sedimentation rate with depth in winter suggests this material was largely derived from material resuspended from the sediment surface. Sedimentation fluxes in steep sided fjords are strongly affected by resuspension and sediment focussing (Hargrave and Kamp-Nielsen, 1977; Wassmann, 1984; Overnell and Young, 1995). These processes, shown schematically in Figure 8.3, involve the

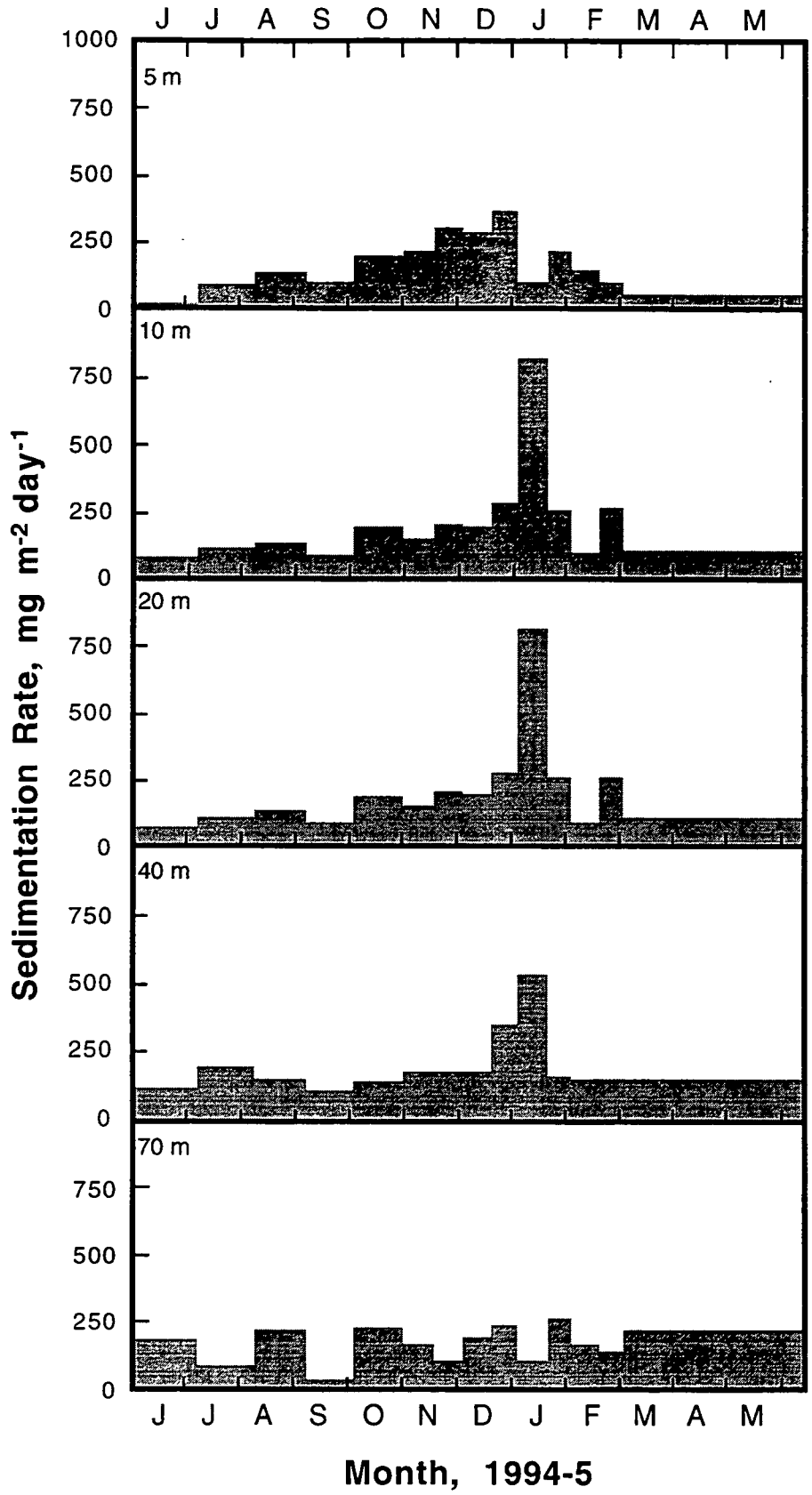

Figure 8.1. Total sedimentation rates (mg m^{-2} day^{-1}) recorded in traps deployed at the Ellis Fjord site from June 1994 and June 1995.

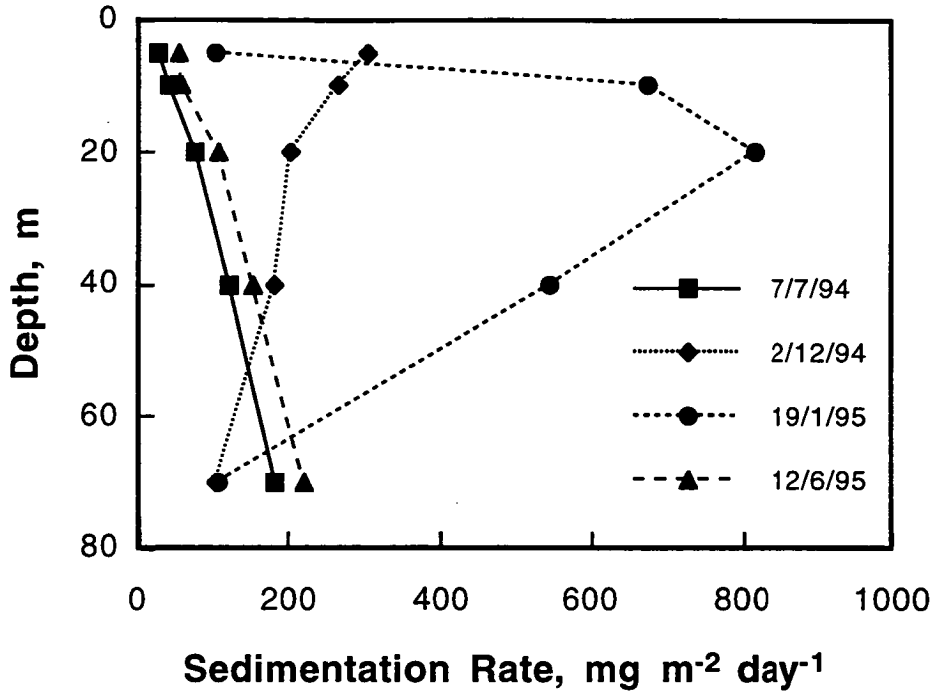

Figure 8.2. Trends in the variation in rates of sedimentation at various depths in Ellis Fjord.

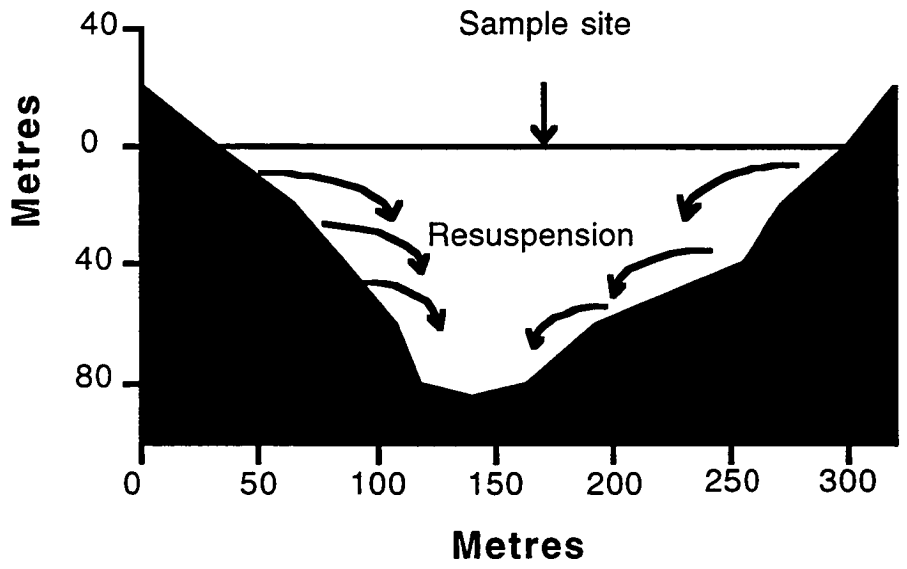

Figure 8.3. Resuspension and sediment focussing in Ellis Fjord. The cross section of the fjord at the sampling site has no vertical exaggeration.

removal of material from the upper slopes of the basin by brine flows (Chapter 6) and other currents and resedimentation deeper in the water column, effectively increasing the rate of sedimentation at the base of the basin. Assuming this to be true, and also that resuspension from the sediment occurred at a constant rate throughout the year, an estimate of 'new' material sedimentation can be made by subtracting the average winter (June - September) fluxes from the spring and summer sedimentation rates. Table 8.1 gives details of total sedimentation at each of the depths over the complete study as well as the new and resuspended fluxes.

8.2.2 Organic Carbon Sedimentation

The rates of OC sedimentation showed similar trends to those of total sedimentation. Maximum OC sedimentation occurred during November and December for the trap at 5 m, and January for the traps at 10, 20 and 40 m (Figure 8.4). The 70 m trap exhibited no coherent seasonal variation in the rate of OC sedimentation. The relationship between trap depth and sedimentation rate showed very similar patterns to those recorded for total sedimentation (Figure 8.2).

Table 8.1. Annual inventories (g m^{-2} yr^{-1}) of total and carbon sedimentation for each trap depth separated into resuspended (Res) and newly formed material (New). The percentage of carbon in each of the pools is also given.

	Total			Carbon			% Carbon		
Depth	Total	Res	New	Total	Res	New	Total	Res	New
5	47	28	19	5.9	1.8	4.1	13	6	21
10	68	31	36	7.8	2.0	5.8	12	6	16
20	64	40	24	6.2	2.4	3.8	10	6	16
40	68	59	9	5.2	3.2	2.0	8	5	23
70	66	66	0	4.5	3.5	1.0	7	5	-

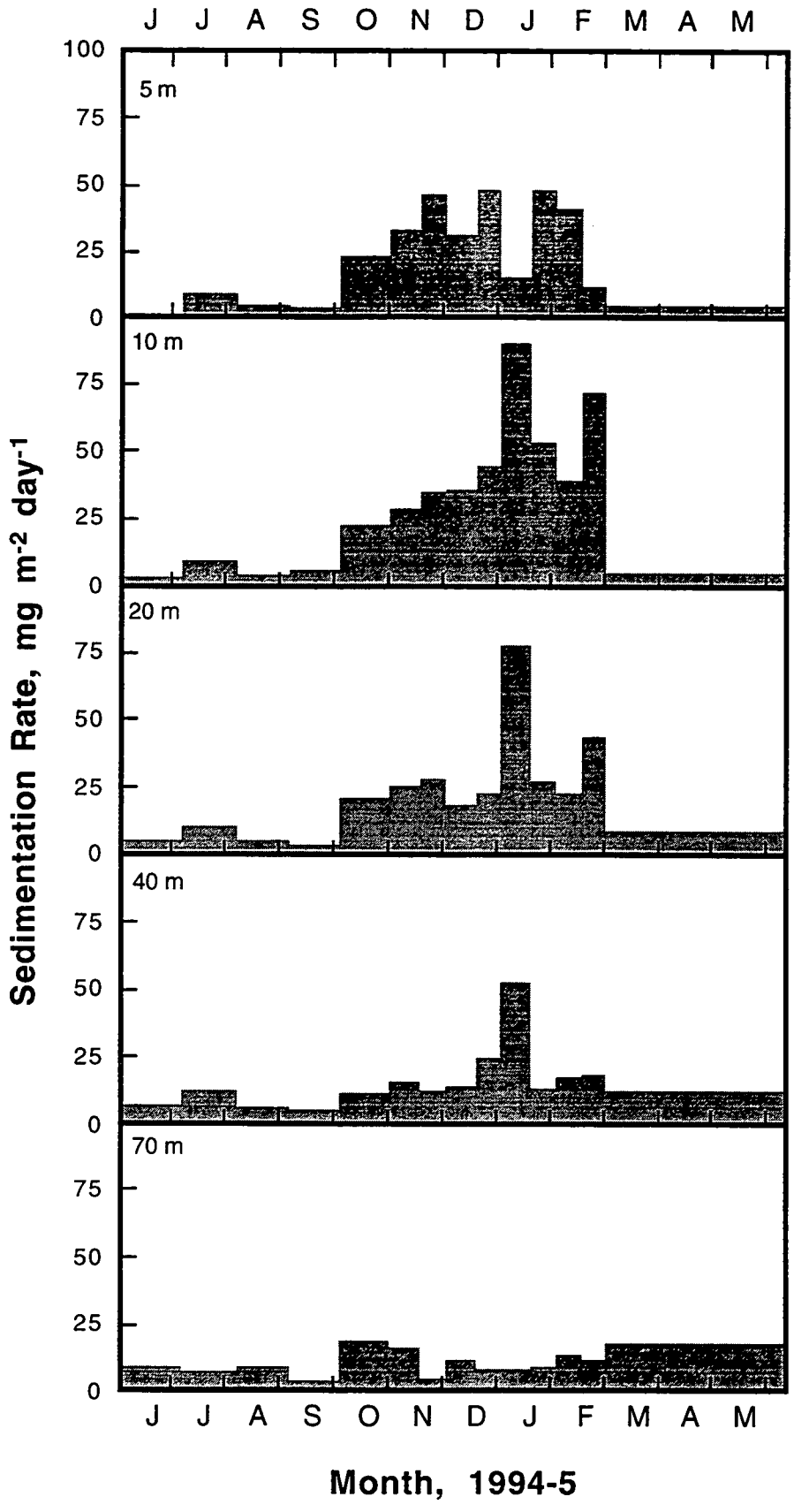

Figure 8.4. Organic carbon sedimentation rates (mg m^{-2} day^{-1}) recorded in traps deployed at the Ellis Fjord site from June 1994 and June 1995.

Organic carbon sedimentation was also separated into resuspended and new fluxes (Table 8.1). Sedimentation of resuspended OC increased steadily with depth, but sedimentation of new OC peaked at 10 m. The calculated rate of sedimentation of new carbon at 70 m was greater than new total sedimentation at this depth. C:N mole ratio and $\delta^{13}C$ data indicated that new material did reach this depth (see below), and that the actual 'new' total flux at 70 m must have been greater than calculated.

The variation in the percentage that OC made up of the total sedimenting material is shown in Figure 8.5. For the traps at 5, 10 and 20 m the percentage was reasonably consistent, showing maxima in November and February. The peaks were far less evident in material from the 40 m traps and even less so at 70 m, where the percentage did not show any consistent trends.

The % C in resuspended material was relatively low, and decreased slightly with depth (Table 8.1). The percentage OC in the new material was considerably higher, though showed no consistent trends with depth.

8.2.3 Carbon to Nitrogen Mole Ratio of the Sedimenting Material

The temporal variation in the C:N mole ratio in the sedimenting organic material is shown in Figure 8.6. The major trend evident was an increase in the ratio during October and November, when it reached 13.4 in material trapped at 10 m and 15.0 at 70 m, followed by a decrease to minimum values in January. The mole ratios at the five trap depths were reasonably consistent, and were always above the Redfield Ratio (6.6; Redfield et al., 1963). Even though there was little seasonal variation in the OC flux at 70 m, the C:N mole ratio indicates that organic material produced near the surface during the spring and summer phytoplankton blooms reached this depth. The annual mass weighted average C:N mole ratio at 5 and 10 m was similar (8.7 and 8.5

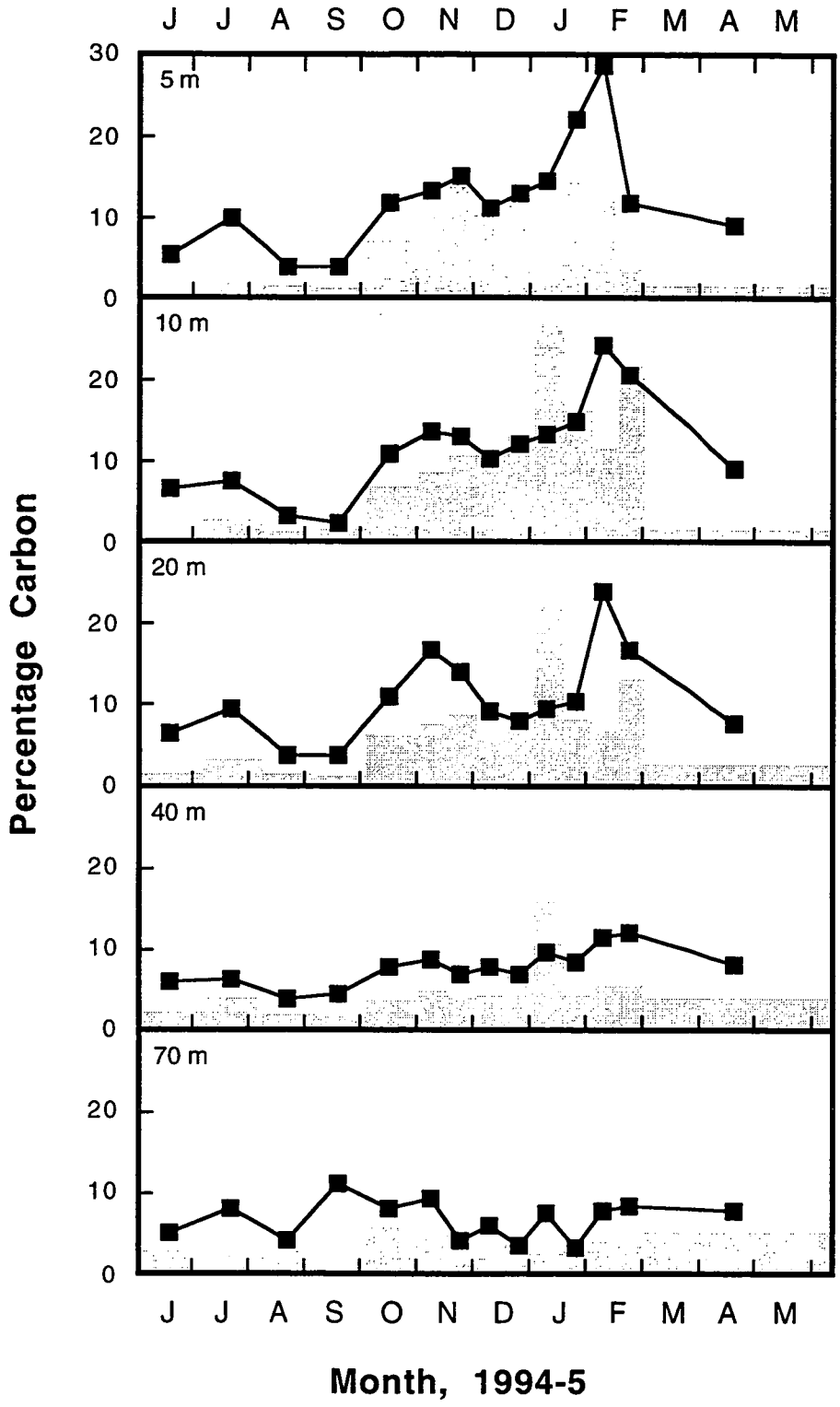

Figure 8.5. Seasonal variations in the percentages of organic carbon in the material caught in the sediment traps at the Ellis Fjord site. The rate of OC sedimentation (Figure 8.4) is plotted in the background for comparison.

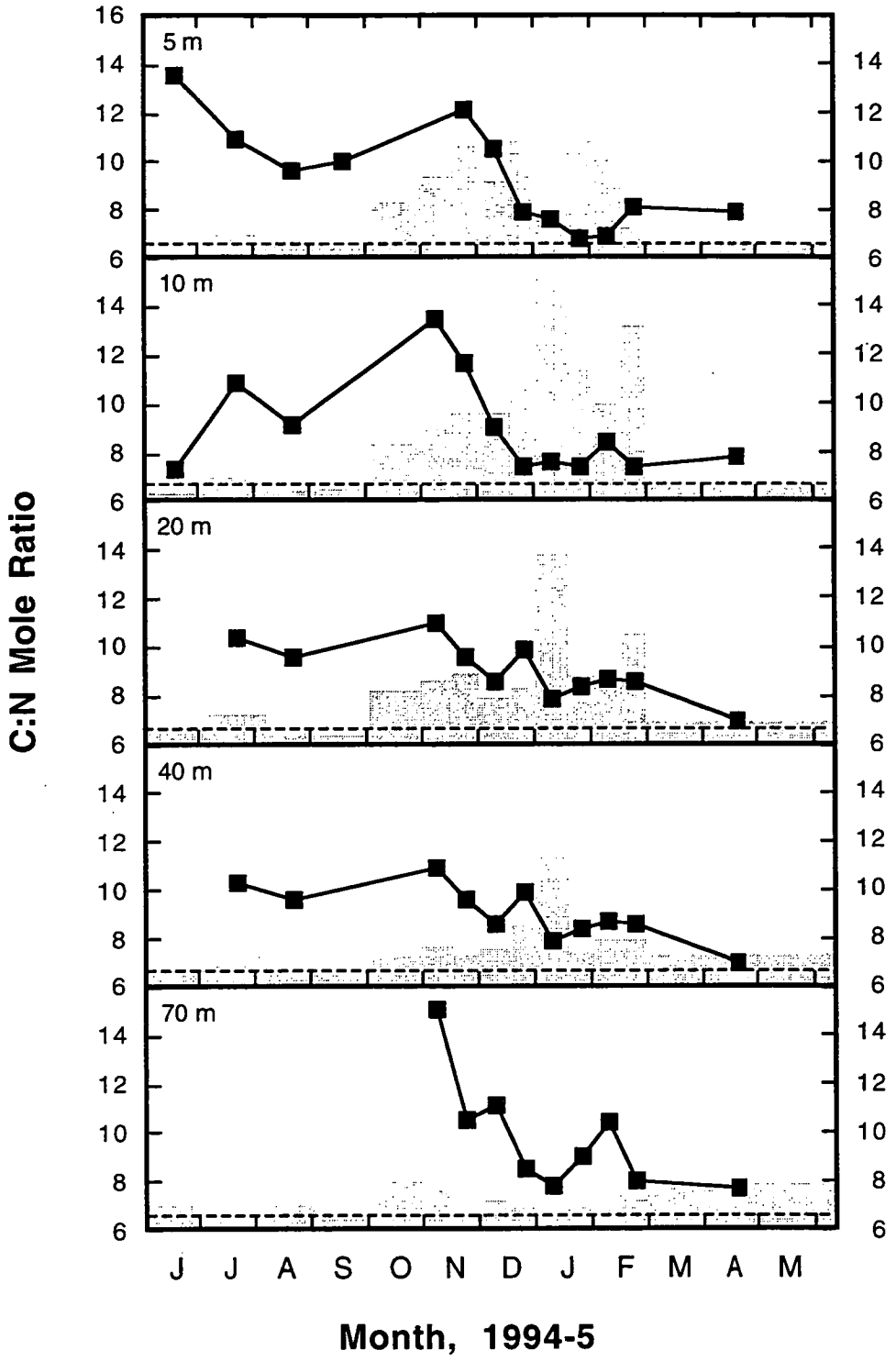

Figure 8.6. The seasonal cycle of the carbon to nitrogen mole ratio in the organic fraction of the sedimenting material. The dashed line is the Redfield Ratio. The rate of OC sedimentation (Figure 8.4) is plotted in the background for comparison.

respectively), and slightly lower than ratios at 20, 40 and 70 m (9.5, 9.4 and 9.5 respectively).

8.2.4 $\delta^{13}C$ of the Sedimenting Organic Carbon

Figure 8.7 shows the seasonal variation of the $\delta^{13}C_{OC}$ of the sedimenting material recorded during the study. $\delta^{13}C_{OC}$ was lowest during winter (-24 ‰ to -20 ‰), but then rose to a maximum at all depths of greater than -15 ‰ in November before decreasing back to near -20 ‰ by the end of the study. There was no peak in $\delta^{13}C_{OC}$ associated with the peak in sedimentation in January and February. During winter $\delta^{13}C_{OC}$ increased slightly with depth, but the reverse was true during spring and summer. The high $\delta^{13}C_{OC}$ recorded at 70 m in spring again implied that organic material from the phytoplankton bloom near the surface reached this depth.

The mass weighted average $\delta^{13}C_{OC}$ for the entire study was between -18.4 ‰ at 5 m and -19.0 ‰ at 70 m.

8.2.5 Characteristics of the Sedimenting Material

The material caught in the sediment traps from the beginning of the study until October generally consisted of unidentifiable organic remains and inorganic detritus (generally termed 'marine snow'), and was largely devoid of identifiable phytoplankton cells. From October to February the sedimenting material at 5, 10 and 20 m was generally dominated by intact diatoms and faecal pellets containing identifiable diatom parts. The deeper traps, in contrast, had reduced abundances of diatoms (which were nearly absent from the 70 m trap material) and a greater percentage of undifferentiated marine snow and, to a lesser extent, faecal pellets.

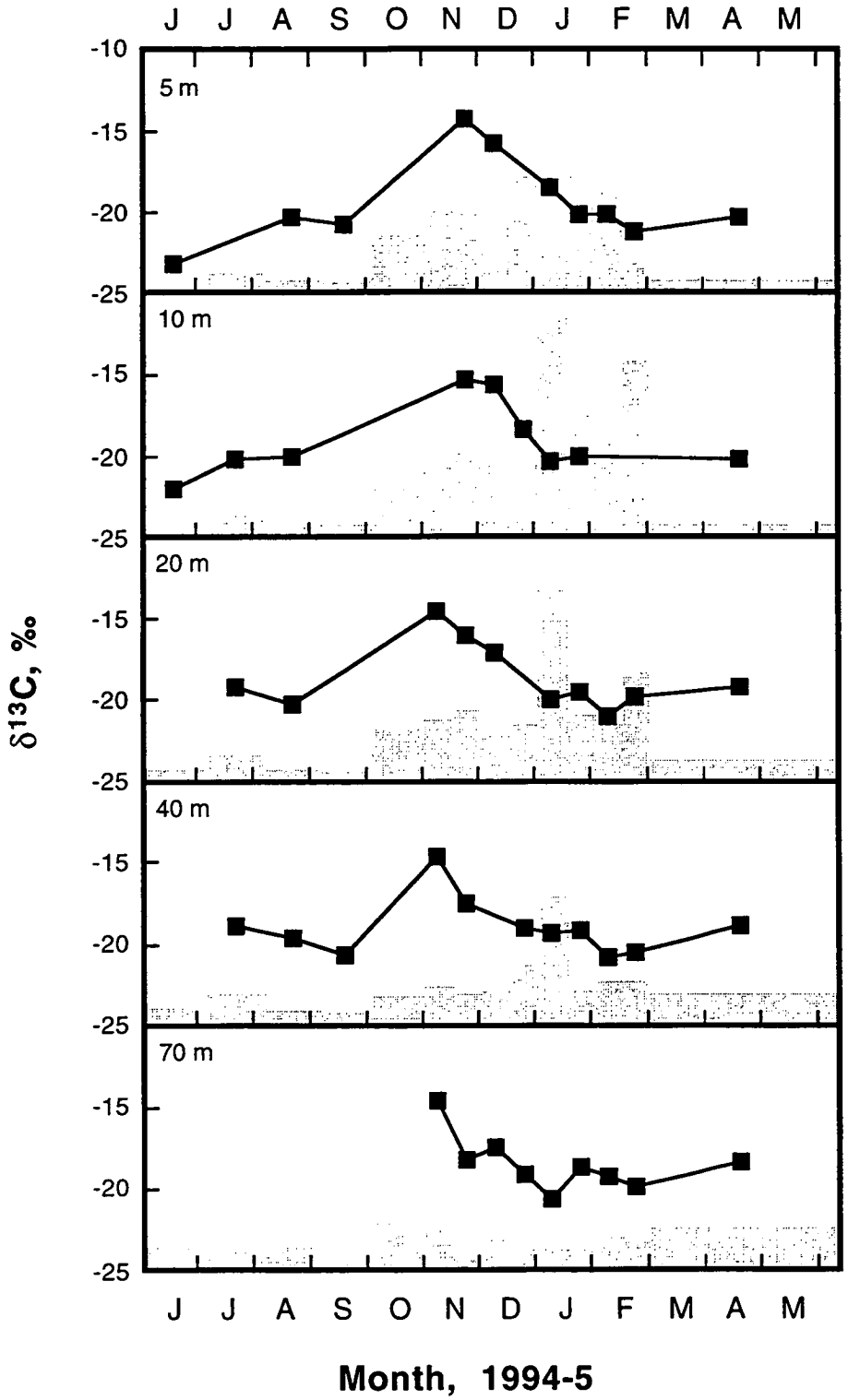

Figure 8.7. Seasonal variation in the $\delta^{13}C$ of the organic fraction of the material caught in the sediment traps at the Ellis Fjord site. The rate of OC sedimentation (Figure 8.4) is plotted in the background for comparison.

Sedimentation of intact diatoms began in late October, when long chains of the diatoms species *Entomoneis kjellmanii*, *Thalassiosira antarctica* and especially *Thalassiosira australis* dominated the trapped material. *Thalassiosira australis* remained the dominant species caught in the traps until mid-December, when it was replaced by a variety of *Fragilariopsis* species, which were present in high abundance until early February. Zooplankton faecal pellets became more numerous from the middle of December, and remained common throughout the rest of the summer. *Thalassiosira dichotomica* was present at low abundance throughout the latter part of the summer, while *Chaetoceros* spp. and a occasional colonies of *Phaeocystis* sp. affin. *antarctica* (Chapter 3) were observed primarily in late December and early January. Very few cells of the flagellates cryptomonad A and *Pyramimonas gelidicola*, both of which were dominant phytoplankton species at times during the summer (Chapter 7), were observed in the traps. From the middle of February until the end of the study, the trap material was again dominated by largely unidentifiable organic material. In contrast to observations at the O'Gorman Rocks site, little visible clastic matter, such as sand grains and silt, was evident in the trap material at any time during the study at the Ellis Fjord site.

Many other species of diatoms apart from those mentioned above were observed in the traps at low relative abundances at various times during the summer. The suite of species observed similar to that recorded at the O'Gorman Rocks site (Chapter 3), though there appeared to be less diversity in the fjord.

Faecal pellets were an important part of the trap material throughout the summer, though were less abundant in November and early December. Two main types of pellets were observed. The first was cigar shaped and about 150 µm in length by 60 µm in diameter, and the other approximately spherical and 100 µm in diameter. The spherical pellets were similar to that pictured in El-Sayed and Fryxell (1993: p 114), and both types were usually full of diatom frustules. The source of the major kinds of

pellets was not determined, though it should be noted that a diverse range of zooplankton species has been recorded in the fjord (Kirkwood, 1993). Unidentified zooplankton eggs were present in the trap material during summer, and were most abundant in early January.

8.2.6 Carbon in the Sediment

A short sediment core obtained at the sampling site consisted of fine green-brown diatomaceous mud. No large pieces of shell material were noted in the core. The OC content of the core is shown in Figure 8.8. Unfortunately, no other chemical or isotopic data were obtained for this core.

Figure 8.8. Organic carbon content (percent) of a sediment core recovered from the Ellis Fjord sampling site.

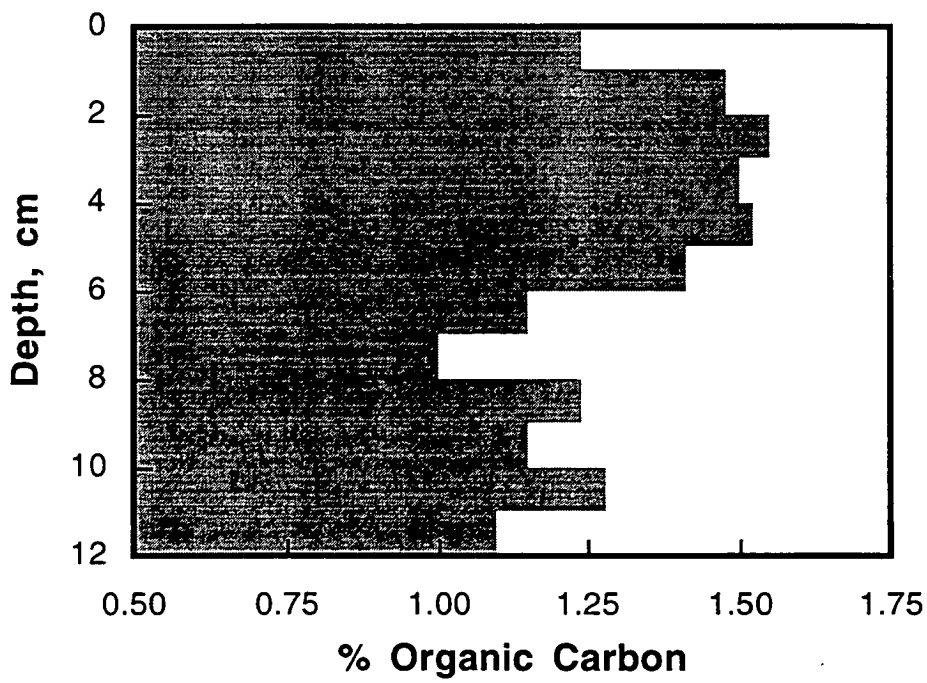

8.3 Discussion

8.3.1 The Cycle of Sedimentation

The general cycle of sedimentation in Ellis Fjord was similar to that observed at the O'Gorman Rocks (Chapter 5) and other Antarctic sites (Platt, 1979; Matsuda et al., 1987b; Fischer et al., 1988; Wefer et al., 1988; Dunbar et al., 1989; Wefer and Fischer, 1991; Nedwell et al., 1993), in that the sedimentation rate was low in winter and higher in summer. The period during which above background fluxes of biogenic material occurred in the fjord, however, was longer than elsewhere. Near the surface, total and OC sedimentation rates were generally above winter background levels between October and February, which reflected the prolonged period of primary productivity in the fjord (Chapter 7).

The situation was less clear deeper in the water column, where resuspension of surface sediment material (discussed in more detail below) became more important and outweighed the signal from the summer biological activity, which was decreased presumably by remineralisation and grazing by zooplankton. At 70 m it was difficult to discern any seasonality in the flux.

The initial increases in sedimentation during October and November were clearly associated with the onset of biological productivity. As discussed in Chapter 7, an intense diatom bloom had developed in the top few metres of the water column by the end of October. At the same time, rates of OC sedimentation rose sharply in the 5 and 10 m traps, but less markedly deeper in the water column. The trap material at this time was dominated by the diatom *Thalassiosira australis*, which was also prominent in the phytoplankton in samples from the water column and presumably in the bottom ice algal mat from which the bloom was derived.

Total and OC sedimentation rates remained at an approximately similar level at 5 m from October until the end of December, which coincided with the period during which maximum water column chl *a* concentrations occurred at 2 and 5 m (Chapter 7). During January and again at the end of February the rates at 5 m dropped, and highest sedimentation rates were recorded at 10 and 20 m. This reflected the shift of the main body of phytoplankton away from the under ice zone to deeper in the water column, as evidenced by the chl *a* maximum being at 5, 10 and/or 20 m during this time (Chapter 7). Thus it appears that, not surprisingly, the rate of sedimentation was closely related to vertical and temporal variations in the phytoplankton community.

The total annual sedimentation flux, *circa* 60 g m^{-2} (Table 8.1), was approximately half that at the offshore site. The sedimentation rate during winter was generally higher at the Ellis Fjord site, but there was not the intense pulse of sedimentation of inorganic material in December and January that occurred at O'Gorman Rocks. This was in part due to the maintenance of the ice cover throughout the study period; if the ice had melted out (as occurs during some summers), it is probable that a greater flux of clastic material would have occurred. The amount of material incorporated into the fjord ice (and ultimately entering the water column) was probably lower than at the offshore site, as the narrow, linear shape of the fjord and its alignment with the prevailing winds minimise deposition of aeolian material.

The annual OC sedimentation rates, which ranged from 7.8 g m^{-2} yr^{-1} at 10 m to 4.5 g m^{-2} yr^{-1} at 70 m (Table 8.1), were lower than calculated for the O'Gorman Rocks site (9.8 g m^{-2}, Chapter 5). If resuspension of organic material is taken into consideration, the fluxes of new OC are reduced even further, with the maximum, recorded at 10 m, of 5.8 g m^{-2} yr^{-1}. As the apparent amount of organic production was quite similar at the two sites (as evidenced by the reduction in the concentrations of nutrients and DIC), the lower sedimentation in the fjord was presumably due to greater recycling of OC within the water column. Organic matter production and remineralisation therefore

appear to be more tightly coupled in the fjord than offshore. Faecal pellets made up a greater percentage of the sedimenting material during the periods of peak phytoplankton production in the fjord than at O'Gorman Rocks, suggesting that zooplankton grazing was more important in the fjord than offshore. The long chains of *Thalassiosira* spp. and *Fragilariopsis* spp. observed in the near surface traps at various times during the summer were largely absent from the 70 m, and to a lesser extent, 40 m traps, indicating that this material had been efficiently grazed and remineralised above these depths.

Most of the identifiable material in the sediment traps consisted of diatom cells. Intact cells of the flagellates cryptomonad A and *Pyramimonas gelidicola* were rarely observed in the trap material, indicating that the a large percentage of the carbon in these species remained suspended or was rapidly remineralised by zooplankton or bacteria. Cells of the dominant diatom at the end of the study, *Thalassiosira dichotomica*, were also scarce in the traps. This was also the case at the O'Gorman Rocks site, indicating that, like the flagellates, this species did not sink particularly rapidly, or was efficiently grazed by the zooplankton community near the surface. Transfer of some of the OC of the flagellates and *Thalassiosira dichotomica* to the sediment presumably occurred in faecal pellets and marine snow.

This study highlights the importance of the bottom ice diatom community as a source of OC. It is in this environment that primary production begins each year, and the material produced by the community is an important source of sedimenting OC. McMinn (1996) recorded a bottom ice OC standing stock of 0.23 g m^{-2} in the Middle Basin of Ellis Fjord, though much higher concentrations have been reported at other Antarctic sites, and there is likely to be considerable variation between localities and years. For example, the standing stock of carbon in bottom ice communities in McMurdo Sound was estimated to be 5 g m^{-2} (Cota and Sullivan, 1990), with the net annual OC production rate in these communities ranging from 4 to 12 g m^{-2} yr^{-1}

(Palmisano and Sullivan, 1983; Knox, 1990). While no direct estimate was made of the bottom ice OC standing stock in the present study, preponderance of diatom species commonly found in such communities (McMinn, 1996) in the traps, makes it clear that this community played an important role in OC sedimentation.

The percentage carbon in the sedimenting material reflected the sediment source throughout the study. The percentage was low in winter, when low OC resuspended sediment made up the bulk of the trapped material, but increased in October and November when actively growing phytoplankton cells were trapped. The subsequent depression of the carbon percentages in December and January was probably the result of dilution by minerals as the ice softened (exacerbated by a decrease in OC standing stock associated with the input of water into the basin (Figure 7.17)), though little microscopic evidence for an increase in clastic material was observed. The decrease in % C was, however, much less dramatic than the drop during the same period at the O'Gorman Rocks site. The increased percentage carbon observed in February suggested that largely intact phytoplankton material again dominated sedimentation.

The vertical distribution of percentage OC (Figure 8.5) shows that the highest percentages were observed in the material closer to the surface, with lower percentages recorded at 40 and 70 m. This was undoubtedly due to the increased relative importance of low carbon resuspended material at depth as well as removal of new carbon from POM during grazing and remineralisation.

The C:N mole ratio of the OC in the sedimenting material was significantly above the Redfield Ratio for nearly all of the study. Unlike material from the O'Gorman Rocks site, the C:N mole ratio exhibited a maximum in October and November during a period of major organic production in the upper few metres of the water column and OC sedimentation (Figure 8.6). Offshore, the maximum occurred in September, which was prior to the onset of the phytoplankton bloom and during a period of low

sedimentation. It would appear that the dominant diatom during October and November at the Ellis Fjord site, *Thalassiosira australis*, which made up the bulk of the sediment trap material at this time, was able to produce organic matter with a C:N mole ratio up to double that of standard particulate organic matter. This relationship, which was probably associated with the continued production of OC after exhaustion of nitrate in the water directly under the ice during this period was consistent with the water chemistry (Chapter 6), and is discussed in more detail below.

8.3.2 The $\delta^{13}C$ of the Sedimenting Organic Carbon

In a similar cycle to that recorded at the O'Gorman Rocks site, the $\delta^{13}C$ of the OC caught in the sediment traps rose from initial winter values of approximately -20 ‰ to -22 ‰ to a maximum of greater than -15 ‰ in spring, which was followed by a subsequent decrease back to *circa* -20 ‰ in December and January. As noted in Chapter 5, the winter $\delta^{13}C_{OC}$ values were significantly higher than recorded for particulate matter in other Antarctic studies at any time of the year (Sackett et al., 1965; Sackett et al., 1974; Bathmann et al., 1991; Rau et al., 1991a, 1991c; Dunbar and Leventer, 1992; Rogers and Dunbar, 1993; Kennedy and Robertson, 1995), and the values during spring have only been exceeded in the Antarctic region by material from the sea ice of McMurdo Sound (Dunbar and Leventer, 1992).

The $\delta^{13}C_{OC}$ of the sedimenting material between July and early October was presumably similar to that of the OC in the surface sediment, as the material trapped during this period was most likely to be largely from this source. The $\delta^{13}C_{OC}$ of material from near the top of a sediment core from Deep Meromictic Basin (Figure 6.1) was reported to be -18.1 ‰ (Bird et al., 1991), and it is probable that resuspended material in Middle Basin had a similar value. The $\delta^{13}C_{OC}$ of material caught during the first trap deployment was significantly lower than that recorded later in winter. This

might have been due to the incomplete mixing of the upper fjord for at least part of this trap deployment (Chapter 6), thus reducing the resuspension flux.

Maximum $\delta^{13}C_{OC}$ values were recorded during the period in which OC sedimentation was dominated by algal material from the lower surface of the ice. This was the same environment that the species responsible for the high spring $\delta^{13}C_{OC}$ in sedimenting carbon at the O'Gorman Rocks site, *Entomoneis kjellmanii*, grew. This species was also present in the phytoplankton at Ellis Fjord in October, but at no time was numerically dominant, and had largely disappeared by mid-November. Fischer (1991) reported that *Thalassiosira* spp. produced OC with relatively high $\delta^{13}C$ (*circa* -24 ‰) compared to other diatom species, for example *Corethron criophilum* (*circa* -34 ‰), and similar results have been reported by other workers (e.g. Kopczynska et al., 1995). It is probable, therefore, that the high $\delta^{13}C_{OC}$ of the trap material was a result of both the presence of a suite of species that was capable of producing high $\delta^{13}C$ material, and the low concentrations of DIC (and therefore $CO_{2(aq)}$) directly under the ice (Chapter 7). The rapid growth of the diatoms in the under ice community may also have acted to increase $\delta^{13}C_{OC}$ (Laws et al., 1995).

The decrease in $\delta^{13}C_{OC}$ in December and January reflected the increased importance of OC production deeper in the water column, as shown by the shift to deeper depths of the maximum chl *a* concentrations, where the relatively high DIC environment made greater isotopic fractionation possible. The species responsible for the primary productivity also changed, with *Porosira socialis* and *Fragilariopsis* spp. becoming more important. It is also possible that these species produced OC with inherently greater isotopic fractionation and thus lower $\delta^{13}C_{OC}$.

8.3.3 The Relationship Between $\delta^{13}C$ of the Sediment Trap Material and DIC in the Water Column

The relationship between the $\delta^{13}C_{OC}$ of the trapped material and $[CO_{2(aq)}]$ is shown in Figure 8.9 along with the line defined by Equation 5.3, which Rau et al. (1991c) suggested reflected the association between these parameters. The data points fall, generally speaking, close to the line, especially considering that the $[CO_{2(aq)}]$ plotted was for the depth of the trap on the day of the trap recovery, and thus did not necessarily reflect the $[CO_{2(aq)}]$ in which the particulate organic matter was produced. The cluster of data points to the right of the line (plotted as crosses) represents some of the data from 70 m, where $[CO_{2(aq)}]$ was generally considerably higher than in the

Figure 8.9. The $\delta^{13}C$ of the sedimenting material plotted against the calculated $[CO_{2(aq)}]$ at the trap depth on the date of recovery. Also shown are the lines suggested by Rau et al. (1991c) to relate the $\delta^{13}C$ of particulate organic matter and $[CO_{2(aq)}]$ in other Antarctic studies (Equation 5.3). The data plotted as crosses are discussed in the text.

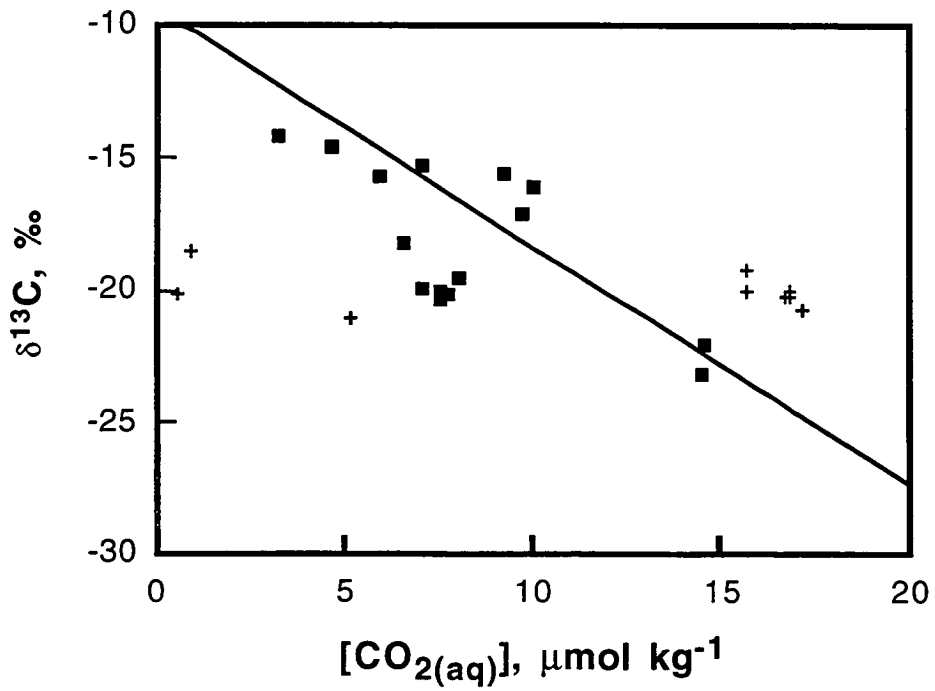

upper water and production was minimal, and from winter samples, when resuspension of material from the sediment made up most of the OC flux. The points to the left hand side of the line (also plotted as crosses) were from near surface samples during periods in January and February where $[CO_{2(aq)}]$ was very low, but the production of high $\delta^{13}C_{OC}$ organic material by diatoms (as distinct from flagellates, which were not so efficiently trapped) was also low.

As for the O'Gorman Rocks site, there was little relationship between temperature and $\delta^{13}C_{OC}$ (data and plot not shown) of the sedimenting organic material, and the data fell nowhere near the line suggested by Rau (1991c) to connect these parameters (this relationship is plotted in Figure 5.8). This again indicated that the relationship was the result of autocorrelation between $[CO_{2(aq)}]$ and temperature in areas of limited DIC drawdown.

8.3.4 Trends in $\delta^{13}C_{OC}$ and the C:N Mole Ratio of the Sediment Trap Material

The relationship between the $\delta^{13}C_{OC}$ and C:N mole ratio of the sedimenting material at the O'Gorman Rocks and Ellis Fjord sites provided an interesting insight into the processes occurring during organic matter production. At the O'Gorman Rocks site, the data show two major trends (indicated by the dashed lines in Figure 8.10): when the C:N mole ratio was high during winter, $\delta^{13}C_{OC}$ was at its lowest, and during spring, when $\delta^{13}C_{OC}$ was high, the C:N mole ratio increased slightly from the Redfield Ratio. In contrast, at the Ellis Fjord site a trend of increasing $\delta^{13}C_{OC}$ of the sedimenting material was generally accompanied by an increase in the C:N mole ratio (indicated by the regression line in Figure 8.10), though there is some evidence of the sedimenting material following the trends observed at O'Gorman Rocks at times.

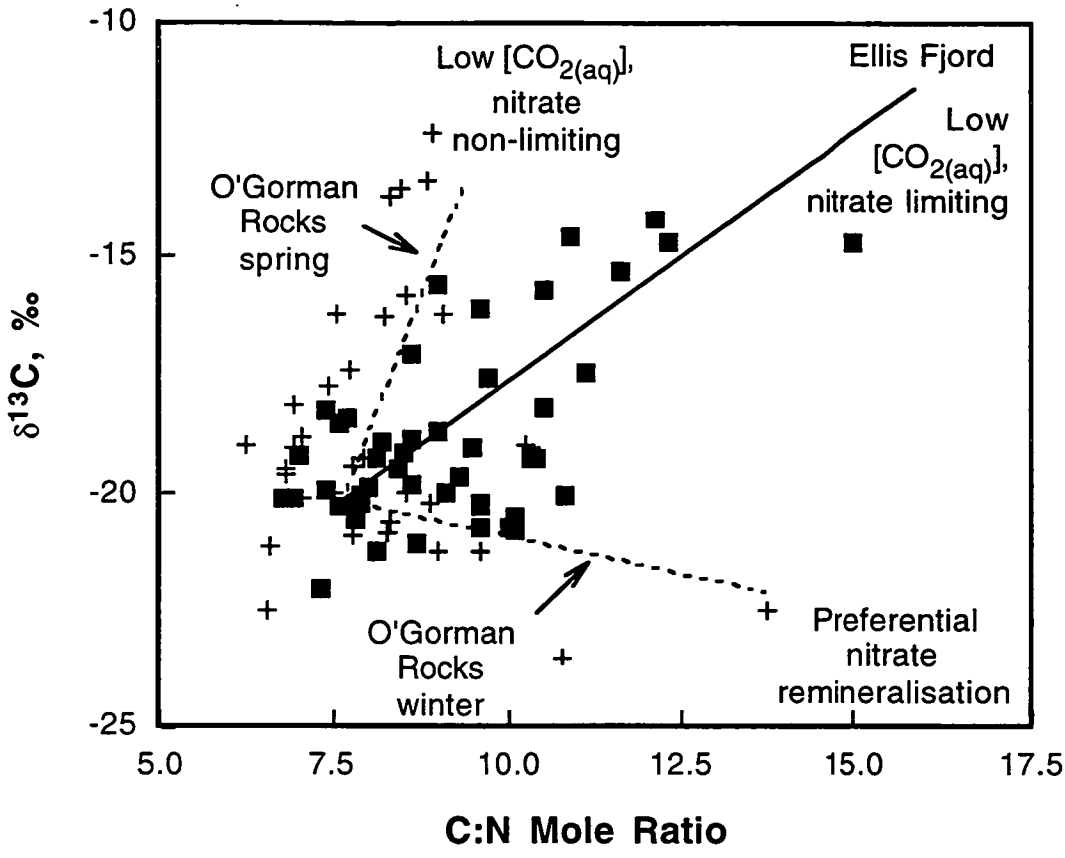

Figure 8.10. Plot of $\delta^{13}C$ versus the C:N mole ratio for sediment trap material from Ellis Fjord (squares) and O'Gorman Rocks (crosses). The solid line is the trend line for the data from the Ellis Fjord site, and the dashed lines represent trends in the data from the O'Gorman Rocks site during the periods indicated.

These observations were consistent with the increased importance of phytoplankton growing close to the undersurface of the ice cover in the sedimenting material at the Ellis Fjord site. As discussed in Chapter 7, it appeared that rapid growth in this community contributed to the extremely low DIC concentrations recorded at 2m from October to the end of the study, and, from the uptake ratios of DIC and nitrate, production of organic material of high C:N mole ratio (Figure 7.17). Both the low DIC concentration and the rapid growth rate would contribute to an increase in $\delta^{13}C_{oc}$ of the organic material formed. The same process is less evident in the data from the O'Gorman Rocks site, as the increase in the C:N mole ratio of the high $\delta^{13}C_{oc}$ material is much less pronounced.

These trends could have stemmed from at least two causes. The diatom species responsible for the bulk of the sedimentation during spring at the O'Gorman Rocks site was *Entomoneis kjellmanii*, whereas in Ellis Fjord *Thalassiosira australis* was responsible. As mentioned above, this latter species appears to be particularly capable of continued primary production at low nitrate concentrations, thus producing material with high C:N mole ratio, whereas the former is less so. This observation might also explain the less well developed mat community at the O'Gorman Rocks site (K. Swadling, personal communication) even though the initial chemical and physical conditions were similar.

The C:N mole ratio results are consistent with previous studies of the chemistry of bottom ice mat material. Cota and Sullivan (1990) reported C:N ratios of between 8 and 14 for a mat community dominated by *Nitzschia stellata* Manguin, *Pleurosigma* sp. and *Entomoneis* sp. in the McMurdo Sound area, while Gleitz et al. (1996a), in their study of crack pool communities derived from ice algae, observed ratios between 7 and 15. In both studies, it appeared that low nitrogen material was being produced by cells held in a (relatively) high light environment where, due to the nature of the surroundings in which the cells were growing, nitrate could become depleted. Gleitz et al (1996b) reported that growth of sea ice diatoms in closed bottle incubations resulted in the production of high $\delta^{13}C_{OC}$ and the reduction of the concentration of DIC to well below that expected if the organic matter produced had the Redfield C:N mole ratio, consistent with the field observations in the present study.

8.3.5 Carbon in the Sediment

The concentration of OC in the sediment core ranged from 1 to 1.5 %, which was similar, though lower, to that at the O'Gorman Rocks site, and it again appeared that the top five cm of the sediment was mixed by bioturbation (Figure 8.8). The carbonate content of the core was not measured, but Bloxham (1993) reported that inorganic

carbon made up approximately 0.3 % of the dried core material at the centre of Middle Basin (Figure 6.1), close to the sampling site. This concentration was for the top 5 cm, and it is possible that, as at O'Gorman Rocks, the percentage of inorganic carbon increased beneath this depth. Bird et al. (1991) reported that OC constituted 2.1 - 3.9 % (dry weight) of a core from Deep Meromictic Basin, with inorganic carbon of 0.5 - 1.5 %. It should be noted, however, that this basin is anoxic beneath a depth of approximately 40 m, and the remineralisation processes occurring in deeper water and at the top of the sediment may be quite different.

The chemical data from the sediment at or near the sampling site in Ellis Fjord have been included in the sedimentation and burial model described below.

8.3.6 A Model of Organic Carbon Production, Remineralisation and Burial

The data obtained in the studies of particulate matter production, resuspension and sedimentation at the Ellis Fjord site can be included in a model of carbon flow through the water column. In the model the water column was divided into 5 boxes, each 1 metre square, and each with a sediment trap at its base. The boxes extended over the depth intervals 2 to 5 m, 5 to 10 m, 10 to 20 m, 20 to 40 m, and 40 to 70 m (numbered boxes 1 to 5 respectively).

The net increase (or decrease) of 'trappable' carbon in the n^{th} box resulting from sedimentation into and out of the box, the resuspension flux, and processes such as photosynthesis, remineralisation, transfer of POC to non-trappable pools such as DOC, or aggregation of colloidal material within the box, was calculated as follows:

$$P_n = S_{n-1} - S_n + R_n \qquad (8.1)$$

where P_n is the net increase of 'trappable' OC in the n^{th} box, S is the vertical sedimentation flux either into (subscript n-1) or out of (subscript n) the n^{th} box and R_n is the net resuspension flux into the n^{th} box (obtained from the data in Table 8.1 by subtracting the resuspension flux for the $n\text{-}1^{th}$ trap from the resuspension flux for the n^{th} trap). Figure 8.11 shows the fluxes entering or leaving a box schematically. The output from the bottom box was used, along with data from the sediment core, as input into a carbon burial model similar to that described in Chapter 5 for sedimentation at the O'Gorman Rocks site.

The carbon fluxes calculated from this model for the complete study (essentially for a period of one year) are shown in Figure 8.12. A number of features are immediately evident. Net production of particulate OC occurred only in the top 10 m, and production was, not surprisingly, greatest in the topmost box. Net loss of POC occurred beneath 10 m, with the greatest loss occurring in the 10 - 20 m box, as well as at the sediment-water interface due to respiration and secondary production by

Figure 8.11. A schematic diagram of the carbon fluxes into and out of the n^{th} box in the model.

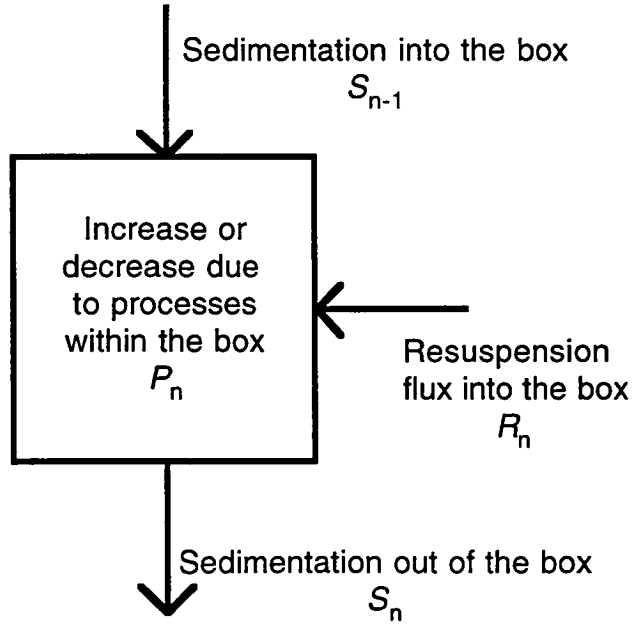

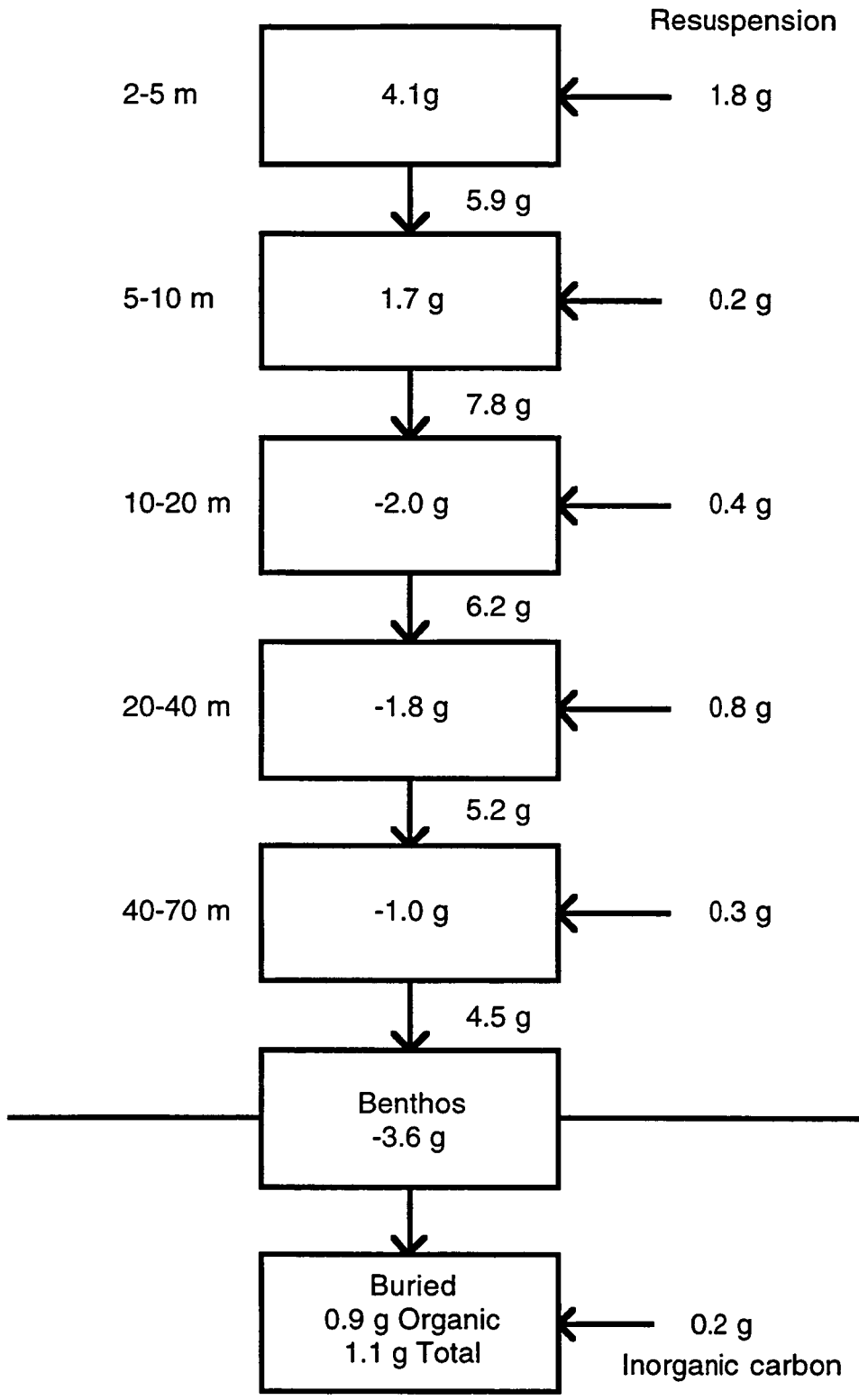

Figure 8.12. Annual carbon flow (g m^{-2}) through the water column and to the sediment at the Ellis Fjord site calculated using the data in Table 8.1 and Section 8.3.6 and the models described in this section and in Chapter 5. The numbers in the rectangles are the net change in 'trappable' OC in the boxes.

benthic organisms. The dominance of respiration beneath 10 m was not unexpected, as the reduced levels of light reaching these depths, especially considering the ice cover, would have limited primary production. Net OC production in the top ten metres totalled 5.84 g $m^{-2} yr^{-1}$, which was low compared to estimated OC production at other Antarctic sites (e.g. Holm-Hansen et al., 1977; Knox, 1990) or even production estimated from the reductions in the concentrations of nutrients in the present study (Chapter 7). However, the sediment trap flux effectively takes into account remineralisation within the top 10 m, and will not include OC produced from photosynthesis but subsequently transferred to the 'untrappable' DOC or metazoan zooplankton pools. Furthermore, the efficiency of trapping was not determined, and the true fluxes could have been considerably greater (or, for that matter, smaller).

The net OC resuspension flux was somewhat surprisingly greatest for the surface box. Physical processes such as tidal ice rafting at the edges of the fjord could have led to the increased resuspension of material from shallow sediment, whereas resuspension at greater depths would depend on currents and the activities of benthic organisms. The OC content of the sediment at shallow depths was also likely to have been much greater than deeper in the fjord, and thus less sediment would have had to have been resuspended for the observed OC flux to occur. This conclusion was tested by developing a similar model for total sedimentation to that above, and calculating the percentage OC in the resuspended flux into each box. The percentage OC calculated was 6.5 % for the top box, but dropped to 5.1 % for the second box and 3.7 % in the bottom box. These data are consistent with the material reaching the sediment at shallower depths (and subsequently resuspended) having higher percentages of OC than that which reached greater depths.

The resuspension flux into the 20 - 40 m box was greater than in the bottom box, which was consistent with occurrence throughout the year of mixing processes

including brine and tidal flows which generally did not penetrate to below 40 m, reducing the effect of turbulence as a resuspension mechanism.

Substitution of the OC fractions from the sedimenting material at 70 m and of the sediment core (and assuming an inorganic carbon content at depth of 0.3 %, equivalent to an annual input of 0.2 g m^{-2} yr^{-1}) into Equation 5.8 indicated that secondary production and remineralisation of OC either at the sediment - water interface or within the sediment itself accounted for 3.7 g m^{-2} yr^{-1}, resulting in the burial of 0.8 g m^{-2} yr^{-1} carbon per year. Assuming that resuspended and new OC are remineralised at the same rate, only approximately 0.2 g m^{-2} yr^{-1} OC produced in the water column by photosynthesis during the year was buried in the sediment at a depth of 70 m during the study.

This calculation, however, only takes into account carbon which falls to the bottom of the fjord, whereas most material would reach the sediment at shallower depths. Table 8.1 shows that the total OC flux decreased with depth (particularly below 20 m), indicating that the amount of carbon reaching the sediment in shallower water was greater than at 70 m. Assuming that the fjord cross section is triangular, that the sedimentation rates were horizontally homogenous, and that the rates varied linearly between the trap depths, the bottom area weighted average sedimentation rate of OC at all depths was calculated to be 5.5 g m^{-2} yr^{-1}. Of this, only 2.6 g m^{-2} yr^{-1} is new carbon, with the rest being resuspended material. However, without knowledge of the relationship between water depth and carbon content of the sediment, it is difficult to estimate average preservation rates of OC throughout the fjord.

As discussed in Chapter 7, there is a major imbalance between the measured and calculated concentrations of OC present at the Ellis Fjord site. It was concluded that this material had either sedimented rapidly from the water column or had been transferred to organisms higher in the food web, such as copepods, which were not

considered in the balance. It is clear from the study of sedimentation described in this chapter that this flux was insufficient to balance the OC inventories. Furthermore, Kirkwood (1993) recorded a maximum integrated zooplankton biomass of only 130 mg m^{-3}, which is also insufficient to account for the missing carbon. The role of advection and spatial variability, which was not measured in this study, must also be considered as reasons for the observed imbalances. Finally, it is possible that the OC is removed rapidly by the well developed filter feeding macrobenthic communities on the steep sides of the fjord (Kirkwood and Burton, 1989). This would require efficient horizontal mixing, so that all fjord water was in contact with the community on a regular basis. Whatever the cause, the inability to balance adequately the fate of OC produced in the water column remains.

8.4. Conclusions

Sedimentation in Ellis Fjord underwent a similar seasonal cycle to that recorded at the O'Gorman Rocks site. However, the nature of the fjord meant that some important differences occurred. For example, the period during which biological productivity occurred was significantly longer, resulting in extended biogenic sedimentation, and resuspension of material from the sides of the fjord played an important role. The seasonal trends OC sedimentation observed in the traps closer to the surface were absent at 70 m. This, along with the lower OC sedimentation rates a this depth, suggested that considerable remineralisation of organic material occurred in the water column.

The carbon to nitrogen mole ratio and the $\delta^{13}C$ of the sedimenting material reflected the importance of the under ice algal mat not only in the production of OC but also in the transfer of high nitrogen, high $\delta^{13}C$ material to the sediment. The relatively quiescent nature of the fjord environment probably aided the formation of the algal mat, as it was better developed than at the O'Gorman Rocks site.

CHAPTER 9

CONCLUSIONS

At the end of Chapter 1 several broad questions about the nature of the carbon cycle in waters surrounding the Antarctic continent were posed. Here the results of this thesis are discussed in terms of these questions, with the goal of extrapolating the conclusions drawn from the nearshore waters of the Vestfold Hills to other neritic and pelagic regions of the Southern Ocean.

The seasonal cycle of primary production at the two study sites - offshore at O'Gorman Rocks (water depth: 23 m) and in semi-enclosed Ellis Fjord (75 m) - differed, in that significant productivity occurred between October and May in the fjord, but from November to February or early March offshore (Chapters 4 and 7). The extended duration of phytoplankton activity in Ellis Fjord indicated that the potential period for primary productivity in the Southern Ocean is much longer than typically observed, and that sufficient light is available at these latitudes for productivity by a well adapted phytoplankton community for over 6 months of the year. The period of production appeared to be strongly influenced by the intensity of mixing of the water column; stronger mixing reduces the time individual phytoplankton cells spend in the relatively high light environment near the surface. In Ellis Fjord, the water column remained stratified for the majority of the year, and deep mixing during winter was not intense. At O'Gorman Rocks, in contrast, winter mixing from ice formation and surface cooling curtailed the summer phytoplankton bloom in autumn and also retarded its initiation in spring.

The intense phytoplankton blooms observed in Ellis Fjord indicated that considerable OC production can occur under ice, and a similar observation was made at the O'Gorman Rocks site, where significant OC production and sedimentation occurred

prior to the break out of the fast ice. From the sediment trap data it is estimated that approximately 20 % of annual production at the offshore site occurred in spring. These results indicate that ice-covered environments must not be ignored in estimating the amount of carbon fixed by phytoplankton in the Southern Ocean. That production in the open ocean often appears to be focussed into an area near the retreating ice edge is again an indication of the importance of stratification rather than limitation of growth of phytoplankton under ice by low light levels.

The balance between measured and calculated concentrations of OC during summer phytoplankton blooms both at O'Gorman Rocks and in Ellis Fjord was poor, with the concentration of OC much lower than calculated from the reduction in the concentrations of DIC and nutrients (Chapter 4 and 7). Similar observations have been made in a number of other Antarctic studies (e.g. Bunt, 1960; Perez, 1994) suggesting that this problem is widespread. If the 'calculated' OC was in fact formed (measurements of DIC and nutrients provide only indirect evidence of OC formation) it must have been removed from the water column by sedimentation, or transferred to carbon pools which were not adequately quantified, such as metazoan zooplankton and higher organisms (Huntley et al., 1991) or the bottom ice algal mat. Both at O'Gorman Rocks and in Ellis Fjord the amount of carbon in the sediment traps accounted for only a small percentage of that missing, suggesting that transfer to unmeasured pools was the major cause for this imbalance. It is possible that bottom ice algal mats detached from the ice in very large flocs (McConville et al., 1985) which were poorly sampled by the traps, and therefore the missing carbon had in fact been transported to deep water or to the sediment, though there is no evidence for this occurring. The problem was exacerbated by the production of high carbon, low nitrogen organic material at low nitrate levels in some communities, which, apart from anything else, called into question the accuracy of OC production calculated from nitrate depletion (Eppley et al., 1983; Chavez and Baker, 1987, Platt et al., 1989).

These observations highlight a problem oft encountered in oceanic studies. It is unreasonable to assume that productivity, remineralisation and sedimentation all occur uniformly, and thus the spatial and temporal uncoupling of production and loss terms for OC will occur. Measuring OC budgets at a particular is site is fraught with danger, as the 'production' measured at the sampling site will have occurred in water before it actually reaches the site, and the sedimentation and remineralisation of OC produced at the sampling site will actually occur down current. Few, if any, natural system will exhibit characteristics of laminar flow, where it might be supposed that each parcel of water passing the sampling site undergoes an identical history. Therefore any attempts to balance the production of OC with actual OC concentrations must be treated with care.

Phytoplankton growth during spring and summer resulted in CO_2 in the surface waters both offshore and in the fjord becoming considerably undersaturated with respect to the atmosphere, with fCO_2 reduced to less than 100 µatm under ice cover, and between 100 and 200 µatm during ice free periods (Chapter 4 and 7). This disequilibrium should result in uptake of atmospheric CO_2 by the ocean during ice free periods. Direct evidence for such uptake was not observed (consistent with at least one other Antarctic study: Karl et al., 1991), and ^{13}C isotopic evidence was equivocal. However, a flux of oxygen, which occurred during periods of open water at O'Gorman Rocks when the gas was supersaturated in the surface water, suggested that there was a concomitant transfer of CO_2 from the atmosphere into the water column. Rough calculations based on oxygen degassing suggested an uptake of CO_2 amounting to an increase of approximately 5 µmol kg^{-1} CO_2 throughout the water column, which was considerably less than the 50 - 90 µmol kg^{-1} calculated using the gas transfer model of Wanninkhof (1993). This imbalance might have been due to effects such as the formation of a thin skin of ice at the water surface, which hindered transport and which was not destroyed by the generally light winds experienced during the open water period.

After the end of the periods of summer productivity, the concentrations of DIC and nutrients at both sites increased steadily throughout winter (Chapters 4 and 7). These increases were consistent with the remineralisation of organic material at relatively shallow depths rather than through deep convective upwelling of nutrient rich deep water, which would have resulted in a sudden jump in concentrations. This conclusion was supported by sediment trap data from Ellis Fjord (Chapter 8). Strong peaks in the rate of OC sedimentation observed in near-surface traps which were associated with periods of high primary productivity decreased in intensity with depth, and at 70 m were virtually indistinguishable from background sedimentation. Furthermore, few intact diatoms were observed in the material trapped at 70 m, whereas they were prevalent in surface traps. Therefore, it appeared that the majority of organic matter was remineralised within the water column in Ellis Fjord. In the open ocean it is probable that a high percentage of OC was remineralised above the depth of the maximum extent of mixed WW layer (*circa* 200 m).

The fugacity of CO_2 at O'Gorman Rocks rose steadily during winter to approximately 360 - 370 µatm, close to the concentration of the gas in the atmosphere (Chapter 4). This observation can be interpreted in two ways. Firstly, the surface of the Southern Ocean could be essentially in equilibrium with the atmosphere at the end of winter, implying that fCO_2 at this time of year has been increasing steadily in concert with atmospheric CO_2 over the last few centuries. Secondly, fCO_2 at the end of winter may have been essentially constant over this period, with maximum fCO_2 controlled by regenerative processes rather than CO_2 uptake from the atmosphere. If so, the area is changing from a putative late winter CO_2 source to the atmosphere to a sink. Further observations during late winter are required to determine which process is occurring. In this regard, it is possible that the recently proposed circum-Antarctic atmospheric wave (White and Peterson, 1996) plays an important role in controlling the uptake of CO_2 by the ocean from the atmosphere, and this needs to be tested.

Organic matter sedimentation in the Antarctic region has been characterised as being 'on for two months, off for ten' (Fischer et al., 1988). This view was in part the result of a study undertaken in the central Weddell Sea, in which measurable sedimentation at a depth of 863 m occurred only during periods from late January to early April, when the site was ice free (Fischer et al., 1988). This assessment, which might lead researchers to put out sediment traps for relatively short periods of time in the belief that sedimentation during the rest of the year is insignificant, is not a true reflection of the situation in neritic waters. Sedimentation at both O'Gorman Rocks and in Ellis Fjord was highest during summer, but a significant proportion of the total flux occurred during the remainder of the year (Chapters 5 and 8). The extended period of sedimentation was, to some extent, a function of the location of the study sites in inshore and shallow waters, as OC production both in bottom ice algal mats and in the shallow and stratified water column prior to the break out of the sea ice was important. However, any study of sedimentation in the Antarctic region should consider a complete annual cycle rather than extrapolate from shorter, typically summer, periods.

A number of different mechanisms by which organic matter can be transferred from where it is produced in the surface water to deep water or to the sediment were identified during this study. Direct sedimentation of diatom cells was important at times, and has also been reported elsewhere (Dunbar et al., 1985; Johnson and Smith, 1986). If the phytoplankton cells were grazed by zooplankton before they can fall from the surface water, a proportion of the carbon will remain in the upper water either as DIC resulting from respiration and DOC lost during sloppy feeding, or will be incorporated into the bodies of zooplankton and organisms in higher trophic levels. Some of the carbon, however, is repackaged into faecal pellets, which typically sediment rapidly. The efficiency of the transfer of carbon from the surface to the sediment will depend in part on the propensity of the phytoplankton species present to undergo sedimentation, and the palatability of the species to zooplankton grazers. Thus the make-up of phytoplankton blooms will play an important role in determining the

rate of carbon sedimentation: if flagellates (such as cryptomonad A, which was at times the dominant phytoplankton species but which did not appear in the sediment traps), or small or particularly palatable diatoms are dominant, relatively less carbon will be lost from surface waters than for blooms comprised of larger, less buoyant species. Changes in dominant phytoplankton species can therefore have a strong influence on the strength of the biological pump. Furthermore, the chemistry of the organic matter in the sediment will depend on the characteristics of the species which made up the bulk of the sedimenting material.

The organic material in the sediment traps at both the O'Gorman Rocks and Ellis Fjord sites (Chapters 5 and 8) had surprisingly high $\delta^{13}C_{OC}$ (annual average *circa* -19 ‰ at both sites) compared to previous Antarctic studies, in which $\delta^{13}C_{OC}$ was often less than -25 ‰. This was due to the sedimentation not only of bottom ice mat material in October and November, which had very high $\delta^{13}C_{OC}$ (up to -13 ‰), but also organic material with relatively high $\delta^{13}C_{OC}$ throughout the balance of the year. Sedimentation of high $\delta^{13}C_{OC}$ material appears to have occurred in the area for many thousands of years, as evidenced by $\delta^{13}C_{OC}$ in marine sediment cores (this study; Bird et al., 1991).

$\delta^{13}C_{OC}$ in sediment cores and sedimentary rocks has been proposed as a proxy for both water temperature (Sackett, 1986) and $[CO_{2(aq)}]$ (and, assuming equilibrium between the aqueous and gaseous phases, the concentration of atmospheric CO_2: Rau et al., 1991b). The data from the present study indicate that $\delta^{13}C_{OC}$ is not a good proxy for temperature, as the high $\delta^{13}C_{OC}$ found suggested (Sackett, 1986; Rau et al., 1991c) water temperatures far higher than those actually recorded. The relationship with $[CO_{2(aq)}]$ appears to hold a little more closely, as the high $\delta^{13}C_{OC}$ in the present study can be attributed to OC production in the low DIC (and therefore low $[CO_{2(aq)}]$) environment in the bottom ice mat and, to a lesser extent, in the highly productive surface water in which the concentration of DIC was also reduced significantly. If this relationship holds, $\delta^{13}C_{OC}$ could also be an indirect measure of mixing depth and

stratification; reduced mixing and increased stratification should result in higher $\delta^{13}C_{OC}$ due to the greater reduction of $[CO_{2(aq)}]$ in the surface waters where primary production occurs. The $\delta^{13}C_{OC}$ in sediment cores should therefore not be interpreted in terms of general relationships between latitude and $[CO_{2(aq)}]$ in equilibrium with the atmosphere (e.g. Rau et al., 1991b), but rather in terms of the history of productivity, stratification and ice cover at the core location.

Studies of phytoplankton identity and biomass in the waters offshore from Davis Base over a period of approximately 15 years indicate that considerable interannual variation occurs in these parameters (Chapter 3 and Perrin et al., 1987; Gibson et al., 1990, 1997; Davidson and Marchant, 1992a; McTaggart, 1994; F. Scott, J. Grey, personal communications). This variation can be attributed in part to stochastic events, such as the timing of the break out of the fast ice and periods of strong winds, which mix the water column and introduce new bodies of water and associated phytoplankton populations into the area. Ultimately, this variation will be reflected in the dynamics of carbon flow through the ecosystem both due to changes in phytoplankton biomass (i.e. net productivity) and speciation. The increasing levels of UVB radiation currently being experienced in the Antarctic region as a result of the annual spring ozone hole could well have an affect, possibly reducing phytoplankton biomass and inducing a shift in the dominant species (Davidson et al., 1996).

The results from this study reinforce the danger of the assumption that results from studies of Antarctic ecosystems undertaken during a single season (often due in part to logistic or funding constraints) are typical of those occurring in other years. Interannual variation does occur, and it is hazardous to assume that data from a particular year are representative, and can be used to predict the behaviour of the systems over extended periods.

APPENDIX A

EXPERIMENTAL METHODOLOGY

A.1 Introduction

This appendix gives details of sample collection and analytical protocols. Also described are the techniques used in the studies of sedimentation rates and sediment cores, and the identification and enumeration of phytoplankton.

A.2 Sampling Dates and Times

Water sample collection dates for the O'Gorman Rocks and Ellis Fjord sites are listed in Tables A.1 and A.2 respectively. A complete set of samples was collected on each date unless otherwise noted. Sampling was carried out at essentially the same time on every trip, which for O'Gorman Rocks was from 10 AM to 1 PM local solar time, and for Ellis Fjord from 11 AM to 2 PM.

A.3 Collection of Water Samples

When ice was present water sampling and other procedures were carried out through 20 cm holes drilled with an ice auger. Every effort was made to keep the hole free of ice to avoid contaminating samples and interfering with action of the sampling bottles. After ice break out at the O'Gorman Rocks site sampling was undertaken from a small boat moored at the site.

Water samples were collected using either a 2 L Go-Flo sampler (General Oceanographics, Miami, USA) or a polycarbonate 2 L Kemmerer bottle (Roberts and Burton, 1992). Both samplers were designed to allow the transfer of water to storage

Table A.1. Sampling dates, O'Gorman Rocks, December 1993 - February 1995

22 December 1993	10 May 1995[3]	21 December 1994[3]
29 December 1993[1]	9 June 1994[3]	28 December 1994[3]
6 January 1994[1]	11 July 1994[3]	4 January 1995[3]
12 January 1994[1]	9 August 1994[3]	8 January 1995[3,4]
19 January 1994[1]	8 September 1994[3]	16 January 1995[1,3]
26 January 1994[1]	7 October 1994[3]	23 January 1995[1]
2 February 1994[1]	21 October 1994	30 January 1995[1,3]
9 February 1994[1]	4 November 1994[3]	13 February 1995[1,3]
15 February 1994[1]	19 November 1994[3]	20 February 1995[1]
24 February 1994[1]	28 November 1994	27 February 1995[1,3]
2 March 1994[1]	7 December 1994[3]	
2 April 1994[2]	14 December 1994[3]	

1. The sampling site was ice free on these dates
2. Dates on which the sediment trap array was initially deployed
3. Dates on which the sediment trap array was recovered and redeployed
4. Sampling restricted to recovery of the sediment trap array

Table A.2. Sampling dates, Ellis Fjord, May 1994 - June 1995. The site was covered by ice throughout the study.

7 May 1994	17 November 1994[2]	19 January 1995[2]
2 June 1994[1]	25 November 1994	27 January 1995
7 July 1994[2]	2 December 1994[2]	2 February 1995[2]
2 August 1994[2]	12 December 1994	17 February 1995[2]
6 September 1994[2]	19 December 1994[2]	2 March 1995[2,3]
3 October 1994[2]	26 December 1994	12 June 1995[3]
17 October 1994	2 January 1995[2]	
31 October 1994[2]	12 January 1995	

1. Date on which the sediment trap array was initially deployed
2. Dates on which the sediment trap array was recovered and redeployed
3. Sampling restricted to recovery of the sediment trap array

containers using nalgene tubing, resulting in minimal exposure of the sample to the atmosphere. The samplers were thus well suited for the acquisition of samples for the analysis of dissolved gases.

All samples were placed in a large, insulated container as soon as possible after collection. The container was kept closed to reduce both light and thermal shock of the samples (both warming in summer and cooling in winter).

A.4 Physical Parameters

A.4.1 Water Temperature and Electrical Conductivity

Water temperature and electrical conductivity were measured using a Platypus Submersible Data Logger (SDL) (Platypus Engineering, Hobart, Australia), which was attached to a marked line and lowered into the water column in 1 m steps. The SDL was kept at each depth for at least 40 s to allow stabilisation of the temperature and conductivity outputs. The data were initially stored internally in the SDL, and were recovered in the laboratory using a personal computer-based interrogation program. Both the temperature and conductivity functions provided data to 2 decimal places (ie 0.01 °C and 0.01 mS cm^{-1}). The precision of the temperature function was better than 0.01 °C, whereas that of the conductivity function was less precise, with output varying by approximately ±0.05 mS cm^{-1} when the SDL was placed in seawater at a constant temperature.

The temperature function of the SDL was calibrated by placing the unit in a container of deionised water (Milli-Q grade) and allowing the water to cool to freezing. The temperature recorded when both ice and water were present was -0.04 °C, instead of the expected 0.00 °C, so all temperature data collected during the study were corrected by +0.04 °C. Calibration of the conductivity function of the SDL was carried out by placing the unit in a 60 L container of seawater, the salinity of which (34.60 psu) had been determined previously using a Yeo-Kal bench top salinometer. This water was allowed to cool to freezing and then rewarm to room temperature a number of times, and the resulting conductivity curves compared to those predicted for the standard calculated from the equations of state for seawater (Fofonoff and Millard, 1983). A slight correction, which increased the measured conductivity by a factor of 1.0222, was applied to all conductivity data.

A.4.2 Water Salinity and Density

Water salinity (psu) was calculated from measured temperature and electrical conductivity using the equations of by Fofonoff and Millard (1983). The ±0.05 mS cm^{-1} variation in the conductivity noted above introduces an error in the calculated salinities of ± 0.07 psu. It is recognised that this error is poor by oceanographic standards, but more accurate and precise equipment was not available.

Water density was calculated from the salinity and temperature also using equations given by Fofonoff and Millard (1983). The approximate density error at 0° C due to the imprecision in the conductivity function was ±0.05 kg m^{-3}.

A.5 Dissolved Inorganic Carbon and Related Parameters

A.5.1 Dissolved Inorganic Carbon

Samples for the determination of DIC were stored in either 500 mL Schott bottles or 250 mL Kimble milk dilution bottles. Prior to use the bottles were wrapped in clean aluminium foil and muffled at 525 °C for 16 hrs. All muffling referred to throughout this appendix was at this temperature and for this length of time.

Water samples were transferred from the Kemmerer or Go-Flo sampling bottle to the storage bottles using a length of nalgene tubing. The storage bottles were filled from the bottom, and water was allowed to overflow by approximately one bottle volume to minimise contact of the sample with the atmosphere. The samples were preserved by addition of 100 µL saturated $HgCl_2$, and a small volume of each sample was removed to provide an air space on closing. The 500 mL bottles were sealed with a ground glass stopper coated lightly with Apiezon L grease, while the 250 mL bottles were tightly sealed with a screw cap.

Both the Kimble and the Schott bottles proved susceptible to breakage in cold conditions in the field due to ice formation in the samples, and several samples were lost. The samples were stored at room temperature until analysis in Hobart.

The concentration of DIC in the samples was determined using a SOMMA (Single Operator Multi-Metabolic Analyzer) system (Johnson et al., 1993) in the CSIRO Division of Oceanography, Hobart, Tasmania. In this system the sample was acidified with phosphoric acid, and the released CO_2 trapped in a solution of triethanolamine in dimethylsulphoxide which also contained an indicator dye. The CO_2 formed an addition product with the ethanolamine, which was then reduced electrochemically. The endpoint of the reduction was determined spectrophotometrically. The system was standardised using seawater of known DIC concentration prepared by the Marine Standards Laboratory, University of California - San Diego, USA. A standard was analysed every ten samples, and little drift in the measured concentration of the standards was observed (± 2 μmol kg^{-1}). The precision of the system, estimated from repeated injections of carbon dioxide using a gas loop, was also about 2 μmol kg^{-1}.

A.5.2 Measurement of pH

An adaptation of the spectrophotometric cresol red method of Byrne and Breland (1989) was used to measure pH in this study. The sodium salt of cresol red was obtained from Aldrich Chemicals.

Samples for the determination of pH were collected in 300 mL biological oxygen demand (BOD) bottles, which had previously been thoroughly washed and rinsed with deionised water. The bottles were rinsed several times with the seawater sample before being completely filled from the bottom and sealed with a ground glass stopper (no air space remained in the bottles after sealing).

On return to the laboratory, the samples were warmed to 25 °C in a water bath, and a small volume removed for use in the reference beam of the spectrophotometer. Forty μL of a 0.002 M solution of the sodium salt of cresol red (the pH of which had been previously adjusted to 8.0 with HCl) was added to the bottle, which was then restoppered and mixed quickly by inversion. The absorbance of the resulting solution was then measured immediately at 433, 573 and 750 nm using a GBC 916 Spectrophotometer with the original sample in the reference beam. The alignment of the diffraction grating of the spectrophotometer was checked by comparison to a didymium standard, and was found to accurate.

The following equation was used to calculate pH at 25 °C (Byrne and Breland, 1989):

$$pH = 7.8614 + 0.004\ (35\text{-}S) + \log_{10}\left(\frac{R - 0.00286}{2.7985 - 0.09025R}\right) \qquad (A.1)$$

where S was the salinity of the sample in psu, and R was defined as:

$$R = \left(\frac{A_{573} - A_{730}}{A_{433} - A_{730}}\right) \qquad (A.2)$$

where A_W was the absorbance of the solution at the wavelength W nm.

The accuracy of this experimental protocol was not determined by comparison to seawater standards, as none were available. However, Bellerby et al. (1995) point out that calibration of spectrophotometric methods for pH determination are dependent solely on the accuracy of the measurement of the absorbance characteristics of the indicator and the alignment of the wavelength function of the spectrophotometer. Given the high precision of spectrophotometric techniques (Byrne and Breland, 1989; Clayton and Byrne, 1993; Zhang and Byrne, 1996), it is probable that the pHs reported here are correct to at least ± 0.01 pH units. The addition of the indicator

slightly altered the pH of the samples, but the small volume used and the adjustment of the pH of the indicator solution to close to that of the samples kept the associated error insignificant. Similarly, the reduction in salinity of the sample from the addition of the indicator was within the instrumental error of the SDL, and had a negligible effect on the calculated pH (as can be seen from Equation A.1).

A number of scales exists for the measurement of pH in seawater (Dickson, 1993). The spectrophotometric method used in this study yields pH on the 'free' scale, pH_f (R. Byrne, personal communication), and the pHs discussed in the text and tabulated in Appendices B and E are on this scale. pH on the seawater scale, pH_{sws}, which takes into account the dissociation of the HSO_4^- ion and HF, was calculated for input into the computer program discussed in Section A.5.3 using to the following equation (Clayton and Byrne, 1993; Dickson, 1993):

$$pH_{sws} = pH_f - \log_{10}\left(1 + \frac{[SO_4^{2-}]}{K_{HSO_4}} + \frac{[F^-]}{K_{HF}}\right) \qquad A.3$$

where $[SO_4^{2-}]$ and $[F^-]$ are the total concentrations of sulphate and fluoride ions in a seawater sample, and K_{HSO4} and K_{HF} are the dissociation constants of the bisulphate ion and hydrofluoric acid, respectively, in the sample. The values for the concentrations and constants were calculated from equations given by Millero (1995) and Lee and Millero (1995).

A.5.3 Calculation of Related Parameters

The concentration of DIC and pH can be used to calculate the concentration of the various inorganic carbon species and other related parameters including Alk_T and fCO_2 in a seawater sample (see, for example, Stumm and Morgan, 1981). To facilitate these calculations, a Quickbasic computer program was obtained from Professor F. J.

Millero, University of Miami, USA. Input of DIC concentration, pH_{sws} at 25 °C, salinity and temperature resulted in the calculation *inter alia* of the following parameters in the sample: total alkalinity; the concentrations of carbonate and bicarbonate ions and carbonic acid; and fCO_2. This program employed the 'best choice' equilibrium constants of Millero (1995) and Lee and Millero (1995).

A.6 Organic Carbon

Two functional pools of organic carbon were measured during the study:
DOC (defined as that material that passed through a Whatman GF/F glass fibre filter with nominal pore size 0.7 μm) and POC (defined as that material trapped on a GF/F filter). The methods used to measure the carbon in these pools are described below.

A.6.1 Dissolved Organic Carbon

Samples for the analysis of DOC were transferred carefully in the field into pre-muffled 125 mL amber glass bottles. Special effort was made not to contaminate the samples during this procedure. The bottles were sealed with screw caps and virgin teflon lined inserts.

On return to the laboratory, the samples were filtered through an all glass system (Figure A.1). The only parts of this system which came into contact with the sample were the funnel, the GF/F filter and the filter support. The funnel was muffled prior to each use of the filtering equipment, as were the GF/F filters, one of which was used for each sample. The filter support, which unfortunately could not be removed from the rest of the set up, was rinsed thoroughly with deionised water and then filtered seawater before use. Thirty mL of each sample was passed through the system before any filtrate was collected. Approximately 60 mL of filtrate was then collected in pre-muffled 125 mL amber bottles, to which 100 μL concentrated HCl was added as a

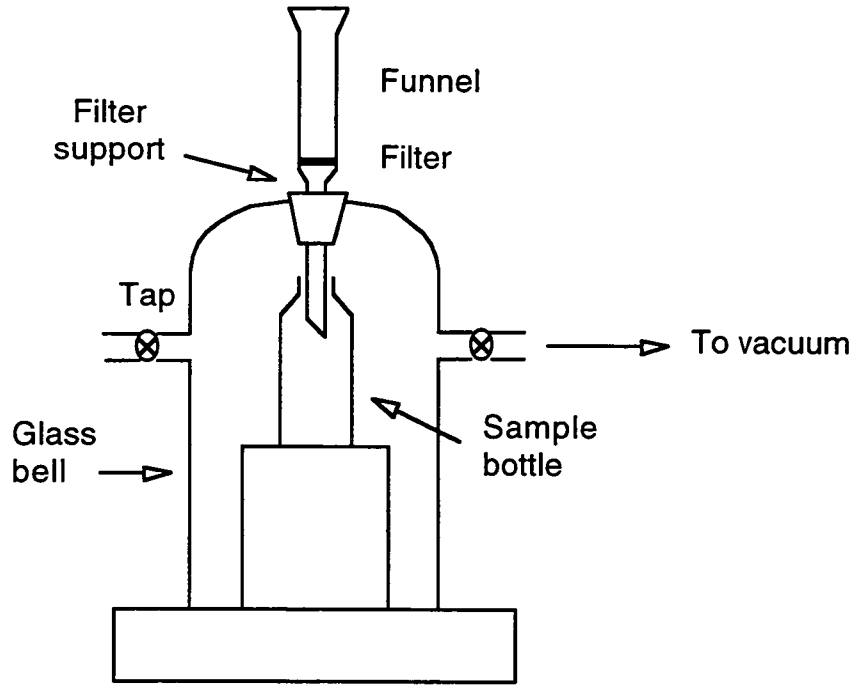

Figure A.1. Diagram of the apparatus used to filter water samples for dissolved organic carbon analysis.

preservative (the samples needed to be acidified later in the analysis protocol to remove DIC; this addition also served this purpose). The samples were sealed as described above, and stored upright at -20 °C until analysis was performed. Every effort was made to reduce sample contamination.

Analysis of DOC was undertaken using a Shimadzu 5000-TOC total organic carbon analyser, which determined OC by oxidising a sample to CO_2 in a column of platinum-coated zeolite balls at a temperature of 680 °C. The gas produced in the reaction column was dried and any halogen present was removed with chemical scrubbers. The amount of CO_2 produced, and thus the concentration of organic carbon, was determined by an internal non-dispersive infra-red gas analyser, the output of which was integrated by the instrument. Inorganic carbon was removed automatically by the instrument from the acidified samples by stripping with CO_2-free gas prior to injection into the reaction column.

Standards were prepared before each sample run by accurate standard addition of a freshly prepared glucose solution to a seawater sample. The resulting calibration curves were linear over the range of carbon concentrations observed in the samples. The precision of the instrument was such that repeated injections of the same seawater sample gave concentrations within a few percent of each other. Accuracy was more difficult to determine due to the 'machine blank', which is the detector response that would occur on injection of a sample with no carbon (Benner and Strom, 1993; Williams et al., 1993). The machine blank for the instrument could not be determined accurately, but must have been less than 15 μmol kg^{-1} carbon, as concentrations this low were measured in some samples.

A.6.2 Particulate Organic Carbon

Samples for the determination of POC were transferred to clean 2 L plastic containers. POC was determined by first filtering the seawater sample through a pre-weighed (to 10 μg), pre-muffled 47 mm GF/F filter, which was subsequently rinsed with a few mL of 1 M HCl to remove carbonates, and then deionised water to wash out any soluble salts. If zooplankton (e.g. copepods) were present, the sample was passed through a 100 μm mesh prior to filtration. The filters were dried at 80 °C overnight, and reweighed in order to determine total particulate matter. The filters were then heated to 525 °C for 16 hrs to oxidise any organic material, and reweighed. Particulate organic matter was determined by difference, and POC calculated assuming that carbon made up 35.8 % of the material, which assumed an average POC composition of $C_{106}H_{263}N_{16}O_{110}P$ (Libes, 1992).

A filter blank was calculated as follows. A 2 L sample of seawater was filtered twice through pre-muffled GF/F filters. This water was then passed through each of ten pre-muffled, pre-weighed 47 mm GF/F filters, which were subsequently rinsed with 1 M HCl and deionised water. The filters were dried and muffled as above, and the

changes in the masses of the filters used to calculate a blank correction for the concentration of POC. All data presented in this thesis have been corrected for this blank. The blank was approximately 10 % of typical uncorrected POC mass. No estimate of the precision or the accuracy of this method was made.

A.7 Carbon Isotopic Ratios in the DIC Pool

Water for the determination of the carbon isotope ratios of the DIC was transferred from the sampling bottle to pre-muffled 500 mL Schott bottles as described above for DIC analysis (Section A.5.1), and were preserved, sealed and stored in the same fashion.

A.7.1 Measurement of the $^{13}C/^{12}C$ Ratio of DIC

The $^{13}C/^{12}C$ ratio of the total carbonate fraction was measured in the Isotope Biogeochemistry Laboratory, University of Hawaii, USA. Samples were acidified, and the resulting CO_2 dried and collected cryogenically. The isotopic ratio of the CO_2 was determined using a Finnigan MAT 252 Ion Ratio mass spectrometer. $^{13}C/^{12}C$ isotopic ratios are quoted on the δ scale with respect to Pee Dee belemnite (PDB) (Craig, 1957):

$$\delta^{13}C = \left(\frac{\left(\frac{^{13}C}{^{12}C}\right)_S - \left(\frac{^{13}C}{^{12}C}\right)_{PDB}}{\left(\frac{^{13}C}{^{12}C}\right)_{PDB}} \right) \times 1000\ ‰ \qquad (A.4)$$

where the subscripts S and PDB refer to the isotope ratios of the sample and the PDB standard respectively. The precision of this measurement was estimated to be $\pm$ 0.1 ‰.

A.7.2 Measurement of the ^{14}C /^{12}C Ratio of DIC

Samples for the measurement of the ^{14}C content of the DIC were sent to the Australian Nuclear Scientific and Technical Organisation, Lucas Heights, NSW (ANSTO). The isotopic ratio was measured by accelerator mass spectrometry methods (Schlosser et al., 1987).

Ratios of $^{14}C/^{12}C$ are quoted on the $\Delta^{14}C$ scale, defined as follows:

$$\Delta^{14}C = \delta^{14}C - 2\,(\delta^{13}C + 25)\left(1+\frac{\delta^{14}C}{1000}\right) \times 1000\ ‰ \qquad (A.5)$$

where $\delta^{14}C$ is defined in a similar manner to $\delta^{13}C$ above (Equation A.4). The standard ratio for the calculation of $\delta^{14}C$ was 0.95 times the $^{14}C/^{12}C$ ratio of the National Bureau of Standard's oxalic acid reference material. Further details of the analyses, including ANSTO sample numbers, are included in Appendix D.

A.8 Chlorophyll

Samples for measurement of chl *a* and chl *b* were transferred to clean, 2 L plastic bottles, and were stored in the dark. On return to the laboratory the samples were filtered through a 47 mm Whatman GF/F glass fibre filter, and the volume of the filtrate recorded (± 10 mL). Samples collected during intense phytoplankton blooms clogged the filter rapidly, so that volumes considerably less than 2 L were filtered. The filters were dried and stored frozen at -20 °C until analysis was undertaken.

The filters were cut up and placed in 90% (v/v) aqueous acetone, agitated ultrasonically for 5 minutes, stored overnight in a freezer at -20 °C, resonicated and finally centrifuged. Absorbance of the resulting solution was measured at 630, 647

664 and 750 nm using the GBC 916 Spectrophotometer with 90% (v/v) aqueous acetone in the reference beam. The equations given by Parsons et al. (1984) were used to calculate the concentration of chl *a*. and chl *b*. The estimated error in the concentrations of both chlorophylls was less than 1 %, and the precision ±0.2 mg m^{-3} at a concentration of 5 mg m^{-3} (Parsons et al., 1984). The detection limit was 0.1 mg m^{-3}. No correction was made for the concentrations of phaeopigments.

A.9 Dissolved Oxygen

Samples for the analysis of DO were transferred into 300 mL BOD bottles using nalgene tubing as described above to minimise exposure of the sample to air, and were fixed with basic potassium iodide and manganous chloride solutions in the field. On return to the laboratory, DO was determined using the standard Winkler method (Parsons et al., 1984). The equilibrium solubility of oxygen at the *in situ* temperature and salinity of each sample was calculated using the equation of Benson and Krause (1984) (allowing for a change of units from µM to µmol kg^{-1}). The percentage oxygen saturation was then calculated by dividing the actual concentration by the equilibrium concentration and multiplying by one hundred.

A.10 Nutrients

Samples for the analysis of nitrate and nitrite, phosphate and silicate were transferred to acid washed 125 mL high density polyethylene bottles, stored at -20 °C, and analysed within 4 weeks of sampling. This storage time would not be expected to result in any sample degradation (McDonald et al., 1986; Kirkwood, 1992; Dore et al., 1996). The method used for nitrate determination did not discriminate between nitrate and nitrite, and throughout this thesis, 'nitrate' refers to the sum of these species. From November 1994 until the end of the study nitrate analyses were performed on the filtrate from the chl *a* analysis immediately after the filtration.

Nutrient analyses were carried out using standard manual wet chemical techniques given in Parsons et al. (1984). Table A.3 gives a short summary of the techniques used and the detection limits and accuracy of each technique.

A.11 Phytoplankton

Samples for the identification and enumeration of phytoplankton were preserved with 0.25 % Lugol's Iodine (prepared following Parsons et al. (1984)) and stored in 1 L glass bottles to aid diatom preservation.

Phytoplankton known volumes of the water samples were initially allowed to sediment in measuring cylinders, and then in 10 mL Utermöhl counting chambers (Utermöhl, 1958). Cells were counted using a Leitz Laborlux inverted microscope at x400. Between 15 and 70 randomly spaced fields of view containing at least 300 cells in total were counted for each sample. The phytoplankton cells were identified to genus and,

Table A.3. A summary of the methods used for analysis of nutrients. Estimates of the detection range and accuracy (at the concentration given in brackets) of the methods is also given (Parsons et al., 1984).

Analysis	Method	Detection Range	Accuracy
Nitrate	Cadmium reduction column/sulphanilamide/N-(1-naphthyl)-ethylenediamine	0.05 - 45 µM	± 0.5 µM (20 µM)
Phosphate	Molybdic acid/ascorbic acid/Sb(III)	0.03 - 5 µM	± 0.03 µM (3 µM)
Silicate	Molybdic acid/metol/oxalic acid/sulfite	0.1 - 140 µM	± 0.25µM (10 µM)

where possible, to species. Diatoms were identified after Priddle and Fryxell (1985) and Medlin and Priddle (1990). Standard errors of the counts were typically 10% of the total for common species. It is recognised that this procedure would not allow the identification and enumeration of small flagellates and picoplankton not readily observable at the magnification used.

A.12 Sediment Traps

Sediment trap arrays were deployed at the O'Gorman Rocks and Ellis Fjord sites from 2 April 1994 to 27 February 1995, and from 2 June 1994 to 12 June 1995 respectively. The sections below describe the design, deployment and retrieval of the traps, as well as the subsequent processing of the samples.

A.12.1 Sediment Trap Design and Deployment

The sediment traps consisted of slightly tapered plastic cylinders with a mouth diameter of 6.8 cm and a depth of 15 cm, giving a mouth diameter to depth ratio of 3.2 (Figure A.2). The traps were placed in wooden brackets, each of which held four individual traps. The brackets were in turn attached to a nylon rope at depths of 5, 10, 15 and 20 m at O'Gorman Rocks, and at 5, 10, 20, 40 and 70 m in Ellis Fjord. When ice cover was present at the sample sites the trap arrays were hung from a length of wood on the surface of the ice. A weight was attached to the end of the rope to keep it vertical. After ice break out at O'Gorman Rocks, the array was hung from a buoy attached to a large weight on the sediment by a separate rope. No poison or high density solutions were used in the traps.

When the sites were ice covered the traps were recovered by drilling a hole through the ice next to the length of wood at the surface and catching the rope to which the brackets were attached with a hook. The rope was carefully pulled up through the ice

Figure A.2. Design of the sediment trap arrays: (a) Side view of sediment traps in bracket; (b) Plan view of bracket.

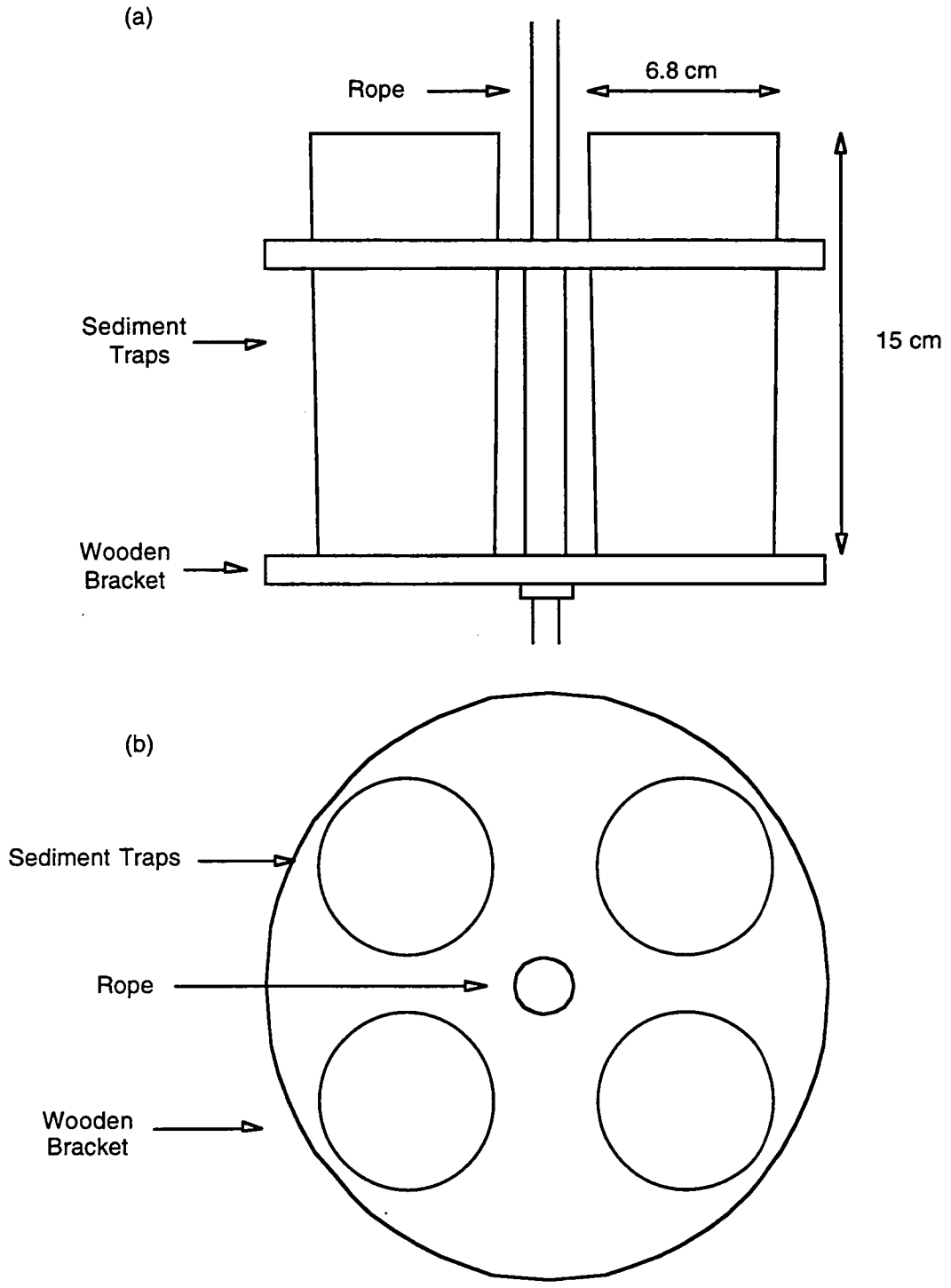

hole and the individual traps removed from the brackets as they reached the surface. The traps were then capped, and, when all had been recovered, new traps were placed in the brackets and the array redeployed. On some occasions traps were lost when they floated free from the brackets during deployment. In the absence of ice, the traps were recovered in a similar fashion from a small boat.

The trap arrays were recovered approximately monthly from the initial deployments until October, after which retrieval was on a fortnightly or weekly basis (Tables A.1 and A.2). The array in Ellis Fjord was left in place at the end of the main study in February 1995, and recovered by members of the 1995 wintering party at Davis Station in June of that year, completing a full year of deployment.

Between October and December 1994, the amphipod *Paramoera walkeri*, a species associated with the undersurface of the ice (Tucker and Burton, 1988), was found regularly in the 5m traps at the O'Gorman Rocks site. Data from these traps have been excluded from the results and discussion presented in Chapter 5 and tabulated in Appendix E. Apart from these occurrences, few problems were experienced with swimmers.

As the break out of the fast ice at the O'Gorman Rocks site became imminent, the brackets at 5, 15 and 20 m were removed from the array to minimise equipment losses if the ice were to break out suddenly. The array was removed completely from the water on 8 January 1995, and repositioned, after the break out of the fast ice on the 13 January, on 16 January. The sedimentation rates during this period were estimated by assuming that for the period 8 - 13 January they were the same as during the preceding time period, and for 13 - 16 January the same as the subsequent period. The array was lost during a period of strong winds in early March 1995. In order to complete a full year of data, the sedimentation rate for the period 27 February - 4 April 1995 was estimated by assuming that the rate dropped exponentially during this period from that

measured for the period 13 - 27 February 1995 to the rate recorded at the start of the study in March the previous year. From observations of water clarity, which increased rapidly early in this period, this assumption appeared to be reasonable.

A.12.2 Total and Organic Sedimentation Rates

Material from three of the sediment traps from each depth were filtered through pre-muffled, pre-weighed GF/F filters. The filters were treated with a few mL 10% HCl to remove carbonates, rinsed with deionised water, and dried at 80 °C overnight. The filters were reweighed, and the total sedimentation rate calculated (correcting for the blank described in Section A.6.2 above). One of the filters was stored for later chemical and isotopic analysis. The other two filters were heated to 525 °C for 16 hours and the amount of organic carbon calculated as described in Section A.6.2, again correcting for the blank.

The total and organic carbon sedimentation rates calculated from the three samples generally agreed quite to very well. The data tabulated in Appendices E and G are the averages of these repeat determinations.

The percentage organic carbon in the sedimenting material was calculated by dividing the rate of organic carbon sedimentation by the total sedimentation rate and multiplying by 100.

A.12.3 C:N Molar Ratio of the Organic Material

The percentages of carbon and nitrogen in the organic material on sections of the dried, non-muffled filters (Section A.12.2) were determined using a Carlo-Erba EA1108 Elemental Analyser at the Central Science Laboratories, University of Tasmania, Hobart. The C:N molar ratios were calculated from these percentages.

A.12.4 Determination of $\delta^{13}C$ of the Sediment Trap Material

Sections of the dried, non-muffled filters were put into quartz tubes, which were placed in a desiccator along with a beaker of concentrated HCl for 2 - 3 days in order to remove any carbonate present. CuO/Cu_2O wire (obtained from Merck) was added to the tubes, which were then evacuated and sealed on a vacuum line. The tubes were heated to 680 °C for 16 hours to oxidise all organic material present to CO_2. The tubes were cracked *in vacuo*, and the CO_2 dried cryogenically on a vacuum line. The gas was collected in an evacuated glass tube which was then sealed.

The $^{13}C/^{12}C$ ratio of the CO_2 in the samples was determined using a Finnigan MAT 252 Ion Ratio mass spectrometer in the Isotope Biogeochemistry Laboratory, University of Hawaii, Honolulu, USA or a VG Sira Series 2 mass spectrometer in the Central Science Laboratory, University of Tasmania, Hobart, Tasmania. The isotopic ratio of a number of samples of which subsamples were sent to both laboratories agreed closely. The ratios are reported on the $\delta^{13}C$ scale.

A.12.5 Description of Material Caught in Sediment Traps

Particulate matter in the fourth sediment trap (Section A.12.1) was allowed to settle, and a sample removed and placed in a 25 mL glass bottle. Glutaraldehyde was added as a preservative at a final concentration of 4%. Use of glass bottles helped in the preservation of diatom frustules. Samples were stored at 4 °C until processed.

Subsamples were transferred to 10 mL Utermöhl counting chambers (Utermöhl, 1958), and allowed to sediment. The material was viewed using a Leitz Laborlux inverted microscope at x400. The general characteristics of the material was noted. Diatoms and other phytoplankton cells were identified to genus and, where possible, to species. The size of faecal pellets was measured using a calibrated graticule.

A.13 Sediment Cores

Short sediment cores 10 - 13 cm long and 4.5 cm in diameter were collected from the O'Gorman Rocks and Ellis Fjord sites using a Glew corer (Glew, 1989). The cores were cut into 1 cm sections in the field, and the sections placed into zip-lock plastic bags. Processing of the samples from Ellis Fjord was undertaken at Davis Station, while the sections of the core from O'Gorman Rocks were returned to the University of Tasmania.

A.13.1 Percentage of Organic Carbon

The percentages of carbon and nitrogen in dried core sections from the O'Gorman Rocks site were determined as described above (Section A.12.3). The percentage organic carbon was determined by subtracting the percentage of inorganic carbon in the core material (Section A.13.3) from the percentage total carbon.

The percentage organic carbon in the core from Ellis Fjord was determined by first drying the core sections thoroughly at 80 °C, weighing, and then heating the sediment at 525 °C for 16 hours. The percentage organic matter was calculated from the weight loss, and percentage organic carbon by multiplying the percentage organic matter by 0.358.

A.13.2 Determination of Inorganic Carbon Content

A weighed sample of the core material was acidified with 100 % phosphoric acid in a closed vacuum flask. The CO_2 produced was dried cryogenically on a vacuum line and was expanded into a known volume. The pressure was measured with a manometer, the amount of gas estimated using the ideal gas equation, and the masses of inorganic carbon and of $CaCO_3$ in the sediment calculated.

A.13.3 $\delta^{13}C$ of Organic Material from the Sediment Cores

Subsamples of core sections were treated 10% HCl to remove carbonates, redried, and ground in the mortar and pestle. The $\delta^{13}C$ of the remaining organic carbon was determined in the Central Science Laboratory, University of Tasmania as described previously (Section A.12.4).

A.13.4 $\delta^{13}C$ of Carbonate Material From the Sediment Cores

Large pieces of shell material (up to 2 cm across) were recovered from 8 - 10 cm in duplicate short core collected from the O'Gorman Rocks site. This material was washed thoroughly with distilled water and dried. It was then heated to 380 °C *in vacuo* for 2 hours to remove any organic matter. The remaining material was acidified with 100% phosphoric acid in an evacuated flask. The CO_2 produced was dried cryogenically, and the $\delta^{13}C$ determined as described in Section A.12.4.

A.14 Atmospheric CO_2 Concentration and Isotope Signature

Atmospheric CO_2 samples were collected on 24 occasions from March 1994 to March 1995 using pre-evacuated glass flasks and a pump system supplied by the CSIRO Division of Atmospheric Research, Melbourne. The sampling site at Davis Station was approximately 500 m upwind from any other station building, and the inlet was at a height of 6 m above ground level. Samples were collected only on days when the wind was blowing at greater than 15 knots from a direction that would minimise anthropogenic contamination. The concentration and $\delta^{13}C$ of the CO_2 in the samples were measured at the CSIRO Division of Atmospheric Research, Melbourne, Victoria using a CARLE Series 400 gas chromatograph and a Finnigan MAT 252 Ion Ratio mass spectrometer respectively.

APPENDIX B

WEATHER CONDITIONS AT DAVIS STATION: DECEMBER 1993 - FEBRUARY 1995

B.1 Introduction

This appendix summarises the weather recorded at Davis Station by members of the Australian Bureau of Meteorology from December 1993 to February 1995. It is likely that the weather at the Ellis Fjord site was slightly colder and windier than at Davis Station.

B.2 Air temperature

Air temperature at Davis was close to the long term average for most of the months of the study, with the monthly mean temperature ranging from -20.6 °C in August 1994 to 2.9 °C in February 1995. Major excursions from the average occurred in May and August 1994, which were significantly colder, and June 1994 and February 1995, which were warmer.

B.3 Wind

The monthly average wind were considerably higher than the long term average except for during the months of December 1993 and August 1994. The total wind run for the study was 26.7 % greater than the average, indicating that the period was particularly windy. During winter, lower wind speeds were correlated to colder weather and stronger wind, warmer conditions.

Figure B.1. Monthly maximum (squares), minimum (diamonds) and average (circles) temperatures, Davis Station, December 1993 - February 1995. Long term average monthly temperatures are indicated by the dashed line.

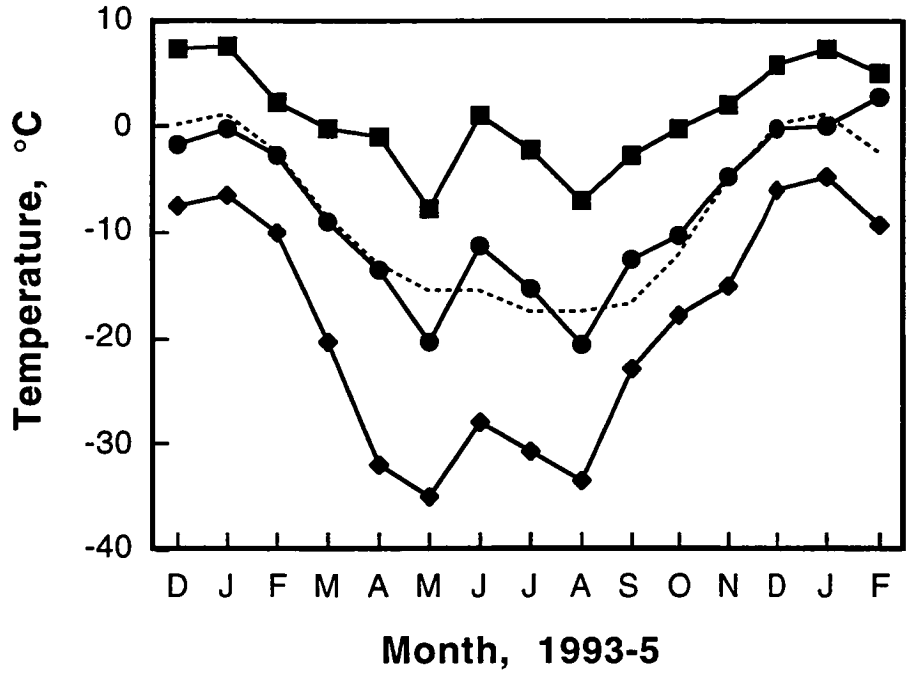

Figure B.2. Monthly average wind speeds, Davis Station, December 1993 - February 1995. Long term average monthly wind speeds are indicated by the dashed line.

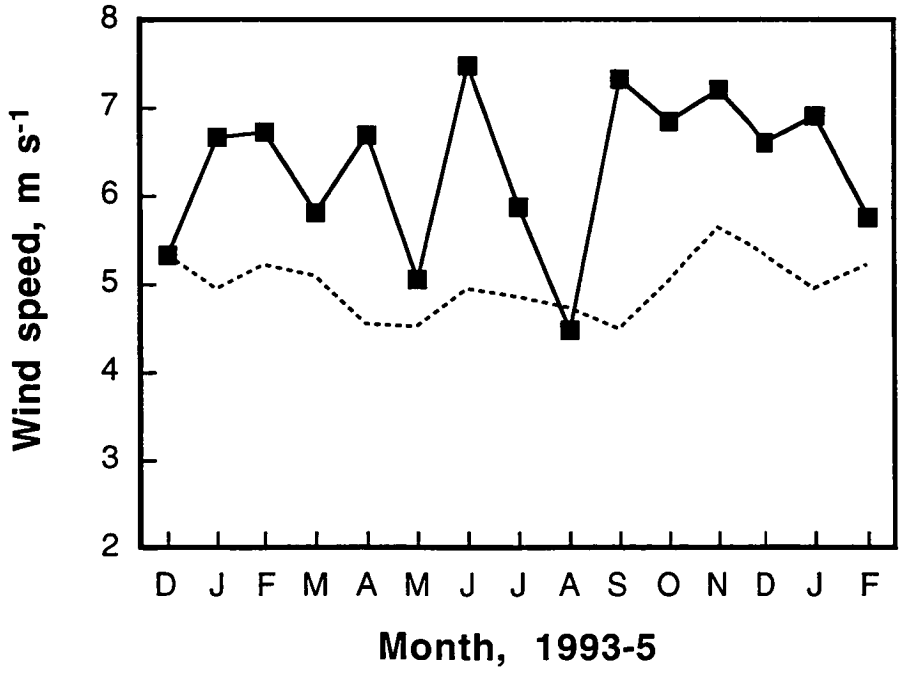

B.4 Sunlight

The average daily sunlight hours generally followed the expected cycle, with longest period of light in summer and zero when the sun did rise above the horizon for six weeks during winter. Far higher sunlight hours than the long term average were recorded in December 1993 and November and December 1994. Water column irradiances would not necessarily follow the same curve as shown in the figure, as the irradiance is also a function of the angle of the sun above the horizon.

Figure B.3. Average daily sunlight hours, Davis Station, December 1993 - February 1995. Long term average monthly sunlight hours are indicated by the dashed line.

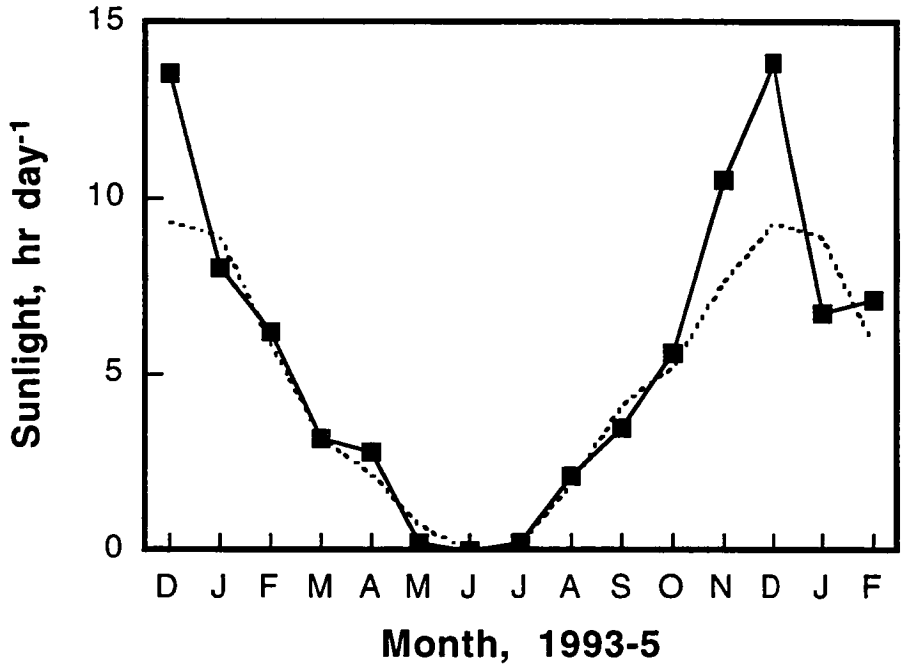

APPENDIX C

O'GORMAN ROCKS: PHYTOPLANKTON CELL COUNTS

This appendix lists phytoplankton cell counts for the water column at the O'Gorman Rocks site between December 1993 and February 1995.

Table C.1. Total cell counts (cells L^{-1}) at the O'Gorman Rocks site.

Date	Depth, m				
	0/2	5	10	15	20
22/12/93	6.08E+06	1.00E+06	1.17E+06	3.31E+05	2.42E+05
29/12/93	6.11E+06	4.73E+06	5.50E+06	6.48E+06	5.08E+06
6/1/94	4.80E+06	2.78E+06	3.53E+06	3.13E+06	3.94E+06
12/1/94	3.33E+06	2.83E+06	3.86E+06	3.01E+06	2.78E+06
19/1/94	4.45E+06	3.55E+06	5.77E+06	5.35E+06	3.78E+06
26/1/94	1.16E+07	1.11E+07	5.95E+06	1.30E+07	5.43E+06
2/2/94	8.47E+06	8.85E+06	8.80E+06		
9/2/94	4.20E+06	1.51E+06	7.98E+05		
15/2/94	1.54E+05		1.59E+05		
24/2/94	1.02E+05	1.30E+05	1.84E+05	1.82E+05	2.54E+05
2/3/94	1.65E+05	2.05E+04	1.80E+05	2.00E+05	2.38E+05
2/4/94	6.26E+04	7.38E+04	8.50E+04	4.44E+04	4.89E+04
10/5/94	5.37E+04	4.97E+04	3.78E+04	9.92E+04	1.61E+05
9/6/94	1.45E+04	1.15E+04	2.06E+04	1.20E+04	1.45E+04
11/7/94	1.49E+04	1.21E+04	1.38E+04	9.10E+03	8.00E+03
9/8/94	5.30E+03	4.06E+03	4.82E+03	4.57E+03	4.62E+03
8/9/94	1.72E+04	1.53E+04	4.82E+03	1.52E+04	1.46E+04
7/10/94	8.13E+03	1.33E+04	1.28E+04	5.46E+03	7.39E+03
21/10/94	2.91E+05	9.66E+04	4.58E+04	2.31E+04	1.30E+04
4/11/94	3.45E+05	2.53E+05	1.33E+05	4.91E+04	8.42E+04
19/11/94	1.86E+06	1.13E+06	4.05E+05	3.42E+05	8.99E+04
28/11/94	6.16E+05	5.22E+05	5.85E+05	2.96E+05	3.48E+05
7/12/94	1.08E+08	7.71E+07	2.42E+07	1.20E+07	8.25E+06
14/12/94	3.81E+07	7.01E+06	3.04E+06	1.17E+06	2.05E+06
21/12/94	8.81E+06	1.57E+06	1.10E+06	5.55E+05	5.04E+05
28/12/94	1.21E+06	4.14E+06	8.86E+06	5.50E+06	4.06E+06
4/1/95	3.08E+07	1.46E+07	1.57E+07	1.20E+07	8.02E+06
16/1/95	3.91E+06	4.23E+06	4.54E+06	2.51E+06	2.08E+06
23/1/95	3.59E+06	3.30E+06	2.25E+06	1.68E+06	1.11E+06
30/1/95	1.11E+06	1.03E+06	1.27E+06	1.00E+06	7.34E+05
13/2/95	6.98E+06	6.94E+06	4.70E+06	5.60E+06	4.29E+06

Table C.1. Continued

Date	Depth, m				
	0/2	5	10	15	20
20/2/95	3.23E+06	2.81E+06	2.63E+06	2.03E+06	2.14E+06
27/2/95	2.22E+06	2.86E+06	2.20E+06	1.96E+06	1.90E+06

Table C.2. Cryptomonad A cell counts (cells L^{-1}) at the O'Gorman Rocks site.

Date	Depth, m				
	0/2	5	10	15	20
22/12/93	3.56E+06	5.28E+05	2.81E+05	7.18E+03	7.90E+03
29/12/93	1.28E+05	7.17E+04	8.20E+04	4.98E+04	5.11E+03
6/1/94	9.98E+04	9.48E+04	7.49E+04	4.93E+04	2.81E+04
12/1/94	1.39E+03	8.11E+04	1.17E+05	3.92E+04	2.37E+03
19/1/94	1.74E+05	6.68E+04	1.52E+05	9.74E+04	9.07E+03
26/1/94	1.11E+06	1.04E+06	4.56E+04	1.07E+05	4.16E+04
2/2/94	8.56E+05	8.83E+05	1.05E+06		
9/2/94	8.07E+04	1.12E+04	0.00E+00		
15/2/94	2.06E+04		1.86E+04		
24/2/94	2.71E+04	2.53E+04	1.20E+04	6.33E+03	5.25E+03
2/3/94	2.75E+03	0.00E+00	1.03E+03	5.23E+02	9.51E+02
2/4/94	1.31E+03	0.00E+00	0.00E+00	3.64E+02	0.00E+00
10/5/94	0.00E+00	8.02E+02	4.35E+02	0.00E+00	1.63E+03
9/6/94	0.00E+00	0.00E+00	0.00E+00	0.00E+00	0.00E+00
11/7/94	9.60E+02	6.73E+02	0.00E+00	0.00E+00	0.00E+00
9/8/94	0.00E+00	0.00E+00	0.00E+00	0.00E+00	0.00E+00
8/9/94	0.00E+00	0.00E+00	0.00E+00	0.00E+00	0.00E+00
7/10/94	4.07E+02	0.00E+00	4.43E+02	0.00E+00	4.11E+02
21/10/94	5.70E+03	1.36E+03	5.09E+02	0.00E+00	4.66E+02
4/11/94	2.50E+04	2.59E+04	1.64E+04	1.87E+04	2.38E+04
19/11/94	2.63E+05	1.23E+05	5.79E+04	4.83E+04	1.30E+04
28/11/94	8.72E+04	3.98E+04	4.63E+04	4.28E+04	1.83E+04
7/12/94	1.02E+08	7.01E+07	2.21E+07	1.09E+07	7.36E+06
14/12/94	3.70E+07	2.01E+07	3.09E+06	6.20E+05	1.54E+06
21/12/94	7.96E+06	1.03E+06	4.90E+05	1.37E+05	1.37E+05
28/12/94	2.76E+05	2.63E+06	5.93E+06	3.30E+06	2.05E+06
4/1/95	1.92E+07	3.01E+06	2.75E+06	4.03E+05	1.43E+05
16/1/95	3.27E+05	4.14E+05	5.01E+05	4.13E+05	1.57E+05
23/1/95	7.00E+05	9.34E+05	2.70E+05	1.89E+05	1.09E+05
30/1/95	4.38E+05	3.87E+05	5.94E+05	3.70E+05	1.46E+05
13/2/95	5.06E+05	5.16E+05	8.80E+04	1.59E+05	1.00E+05
20/2/95	1.36E+05	8.24E+04	1.45E+05	5.08E+04	6.22E+04
27/2/95	1.60E+05	3.99E+04	4.49E+04	3.44E+04	3.00E+04

Table C.3. Diatom cell counts (all species) (cells L^{-1}) at the O'Gorman Rocks site.

Date	Depth, m				
	0/2	5	10	15	20
22/12/93	1.45E+05	6.58E+04	1.88E+05	9.14E+04	7.84E+04
29/12/93	7.06E+05	4.23E+05	5.30E+05	6.19E+05	5.62E+05
6/1/94	1.20E+06	1.12E+06	1.15E+06	8.20E+05	1.20E+06
12/1/94	2.79E+06	2.41E+06	3.12E+06	2.34E+06	1.84E+06
19/1/94	3.92E+06	3.14E+06	5.17E+06	4.89E+06	3.37E+06
26/1/94	1.03E+07	9.81E+06	5.50E+06	1.23E+07	5.01E+06
2/2/94	7.17E+06	7.58E+06	7.11E+06		
9/2/94	3.76E+06	1.39E+06	6.40E+05		
15/2/94	5.97E+04		7.50E+04		
24/2/94	4.55E+04	6.09E+04	8.75E+04	9.60E+04	1.71E+05
2/3/94	1.25E+05	1.57E+05	1.53E+05	1.37E+05	1.78E+05
2/4/94	3.98E+04	4.86E+04	5.74E+04	3.05E+04	3.68E+04
10/5/94	4.54E+04	4.25E+04	3.22E+04	8.82E+04	1.44E+05
9/6/94	7.74E+03	8.27E+03	7.23E+03	6.55E+03	2.31E+03
11/7/94	8.16E+03	4.71E+03	5.80E+03	5.92E+03	4.36E+03
9/8/94	2.32E+03	1.80E+03	2.01E+03	2.67E+03	2.31E+03
8/9/94	7.29E+03	1.35E+03	2.01E+03	0.00E+00	1.92E+03
7/10/94	4.07E+03	7.65E+03	6.64E+03	8.41E+02	0.00E+00
21/10/94	2.76E+05	8.98E+04	4.02E+04	1.48E+04	3.26E+03
4/11/94	2.90E+05	2.03E+05	9.48E+04	1.73E+04	3.34E+04
19/11/94	4.24E+05	2.51E+05	1.12E+05	5.57E+04	6.48E+03
28/11/94	1.80E+05	1.95E+05	1.74E+04	8.86E+04	1.47E+05
7/12/94	3.09E+04	1.64E+05	8.21E+04	1.52E+05	1.67E+05
14/12/94	3.57E+04	1.28E+05	2.20E+05	2.95E+05	5.69E+04
21/12/94	2.60E+05	3.16E+05	3.00E+05	3.39E+05	3.00E+05
28/12/94	7.08E+05	1.20E+06	2.79E+06	2.05E+06	1.95E+06
4/1/95	1.09E+07	1.08E+07	1.26E+07	1.10E+07	7.73E+06
16/1/95	3.42E+06	3.63E+06	3.85E+06	2.00E+06	1.77E+06
23/1/95	2.51E+06	2.00E+06	1.74E+06	1.31E+06	8.84E+05
30/1/95	2.93E+05	3.44E+05	3.86E+05	3.94E+05	4.02E+05
13/2/95	4.90E+06	5.12E+06	4.17E+06	4.36E+06	3.56E+06
20/2/95	2.15E+06	2.02E+06	1.87E+06	1.68E+06	1.71E+06
27/2/95	1.68E+06	2.41E+06	1.95E+06	1.96E+06	1.90E+06

Table C.4. *Phaeocystis* cf. *antarctica* cell counts (cells L^{-1}) at the O'Gorman Rocks site.

Date	Depth, m				
	0/2	5	10	15	20
22/12/93	1.38E+06	3.12E+05	6.42E+05	2.26E+05	1.52E+05
29/12/93	5.20E+06	4.20E+06	4.88E+06	5.77E+06	4.41E+06
6/1/94	3.33E+06	1.26E+06	2.07E+06	2.02E+06	2.46E+06
12/1/94	5.29E+04	1.90E+05	1.22E+05	2.17E+05	2.26E+05
19/1/94	5.14E+04	6.10E+04	7.60E+04	8.53E+04	7.25E+04

Table C.4. Continued

Date	Depth, m				
	0/2	5	10	15	20
26/1/94	8.38E+04	1.34E+05	1.60E+05	2.15E+05	1.45E+05
2/2/94	2.83E+05	2.47E+05	4.12E+05		
9/2/94	2.48E+05	5.32E+04	4.65E+04		
15/2/94	2.23E+03		4.07E+03		
24/2/94	0.00E+00	1.86E+03	2.19E+03	0.00E+00	2.62E+03
2/3/94	4.59E+02	0.00E+00	0.00E+00	3.56E+02	2.85E+02
2/4/94	1.31E+03	6.53E+02	0.00E+00	0.00E+00	4.18E+02
10/5/94	0.00E+00	0.00E+00	0.00E+00	0.00E+00	0.00E+00
9/6/94	0.00E+00	0.00E+00	0.00E+00	0.00E+00	0.00E+00
11/7/94	0.00E+00	2.69E+03	1.34E+03	0.00E+00	0.00E+00
9/8/94	0.00E+00	0.00E+00	0.00E+00	0.00E+00	0.00E+00
8/9/94	0.00E+00	0.00E+00	0.00E+00	0.00E+00	0.00E+00
7/10/94	0.00E+00	0.00E+00	0.00E+00	0.00E+00	0.00E+00
21/10/94	0.00E+00	0.00E+00	0.00E+00	0.00E+00	0.00E+00
4/11/94	0.00E+00	0.00E+00	0.00E+00	6.92E+02	0.00E+00
19/11/94	2.01E+05	1.18E+05	3.06E+04	3.71E+04	4.54E+04
28/11/94	2.91E+05	2.12E+05	3.13E+05	1.53E+05	1.56E+05
7/12/94	6.18E+04	6.14E+05	6.57E+05	3.74E+05	2.89E+05
14/12/94	3.93E+05	2.63E+05	1.32E+05	9.25E+04	1.49E+05
21/12/94	6.04E+04	1.00E+04	1.29E+05	4.40E+03	4.00E+03
28/12/94	6.25E+04	4.31E+04	4.19E+04	1.62E+04	0.00E+00
4/1/95	5.60E+04	4.17E+05	3.44E+04	2.68E+04	0.00E+00
16/1/95	2.24E+04	1.84E+04	1.45E+04	0.00E+00	2.71E+04
23/1/95	2.29E+04	0.00E+00	0.00E+00	0.00E+00	0.00E+00
30/1/95	9.03E+03	0.00E+00	0.00E+00	5.82E+03	1.16E+04
13/2/95	0.00E+00	3.44E+04	2.93E+04	0.00E+00	0.00E+00
20/2/95	5.45E+03	0.00E+00	3.71E+03	0.00E+00	0.00E+00
27/2/95	0.00E+00	0.00E+00	0.00E+00	0.00E+00	0.00E+00

Table C.5. Dinoflagellate cell counts (all species) (cells L^{-1}) at the O'Gorman Rocks site.

Date	Depth, m				
	0/2	5	10	15	20
22/12/93	9.44E+05	8.71E+04	8.30E+04	4.55E+03	3.38E+03
29/12/93	5.76E+04	4.29E+04	4.72E+03	3.24E+04	6.00E+03
6/1/94	7.78E+03	1.04E+04	7.27E+04	1.27E+04	2.69E+04
12/1/94	1.11E+04	1.29E+04	2.17E+04	6.12E+03	4.73E+03
19/1/94	6.44E+04	2.61E+04	3.18E+04	2.74E+04	1.75E+04
26/1/94	3.05E+04	6.40E+04	6.12E+04	4.24E+04	5.61E+04
2/2/94	1.48E+05	1.19E+05	1.55E+05		
9/2/94	1.10E+05	4.09E+04	9.70E+04		
15/2/94	6.91E+04		5.43E+04		
24/2/94	2.43E+04	3.88E+04	6.33E+04	6.85E+04	6.56E+04
2/3/94	3.53E+04	8.49E+03	2.48E+04	2.67E+04	2.76E+04

Table C.5. Continued

Date	Depth, m				
	0/2	5	10	15	20
2/4/94	1.83E+04	2.11E+04	2.38E+04	1.24E+04	1.04E+04
10/5/94	7.80E+03	1.52E+04	4.78E+03	9.74E+03	1.47E+04
9/6/94	5.81E+03	3.24E+03	1.22E+04	5.09E+03	7.05E+03
11/7/94	4.80E+03	5.72E+03	6.69E+03	3.19E+03	3.00E+03
9/8/94	2.98E+03	3.15E+03	2.81E+03	1.91E+03	1.92E+03
8/9/94	6.63E+03	1.13E+04	2.81E+03	1.14E+04	1.15E+04
7/10/94	3.66E+03	5.61E+03	5.31E+03	4.20E+03	4.93E+03
21/10/94	7.98E+03	5.44E+03	5.09E+03	7.87E+03	8.38E+03
4/11/94	3.01E+04	2.34E+04	2.18E+04	1.11E+04	2.54E+04
19/11/94	9.29E+05	6.34E+05	2.04E+05	1.86E+05	2.41E+04
28/11/94	4.65E+04	7.52E+04	8.10E+04	1.22E+04	2.14E+04
7/12/94	6.21E+06	5.81E+06	1.37E+06	5.45E+05	4.31E+05
14/12/94	5.36E+05	3.69E+05	2.01E+05	1.51E+05	2.99E+05
21/12/94	5.16E+05	4.05E+05	1.53E+05	6.61E+04	4.00E+04
28/12/94	1.51E+05	2.42E+05	9.77E+04	1.19E+05	5.69E+04
4/1/95	2.52E+05	1.49E+05	1.03E+05	2.95E+05	7.13E+04
16/1/95	1.34E+05	1.54E+05	1.74E+05	8.25E+04	1.08E+05
23/1/95	1.83E+05	1.59E+05	2.10E+05	1.34E+05	5.69E+04
30/1/95	1.85E+05	1.06E+05	1.08E+05	1.01E+05	9.31E+04
13/2/95	7.99E+04	1.03E+05	5.87E+04	1.32E+05	5.02E+04
20/2/95	8.71E+04	3.75E+04	3.71E+04	5.08E+04	8.95E+04
27/2/95	2.49E+04	4.49E+04	1.20E+05	6.87E+04	7.00E+04

Table C.6. *Pyramimonas gelidicola* cell counts (cells L^{-1}) at the O'Gorman Rocks site.

Date	Depth, m				
	0/2	5	10	15	20
22/12/93	1.45E+04	3.87E+03	3.79E+03	2.39E+02	0.00E+00
29/12/93	1.27E+04	3.98E+03	2.45E+03	7.66E+03	1.20E+03
6/1/94	1.30E+03	0.00E+00	0.00E+00	7.04E+02	7.00E+02
12/1/94	0.00E+00	0.00E+00	0.00E+00	0.00E+00	0.00E+00
19/1/94	0.00E+00	0.00E+00	0.00E+00	0.00E+00	0.00E+00
26/1/94	0.00E+00	0.00E+00	0.00E+00	0.00E+00	0.00E+00
2/2/94	0.00E+00	0.00E+00	0.00E+00		
9/2/94	3.23E+03	5.60E+03	2.73E+03		
15/2/94	5.58E+02		1.74E+03		
24/2/94	0.00E+00	0.00E+00	0.00E+00	0.00E+00	0.00E+00
2/3/94	0.00E+00	0.00E+00	0.00E+00	0.00E+00	0.00E+00
2/4/94	0.00E+00	0.00E+00	0.00E+00	0.00E+00	0.00E+00
10/5/94	0.00E+00	0.00E+00	0.00E+00	0.00E+00	0.00E+00
9/6/94	0.00E+00	0.00E+00	0.00E+00	0.00E+00	0.00E+00
11/7/94	0.00E+00	0.00E+00	0.00E+00	0.00E+00	0.00E+00
9/8/94	0.00E+00	0.00E+00	0.00E+00	0.00E+00	0.00E+00
8/9/94	0.00E+00	0.00E+00	0.00E+00	0.00E+00	0.00E+00

Table C.6. Continued

Date	Depth, m				
	0/2	5	10	15	20
7/10/94	0.00E+00	0.00E+00	0.00E+00	0.00E+00	0.00E+00
21/10/94	0.00E+00	0.00E+00	0.00E+00	0.00E+00	0.00E+00
4/11/94	0.00E+00	0.00E+00	0.00E+00	0.00E+00	0.00E+00
19/11/94	0.00E+00	0.00E+00	0.00E+00	0.00E+00	0.00E+00
28/11/94	0.00E+00	0.00E+00	0.00E+00	0.00E+00	0.00E+00
7/12/94	0.00E+00	0.00E+00	0.00E+00	0.00E+00	0.00E+00
14/12/94	0.00E+00	0.00E+00	0.00E+00	0.00E+00	0.00E+00
21/12/94	0.00E+00	0.00E+00	0.00E+00	0.00E+00	0.00E+00
28/12/94	5.21E+03	0.00E+00	0.00E+00	1.08E+04	0.00E+00
4/1/95	3.36E+05	1.79E+05	0.00E+00	5.37E+04	7.13E+04
16/1/95	4.77E+03	2.50E+03	0.00E+00	5.16E+03	1.08E+04
23/1/95	1.70E+05	2.01E+05	3.24E+04	5.00E+04	6.21E+04
30/1/95	1.72E+05	1.88E+05	1.74E+05	1.20E+05	8.15E+04
13/2/95	1.49E+06	1.17E+06	3.52E+05	9.52E+05	5.77E+05
20/2/95	8.50E+05	6.67E+05	5.71E+05	2.54E+05	2.72E+05
27/2/95	3.64E+05	3.64E+05	7.98E+04	2.99E+05	2.80E+05

APPENDIX D

O'GORMAN ROCKS: CHEMICAL AND PHYSICAL DATA

Presented in this appendix are tables of chemical and physical data recorded in the water column at the O'Gorman Rocks site between December 1993 and February 1995.

Table D.1. Temperature, salinity and concentrations of nitrate, phosphate, silicate and dissolved oxygen at the O'Gorman Rocks site.

Date	Depth m	Temp ℃	Salinity psu	$NO_3^{-(1)}$ µmol kg^{-1}	PO_4^{3-} µmol kg^{-1}	H_4SiO_4 µmol kg^{-1}	O_2 µmol kg^{-1}
22/12/93	2	-0.89	33.66	8.5	0.93	41.2	
22/12/93	5	-0.56	33.84	17.3	1.26	46.0	480
22/12/93	10	-1.09	34.03	23.9	1.54	45.9	400
22/12/93	15	-1.20	33.96	24.8	1.63	52.0	
22/12/93	20	-1.26	33.97	23.4	1.61	50.1	371
29/12/93	0	0.04	33.39	13.0	1.06	48.5	419
29/12/93	5	-0.27	33.45	13.0	1.08	56.6	429
29/12/93	10	-0.38	33.54	12.5	1.07	49.2	439
29/12/93	15	-1.00	33.64	13.0	1.21	42.5	440
29/12/93	20	-0.96	33.69	17.1	1.44	35.6	416
6/1/94	0	-1.13	33.60	17.2	1.34	51.6	380
6/1/94	5	-1.16	33.49	17.1	1.31	48.1	381
6/1/94	10	-1.16	33.43	17.7	1.32	54.7	380
6/1/94	15	-1.12	33.48	17.5	1.35	53.1	375
6/1/94	20	-1.16	33.48	17.5	1.32	54.3	347
12/1/94	0	-0.40	33.37	11.5	0.88	47.6	411
12/1/94	5	-0.09	33.16	11.4	0.87	53.0	417
12/1/94	10	-0.66	33.23	10.5	0.80	49.6	429
12/1/94	15	-0.93	33.32	15.4	1.11	50.4	406
12/1/94	20	-1.13	33.44	18.3	1.38	51.1	377
19/1/94	0	-0.88	33.04	9.5	0.72	43.0	412
19/1/94	5	-0.86	32.86	9.3	0.77	41.0	407
19/1/94	10	-0.88	32.88	7.5	0.62	33.6	413
19/1/94	15	-1.20	33.09	10.6	0.84	41.6	396
19/1/94	20	-1.16	33.14	13.8	1.07	40.6	380
26/1/94	0	-0.66	32.30	0.3	0.55	41.7	458
26/1/94	5	-0.39	32.55	0.4	0.53	39.4	457
26/1/94	10	-0.70	32.79	1.7	0.51	40.8	436
26/1/94	15	-0.88	32.98	4.9	0.66	41.8	419

Table D.1. Continued

Date	Depth m	Temp ℃	Salinity psu	NO_3^- µmol kg^{-1}	PO_4^{3-} µmol kg^{-1}	H_4SiO_4 µmol kg^{-1}	O_2 µmol kg^{-1}
26/1/94	20	-1.14	33.22	10.9	1.11	47.1	382
2/2/94	0	-0.82	32.88	4.4	0.61	40.0	408
2/2/94	5	-0.84	32.85	4.0	0.56	39.4	410
2/2/94	10	-0.83	32.83				407
2/2/94	15	-0.87	32.87				
2/2/94	20	-1.01	33.02				
9/2/94	0	-1.14	32.94	5.1	0.79	45.3	395
9/2/94	5	-1.13	32.90	9.2	0.83	40.9	379
9/2/94	10	-1.16	32.93	11.6	1.00	48.0	348
9/2/94	15	-1.18	32.95				
9/2/94	20	-1.18	32.95				
16/2/94	0	-1.26	33.06	15.3	1.38	39.4	356
16/2/94	5	-1.30	33.04				
16/2/94	10	-1.28	33.08				
16/2/94	15	-1.30	33.10				
16/2/94	20	-1.31	33.10				
24/2/94	0	-1.48	33.19	14.3	1.21	40.4	284
24/2/94	5	-1.47	33.18	15.3	1.21	41.6	311
24/2/94	10	-1.40	33.22	16.6	1.30	43.6	307
24/2/94	15	-1.42	33.24	17.1	1.29	41.4	338
24/2/94	20	-1.43	33.25	16.5	1.30	27.0	314
2/3/94	0	-1.63	33.20	16.3	1.23	40.7	345
2/3/94	5	-1.62	33.25	16.9	1.26	40.3	349
2/3/94	10	-1.62	33.24	16.5	1.31	38.3	376
2/3/94	15	-1.61	33.26	16.7	1.26	41.5	365
2/3/94	20	-1.61	33.23	17.1	1.31	35.4	379
2/4/94	2	-1.82	33.27	22.3	1.55	46.0	351
2/4/94	5	-1.82	33.42	21.9	1.57	38.7	343
2/4/94	10	-1.82	33.50	22.4	1.54	44.5	345
2/4/94	15	-1.82	33.49	22.6	1.55	38.2	349
2/4/94	20	-1.82	33.49	23.0	1.46	36.5	347
10/5/94	2	-1.89	33.35	24.1	2.01	44.7	332
10/5/94	5	-1.88	33.48	24.4	1.89	46.1	322
10/5/94	10	-1.88	33.57	24.1	1.92	47.1	324
10/5/94	15	-1.87	33.55	24.1	1.93	48.1	315
10/5/94	20	-1.88	33.66	24.1	1.94	49.6	330
9/6/94	2	-1.90	33.42	24.5	2.08	48.3	328
9/6/94	5	-1.89	33.52	24.9	2.05	51.2	322
9/6/94	10	-1.89	33.60	25.1	2.08	50.7	323
9/6/94	15	-1.89	33.66	24.8	2.02	49.7	327
9/6/94	20	-1.88	33.79	24.9	2.01	49.6	322
11/7/94	2	-1.88	33.49	25.4	1.95	51.4	322
11/7/94	5	-1.87	33.56	25.4	2.08	54.0	316
11/7/94	10	-1.88	33.64	25.2	1.99	53.9	316
11/7/94	15	-1.89	33.77	25.2	2.12	54.1	317
11/7/94	20	-1.89	33.91	25.3	2.15	54.9	300
9/8/94	2	-1.90	32.72	25.8	1.88	61.6	325
9/8/94	5	-1.90	33.84	26.1	1.90	59.7	317
9/8/94	10	-1.89	33.92	26.3	1.91	59.0	315
9/8/94	15	-1.90	34.03	26.0	1.92	59.4	325
9/8/94	20	-1.90	34.03	26.5	1.89	59.5	301
8/9/94	2	-1.91	33.61	24.9	1.92	59.9	312
8/9/94	5	-1.91	33.78	26.7	1.96	63.6	306

Table D.1. Continued

Date	Depth m	Temp ℃	Salinity psu	NO_3^- µmol kg^{-1}	PO_4^{3-} µmol kg^{-1}	H_4SiO_4 µmol kg^{-1}	O_2 µmol kg^{-1}
8/9/94	10	-1.90	33.93	26.7	1.98	62.7	296
8/9/94	15	-1.90	34.03	26.7	1.96	62.5	300
8/9/94	20	-1.90	34.08	26.8	1.97	62.5	303
7/10/94	2	-1.89	34.43	27.3	2.04	65.7	324
7/10/94	5	-1.89	34.13	27.5	1.98	64.5	297
7/10/94	10	-1.90	33.99	27.6	2.07	66.8	322
7/10/94	15	-1.89	34.08	27.9	2.00	67.2	321
7/10/94	20	-1.90	34.13	27.5	1.94	66.5	313
21/10/94	2	-1.86	34.98	21.9	1.98	62.5	330
21/10/94	5	-1.88	34.11	27.0	1.95	64.0	321
21/10/94	10	-1.89	33.92	25.7	1.94	65.3	326
21/10/94	15	-1.89	34.02	25.5	1.95	64.3	312
21/10/94	20	-1.89	34.02	25.4	1.95	65.3	317
4/11/94	2	-1.86	34.49	26.9	1.89	65.5	322
4/11/94	5	-1.87	34.25	25.2	1.88	62.7	327
4/11/94	10	-1.87	34.06	26.5	1.89	64.4	317
4/11/94	15	-1.88	33.96	26.7	1.88	63.8	329
4/11/94	20	-1.85	34.03	22.0	1.71	52.9	325
19/11/94	2	-1.77	33.99	22.1	1.67	59.7	354
19/11/94	5	-1.79	33.97	24.4	1.74	61.2	338
19/11/94	10	-1.82	33.94	23.9	1.82	61.6	337
19/11/94	15	-1.83	33.95	25.5	1.90	62.3	339
19/11/94	20	-1.77	33.93	24.9	1.87	60.2	340
28/11/94	2	-1.57	34.13	21.4	1.62	59.0	364
28/11/94	5	-1.56	33.96	23.4	1.61	58.9	363
28/11/94	10	-1.65	33.83	23.1	1.63	59.5	366
28/11/94	15	-1.70	33.88	23.1	1.64	58.6	368
28/11/94	20	-1.77	33.87	22.6	1.71	58.3	366
7/12/94	2	-1.59	34.28	7.5	0.98	50.8	519
7/12/94	5	-1.61	33.95	9.1	1.57	57.2	420
7/12/94	10	-1.63	33.72	9.7	1.67	57.0	441
7/12/94	15	-1.66	33.81	17.2	1.52	62.4	400
7/12/94	20	-1.57	33.81	18.9	1.53	61.5	378
14/12/94	2	-1.39	33.51	2.6	0.59	44.4	520
14/12/94	5	-1.48	33.85	19.0	1.15	51.7	385
14/12/94	10	-1.56	33.74	19.9	1.40	54.7	380
14/12/94	15	-1.63	33.68	19.4	1.63	60.7	349
14/12/94	20	-1.64	33.79	23.9	1.87	64.6	331
21/12/94	2	-0.69	33.97	0.1	0.49	22.9	478
21/12/94	5	-0.52	34.06	9.8	0.73	28.9	398
21/12/94	10	-1.12	33.68	6.2	0.99	38.0	405
21/12/94	15	-1.32	33.67	15.2	1.06	43.3	407
21/12/94	20	-1.44	33.70	15.7	1.58	54.3	362
28/12/94	2	0.12	34.22	0.4	0.39	26.5	376
28/12/94	5	-0.32	34.16	0.1	0.54	41.1	511
28/12/94	10	-0.63	33.70	5.3	1.08	44.7	506
28/12/94	15	-0.79	33.70	10.0	1.74	44.4	425
28/12/94	20	-1.13	33.83	11.4	1.43	46.0	400
4/1/95	2	0.58	33.11	0.2	0.54	13.3	540
4/1/95	5	0.51	33.47	0.3	0.46	19.4	516
4/1/95	10	0.41	33.48	5.8	0.63	23.4	426
4/1/95	15	0.18	33.54	7.0	0.81	28.4	434
4/1/95	20	-0.55	33.66	8.1	0.52	35.5	422

Table D.1. Continued

Date	Depth m	Temp ℃	Salinity psu	NO_3^- µmol kg^{-1}	PO_4^{3-} µmol kg^{-1}	H_4SiO_4 µmol kg^{-1}	O_2 µmol kg^{-1}
16/1/95	0	1.43	32.67	7.5	0.67	29.7	401
16/1/95	5	0.87	32.95	7.3	0.67	27.1	393
16/1/95	10	0.16	33.12	7.5	0.84	28.1	408
16/1/95	15	-0.14	33.21	9.9	0.96	30.4	376
16/1/95	20	-0.27	33.30	9.2	0.97	31.8	375
23/1/95	0	-0.02	32.86	6.3	1.08	32.1	378
23/1/95	5	-0.08	32.96	3.9	0.90	32.1	365
23/1/95	10	-0.14	33.08	7.8	0.77	35.5	364
23/1/95	15	-0.22	33.11	9.3	1.17	35.4	337
23/1/95	20	-0.27	33.22	11.4	1.34	37.3	334
30/1/95	0	-0.74	32.64	14.1	1.32	34.0	335
30/1/95	5	-0.75	32.51	13.8	1.32	39.4	334
30/1/95	10	-0.74	32.64	14.6	1.37	39.3	343
30/1/95	15	-0.61	32.82	14.0	1.40	39.7	336
30/1/95	20	-0.57	32.97	14.3	1.42	40.6	321
13/2/95	0	0.06	31.94	1.7	0.43	47.3	456
13/2/95	5	0.08	32.09	1.5	0.43	47.5	465
13/2/95	10	-0.47	32.67	7.1	0.65	50.6	436
13/2/95	15	-0.51	32.81	6.2	0.82	51.1	384
13/2/95	20	-0.52	32.91	12.2	0.49	47.4	367
20/2/95	0	-0.71	32.47	10.1	0.79	54.4	398
20/2/95	5	-0.75	32.49	11.4	0.81	53.8	394
20/2/95	10	-0.85	32.76	13.3	1.04	58.5	381
20/2/95	15	-0.89	32.80	18.6	1.22	60.3	372
20/2/95	20	-0.89	32.89	18.5	1.22	58.4	359
27/2/95	0	-1.61	32.60	8.7	0.71	50.5	388
27/2/95	5	-1.63	32.62	10.1	0.76	51.6	396
27/2/95	10	-1.34	32.88	15.6	0.88	54.9	374
27/2/95	15	-1.27	32.98	13.1	1.09	56.7	361
27/2/95	20	-1.27	33.17	19.3	1.28	59.5	346

1. The concentration given for nitrate is actually the sum of the concentrations of nitrate and nitrite, as the method used for this analysis did not discriminate between these species (Appendix A).

Table D.2. Further chemical parameters for samples from the O'Gorman Rocks Site. Chl *a*, pH_f and DIC were measured experimentally, while $[CO_{2(aq)}]$ fCO_2 and Alk_T were calculated as described in Appendix A.

Date	Depth m	Chl *a* mg m^{-3}	pH_f	DIC µmol kg^{-1}	$[CO_{2(aq)}]$ µmol kg^{-1}	fCO_2 µatm	Alk_T µeq kg^{-1}
22/12/93	2	3.19	8.13	1718	5.2	79	2058
22/12/93	5	1.84	7.85	1938	12.5	193	2133
22/12/93	10	1.42	7.76	2177	17.2	261	2346
22/12/93	15	1.71	7.75	2173	17.9	270	2334
22/12/93	20	1.18	7.74	2181	18.2	273	2341
29/12/93	0	4.77	7.93	2093	10.8	170	2344
29/12/93	5	5.03	7.93	2097	10.8	167	2359
29/12/93	10	4.72	7.94	2096	10.4	132	2354
29/12/93	15	6.63	7.94	2107	10.5	159	2364
29/12/93	20	6.56	7.89	2121	11.9	181	2353
6/1/94	0	4.45	7.85	2103	13.3	201	2308
6/1/94	5	4.17	7.84	2107	13.6	205	2309
6/1/94	10	4.23	7.84	2108	13.6	204	2310
6/1/94	15	4.26	7.85	2109	13.2	199	2317
6/1/94	20	4.35	7.84	2109	13.7	207	2309
12/1/94	0	5.65	7.94	2039	10.4	161	2287
12/1/94	5	4.90	7.94	2046	10.5	164	2294
12/1/94	10	7.66	7.96	2039	9.8	151	2297
12/1/94	15	8.08	7.90	2082	11.7	178	2310
12/1/94	20	4.69	7.80	2121	15.1	228	2304
19/1/94	0	10.48	7.95	2032	9.8	150	2287
19/1/94	5	11.21	7.95	2034	10.1	153	2284
19/1/94	10	11.30	7.93	2040	10.4	158	2283
19/1/94	15	10.56	7.93	2093	10.8	163	2337
19/1/94	20	7.16	7.85	2092	13.3	199	2295
26/1/94	0	15.68	8.13	1938	5.9	91	2293
26/1/94	5	16.96	8.12	1943	6.2	96	2290
26/1/94	10	17.56	8.09	2009	6.8	104	2348
26/1/94	15	16.09	8.01	2004	8.3	126	2291
26/1/94	20	9.98	7.87	2091	12.6	189	2304
2/2/94	0	13.59	7.98	2005	9.0	137	2274
2/2/94	5	14.53	7.96	2007	9.6	146	2262
2/2/94	10	13.61					
2/2/94	15						
2/2/94	20						
9/2/94	0	6.65	7.98	2024	9.2	138	2292
9/2/94	5	4.52	7.91	2050	11.0	165	2282
9/2/94	10	2.48	7.89				
9/2/94	15						
9/2/94	20						
16/2/94	0	0.62	7.83				
16/2/94	5						
16/2/94	10	0.44					
16/2/94	15						
16/2/94	20						
24/2/94	0	0.11	7.87	2080	12.5	186	2291
24/2/94	5	0.10	7.86	2088	12.8	189	2297

Table D.2. Continued

Date	Depth	Chl *a*	pH_f	DIC	$[CO_{2(aq)}]$	fCO_2	Alk_T
	m	mg m^{-3}		µmol kg^{-1}	µmol kg^{-1}	µatm	µeq kg^{-1}
24/2/94	10	0.12	7.85	2110	13.2	196	2316
24/2/94	15	0.15	7.84	2109	13.6	202	2309
24/2/94	20	0.27	7.82	2150	14.5	216	2344
2/3/94	0	0.13	7.85	2091	13.1	193	2295
2/3/94	5	0.14	7.86	2094	12.8	189	2303
2/3/94	10	0.14	7.86	2094	13.0	191	2301
2/3/94	15	0.13	7.85	2095	13.1	193	2300
2/3/94	20	0.14	7.86	2094	12.7	188	2304
2/4/94	2	0.24	7.77				
2/4/94	5	0.30	7.70	2139	19.7	288	2277
2/4/94	10	0.28	7.72	2156	18.9	277	2303
2/4/94	15	0.24	7.75	2160	17.6	259	2317
2/4/94	20	0.33	7.75				
10/5/94	2	0.16	7.67	2195	21.8	319	2323
10/5/94	5	0.13	7.68	2185	21.2	310	2317
10/5/94	10	0.13	7.68	2181	21.5	315	2310
10/5/94	15	0.13	7.68	2190	21.6	316	2320
10/5/94	20	0.14	7.67	2188	21.8	319	2316
9/6/94	2	0.14	7.66	2194	22.6	330	2317
9/6/94	5	0.19	7.67				
9/6/94	10	0.14	7.66	2191	22.3	327	2315
9/6/94	15	0.14	7.66	2126	21.7	318	2248
9/6/94	20	0.16	7.66	2146	22.3	327	2266
11/7/94	2	0.14	7.64	2255	24.6	361	2370
11/7/94	5	0.16	7.65	2209	23.0	346	2326
11/7/94	10	0.13	7.63	2193	24.3	355	2305
11/7/94	15	0.13	7.65	2194	23.3	341	2313
11/7/94	20	0.13	7.61	2210	25.8	348	2315
9/8/94	2	0.15	7.65	2230	24.0	349	2344
9/8/94	5	0.10	7.64				
9/8/94	10	0.08	7.65	2221	23.5	345	2341
9/8/94	15	0.09	7.62	2223	25.6	375	2331
9/8/94	20	0.10	7.63	2230	24.9	365	2343
8/9/94	2	0.18	7.63	2239	25.0	366	2351
8/9/94	5	0.13	7.63	2227	24.6	360	2341
8/9/94	10	0.10	7.63	2220	24.7	362	2333
8/9/94	15	0.10	7.63	2198	24.3	357	2311
8/9/94	20	0.09	7.63	2228	24.9	365	2341
7/10/94	2	0.08	7.63	2233	24.9	366	2347
7/10/94	5	0.12	7.64	2228	24.1	353	2346
7/10/94	10	0.13	7.64	2221	23.7	347	2340
7/10/94	15	0.10	7.64	2230	24.0	353	2348
7/10/94	20	0.09	7.64	2234	24.4	358	2351
21/10/94	2	0.86	7.64	2197	23.4	346	2318
21/10/94	5	1.17	7.65	2226	23.5	345	2348
21/10/94	10	0.76	7.65	2228	23.3	341	2351
21/10/94	15	0.36	7.66	2226	22.6	332	2353
21/10/94	20	0.55	7.65	2223	23.5	344	2344
4/11/94	2	1.59	7.67	2218	21.7	320	2352
4/11/94	5	1.91	7.66	2217	23.0	338	2341
4/11/94	10	0.52	7.66	2219	23.0	338	2343
4/11/94	15	0.36	7.65	2220	23.6	346	2340
4/11/94	20	0.25	7.65	2220	23.2	342	2342

Table D.2. Continued

Date	Depth m	Chl *a* mg m^{-3}	pH_f	DIC µmol kg^{-1}	$[CO_{2(aq)}]$ µmol kg^{-1}	fCO_2 µatm	Alk_T µeq kg^{-1}
19/11/94	2	4.16	7.78	2141	15.9	235	2318
19/11/94	5	2.46	7.77	2165	16.8	247	2335
19/11/94	10	1.80	7.74	2198	18.2	268	2358
19/11/94	15	0.54	7.75				
19/11/94	20	0.75	7.75	2196	17.7	260	2361
28/11/94	2	1.73	7.75	2162	17.5	261	2326
28/11/94	5	1.70	7.77	2166	16.5	245	2341
28/11/94	10	1.57	7.76	2175	17.3	256	2341
28/11/94	15	2.01	7.76	2175	17.2	254	2342
28/11/94	20	1.66	7.75	2179	17.4	256	2344
7/12/94	2	23.71	8.22	1980	4.6	69	2429
7/12/94	5	16.76	8.08	2096	7.0	105	2451
7/12/94	10	13.99	8.13	2120	6.3	93	2512
7/12/94	15	3.66	7.94	2108	10.4	153	2367
7/12/94	20	2.38	8.00	2151	8.9	133	2455
14/12/94	2	2.26	8.23	1959	4.5	67	2405
14/12/94	5	0.44	7.96	2160	10.0	149	2438
14/12/94	10	1.88	7.80	2152	15.2	225	2339
14/12/94	15	1.94	7.82	2179	14.8	218	2375
14/12/94	20	2.21	7.75	2196	17.8	264	2359
21/12/94	2	8.96	8.30				
21/12/94	5	3.68	8.59				
21/12/94	10	5.47	8.44				
21/12/94	15	1.64	8.47				
21/12/94	20	3.78	8.40				
28/12/94	2	1.10	8.25	1592	3.5	56	2006
28/12/94	5	12.53	8.29	1406	2.8	44	1811
28/12/94	10	9.31	8.21	2072	5.0	77	2526
28/12/94	15	14.01	8.04	2107	8.1	123	2430
28/12/94	20	9.40	7.99	2129	9.2	139	2422
4/1/95	2	8.15	8.04	1963	7.8	126	2263
4/1/95	5	6.52	8.01	2010	8.6	137	2301
4/1/95	10	14.12	7.96	2069	10.0	160	2335
4/1/95	15	11.91	7.89	2075	12.0	191	2300
4/1/95	20	11.03	7.85	2086	13.1	202	2294
16/1/95	0	5.44	8.02	2013	8.6	142	2303
16/1/95	5	6.51	8.01	2021	8.7	142	2308
16/1/95	10	7.38	8.01	2061	8.9	140	2351
16/1/95	15	6.21	7.92	2073	11.0	172	2315
16/1/95	20	7.80	7.97	2063	9.7	151	2331
23/1/95	0	5.44	7.90	2044	11.5	181	2269
23/1/95	5	5.94	7.91	2090	11.6	182	2322
23/1/95	10	3.66	7.90	2070	11.8	184	2296
23/1/95	15	3.50	7.89	2057	12.1	188	2276
23/1/95	20	2.47	7.82	2101	14.7	229	2288
30/1/95	0	1.34	7.81	2083	14.7	224	2264
30/1/95	5	1.40	7.83	2084	14.1	214	2272
30/1/95	10	1.25	7.68	2080	21.0	321	2201
30/1/95	15	1.18	7.80	2102	15.4	235	2279
30/1/95	20	1.33	7.81	2105	15.1	232	2286
13/2/95	0	12.43	8.06	1947	7.3	114	2251
13/2/95	5	14.71	8.07	1942	7.1	111	2254
13/2/95	10	13.98	8.02	2017	8.4	129	2306

Table D.2. Continued

Date	Depth m	Chl *a* mg m^{-3}	pH_f	DIC µmol kg^{-1}	$[CO_{2(aq)}]$ µmol kg^{-1}	fCO_2 µatm	Alk_T µeqkg^{-1}
13/2/95	15	9.77	7.92	2045	11.0	169	2279
13/2/95	20	4.13	7.84	2092	13.7	211	2289
20/2/95	0	7.95	7.89	2019	11.6	176	2236
20/2/95	5	9.58	8.00	2022	8.7	133	2300
20/2/95	10	8.96	8.00	2064	8.9	135	2348
20/2/95	15	6.94	7.96	2054	9.8	149	2312
20/2/95	20	6.07	7.93	2090	10.7	162	2337
27/2/95	0	7.43	7.91	2035	11.0	162	2262
27/2/95	5	9.13	7.94	2036	10.1	149	2281
27/2/95	10	8.63	7.86	2073	12.8	191	2278
27/2/95	15	4.78	7.84	2082	13.4	200	2280
27/2/95	20	5.83	7.85	2071	13.1	196	2273

Table D.3. Concentrations of DOC, POC and total organic carbon at the O'Gorman Rocks site.

Date	Depth m	DOC µmol kg^{-1}	POC µmol kg^{-1}	Total µmol kg^{-1}
4/11/94	2	80	10	90
4/11/94	5	90	10	100
4/11/94	10	69	6	75
4/11/94	15	91	7	98
4/11/94	20	77	0	77
19/11/94	2	89	30	119
19/11/94	5	94	12	106
19/11/94	10	72	7	78
19/11/94	15	105	0	105
19/11/94	20	83	1	84
28/11/94	2	73	18	91
28/11/94	5	57	14	71
28/11/94	10	67	10	77
28/11/94	15	69	10	79
28/11/94	20	74	12	86
7/12/94	2	157	563	720
7/12/94	5	103	345	449
7/12/94	10	146	165	311
7/12/94	15	86	29	115
7/12/94	20	85	30	115
14/12/94	2	119	105	224
14/12/94	5	72	22	95
14/12/94	10	71	15	86
14/12/94	15	67	3	71
14/12/94	20	63	13	77
21/12/94	2	106	85	191
21/12/94	5	67	39	107
21/12/94	10	65	24	89
21/12/94	15	77	20	97
21/12/94	20	62	18	80

Table D.3. Continued

Date	Depth m	DOC μmol kg^{-1}	POC μmol kg^{-1}	Total μmol kg^{-1}
28/12/94	2	102	18	121
28/12/94	5	86	36	122
28/12/94	10	80	28	108
28/12/94	15	79	23	102
28/12/94	20	78	9	87
4/1/95	2	102	73	176
4/1/95	5	67	60	127
4/1/95	10	86	60	145
4/1/95	15	53	55	108
4/1/95	20	58	39	97
16/1/95	0	78	25	104
16/1/95	5	69	25	94
16/1/95	10	74	32	106
16/1/95	15	67	32	99
16/1/95	20	71	16	87
23/1/95	0	70	20	90
23/1/95	5	79	21	100
23/1/95	10	78	15	93
23/1/95	15	70	7	77
23/1/95	20	75	7	82
30/1/95	0	74	11	84
30/1/95	5	76	18	94
30/1/95	10	71	15	86
30/1/95	15	72	8	80
30/1/95	20	65	5	71
13/2/95	0	78	20	98
13/2/95	5	69	37	106
13/2/95	10	69	26	96
13/2/95	15	75	27	102
13/2/95	20	67	17	84

Table D.4. $\delta^{13}C_{DIC}$ and $\Delta^{14}C_{DIC}$ at the O'Gorman Rocks site. Also given are the estimated 1σ counting error in the $\Delta^{14}C_{DIC}$ value and the ANSTO sample number. All samples were collected from 10 m.

Date	$\delta^{13}C_{DIC}$ ‰	$\Delta^{14}C_{DIC}$ ‰	Error ‰	ANSTO sample no.
10/5/94	1.10	-93.0	6.8	OZB367U
9/6/94	0.92	-91.7	4.6	OZB368U
10/7/94	1.01	-86.4	5.2	OZB369U
9/8/94	0.25	-87.2	6.9	OZB370U
8/9/94	-0.27	-108.4	4.6	OZB371U
7/10/94	0.63	-104.3	7.5	OZB372U
21/10/94	0.85			
4/11/94	0.92			
19/11/94	0.81	-107.6	6.1	OZB537U
28/11/94	1.23			
7/12/94	1.61	-107.5	6.5	OZB538U

Table D.4. Continued

Date	$\delta^{13}C_{DIC}$ ‰	$\Delta^{14}C_{DIC}$ ‰	Error ‰	ANSTO sample no.
14/12/94	1.07			
4/1/95	1.98			
16/1/95	2.22	-110.8	3.8	OZB539U
23/1/95	1.83			
13/2/95	2.16			
27/2/95	1.90			

APPENDIX E

O'GORMAN ROCKS: SEDIMENT TRAP AND CORE DATA

This appendix gives the results of the sediment trap study carried out at the O'Gorman Rocks site. Data from the short sediment core collected at the same site are also presented.

Table E.1. Sediment flux and chemical data for the sediment trap array positioned at the O'Gorman Rocks site. The C:N mole ratio and $\delta^{13}C$ are for the organic fraction of the sediment trap material.

Trap deploy-ment date	Trap recovery date	Trap days	Depth m	Total flux mg m^{-2} day^{-1}	Carbon flux mg m^{-2} day^{-1}	C:N mole ratio	$\delta^{13}C$ ‰
2/4/94	10/5/94	38	5	136	9.0	7.6	
2/4/94	10/5/94	38	10	152	8.4		
2/4/94	10/5/94	38	15	138	9.2	7.8	-19.45
2/4/94	10/5/94	38	20	185	14.5	8.5	-19.33
10/5/94	9/6/94	30	5	86	9.1		
10/5/94	9/6/94	30	10	168	13.3		
10/5/94	9/6/94	30	15	147	11.8	8.3	-20.59
10/5/94	9/6/94	30	20	177	10.1		
9/6/94	11/7/94	32	5	182	11.0		
9/6/94	11/7/94	32	10	158	1.9	8.7	
9/6/94	11/7/94	32	15	166	9.1	8.9	-20.19
9/6/94	11/7/94	32	20	248	16.8	8.3	-20.83
11/7/94	9/8/94	29	5	152	9.8	9.0	-21.24
11/7/94	9/8/94	29	10	136	7.6		
11/7/94	9/8/94	29	15	126	7.2		
11/7/94	9/8/94	29	20	181	11.3		
9/8/94	8/9/94	30	5	36	0.9	13.7	-22.45
9/8/94	8/9/94	30	10	73	2.3	9.6	-21.22
9/8/94	8/9/94	30	15	76	2.7	9.6	
9/8/94	8/9/94	30	20	166	8.6	7.9	-19.25
8/9/94	7/10/94	29	5	29	2.4	10.8	-23.49
8/9/94	7/10/94	29	10	48	2.4		
8/9/94	7/10/94	29	15	73	6.0		
8/9/94	7/10/94	29	20	111	8.7		
7/10/94	4/11/94	28	5	103	13.9	9.1	-16.23

Table E.1. Continued

Trap deploy-ment date	Trap recovery date	Trap days	Depth m	Total flux mg m^{-2} day^{-1}	Carbon flux mg m^{-2} day^{-1}	C:N mole ratio	$\delta^{13}C$ ‰
7/10/94	4/11/94	28	10	103	9.6	8.3	-13.67
7/10/94	4/11/94	28	15	38	2.9	10.2	-18.96
7/10/94	4/11/94	28	20	125	12.3	8.5	-15.80
4/11/94	19/11/94	15	5	209	28.2	8.5	-13.53
4/11/94	19/11/94	15	10	231	28.7	8.8	-13.36
4/11/94	19/11/94	15	15	224	27.3	9.2	
4/11/94	19/11/94	15	20	239	23.6	8.9	-12.32
19/11/94	7/12/94	18	5	507	86.3	8.2	-16.26
19/11/94	7/12/94	18	10	472	77.3	7.7	-17.39
19/11/94	7/12/94	18	15	460	70.9	7.5	-16.24
19/11/94	7/12/94	18	20	453	71.2	6.9	-19.01
7/12/94	14/12/94	7	10	540	79.9	7.8	-20.87
7/12/94	14/12/94	7	15	570	85.8	7.0	-20.08
7/12/94	14/12/94	7	20	568	77.3	6.6	-22.47
14/12/94	21/12/94	7	10	366	42.2	6.8	-19.61
14/12/94	21/12/94	7	15	361	58.9	7.5	-19.97
14/12/94	21/12/94	7	20	347	57.3	6.6	-21.10
21/12/94	28/12/94	7	10	628	63.6	6.8	-19.48
28/12/94	4/1/95	7	10	1530	144.1	6.2	-18.98
4/1/95	8/1/95	4	10	2557	161.0	6.5	
16/1/95	30/1/95	14	10	238	25.3	8.5	-19.98
30/1/95	13/2/95	14	15	488	60.6	6.9	
30/1/95	13/2/95	14	20	673	61.8	6.9	-18.16
13/2/95	27/2/95	14	15	678	42.2	7.4	-17.75
13/2/95	27/2/95	14	20	1378	115.3	7.1	-18.79

Table E.2. Chemical characteristics of the short sediment core recovered from the O'Gorman Rocks site. The C:N mole ratio and the $\delta^{13}C$ are for the organic fraction of the core.

Segment depth, cm	% Water	% C organic	% C inorganic	C:N mole ratio	$\delta^{13}C$ ‰
0-1	85.4	2.99	0.08	7.3	-19.40
1-2	76.2	2.82	0.01	7.5	-19.57
2-3	74.0	3.01	0.00	7.3	-18.82
3-4	72.9	3.17	0.00	7.4	-19.18
4-5	71.2	2.97	0.04	7.5	-19.30
5-6	68.8	2.96	0.37	7.2	-19.42
6-7	70.8	3.11	0.26	7.4	-19.44
7-8	70.0	2.49	0.36	7.1	-19.73
8-9	68.0	2.03	0.51	6.2	-19.86
9-10	66.1	2.27	0.61	7.1	-19.46
10-13	65.7	2.12	0.44	6.5	-19.22

APPENDIX F

ELLIS FJORD: CHEMICAL AND PHYSICAL DATA

This appendix presents tables of chemical and physical data recorded in the water column at the Ellis Fjord site between May 1994 and February 1995.

Table F.1. Temperature, salinity and concentrations of nitrate, phosphate, silicate and dissolved oxygen at the Ellis Fjord site.

Date	Depth m	Temp ℃	Salinity psu	$NO_3^{-(1)}$ µmol kg^{-1}	PO_4^{3-} µmol kg^{-1}	H_4SiO_4 µmol kg^{-1}	O_2 µmol kg^{-1}
7/5/94	2	-1.27	33.67	8.3	1.62	40.5	445
7/5/94	5	-1.56	33.65	7.3	1.63	37.3	388
7/5/94	10	-1.67	33.74	10.7	1.80	37.5	333
7/5/94	20	-1.70	33.74	8.6	1.82	37.5	346
7/5/94	40	-1.66	33.81	16.1	1.90	45.1	330
7/5/94	70	-1.74	34.49	20.4	2.40	59.4	289
2/6/94	2	-1.84	33.94	15.5	2.06	45.5	331
2/6/94	5	-1.85	33.99	17.2	2.02	47.2	327
2/6/94	10	-1.86	33.81	17.8	2.00	45.6	314
2/6/94	20	-1.87	33.82	18.4	2.04	46.0	321
2/6/94	40	-1.87	33.84	19.3	2.06	47.6	325
2/6/94	70	-1.74	34.49	23.5	2.61	62.9	258
8/7/94	2	-1.84	34.21	21.3	2.17	48.1	305
8/7/94	5	-1.85	34.32	20.8	2.12	49.7	301
8/7/94	10	-1.86	33.88	21.1	2.12	50.0	305
8/7/94	20	-1.87	33.89	21.2	2.07	48.7	306
8/7/94	40	-1.87	33.88	21.4	2.16	49.8	302
8/7/94	70	-1.74	34.49	23.4	2.47	59.5	270
2/8/94	2	-1.91	32.83	21.7	2.07	50.9	299
2/8/94	5	-1.91	33.56	22.1	2.04	56.2	297
2/8/94	10	-1.91	33.64	22.2	2.03	56.5	296
2/8/94	20	-1.90	33.92	22.4	2.04	56.5	295
2/8/94	40	-1.89	34.00	22.5	2.04	57.0	290
2/8/94	70	-1.75	34.50	24.1	2.47	74.6	252
6/9/94	2	-1.91	33.65	21.7	2.08	59.6	288
6/9/94	5	-1.91	33.84	22.5	2.10	58.3	275
6/9/94	10	-1.91	33.94	22.5	2.14	59.9	275
6/9/94	20	-1.90	34.02	22.4	2.11	59.8	280
6/9/94	40	-1.90	34.11	23.1	2.12	60.0	278
6/9/94	70	-1.74	34.35	23.2	2.12	60.1	214
3/10/94	2	-1.89	34.17	23.7	2.17	60.9	279

Table F.1. Continued

Date	Depth m	Temp ℃	Salinity psu	NO_3^- µmol kg^{-1}	PO_4^{3-} µmol kg^{-1}	H_4SiO_4 µmol kg^{-1}	O_2 µmol kg^{-1}
3/10/94	5	-1.89	34.12	23.4	2.20	61.6	276
3/10/94	10	-1.89	34.12	24.1	2.17	61.3	277
3/10/94	20	-1.89	34.06	24.1	2.15	61.5	274
3/10/94	40	-1.89	34.10	24.1	2.19	61.8	277
3/10/94	70	-1.74	34.35	24.0	2.18	61.4	221
17/10/94	2	-1.89	34.17	23.6	2.10	59.6	296
17/10/94	5	-1.89	34.12	23.5	2.09	61.8	289
17/10/94	10	-1.89	34.12	23.4	2.07	61.6	289
17/10/94	20	-1.89	34.06	23.7	2.08	61.6	286
17/10/94	40	-1.89	34.10	23.6	2.09	61.2	288
17/10/94	70	-1.74	34.45	24.4	2.63	67.3	215
31/10/94	2	-1.77	34.92	23.0	2.15	18.4	302
31/10/94	5	-1.86	34.57	23.0	1.90	59.9	295
31/10/94	10	-1.86	34.27	22.7	2.35	60.5	301
31/10/94	20	-1.87	34.13	21.8	2.29	61.0	289
31/10/94	40	-1.88	34.19	23.4	2.30	60.5	289
31/10/94	70	-1.73	34.34	25.7	2.71	81.6	217
17/11/94	2	-1.69	34.52	3.2	1.36	18.9	885
17/11/94	5	-1.83	34.30	16.3	1.66	42.0	482
17/11/94	10	-1.86	34.18	22.9	2.08	57.5	386
17/11/94	20	-1.86	34.12	23.3	2.05	57.7	322
17/11/94	40	-1.87	34.18	23.4	2.12	59.9	293
17/11/94	70	-1.73	34.34	24.2	2.75	93.7	210
25/11/94	2	-1.42	29.29	9.1	1.50	27.0	755
25/11/94	5	-1.79	34.15	15.1	1.62	36.6	590
25/11/94	10	-1.83	34.09	21.0	1.84	50.2	471
25/11/94	20	-1.81	34.06	16.8	1.88	52.9	494
25/11/94	40	-1.83	34.17	22.9	1.43	66.2	311
25/11/94	70	-1.73	34.34	25.5	2.61	82.3	224
2/12/94	2	-1.66	31.35	9.6	1.35	18.8	704
2/12/94	5	-1.79	34.15	9.6	1.61	36.9	604
2/12/94	10	-1.81	34.07	18.4	1.85	46.3	530
2/12/94	20	-1.78	34.17	20.5	2.04	54.4	402
2/12/94	40	-1.79	34.17	22.8	2.03	56.1	332
2/12/94	70	-1.73	34.34	27.5	2.54	78.2	233
12/12/94	2	-1.57	32.30	7.4	0.94	42.5	587
12/12/94	5	-1.70	34.09	17.2	1.49	53.2	377
12/12/94	10	-1.74	34.05	21.4	1.81	56.7	346
12/12/94	20	-1.71	34.15	19.8	1.93	60.3	323
12/12/94	40	-1.78	34.22	22.9	2.02	60.5	315
12/12/94	70	-1.74	34.39	31.2	2.93	93.2	174
19/12/94	2	-1.48	30.73	5.9	0.86	30.3	654
19/12/94	5	-1.58	33.81	20.1	1.35	54.0	339
19/12/94	10	-1.63	33.92	21.2	1.74	54.5	335
19/12/94	20	-1.66	34.13	21.2	1.79	55.8	328
19/12/94	40	-1.77	34.15	22.1	1.95	56.0	289
19/12/94	70	-1.74	34.29	25.4	2.74	81.1	213
26/12/94	2	-0.89	20.26	0.3	0.28	18.9	600
26/12/94	5	-1.30	33.73	8.9	0.99	35.2	414
26/12/94	10	-1.43	33.73	10.1	1.11	39.7	385
26/12/94	20	-1.54	33.85	16.5	1.37	53.7	357
26/12/94	40	-1.74	34.11	22.5	1.58	52.0	302

Table F.1. Continued

Date	Depth m	Temp ℃	Salinity psu	NO_3^- µmol kg^{-1}	PO_4^{3-} µmol kg^{-1}	H_4SiO_4 µmol kg^{-1}	O_2 µmol kg^{-1}
26/12/94	70	-1.73	34.24	26.4	1.75	79.4	200
2/1/95	2	-1.00	22.83	0.1	0.40	25.5	703
2/1/95	5	-1.10	33.46	8.6	0.82	32.4	406
2/1/95	10	-1.22	33.50	11.9	1.22	37.2	460
2/1/95	20	-1.37	33.76	15.3	1.47	43.2	446
2/1/95	40	-1.72	34.09	22.6	1.96	49.4	344
2/1/95	70	-1.73	34.24	28.2	2.67	87.0	172
12/1/95	2	-0.54	20.38	0.1	0.36	17.0	440
12/1/95	5	-0.85	33.33	6.6	0.63	23.7	443
12/1/95	10	-1.06	33.28	13.7	0.94	30.7	388
12/1/95	20	-1.21	33.58	14.6	1.49	43.7	369
12/1/95	40	-1.72	34.09	19.6	1.95	54.5	405
12/1/95	70	-1.74	34.25	24.9	1.19	36.7	220
19/1/95	2	-0.46	24.17	0.0	0.84	28.1	600
19/1/95	5	-0.40	32.83	12.2	1.51	44.7	397
19/1/95	10	-0.57	33.02	10.5	1.38	41.1	39
19/1/95	20	-1.08	33.38	14.0	1.60	46.1	299
19/1/95	40	-1.72	34.09	22.4	2.13	59.6	297
19/1/95	70	-1.73	34.24	27.7	1.51	43.9	204
27/1/95	2	-0.54	23.60	0.1	1.26	16.8	655
27/1/95	5	-0.32	32.90	7.2	1.12	30.2	396
27/1/95	10	-0.44	33.07	7.7	1.22	31.2	406
27/1/95	20	-0.82	33.19	9.6	1.19	33.9	428
27/1/95	40	-1.72	34.00	19.5	2.12	55.9	285
27/1/95	70	-1.73	34.28	32.0	2.47	71.0	184
2/2/95	2	-0.40	27.58	0.8	0.88	24.3	494
2/2/95	5	-0.30	32.73	10.7	1.08	31.5	336
2/2/95	10	-0.42	32.91	9.8	1.15	33.4	311
2/2/95	20	-0.65	33.10	11.00	1.26	33.1	378
2/2/95	40	-1.71	34.04	15.9	1.82	48.6	331
2/2/95	70	-1.74	34.15	20.9	2.83	75.6	218
17/2/95	2	-0.36	30.54	0.0	0.41	20.9	559
17/2/95	5	-0.20	32.67	3.4	0.62	49.6	447
17/2/95	10	-0.27	32.79	5.8	1.05	52.5	406
17/2/95	20	-0.47	32.95	9.1	1.99	51.6	398
17/2/95	40	-1.69	34.01	15.1	1.99	50.9	308
17/2/95	70	-1.73	34.17	17.1	2.32	97.9	218

1. The concentration given for nitrate is actually the sum of the concentrations of nitrate and nitrite, as the method used for this analysis did not discriminate between these species (Appendix A).

Table F.2. Further chemical parameters for samples from the Ellis Fjord Site. Chlorophyll *a*, pH_f and DIC were measured experimentally, while the concentration of $CO_{2(aq)}$, fCO_2 and Alk_T were calculated as described in Appendix A.

Date	Depth m	Chl *a* mg m^{-3}	pH_f	DIC µmol kg^{-1}	$[CO_{2(aq)}]$ µmol kg^{-1}	fCO_2 µatm	Alk_T µeq kg^{-1}
7/5/94	2	1.20	8.03	2054	8.0	120	2365
7/5/94	5	0.47	7.95	2098	10.1	150	2360
7/5/94	10	0.38	7.85	2170	13.7	202	2381
7/5/94	20	0.21	7.84	2168	13.8	203	2376
7/5/94	40	0.22	7.82	2168	14.7	217	2364
7/5/94	70	0.15	7.66	2258	23.3	345	2385
2/6/94	2	0.08	7.77	2149	16.3	239	2323
2/6/94	5	0.04	7.77	2195	16.6	244	2371
2/6/94	10	0.04	7.77	2194	17.0	250	2365
2/6/94	20	0.02	7.76	2189	17.5	256	2354
2/6/94	40	0.03	7.75	2194	17.7	259	2358
2/6/94	70	0.01	7.60	2300	27.3	405	2407
8/7/94	2	0.16	7.71	2242	20.1	295	2391
8/7/94	5	0.21	7.71	2212	19.7	290	2361
8/7/94	10	0.11	7.71	2209	19.7	289	2356
8/7/94	20	0.19	7.71	2207	19.7	289	2354
8/7/94	40	0.20	7.71	2212	19.9	291	2358
8/7/94	70	0.17	7.60	2279	27.2	402	2385
2/8/94	2	0.10	7.69	2248	21.3	310	2384
2/8/94	5	0.08	7.69	2240	21.3	311	2377
2/8/94	10	0.07	7.69	2222	21.2	310	2358
2/8/94	20	0.10	7.68	2227	21.4	313	2363
2/8/94	40	0.07	7.69	2231	21.3	312	2369
2/8/94	70	0.08	7.66	2275	23.3	344	2404
6/9/94	2	0.11	7.65	2273	23.7	347	2396
6/9/94	5	0.07	7.65	2274	22.8	334	2294
6/9/94	10	0.05	7.66	2244	23.1	338	2370
6/9/94	20	0.06	7.66	2243	23.0	338	2369
6/9/94	40	0.05	7.66	2224	22.9	336	2349
6/9/94	70	0.08	7.65	2291	23.8	352	2418
3/10/94	2	0.30	7.65	2268	23.7	348	2393
3/10/94	5	0.10	7.65	2256	23.6	346	2380
3/10/94	10	0.11	7.66	2255	23.1	340	2382
3/10/94	20	0.10	7.66	2257	23.2	340	2384
3/10/94	40	0.10	7.66	2256	23.2	340	2382
3/10/94	70	0.11	7.65	2240	23.3	345	2365
17/10/94	2	3.44	7.67	2253	22.7	333	2383
17/10/94	5	0.64	7.66	2268	23.4	343	2395
17/10/94	10	0.55	7.66	2265	23.4	343	2391
17/10/94	20	0.63	7.66	2263	23.4	343	2389
17/10/94	40	0.35	7.66	2263	23.5	344	2388
17/10/94	70	0.26	7.62	2317	26.2	388	2431
31/10/94	2	22.57	7.67	2256	22.5	333	2391
31/10/94	5	13.17	7.67	2255	22.4	331	2388
31/10/94	10	3.23	7.68	2254	21.9	322	2390
31/10/94	20	2.15	7.68	2254	21.7	320	2391
31/10/94	40	0.58	7.68	2254	21.8	321	2390

Table F.2. Continued

Date	Depth m	Chl *a* mg m^{-3}	pH_f	DIC µmol kg^{-1}	$[CO_{2(aq)}]$ µmol kg^{-1}	fCO_2 µatm	Alk_T µeq kg^{-1}
31/10/94	70	1.34	7.58	2253	28.3	418	2350
17/11/94	2	2.61	8.58	1431	1.1	17	2108
17/11/94	5	5.13	8.48	1967	2.1	31	2684
17/11/94	10	2.65	8.44	2150	2.6	38	2865
17/11/94	20	0.47	8.13	2190	6.4	94	2600
17/11/94	40	0.48	7.97	2246	10.2	150	2536
17/11/94	70	0.30	7.53	2324	33.3	493	2404
25/11/94	2	20.58	8.34				
25/11/94	5	10.93	8.26	1444	3.0	45	1838
25/11/94	10	3.93	7.98	2059	9.0	133	2341
25/11/94	20	2.61	8.01	2034	8.2	121	2333
25/11/94	40	0.64	7.98	2206	9.6	142	2502
25/11/94	70	0.56	7.51	2303	35.2	520	2374
2/12/94	2	10.51	8.82	1037	0.4	6	1749
2/12/94	5	5.93	8.33	1682	2.9	42	2178
2/12/94	10	3.63	8.15	1999	5.7	83	2391
2/12/94	20	1.87	7.95	2014	9.6	141	2274
2/12/94	40	0.47	7.87	2234	13.0	192	2465
2/12/94	70	0.87	7.48	2288	38.0	562	2347
12/12/94	2	8.76	8.20	1759	4.4	64	2143
12/12/94	5	5.83	7.97	2138	9.6	142	2422
12/12/94	10	3.53	7.85	2181	13.6	201	2394
12/12/94	20	2.09	7.98	2221	15.8	234	2402
12/12/94	40	2.67	7.81	2238	15.3	225	2437
12/12/94	70	0.55	7.44	2346	43.2	639	2392
19/12/94	2	0.78	8.46	1021	1.3	19	1434
19/12/94	5	1.60	8.05	2185	8.0	119	2524
19/12/94	10	1.39	7.88	2182	12.5	185	2414
19/12/94	20	1.24	7.86	2205	13.2	196	2429
19/12/94	40	1.23	7.82	2222	15.0	221	2422
19/12/94	70	0.34	7.51	2283	35.0	517	2353
26/12/94	2	1.18	8.69	197			
26/12/94	5	6.12	7.90	642			
26/12/94	10	7.00	7.89	2118	11.9	178	2349
26/12/94	20	3.89	7.79	2180	16.0	238	2362
26/12/94	40	2.03	7.73	2114	18.0	266	2266
26/12/94	70	1.19	7.50	2279	36.3	537	2343
2/1/95	2	4.44	8.51	1074	1.3	19	1437
2/1/95	5	10.01	8.02	2082	8.5	128	2384
2/1/95	10	8.21	7.99	2026	8.8	132	2308
2/1/95	20	10.00	7.87	2059	11.8	176	2282
2/1/95	40	1.67	7.76	2054	16.0	236	2219
2/1/95	70	1.89	7.48	2336	38.9	575	2395
12/1/95	2	3.29	8.77	337	0.2	3	604
12/1/95	5	9.14	8.23	1692	3.9	60	2097
12/1/95	10	5.51	8.07	2082	7.4	112	2417
12/1/95	20	4.65	7.94	2105	10.3	155	2365
12/1/95	40	2.74	7.91	2195	11.7	172	2444
12/1/95	70	3.20	7.48	2067	34.2	506	2124
19/1/95	2	6.92	8.44	722	1.1	16	988
19/1/95	5	3.59	7.95	2060	10.1	156	2315
19/1/95	10	4.19	7.95	2057	10.1	155	2313

Table F.2. Continued

Date	Depth m	Chl *a* mg m^{-3}	pH_f	DIC µmol kg^{-1}	$[CO_{2(aq)}]$ µmol kg^{-1}	fCO_2 µatm	Alk_T µeq kg^{-1}
19/1/95	20	1.80	7.97	2178	9.9	150	2462
19/1/95	40	1.38	7.79	2236	16.2	239	2423
19/1/95	70	2.19	7.48	2290	38.3	566	2348
27/1/95	2	11.26	8.33	1755	3.5	52	2133
27/1/95	5	3.59	8.06	1131	4.3	66	1354
27/1/95	10	3.30	8.06	2048	7.5	115	2376
27/1/95	20	2.33	8.00	2076	8.8	135	2366
27/1/95	40	0.72	7.78	2199	16.2	239	2380
27/1/95	70	0.58	7.44	2349	44.2	654	2392
2/2/95	2	7.91	8.52	1640	1.8	27	2210
2/2/95	5	1.36	7.94	2029	10.4	160	2273
2/2/95	10	2.06	7.99	2131	9.5	146	2415
2/2/95	20	1.42	7.93	2077	10.8	165	2321
2/2/95	40	0.89	7.81	2140	14.9	220	2329
2/2/95	70	0.64	7.58	2284	28.7	424	2381
17/2/95	2	9.01	8.67	973	0.7	10	1519
17/2/95	5	14.17	8.35	1993	3.3	52	2552
17/2/95	10	7.03	8.09	2027	6.9	107	2370
17/2/95	20	3.18	8.02	2055	8.4	129	2354
17/2/95	40	0.54	7.77	2225	16.9	250	2403
17/2/95	70	0.42	7.66	2306	23.5	347	2436

Table F.3. Concentrations of DOC, POC and total organic carbon at the Ellis Fjord site.

Date	Depth m	DOC µmol kg^{-1}	POC µmol kg^{-1}	Total µmol kg^{-1}
31/10/94	2	112	37	149
31/10/94	5	63	13	76
31/10/94	10	106	10	116
31/10/94	20	89	1	90
31/10/94	40	62	7	69
31/10/94	70	97	4	101
17/11/94	2	144	79	223
17/11/94	5	98	55	153
17/11/94	10	76	8	84
17/11/94	20	72	10	82
17/11/94	40	77	0	77
17/11/94	70	83	0	83
25/11/94	2	166	86	252
25/11/94	5	147	48	195
25/11/94	10	111	20	131
25/11/94	20	96	7	103
25/11/94	40	80	4	84
25/11/94	70	79	0	79
2/12/94	2	185	68	253
2/12/94	5	88	32	120

Table F.3. Continued

Date	Depth m	DOC µmol kg^{-1}	POC µmol kg^{-1}	Total µmol kg^{-1}
2/12/94	10	102	2	104
2/12/94	20	86	0	86
2/12/94	40	65	0	65
2/12/94	70	68	0	68
12/12/94	2	130	72	202
12/12/94	5	86	18	104
12/12/94	10	80	26	106
12/12/94	20	59	2	61
12/12/94	40	75	1	76
12/12/94	70	72	0	72
19/12/94	2	117	18	135
19/12/94	5	79	0	79
19/12/94	10	71	0	71
19/12/94	20	76	0	76
19/12/94	40	74	0	74
19/12/94	70	72	0	72
26/12/94	2	119	0	119
26/12/94	5	88	13	101
26/12/94	10	92	19	111
26/12/94	20	78	27	105
26/12/94	40	77	7	84
26/12/94	70	76	0	76
2/1/95	2	97	53	150
2/1/95	5	67	36	103
2/1/95	10	66	26	92
2/1/95	20	74	18	92
2/1/95	40	70	4	74
2/1/95	70	56	0	56
12/1/95	2	89	36	125
12/1/95	5	68	27	95
12/1/95	10	72	21	93
12/1/95	20	73	25	98
12/1/95	40	78	2	80
12/1/95	70	93	6	99
19/1/95	2	139	73	212
19/1/95	5	105	36	141
19/1/95	10	101	13	114
19/1/95	20	86	7	93
19/1/95	40	75	2	77
19/1/95	70	73	5	78
27/1/95	2	148	132	280
27/1/95	5	111	33	144
27/1/95	10	67	22	89
27/1/95	20	78	12	90
27/1/95	40	63	4	67
27/1/95	70	59	6	65
2/2/95	2	100	81	181
2/2/95	5	93	15	108
2/2/95	10	68	23	91
2/2/95	20	88	12	100
2/2/95	40	68	7	75
2/2/95	70	61	5	66

Table F.4. $\delta^{13}C_{DIC}$ at the Ellis Fjord site. All samples were collected from 10 m.

Date	$\delta^{13}C_{DIC}$ ‰
2/6/94	1.13
2/8/94	0.91
6/9/94	0.87
3/10/94	0.81
17/10/94	0.86
31/10/94	0.82
17/11/94	1.11
25/11/94	1.01
12/12/94	1.12
19/12/94	1.20
26/12/94	1.51
2/1/95	1.67
12/1/95	1.60
19/1/95	1.76
27/1/95	1.79

APPENDIX G

ELLIS FJORD: SEDIMENT TRAP AND CORE DATA

This appendix gives results of the sediment trap study carried out at the Ellis Fjord site. Data from the short sediment core collected at the same site are also presented.

Table G.1. Sediment flux and chemical data for the sediment trap array positioned at the Ellis Fjord site. The C:N mole ratio and $\delta^{13}C$ are for the organic fraction of the sediment trap material.

Trap deploy-ment date	Trap recovery date	Trap days	Depth m	Total flux mg m^{-2} day^{-1}	Carbon flux mg m^{-2} day^{-1}	C:N mole ratio	$\delta^{13}C$ ‰
2/6/94	7/7/94	35	5	24	1.3	7.5	-23.20
2/6/94	7/7/94	35	10	40	2.7	7.3	-22.00
2/6/94	7/7/94	35	20	74	4.8		
2/6/94	7/7/94	35	40	121	7.2	9.3	
2/6/94	7/7/94	35	70	181	9.3		
7/7/94	8/8/94	32	5	88	8.7	10.9	
7/7/94	8/8/94	32	10	115	8.9	10.8	-20.06
7/7/94	8/8/94	32	20	111	10.6	10.3	-19.25
7/7/94	8/8/94	32	40	200	12.6	8.6	-18.85
7/7/94	8/8/94	32	70	87	7.2		
8/8/94	6/9/94	29	5	132	5.1	9.6	-20.22
8/8/94	6/9/94	29	10	123	4.1	9.1	-19.98
8/8/94	6/9/94	29	20	134	5.0	9.6	-20.25
8/8/94	6/9/94	29	40	155	5.8	9.3	-19.66
8/8/94	6/9/94	29	70	216	9.2		
6/9/94	3/10/94	27	5	101	3.9	10.0	-20.75
6/9/94	3/10/94	27	10	216	5.4		
6/9/94	3/10/94	27	20	87	3.3		
6/9/94	3/10/94	27	40	110	5.0	9.6	-20.71
6/9/94	3/10/94	27	70	31	3.4		
3/10/94	31/10/94	28	5	194	23.2		
3/10/94	31/10/94	28	10	205	22.7		
3/10/94	31/10/94	28	20	189	20.6		
3/10/94	31/10/94	28	40	147	11.5		
3/10/94	31/10/94	28	70	229	18.8		
31/10/94	17/11/94	17	5	230	33.0		
31/10/94	17/11/94	17	10	211	28.8	13.4	

Table G.1. Continued

Trap deploy-ment date	Trap recovery date	Trap days	Depth m	Total flux mg m^{-2} day^{-1}	Carbon flux mg m^{-2} day^{-1}	C:N mole ratio	$\delta^{13}C$ ‰
31/10/94	17/11/94	17	20	148	25.0	10.9	-14.59
31/10/94	17/11/94	17	40	181	15.8	12.3	-14.69
31/10/94	17/11/94	17	70	168	16.0	11.9	-14.68
17/11/94	2/12/94	15	5	303	45.7	12.1	-14.19
17/11/94	2/12/94	15	10	266	34.9	11.6	-15.34
17/11/94	2/12/94	15	20	202	28.1	9.6	-16.09
17/11/94	2/12/94	15	40	181	12.7	9.7	-17.57
17/11/94	2/12/94	15	70	102	4.5	10.5	-18.21
2/12/94	19/12/94	17	5	282	31.4	10.5	-15.74
2/12/94	19/12/94	17	10	335	35.1	9.0	-15.58
2/12/94	19/12/94	17	20	196	18.3	8.6	-17.07
2/12/94	19/12/94	17	40	180	14.2	10.2	
2/12/94	19/12/94	17	70	193	11.7	11.1	-17.46
19/12/94	2/1/95	14	5	363	47.6	7.9	
19/12/94	2/1/95	14	10	361	44.4	7.4	-18.26
19/12/94	2/1/95	14	20	278	22.1	9.9	
19/12/94	2/1/95	14	40	360	24.5	9.5	-19.04
19/12/94	2/1/95	14	70	237	8.4	8.5	-19.17
2/1/95	19/1/95	17	5	103	14.9	7.6	-18.54
2/1/95	19/1/95	17	10	673	89.6	7.6	-20.30
2/1/95	19/1/95	17	20	816	77.3	7.9	-20.03
2/1/95	19/1/95	17	40	545	52.1	8.1	-19.27
2/1/95	19/1/95	17	70	105	7.8	7.8	-20.57
19/1/95	2/2/95	14	5	215	47.7	6.8	-20.11
19/1/95	2/2/95	14	10	354	53.3	7.4	-19.95
19/1/95	2/2/95	14	20	257	26.6	8.4	-19.51
19/1/95	2/2/95	14	40	163	13.5	10.3	-19.23
19/1/95	2/2/95	14	70	258	8.9	9.0	-18.71
2/2/95	17/2/95	15	5	140	40.5	6.9	-20.11
2/2/95	17/2/95	15	10	160	38.8	8.4	
2/2/95	17/2/95	15	20	94	22.5	8.7	-21.08
2/2/95	17/2/95	15	40	158	17.9	10.1	-20.80
2/2/95	17/2/95	15	70	169	1.4	10.4	-19.26
17/2/95	2/3/95	13	5	99	11.9	8.1	-21.25
17/2/95	2/3/95	13	10	344	70.9	7.4	
17/2/95	2/3/95	13	20	260	43.6	8.6	-19.83
17/2/95	2/3/95	13	40	154	18.3	10.1	-20.50
17/2/95	2/3/95	13	70	135	11.3	8.0	-19.89
2/3/95	12/6/95	102	5	54	5.0	7.9	-20.23
2/3/95	12/6/95	102	10	56	5.1	7.8	-20.19
2/3/95	12/6/95	102	20	103	8.3	7.0	-19.23
2/3/95	12/6/95	102	40	152	12.4	8.2	-18.90
2/3/95	12/6/95	102	70	221	17.5	7.7	-18.44

Table G.2. Organic carbon content of the short sediment core recovered from the Ellis Fjord site.

Segment depth, cm	% Organic C
0-1	1.74
1-2	2.07
2-3	2.16
3-4	2.10
4-5	2.12
5-6	1.97
6-7	1.61
7-8	1.39
8-9	1.74
9-10	1.61
10-11	1.79
11-12	1.54

REFERENCES

Ackley, S.F., and Sullivan, C.W. (1994) Physical controls on the development and characteristics of Antarctic sea ice biological communities - a review and synthesis. Deep-Sea Research, 41:1583-1604.

Adamson, D.A., and Pickard, J. (1986b) Physiography and geomorphology of the Vestfold Hills. In: (J. Pickard, editor) Antarctic Oasis. Academic Press, Sydney. pp. 99-139.

Allison, C.E., Francey, R.J., Welch, E.D. (1996) $\delta^{13}C$ of *in situ* extracted baseline CO_2. In: (R.J. Francey, A.L. Dick, and N. Derek, editors) Baseline Atmospheric Program, Australia, 1994-5. Bureau of Meteorology and CSIRO Division of Atmospheric Research, Melbourne. pp. 104-105.

Anderson, L.G., and Jones, E.P. (1991) The transport of CO_2 into Arctic and Antarctic Seas: Similarities and differences in the driving processes. Journal of Marine Systems, 2: 81-95.

Archer, S.D., Leakey, R.J.G., Burkill, P.H., and Sleigh, M.A. (1996a) Microbial dynamics in coastal waters off East Antarctica: Herbivory by heterotrophic dinoflagellates. Marine Ecology Progress Series, 138: 239-255.

Archer, S.D., Leakey, R.J.G., Burkill, P.H., Sleigh, M.A. and Appleby, C.J. (1996b) Microbial ecology of sea ice at a coastal Antarctic site: community composition, biomass and temporal change. Marine Ecology Progress Series, 135: 179-195.

Arthur, M.A., Dean, W.E., and Claypool, G.E. (1985) Anomalous 13-C enrichment in modern marine organic carbon. Nature, 315: 216-218.

Barry, J.P. (1988) Hydrographic patterns in McMurdo Sound, Antarctica, and their relationship to local biotic communities. Polar Biology, 8: 367-376.

Bathmann, U., Fischer, G., Müller, P.J., and Gerdes, D. (1991) Short-term variations in particulate matter sedimentation of Kapp Norvegia, Weddell Sea, Antarctica: relation to water mass advection, ice cover, plankton biomass and feeding activity. Polar Biology, 11:185-195.

Beggs, H.M. (1995) Air-sea exchange of CO_2 over the Antarctic seasonal ice zone. Ph.D. Thesis, University of Tasmania. Unpublished.

Bellerby, R.G.J., Turner, D.R., and Robertson, J.E. (1995) Surface pH and pCO_2 distributions in the Bellingshausen Sea, Southern Ocean, during the early austral summer. Deep-Sea Research II, 42: 1093-1107.

Benner, R., and Strom, M. (1993) A critical evaluation of the analytical blank associated with DOC measurements by high-temperature catalytic oxidation. Marine Chemistry, 41: 153-160.

Benson, B.B., and Krause, D. Jr. (1984) The concentration and isotopic fractionation of oxygen dissolved in freshwater and seawater in equilibrium with the atmosphere. Limnology and Oceanography, 29: 620-632.

Berger, W.H., Fischer, K., Lai, C., and Wu, G. (1988) Ocean carbon flux: Global maps of primary production and export production. In: (C.R. Agregian, editor) Biogeochemical cycling and fluxes between the deep euphotic zone and other realms. Research Report 88-1, NOAA Undersea Research Progress, Silver Springs, Maryland, USA. pp. 131-176.

Biggs, D.C., Berkowitz, S.P., Altabet, M.A., Bidigare, R.R., DeMaster, D.J., Macko, S.A., Ondrusek, M.E., and Noh, I. (1989). Cooperative study of upper ocean particulate fluxes. Proceedings of the Ocean Drilling Program, Initial Reports, 119: 109-120.

Billen, G., and Fontigny, A. (1987) Dynamics of a *Phaeocystis*-dominated bloom in Belgian coastal waters. II. Bacterioplankton dynamics. Marine Ecology Progress Series, 37: 249-257.

Bird, M.I., Chivas, A.R., Radnell, C.J. and Burton, H.R. (1991) Sedimentological and stable-isotope evolution of lakes in the Vestfold Hills, Antarctica. Palaeogeography, Palaeoclimatology, Palaeoecology, 84: 109-130.

Bloesch, J., and Burns, N.M. (1980) A critical review of sediment trap technique. Schweizer Zeitschrift für Hydrobiologie, 42: 15-55.

Blomqvist, S., and Håkanson, L. (1981) A review on sediment traps in aquatic environments. Archiv für Hydrobiologie, 91: 101-132.

Blomqvist, S., and Kofoed, C. (1981) Sediment trapping - a subaquatic *in situ* experiment. Limnology and Oceanography, 26: 585-590.

Bloxham, J.J. (1993) Recent sedimentation and facies distribution within Ellis Fjord, the Vestfold Hills: Source and distribution of sediments through particle size and faunal analyses. Honours Thesis, University of Tasmania. Unpublished.

Bölter, M., and Dawson, R. (1982) Heterotrophic utilisation of biochemical compounds in Antarctic waters. Netherlands Journal of Sea Research, 16: 315-322.

Bouquegneau, J.M., Gieskes, W.W.C., Kraay, G.W., and Larsson, A.M. (1992) Influence of physical and biological processes on the concentration of O_2 in the ice-covered Weddell Sea in the spring of 1988. Polar Biology, 12: 163-170.

Broecker, W.S., and Peng, T.-H. (1982) Tracers in the sea. Eldigio Press, Palisades, New York, USA. 690 pp.

Broecker, W.S., and Peng, T.-H. (1993) What caused the glacial to interglacial CO_2 change. In: (M. Heimann, editor) The global carbon cycle. NATO Advanced Research Institute, Springer-Verlag, New York, USA. pp. 413-429.

Brzezinski, M.A. (1985) The Si:C:N ratio of marine diatoms: interspecific variability and the effect of some environmental variables. Journal of Phycology, 21: 347-357.

Buck, K.R., Bolt, P.A., Bentham, W.N., and Garrison, D.L. (1992) A dinoflagellate cyst from Antarctic sea ice. Journal of Phycology, 28: 15-18.

Budd, W.F. (1991) Antarctica and global change. Climatic Change, 18: 271-299.

Buesseler, K.O. (1991) Do upper-ocean sediment traps provide an accurate record of particle flux? Nature, 353: 420-423.

Buma, A.G.J., Gieskes, W.W.C., and Thomsen, H.A. (1992) Abundance of Cryptophyceae and chlorophyll *b*-containing organisms in the Weddell-Scotia Confluence area in the spring of 1988. Polar Biology, 12: 43-52.

Bunt, J.S. (1960) Introductory studies: hydrology and plankton, Mawson, June 1956 - February 1957. Australian National Antarctic Research Expeditions Reports Series B, Volume III, Publication 56. Antarctic Division, Department of External Affairs, Melbourne, Australia. 135 pp.

Burch, M.D. (1988) Annual cycle of phytoplankton in Ace Lake, an ice-covered saline, meromictic lake. Hydrobiologia, 165: 59-75.

Burkholder, P.R., and Mandelli, E.F. (1965) Carbon assimilation of marine phytoplankton in Antarctica. Proceedings of the National Academy of Science of the USA, 54: 437-444.

Burton, H.R., and Campbell, P.J. (1980) The climate of the Vestfold Hills, Davis Station, Antarctica, with a note on its effect on the hydrology of Deep Lake. ANARE Scientific Reports, Series D, 129: 1-50.

Byrne, R.H., and Breland, J.A. (1989) High precision multiwavelength pH determinations in seawater using cresol red. Deep-Sea Research, 40: 629-641.

Cadée, G.C. (1992) Organic carbon in the upper layer and its sedimentation during the ice-retreat period in the Scotia-Weddell Sea, 1988. Polar Biology, 12: 253-259.

Chavez, F.P., and Barber, R.T. (1987) An estimate of new production in the equatorial Pacific. Deep-Sea Research, 34: 1229-1243.

Clarke, A., and Leakey, R.J.G. (1996) The seasonal cycle of phytoplankton, macronutirents, and the microbial community in a nearshore Antarctic marine ecosystem. Limnology and Oceanography, 41: 1281-1294.

Clayton, T.D., and Byrne, R.H. (1993) Spectrophotometric seawater pH measurements: total hydrogen ion concentration scale calibration of m-cresol purple and at-sea results. Deep-Sea Research, 40: 2115-2129.

Codispoti, L.A., Friedrich, G.E., and Hood, D.W. (1986) Variability in the inorganic carbon system over the southeastern Bering Sea shelf during spring 1980 and spring-summer 1981. Continental Shelf Research, 5: 133-160.

Codispoti, L.A., Friedrich, G.E., Iverson, R.L., and Hood, D.W. (1982) Temporal changes in the inorganic carbon system of the south-eastern Bering Sea during Spring 1980. Nature, 296: 242-245.

Colbeck, G. (1977) Hydrographic project, Davis 1976. Antarctic Division Technical Memorandum, 66: 1-44.

Collerson, K.D., and Sheraton, J.W. (1986) Bedrock geology and crustal evolution of the Vestfold Hills. In: (J. Pickard, editor) Antarctic Oasis. Academic Press, Sydney. pp. 21-62.

Copin-Montégut, C., and Copin-Montégut, G. (1978) The chemistry of particulate matter from the south Indian and Antarctic Oceans. Deep-Sea Research, 25: 911-931.

Copin-Montégut, C., and Copin-Montégut, G. (1983) Stoichiometry of carbon, nitrogen, and phosphorus in marine particulate matter. Deep-Sea Research, 30: 31-46.

Cota, G.F., and Sullivan, C.W. (1990) Photoadaption, growth and production of bottom ice algae in the Antarctic. Journal of Phycology, 26: 399-411.

Craig, H. (1957) Isotopic standards for carbon and oxygen and correction factors for mass spectrometry analysis of carbon dioxide. Geochimica et Cosmochimica Acta, 3: 133-149.

Croome, R.J.L., van den Hoff, J., and Burton, H.R. (1987) Observations of the heliozoan genera *Pinaciaphora* and *Acanthocystis* (Heliozoa, Sarcodina, Protozoa) from Ellis Fjord. Polar Biology, 8: 23-28.

Davidson, A.T., and Marchant, H.J. (1992a) Protist abundance and carbon concentration during a *Phaeocystis*-dominated bloom at an Antarctic coastal site. Polar Biology, 12: 387-395.

Davidson, A.T., and Marchant, H.J. (1992b) The biology and ecology of *Phaeocystis* (Prymnesiophyceae). Progress in Phycological Research, 8: 1-44.

Davidson, A.T., Marchant, H.J., and de la Mare, W.K. (1996) Natural UVB exposure changes the species composition of Antarctic phytoplankton in mixed culture. Aquatic Microbial Ecology, 10: 299-305.

de Baar, H.J.W., Buma, A.G.J., Nolting, R.F., Cadée, G.C., Jacques, G., and Treguér, P.J. (1990) On iron limitation of the Southern Ocean: Experimental observations in the Weddell and Scotia Seas. Marine Ecology Progress Series, 65: 105-122.

de Baar, H.J.W., de Jong, J.T.M., Bakker, D.C.E., Löscher, B.M., Veth, C., Bathmann, U., and Smetacek, V. (1995) Importance of iron for plankton blooms and carbon dioxide drawdown in the Southern Ocean. Nature, 373: 412-415.

DeMaster, D.J. (1981) The supply and accumulation of silica in the marine environment. Geochimica et Cosmochimica Acta, 45: 1715-1732.

DeMaster, D.J., Dunbar, R.B., Gordon, L.I., Leventer, A.R., Morrison, J.M., Nelson, D.M., Nittrouer, C.A., and Smith, W.O. Jr. (1992) Cycling and accumulation of biogenic silica and organic matter in high-latitude environments: The Ross Sea. Oceanography, 5: 146-153.

Descolas-Gros, C., and Fontugne, M.R. (1990) Stable carbon isotope fractionation by marine phytoplankton during photosynthesis. Plant, Cell and Environment, 13: 207-218.

Dickson, A.G. (1993) The measurement of pH in seawater. Marine Chemistry, 44: 131-143.

Dieckmann, G.S., Spindler, M., Lange, M.A., Ackley, S.F., and Eicken, H. (1991) Antarctic sea ice: a habitat for the foraminifer *Neogloboquadrina pachyderma*. Journal of Foraminiferal Research, 21: 182-189.

Domanov, M.M., and Lipski, M. (1990) Annual cycle of chlorophyll *a* and primary production of phytoplankton in Admiralty Bay (Antarctica). Polish Archives of Hydrobiology, 37: 471-478.

Dore, J.E., Houlihan, T., Hebel, D.V., Tien, G., Tupas, L., and Karl, D.M. (1996) Freezing as a method of sample preservation for the analysis of dissolved inorganic nutrients in seawater. Marine Chemistry, 53: 173-185.

Dunbar, R.B. (1984) Sediment trap experiments on the Antarctic continental margin. Antarctic Journal of the United States, 19: 70-71.

Dunbar, R.B., and Leventer, A. (1992) Seasonal variation in carbon isotopic composition of antarctic sea ice and open-water plankton communities. Antarctic Journal of the United States, 27: 79-81.

Dunbar, R.B., Anderson, J.B., and Domack, E.W. (1985) Oceanographic influences on sedimentation along the Antarctic continental shelf. Antarctic Research Series, 43: 291-312.

Dunbar, R.B., Leventer, A., and Stockton, W.L. (1989) Biogenic sedimentation in McMurdo Sound, Antarctica. Marine Geology, 85: 155-179.

Eadie, B.J., and Jeffrey, L.M. (1973) $\delta^{13}C$ analysis of oceanic particulate organic matter. Marine Chemistry, 1: 199-209.

El-Sayed, S.Z. (1987) Biological productivity of Antarctic waters: Present paradoxes and emerging patterns. In: (S.Z. El-Sayed and A.P. Tomo, editors) Antarctic aquatic biology. SCAR, Cambridge. pp. 1-21.

El-Sayed, S.Z. (1988) Productivity of the Southern Ocean: A closer look. Comparative Biochemistry and Physiology, 90B: 489-498.

El-Sayed, S.Z., and Fryxell, G.A. (1993) Phytoplankton. In: (E.I. Friedmann, editor) Antarctic Microbiology. Wiley-Liss. New York, USA. pp. 65-122.

El-Sayed, S.Z., and Taguchi, S. (1981) Primary production and standing crop along the ice-edge in the Weddell Sea. Deep-Sea Research, 28:1017-1032.

Eppley, R.W., Renger, E.H., and Betzer, P.R. (1983) The residence time of particulate organic carbon in the surface layer of the ocean. Deep-Sea Research, 30: 311-323.

Everitt, D.A., and Thomas, D.P. (1986) Observations of seasonal changes in diatoms at inshore localities near Davis Station, East Antarctica. Hydrobiologia, 139: 3-12.

Everitt, D.A., Poore, G.C.B., and Pickard, J. (1980) Marine benthos from Davis Station, Eastern Antarctica. Australian Journal of Marine and Freshwater Research, 31: 829-836.

Fairhall, A.W., Broadford, P., Yang, I.C., and Young, A.W. (1971) Carbon-14 in the southern oceans from nuclear bombs. Antarctic Journal of the United States, 6: 163-164.

Falkowski, P.G. (1991) Species variability in the fractionation of ^{13}C and ^{12}C by marine phytoplankton. Journal of Plankton Research, 13: 21-28.

Fischer, G. (1991) Stable carbon isotope ratios of plankton carbon and sinking organic matter from the Atlantic section of the Southern Ocean. Marine Chemistry, 35: 581-596.

Fischer, G., Fütterer, D., Gersonde, R., Honjo, S., Ostermann, D., and Wefer, G. (1988) Seasonal variability of particle flux in the Weddell Sea and its relation to sea ice. Nature, 335:426-428.

Fofonoff, N.P., and Millard, R.C. (1983) Algorithms for computation of fundamental properties of seawater. UNESCO Technical Papers in Marine Science 44, 53 pp.

Fontugne, M., and Duplessy, J.-C. (1981) Organic carbon isotopic fractionation by marine phytoplankton in the temperature range -1 to 31 °C. Oceanologica Acta, 4: 85-90.

Foster, T.D. (1984) The marine environment. In: (R.M. Laws, editor) Antarctic Ecology. Volume 2. Academic Press, London, U.K. pp. 345-371.

Foster, T.D., and Carmack, E.C. (1976) Frontal zone mixing and Antarctic bottom water formation in the Southern Weddell Sea. Deep-Sea Research, 21: 301-317.

Fry, B. (1996) $^{13}C/^{12}C$ fractionation by marine diatoms. Marine Ecology Progress Series 134: 283-294.

Fry, B., and Wainwright, S.C. (1991) Diatom sources of ^{13}C-rich carbon in the marine food webs. Marine Ecology Progress Series, 76: 149-157.

Fukuchi, M., Tanimura, A., and Ohtsuka, H. (1984) Seasonal change of chlorophyll *a* under fast ice in Lützow-Holm Bay, Antarctica. Memoirs of the National Institute for Polar Research, Special Issue, 32: 51-59.

Fukuchi, M., Tanimura, A., Ohtsuka, H., and Hoshiai, T. (1985) Marine biological data of BIOMASS programme at Syowa Station in the 1982 winter (JARE-23). JARE Data Reports 98, 113 pp.

Fukui, F., Otomo, K., and Okabe, S. (1992) Nutrients depression in the blooming area of Prydz Bay, Antarctica. Memoirs of the National Polar Research Institute, Special Issue, 44: 43-54.

Gade, H.G., Lake, R.A., Lewis, E.L., and Walker, E.R. (1974) Oceanography of an Arctic Bay. Deep-Sea Research, 21: 547-571.

Gaillard, J-F., Pauwels, H., and Michard, G. (1989) Chemical diagenesis in coastal marine sediments. Oceanologica Acta, 12:175-187.

Gallagher, J.B., and Burton, H.R. (1988) Seasonal mixing of Ellis Fjord, Vestfold Hills, East Antarctica. Estuarine, Coastal and Shelf Science, 27: 363-380.

Gallagher, J.B., Burton, H.R., and Calf, G.E. (1989) Meromixis in an Antarctic fjord: a precursor to meromictic lakes on an isostatically rising coastline. Hydrobiologia, 172: 235-254.

Garrison, D.L., and Buck, K.R. (1989) The biota of Antarctic pack ice in the Weddell Sea and Antarctic Peninsula regions. Polar Biology, 10: 211-219.

Garrison, D.L., Sullivan, C.W., and Ackley, S.F. (1986) Sea ice microbial communities in the Antarctic. BioScience, 36: 243-250.

Garrison, D.L., Buck, K.R., and Fryxell, G.A. (1987) Algal assemblages in Antarctic pack ice and in ice-edge plankton. Journal of Phycology, 23: 564-572.

Gibson, J.A.E., and Burton, H.R. (1996) Meromictic Antarctic lakes as recorders of climate change: The structures of Ace Lake and Organic Lake, Vestfold Hills, Antarctica. Papers and Proceedings of the Royal Society of Tasmania, 130:73-78.

Gibson, J.A.E., Ferris, J.M., van den Hoff, J., and Burton, H.R. (1989) Temperature profiles of saline lakes of the Vestfold Hills, Antarctica. ANARE Research Notes, 67: 1-75.

Gibson, J.A.E., Garrick, R.C., Burton, H.R., and McTaggart, A.R. (1990a) Dimethylsulfide and the alga *Phaeocystis pouchetii* in Antarctic coastal waters. Marine Biology, 104: 339-346.

Gibson, J.A.E., Garrick, R.C., and Burton, H.R. (1990b) Seasonal fluctuation of bacterial numbers near the Antarctic Continent. Proceedings of the NIPR Symposium on Polar Biology, 3: 16-22..

Gibson, J.A.E., Swadling, K.M., and Burton, H.R. (1997) Interannual variation in dominant phytoplankton species and biomass near Davis Station, East Antarctica. Proceedings of the NIPR Symposium on Polar Biology, 10: 78-90.

Gleitz, M., Rutgers van der Loeff, M., Thomas, D.N., Dieckmann, G.S. and Millero, F.J. (1995) Comparison of summer and winter inorganic carbon, oxygen and nutrient concentrations in Antarctic sea-ice brine. Marine Chemistry, 51: 81-91.

Gleitz, M., Grossmann, S., Scharek, R., and Smetacek. V. (1996a) Ecology of diatom and bacterial assemblages in water associated with melting summer sea ice in the Weddell Sea, Antarctica. Antarctic Science, 8: 135-146.

Gleitz, M., Kukert, H., Riebesell, U., and Dieckmann, G.S. (1996b) Carbon acquisition and growth of Antarctic sea ice diatoms in closed bottle incubations. Marine Ecology Progress Series, 135: 169-177.

Glew, J.R. (1989) A new type of mechanism for sediment samples. Journal of Paleolimnology, 2: 241-243.

Gordon, A.L., and Huber, B.A. (1990) Southern Ocean winter mixed layer. Journal of Geophysical Research, 95: 11655-11672.

Gordon, A.L., Chen, C.T.A., and Metcalf, W.G. (1984) Winter mixed layer entrainment of Weddell Deep Water. Journal of Geophysical Research, 89: 637-640.

Gordon, J.E., and Harkness, D.D. (1992) Magnitude and geographic variation of the radiocarbon content in Antarctic marine life: implications for reservoir corrections in radiocarbon dating. Quaternary Science Reviews, 11: 697-708.

Guillard, R.R.L., and Hellebust, J.A. (1971) Growth and the production of extracellular substances by two strains of *Phaeocystis pouchetii*. Journal of Phycology, 7: 330-338.

Håkanson, L., Floderus, S., and Wallin, M. (1989) Sediment trap assemblages: a methodological description. Hydrobiologia, 176/7: 481-490.

Hargrave, B.T., and Kamp-Nielsen, L. (1977) Accumulation of sedimentary organic matter at the base steep bottom gradients. In: (H.L. Golterman, editor) Interactions between sediment and freshwater. Dr W. Junk, the Hague. pp. 168-173.

Hart, T.J. (1934) On the phytoplankton of the south-west Atlantic and Bellingshausen Sea. Discovery Reports, 8: 1-268.

Hickel, W. (1984) Seston in the Wadden Sea of Sylt (German Bight, North Sea). Netherlands Institute of Sea Research, Publications Series, 10: 113-131.

Hill, D.R.A. (1991) A revised circumscription of *Cryptomonas* (Cryptophyceae) based on examination of Australian strains. Phycologia, 30: 170-188.

Hinga, K.R., Arthur, M.A., Pilson, M.E.Q., and Whitaker, D. (1994) Carbon isotope fractionation by marine phytoplankton in culture: The effects of CO_2 concentration, pH, temperature, and species. Global Biogeochemical Cycles, 8: 91-102.

Holm-Hansen, O. (1985) Nutrient cycles in the Antarctic marine ecosystem. In: (W.R. Siegfried, P.R. Condy and R.M. Laws, editors) Antarctic nutrient cycles and food webs. Springer-Verlag, Berlin, Germany. pp. 6-10.

Holm-Hansen, O., El-Sayed, S.Z., Franchesini, G.A., Cuhel, G.A., and Cuhel, R.L. (1977) Primary production and the factors controlling phytoplankton growth in the Southern Ocean. In: (G. Llano, editor) Adaptations within the Antarctic ecosystem. Gulf Publishing Co., Texas. pp. 11-73.

Holm-Hansen, O., Mitchell, B.G., Hewes, C.D., and Karl, D.M. (1989) Phytoplankton blooms in the vicinity of Palmer Station, Antarctica. Polar Biology, 10: 49-57.

Holm-Hansen, O., Amos, A.F., Silva, N.S., Villafane, V., and Helbling, E.W. (1994) *In situ* evidence for a nutrient limitation of phytoplankton growth in pelagic Antarctic waters. Antarctic Science, 6: 315-324.

Honjo, S. (1990) Particle fluxes and modern sedimentation in the polar oceans. In: (W.O. Smith Jr, editor) Polar Oceanography, Academic Press, San Diego. pp. 687-739.

Horner, R., and Schrader, G.C. (1982) Relative contributions of ice-algae, phytoplankton, and benthic microalgae to primary production in nearshore regions of the Beaufort Sea. Arctic, 35: 485-503.

Houghton, J.T., Callander, B.A., and Varney, S.K. (1992) Climatic change 1992: The supplementary report to the IPCC scientific assessment. Cambridge University Press, Cambridge, UK. 200 pp.

Humphries, S.E. (1987) SIBEX II cruise to the Prydz Bay region, 1985: nutrient data. ANARE Research Notes, 45: 1-101.

Huntley, M.E., Lopez, M.D.G., and Karl, D.M. (1991a) Top predators in the Southern Ocean: a major leak in the biological carbon pump. Science, 253: 64-66.

Huntley, M., Karl, D.M., Niiler, P., and Holm-Hansen, O. (1991b) Research on Antarctic Coastal Ecosystems (RACER): an interdisciplinary field experiment. Deep-Sea Research, 38: 911-941.

Jacques, G. (1983) Some ecophysiological aspects of Antarctic phytoplankton. Polar Biology, 2: 27-33.

Jacques, G., and Panouse, M. (1991) Biomass and composition of size fractionated phytoplankton in the Weddell Scotia Confluence area. Polar Biology, 11: 315-328.

Jahnke, R.A. (1996) The global ocean flux of particulate organic carbon: areal distribution and magnitude. Global Biogeochemical Cycles, 10: 71-88.

Janse, I., van Rijssel, M., Gottschal, J.C., Lancelot, C., and Gieskes, W.W.C. (1996) Carbohydrates in the North Sea during spring blooms of *Phaeocystis*: a specific fingerprint. Aquatic Microbial Ecology, 10: 97-103.

Jennings, J.C., Gordon, L.I., and Nelson, D.M. (1984) Nutrient depletion indicates high primary productivity in the Weddell Sea. Nature, 309: 51-54.

Johnson, K.M., Wills, K.D., Butler, D.B., Johnson, W.K., and Wong, C.S. (1993) Coulometric total carbon dioxide analysis for marine studies: maximizing the performance of an automated gas extraction system and coulometric detector. Marine Chemistry, 44: 167-187.

Jones, E.P., and Coote, A.R. (1981) Oceanic CO_2 produced by the precipitation of $CaCO_3$ from brines in sea ice. Journal of Geophysical Research, 86: 11041-11043.

Jones, E.P., Nelson, D.M., and Tréguer, P. (1990). Chemical oceanography. In: (W.O. Smith Jr, editor) Polar Oceanography, Academic Press, San Diego. pp. 407-476.

Kang, S-H., and Fryxell, G.A. (1992) *Fragilariopsis cylindrus* (Grunow) Krieger: The most abundant diatom in water column assemblages of Antarctic marginal ice-edge zones. Polar Biology, 12: 609-627.

Kantha, L.H. (1979) Turbulent entrainment at the buoyancy interface due to convective turbulence. In: (H.J. Freeland, D.M. Farmer and C.D. Levings, editors) Fjord Oceanography. Plenum Press, New York, USA. pp. 205-213.

Karl, D.M., Tilbrook, B.D., and Tien, G. (1991) Seasonal coupling of organic matter production and particle flux in the western Bransfield Strait, Antarctica. Deep-Sea Research, 38: 1127-1143.

Keeling, C.D. (1973) Industrial production of carbon dioxide from fossil fuel and limestone. Tellus, 25: 174-198.

Keeling, C.D. (1993) Seasonal carbon cycling in the Sargasso Sea. In: (M. Heimann, editor) Global carbon cycle. NATO Advanced Research Institute, Springer-Verlag, New York, USA. pp. 413-429.

Keeling, R.F., Piper, S.C., and Heimann, M. (1996) Global and hemispheric CO_2 sinks deduced from changes in atmospheric O_2 concentration. Nature, 381: 218-221.

Keir, R.S. (1993) Are atmospheric CO_2 content and Pleistocene climate connected by wind speed over a polar Mediterranean Sea. Global and Planetary Change. 8: 59-68.

Kennedy, H., and Robertson, J. (1995) Variations in the isotopic composition of particulate organic carbon in the surface waters along an 88° W transect from 67°S to 54°S. Deep-Sea Research, 42: 1109-1122.

Kirkwood, D.S. (1992) Stability of solutions of nutrient salts during storage. Marine Chemistry, 38: 151-164.

Kirkwood, J.M. (1993) Zooplankton community dynamics and diel vertical migration in Ellis Fjord, Vestfold Hills, Antarctica. Ph.D. thesis, Monash University. Unpublished.

Kirkwood, J.M., and Burton, H.R. (1987) Three new zooplankton nets designed for under-ice sampling; with preliminary results of collections made from Ellis Fjord, Antarctica, during 1985. Proceedings of the NIPR Symposium on Polar Biology, 1: 112-122.

Kirkwood, J.M., and Burton, H.R. (1988) Macrobenthic species assemblages in Ellis Fjord, Vestfold Hills, Antarctica. Marine Biology, 97: 445-457.

Knox, G.A. (1990) Primary production and consumption in McMurdo Sound, Antarctica. In: (K.R. Kerry and G. Hempel, editors) Antarctic ecosystems: Ecological change and conservation. Springer-Verlag, Berlin. pp. 115-128.

Kopczynska, E.E. (1992) Dominance of microflagellates over diatoms in the Antarctic areas of deep vertical mixing and krill concentrations. Journal of Plankton Research, 14: 1031-1054.

Kopczynska, E.E., Goeyens, L., Semeneh, M., and Dehairs, F. (1995) Phytoplankton composition and cell carbon distribution in Prydz Bay, Antarctica: relation to organic particulate matter and its $\delta^{13}C$ values. Journal of Plankton Research, 17: 685-707.

Krebs, W.N. (1983) Ecology of neritic marine diatoms, Arthur Harbor, Antarctica. Micropaleontology, 29: 267-297.

Kroopnick, P. (1974) The dissolved O_2 - CO_2 - ^{13}C system in the eastern equatorial Pacific. Deep-Sea Research, 21: 211-227.

Laws, E.A., Popp, B.N., Bidigare, R.T., Kennicutt, M.C., and Macko, S.A. (1995) Dependence of phytoplankton carbon isotopic composition on growth rate and $[CO_2]_{aq}$: Theoretical considerations and experimental results. Geochimica et Cosmochimica Acta., 59: 1131-1138.

Leakey, R.J.G., Archer, S.D., and Grey, J. (In press) Microbial dynamics in coastal waters of Eastern Antarctica: Bacterial production and nanoflagellate bacteriovory. Marine Ecology Progress Series.

Ledford-Hoffmann, P.A., DeMaster, D.J., and Nittrouer, C.A. (1986) Biogenic silica accumulation in the Ross Sea and the importance of Antarctic shelf deposits in the marine silica budget. Geochimica et Cosmochimica Acta, 50: 2099-2110.

Lee, K., and Millero, F.J. (1995) Thermodynamic studies of the carbonate system in seawater. Deep-Sea Research, 42: 2035-2061.

Leventer, A. (1991) Sediment trap diatom assemblages from the northern Antarctic Peninsula region. Deep-Sea Research, 38:1127-1143.

Libes, S.M. (1992) An introduction to marine biogeochemistry. John Wiley and Sons, New York, 734 pp.

Liss, P.S., and Merlivat, L. (1986) Air-sea gas exchange rates: introduction and synthesis. In: (P. Buat-Menard, editor): The role of air-sea exchange in geochemical cycling. D. Reidel, Norwell, Massachusetts, USA. pp. 113-127.

Lubin, D., Frederick, J.E., Booth, C.R., Lucas, T., and Neuschuler, D. (1989) Measurements of enhanced springtime ultraviolet radiation at Palmer Station, Antarctica. Geophysical Research Letters, 16: 783-785.

Machta, L. (1973) The role of the oceans and the biosphere in the CO_2 cycle. In: (D. Dyrssen and D. Jagner, editors): The changing chemistry of the oceans. Nobel Symposium 20. Almquist and Wiksell, Stockholm, Sweden. pp. 121-145.

Maksimov, I.V. (1958) A study of the Antarctic westward coastal current. Soviet Antarctic Expedition Information Bulletin (English Translation). Elsevier, Amsterdam. Vol 1, pp. 79-81.

Marchant, H.J., and Perrin, R.A. (1990) Seasonal abundance and species composition of choanoflagellates (Acanthoecideae) at Antarctic coastal sites. Polar Biology, 10: 499-505.

Marchant, H.J., van den Hoff, J., and Burton, H.R. (1987) Loricate choanoflagellates from Ellis Fjord, Antarctica, including the description of *Acanthocorbis tintinnabulum* sp. nov. Proceeding of the NIPR Symposium Polar Biology, 1: 10-22.

Martin, J.H., Gordon, R.M., and Fitzwater, S.E. (1990) Iron in Antarctic waters. Nature, 345: 156-158.

Martin, J.H., Gordon, R.M., and Fitzwater, S.E. (1991) The case for iron. Limnology and Oceanography, 36: 1793-1802.

Matsuda, O., Ishikawa, S., and Kawaguchi, K. (1986) Experimental decomposition of particulate organic matter collected under the fast ice in Lützow-Holm Bay, Antarctica, with special reference to the fate of carbon, nitrogen and phosphorus. Memoirs of the National Institute for Polar Research, Special Issue, 44; 67-85.

Matsuda, O., Ishikawa, S., and Kawaguchi, K. (1987a) Oceanographic and marine biological data based on the routine observations near Syowa Station between February 1984 and January 1985 (JARE-25). JARE Data Reports 121, 21 pp.

Matsuda, O., Ishikawa, S., and Kawaguchi, K. (1987b) Seasonal variation of downward flux of particulate organic matter under the antarctic fast ice. Proceedings of the NIPR Symposium of Polar Biology, 1: 23-34.

McConville, M.J., and Wetherbee, R. (1983) The bottom-ice microalgal community from annual ice in the inshore waters of East Antarctica. Journal of Phycology, 19: 431-439.

McConville, M.J., Mitchell, C., and Wetherbee, R. (1985) Patterns of carbon assimilation in a microalgal community from annual sea ice, East Antarctica. Polar Biology, 4: 135-141.

McDonald, R.W., McLaughlin, F.A., and Wang, L. (1986) The storage of reactive silicate samples by freezing. Limnology and Oceanography, 23: 508-517.

McMeekin, T.A. (1988) Preliminary observations on psychrotrophic and psychrophilic, heterotrophic bacteria from antarctic water samples. Hydrobiologia, 165: 35-40.

McMinn, A. (1994) Preliminary investigation of a method for determining past winter temperatures at Ellis Fjord, eastern Antarctica, from fast ice assemblages. Memoirs of the Japanese Institute for Polar Research, Special Issue, 50: 34-40.

McMinn, A. (1996) Preliminary investigation of the contribution of fast-ice algae to the spring phytoplankton bloom in Ellis Fjord, eastern Antarctica. Polar Biology, 16: 301-307.

McMinn, A., and Hodgson, D. (1993) Summer phytoplankton succession in Ellis Fjord, eastern Antarctica. Journal of Plankton Research, 15: 925-938.

McMinn, A., Gibson, J., Hodgson, D., and Aschmann, J. (1995) Nutrient limitation in Ellis Fjord, eastern Antarctica. Polar Biology, 15: 269-276.

McTaggart, A.R. (1994) Dimethylsulfide and iodine in Australian waters. Ph.D. thesis, University of New South Wales. Unpublished.

Medlin, L.K., and Priddle, J. (1990) Polar Marine Diatoms. British Antarctic Survey, Cambridge, UK. 214 pp.

Medlin, L.K., Lange, M., and Baumann, M.E.M. (1994) Genetic differentiation among three colony-forming species of *Phaeocystis*: further evidence for the phylogeny of the Prymnesiophyta. Phycologia, 33: 199-212.

Mikkelsen, K. (1935) Opdagelsen av Ingrid Christensen Land. Norsk Geografisk Tidsskrift, 5: 372-376

Millero, F.J. (1995) Thermodynamics of the carbon dioxide system in the oceans. Geochimica et Cosmochimica Acta, 59: 661-677.

Mitchell, C., and Beardall, J. (1996) Inorganic carbon uptake by an Antarctic sea-ice diatom, *Nitzschia frigida*. Polar Biology, 16: 95-99.

Mook, W.G., Bommerson, J.C., and Staverman, W.H. (1974) Carbon isotope fractionation between dissolved bicarbonate and gaseous carbon dioxide. Earth and Planetary Science Letters, 22: 169-176.

Nedwell, D.B., Walker, T.R., Ellis-Evans, J.C., and Clarke, A. (1993) Measurements of seasonal rates and annual budgets of organic carbon fluxes in an Antarctic coastal environment at Signy Island, South Orkney Islands, suggest a broad balance between production and decomposition. Applied and Environmental Microbiology, 59: 3989-3995.

Nelson, D.M., and Smith, W.O. Jr. (1986) Phytoplankton bloom dynamics of the western Ross Sea ice edge - II. Mesoscale cycling of nitrogen and silicon. Deep-Sea Research, 33: 1389-1412.

Nelson, D.M., Smith, W.O. Jr, Gordon, L.I., and Huber, B.A. (1987) Spring distribution of density, nutrients and phytoplankton biomass in the ice edge zone of the Weddell-Scotia Sea. Journal of Geophysical Research, 92: 7181-7190.

Nelson, D.M., and Tréguer, P. (1992) The role of silicon as a limiting nutrient to Antarctic diatoms: evidence from kinetic studies in the Ross Sea ice-edge zones. Marine Ecology Progress Series, 80:255-264.

Nelson, K.H., and Thompson, T.G. (1954) Deposition of salts from seawater by frigid concentration. Journal of Marine Research, 13: 166-182.

Nolting, R.F., de Baar, H.J.W., van Bennekom, A.J., and Masson, A. (1991) Cadmium, copper and iron in the Scotia, Weddell Sea and the Weddell/Scotia confluence. Marine Chemistry, 35: 219-243.

Nozaki, Y., Cochran, J.K., Turekian, K.K., and Keller, G. (1977) Radiocarbon and ^{210}Pb distributions in submersible-taken deep sea cores from Project FAMOUS. Earth and Planetary Science Letters 34: 167-173.

Overnell, J., and Young, S. (1995) Sedimentation and carbon flux in a Scottish sea loch, Loch Linne. Estuarine, Coastal and Shelf Science, 41:361-376.

Palmisano, A.C., and Sullivan, C.W. (1983) Sea ice microbial communities (SIMCO). I. Distribution, abundance, and primary production of ice microalgae in McMurdo Sound, Antarctica in 1980. Polar Biology, 2: 171-177.

Palmisano, A.C., SooHoo, J.B., and Sullivan, C.W. (1985) Photosynthesis-irradiance relationships in sea ice microalga from McMurdo Sound, Antarctica. Journal of Phycology, 21: 341 - 346.

Palmisano, A.C., SooHoo, J.B., SooHoo, S.L., Kottmeier, S.T., Craft, L.L., and Sullivan, C.W. (1986) Photoadaptation in *Phaeocystis pouchetii* advected beneath annual sea ice in McMurdo Sound, Antarctica. Journal of Plankton Research, 8: 891-906.

Palmisano, A.C., Lizotte, M.P., Smith, G.A., Nichols, P.D., White, D.C., and Sullivan, C.W. (1988) Changes in photosynthetic carbon assimilation in Antarctic sea ice diatoms during spring bloom variation. Journal of Experimental Marine Biology and Ecology, 116: 1-13.

Parsons, T.R., Maita, Y., and Lalli, C.M. (1984) A Manual of Chemical and Biological Methods of Seawater Analysis. Pergamon Press, Oxford. 173 pp.

Peinert, R., von Bodungen, B., and Smetacek, V. (1989) Food web structures and loss rates. In: (W.H. Berger, V.S. Smetacek and G. Wefer, editors) Productivity of the ocean: present and past. John Wiley & Sons, London. pp. 35-48.

Peng, T.-H., Broecker, W.S., Kipphut, G., and Shackleton, N. (1977) Benthic mixing in deep sea cores as determined by 14C dating and its implications regarding climate stratigraphy and the fate of fossil fuel CO_2. In: (N. Andersen and A. Malahoff, editors) The fate of fossil fuel CO_2 in the ocean. Plenum Press, New York. pp. 355-374

Perez, F.F., Figueiras, F.G., and Rios, A.F. (1994) Nutrient depletion and particulate matter near the ice-edge in the Weddell Sea. Marine Ecology Progress Series, 112: 143-153

Perrin, R.A., Lu, P., and Marchant, H.J. (1987) Seasonal variation in marine phytoplankton and ice algae at a shallow antarctic coastal site. Hydrobiologia, 146: 33-46.

Pickard, J. (1986) Antarctic oases, Davis station and the Vestfold Hills. In: (J. Pickard, editor) Antarctic Oasis. Academic Press, Sydney. pp. 1-19.

Platt, H.M. (1979) Sedimentation and the distribution of organic matter in a sub-Antarctic marine bay. Estuarine and Coastal Marine Science 9: 51-63.

Platt, T., Harrison, W.G., Lewis, M.R., Li, W.K.W., Sathyendranath, S., Smith, R.E., and Vezina, A.F. (1989) Biological production of the oceans: the case for consensus. Marine Ecology Progress Series, 52: 77-88.

Poisson, A.T., and Chen, C-T.A. (1987) Why is there little anthropogenic CO_2 in the Antarctic Bottom Water? Deep-Sea Research, 34: 1255-1275.

Popp, B.N., Takigiku, R., Hayes, J.M., Louda, J.W., and Baker, E.W. (1989) The post-Paleozoic chronology and mechanisms of ^{13}C depletion in primary marine organic matter. American Journal of Science, 289: 436-454.

Post, W.M., Peng, T.-H., Emmanuel, W.R., King, A.W., Dale, H., and DeAngelis, D.L. (1990) The global carbon cycle. American Scientist, 78: 310-326.

Priddle, J., and Fryxell, G. (1985) Handbook of the common plankton diatoms of the Southern Ocean: Centrales except the genus *Thalassiosira*. British Antarctic Survey, Cambridge, UK. 159 pp.

Quay, P.D., Tilbrook, B., and Wong, C.S. (1992) Oceanic uptake of fossil fuel CO_2: Carbon-13 evidence. Science, 256: 74-79

Rao, P.C. (1996) Modern carbonates. Tropical, temperate, polar: Introduction to sedimentology and geochemistry. Carbonates, Hobart. 206 pp.

Rau, G.H., Takahashi, T., and Des Marais, D.J. (1989) Latitudinal variations in plankton $\delta^{13}C$: implications for CO_2 and productivity in past oceans. Nature, 341: 516-518.

Rau, G.H., Sullivan, C.W., and Gordon, L.I. (1991a) $\delta^{13}C$ and $\delta^{15}N$ variations in Weddell Sea particulate organic matter. Marine Chemistry, 35: 355-369.

Rau, G.H., Froelich, P.N., Takahashi, T., and Des Marais, D.J. (1991b) Does sedimentary organic $\delta^{13}C$ record variations in quaternary ocean $[CO_2(aq)]$? Paleooceanography, 6: 335-347.

Rau, G.H., Takahashi, T., Des Marais, D.J., and Sullivan, C.W. (1991c) Particulate organic matter $\delta^{13}C$ variations across the Drake Passage. Journal of Geophysical Research, 96: 15131-15135.

Rau, G.H., Takahashi, T., Des Marais, D.J., Repeta, D.J., and Martin, J.H. (1992) The relationship between $\delta^{13}C$ of organic matter and $[CO_2(aq)]$ in ocean surface water: Data from a JGOFS site in the northeast Atlantic Ocean and a model. Geochimica et Cosmochimica Acta, 56: 1413-1419.

Redfield, A.C., Ketchum, B.H., and Richards, F.A. (1963) The influence of organisms on the composition of sea water. In: (M.N. Hill, editor) The Sea. Volume 2. Interscience, New York, USA. pp. 26-77.

Riebesell, U., Wolf-Gladrow, D.A., and Smetacek, V. (1993) Carbon dioxide limitation of marine phytoplankton growth rates. Nature, 361: 249-251.

Rivkin, R.B., Legendre, L., Deibel, D., Tremblay, J.-E., Klein, B., Crocker, K., Roy, S., Silverberg, N., Lovejoy, C., Mesplé, F., Romero, N., Anderson, M.R., Matthers, P., Savenkoff, C., Vézina, A., Therriault, J.-C., Wesson, J., Bérubé, C., and Ingram, R.G. (1996) Vertical flux of biogenic carbon in the ocean: Is there food web control. Science, 272: 1163-1166.

Roberts, N.J., and Burton, H.R. (1992) Sampling volatile organics from a meromictic Antarctic lake. Polar Biology, 13: 359-361.

Robertson., J.E., and Watson, A.J. (1995) A summertime sink for atmospheric carbon dioxide in the Southern Ocean between 88° W and 80° E. Deep-Sea Research II, 42: 1081-1091.

Rogers, J.C., and Dunbar, R.B. (1993) Carbon isotopic composition of particulate organic carbon in Ross Sea surface waters during austral summer. Antarctic Journal of the United States, 28: 81-83.

Rotty, R.M. (1977) Global carbon dioxide production from fossil fuels and cement A.D. 1950 - A.D. 2000. In: (N.R. Andersen and A. Malahoff, editors) The fate of fossil fuel CO_2 in the ocean. Plenum Press. New York, USA. pp. 167-181.

Sackett, W.M. (1986a) $\delta^{13}C$ signatures of organic carbon in southern high latitude deep sea sediments: Paleotemperature implications. Organic Geochemistry, 9: 63-68

Sackett, W.M. (1986b) Organic carbon in sediments underlying the Ross Ice Shelf. Organic Geochemistry, 9: 135-137

Sackett, W.M., Eadie, B.J., and Exner, M.E. (1974) Stable isotope composition in marine plankton and sediments. In: (B. Tissot and F. Biener, editors) Advances in organic geochemistry. Pergamon. Oxford, UK. pp. 661 - 671.

Sackett, W.M., Eckelmann, W.R., Bender, M.L., and Bé, A.W.H. (1965) Temperature dependence of carbon isotope composition in marine plankton and sediments. Science, 148: 235-237.

Sakshaug, E., and Holm-Hansen, O. (1984) Factors governing pelagic production in Polar Oceans. In: (O. Holm-Hansen, L. Bolis and R. Gilles, editors) Marine phytoplankton and productivity. Springer-Verlag, Berlin. pp. 1-18.

Sakshaug, E., and Skjoldal, H.R. (1989) Life at the ice edge. Ambio, 18: 60-67.

Sambrotto, R.N., Savidge, G., Robinson, C., Boyd, P., Takahashi, T., Karl, D.M., Langdon, C., Chipman, D., Marra, J., and Codispoti, L. (1993) Elevated consumption of carbon relative to nitrogen in the surface ocean. Nature, 363: 248-250.

Sarmiento, J.L., and Le Quéré, C. (1996) Oceanic carbon dioxide uptake in a model of century-scale global warming. Science, 274: 1346-1350

Schlosser, P., Kromer, B., Weppernig, R., Loosli, H.H., Bayer, R., Bonani, G., and Suter, M. (1994) The distribution of ^{14}C and ^{39}Ar in the Weddell Sea. Journal of Geophysical Research, 99: 10275-10287.

Schlosser, P., Pfleiderer, C., Kromer, B., Levin, I., Münnich, K.O., Bonani, G., Suter, M., and Wölfli, W. (1987) Measurement of small volume oceanic ^{14}C samples by accelerator mass spectrometry. Radiocarbon, 29: 347-352.

Shabica, S.V., Hedgpeth, J.W., and Park, P.K. (1977) Dissolved oxygen and pH increases by primary productivity in the surface water of Arthur Harbor, Antarctica, 1970-1971. In: (G. Llano, editor) Adaptations within Antarctic ecosystems. Smithsonian Institute, Washington DC, USA, pp. 83-97.

Shirtcliffe, T.G.L. (1964) Lake Bonney: Cause of elevated temperatures. Journal of Geophysical Research, 69: 5257-5268.

Siegenthaler, U., and Oeschger, H. (1987) Biospheric CO_2 emissions during the past 200 years reconstructed by deconvolution of ice core data. Tellus, 39B: 140-154.

Siegenthaler, U., and Sarmiento, J.L. (1993) Atmospheric carbon dioxide and the ocean. Nature, 365: 119-125.

Simon, V. (1986) Le systeme assimilation-regeneration des sels nutritifs de l'eau de surface dans le secteur indien de l'Ocean Austral. Marine Biology, 92: 431-442.

Skerratt, J.H., Nichols, P.D., McMeekin, T.A., and Burton, H.R. (1995) Seasonal and inter-annual changes in planktonic biomass and community structure in eastern Antarctica using signature lipids. Marine Chemistry, 51: 93-113.

Smetacek, V., Scharek, R., and Nöthig, E. (1990) Seasonal and regional variation in the pelagial and its relationship to the life history cycle of krill. In: (K.R. Kerry and G. Hempel, editors) Antarctic ecosystems: Ecological change and conservation. Springer-Verlag, Berlin. pp. 103-114.

Smethie, W.M., Takahashi, T.T., Chipman, D.W., and Ledwell, J.R. (1985) Gas exchange and CO_2 flux in the tropical Atlantic Ocean determined from ^{222}Rn and pCO_2 measurements. Journal of Geophysical Research, 90: 7005-7022.

Smith, N.R., Dong, Z., Kerry, K.R., and Wright, S. (1984) Water masses and circulation in the region of Prydz Bay, Antarctica. Deep-Sea Research, 31: 1121-1147.

Smith, S.V., and Hollibaugh, J.T. (1993) Coastal metabolism and the oceanic organic carbon balance. Reviews of Geophysics, 31: 75-89.

Smith, S.V., and Mackenzie, F.T. (1991) Comments on the role of oceanic biota as a sink for anthropogenic CO_2 emissions. Global Biogeochemical Cycles, 5: 189-190.

Smith, W.O. Jr (1987) Phytoplankton dynamics in marginal ice zones. Oceanography and Marine Biology, 25: 11-38.

Smith, W.O. Jr (1993) Nitrogen uptake and new production in the Greenland Sea: The spring *Phaeocystis* bloom. Journal of Geophysical Research, 98: 4681-4688.

Smith, W.O. Jr, and Nelson, D.M. (1986) Importance of ice edge phytoplankton production in the Southern Ocean. BioScience, 36: 251-257.

Smith, W.O. Jr, and Nelson, D.M. (1990) Phytoplankton growth and new production in the Weddell Sea marginal ice zone in the austral spring and autumn. Limnology and Oceanography, 35: 809-921.

Smith, W.O. Jr, and Sakshaug, E. (1990) Polar Phytoplankton, In: (W.O. Smith Jr, editor) Polar Oceanography, Academic Press, San Diego. pp. 477-525.

Smith, W.O. Jr, Codispoti, L.A., Nelson, D.M., Manley, T., Buskey, E.J., Niebauer, H.J., and Cota, G.F. (1991) Importance of *Phaeocystis* blooms in the high-latitude ocean carbon cycle. Nature, 352: 514-516.

Sommer, L. (1986) Nitrate and silicate competition among Antarctic phytoplankton. Marine Biology, 91: 345-351.

Steele, L.P., Beardsmore, D.J., Pearman, G.I. and Da Costa, D.A. (1996) Baseline carbon dioxide monitoring, In: (R.J. Francey, A.L. Dick, and N. Derek, editors) Baseline Atmospheric Program, Australia, 1994-5. Bureau of Meteorology and CSIRO Division of Atmospheric Research, Melbourne. p. 103

Streten, N.A. (1969) Aspects of the frequency of calms in Antarctica. Polar Record, 14: 463-470.

Streten, N.A. (1986) Climate of the Vestfold Hills. In: (J. Pickard, editor): Antarctic Oasis. Terrestrial Environments of the Vestfold Hills. Academic Press, Sydney. pp. 141-161.

Stucchi, D.J. (1979) The tidal jet in Rupert-Holberg Inlet. In: (H.J. Freeland, D.M. Farmer and C.D. Levings, editors) Fjord Oceanography. Plenum Press. New York. pp. 491-497.

Stumm, W., and Morgan, J.J. (1981) Aquatic Chemistry. Wiley-Interscience, New York. 780 pp.

Suess, H.E., and Revelle, R. (1957) Carbon dioxide exchange between atmosphere and ocean and the question of an increase of atmospheric CO_2 during the last decade. Tellus, 9: 18-27.

Sullivan, C.W., McClain, C.R., Comiso, J.C., and Smith, W.O. Jr (1988) Phytoplankton standing crops within an Antarctic ice edge assessed by satellite remote sensing. Journal of Geophysical Research, 93: 12487-12498.

Sundquist, E.T. (1993) The global carbon dioxide budget. Science, 259: 934-941.

Suzuki, Y. (1995) The global carbon cycle and the role of the ocean. Geoscience reports of the Shizuoka University, 22: 23-36.

Sverdrup, H.U. (1953) On conditions for the vernal blooming of phytoplankton. Journal du Conseil Internationale Permanent pour l'Exploration de la Mer, 18: 287-295.

Swadling, K.M., Gibson, J.A.E., Ritz, D.A., Nichols, P.D., and Hughes, D.E. (In press) Grazing of phytoplankton by copepods in eastern Antarctic coastal waters. Marine Biology.

Takahashi, T. (1989) The carbon dioxide puzzle. Oceanus, 32: 22-29.

Takahashi, T., and Chipman, D. (1982) Carbon dioxide partial pressure in surface waters of the southern ocean. Antarctic Journal of the United States, 17: 103-104.

Takahashi, T., Olafsson, J., Goddard, J.G., Chipman, D.W., and Sutherland, S.C. (1993) Seasonal variations of CO_2 and nutrients in the high-latitude surface oceans: a comparative study. Global Biogeochemical Studies, 7: 843-878.

Tans, P.P., and Bakwin, P.S. (1995) Climate change and carbon dioxide forever. Ambio, 24: 376-378.

Tans, P.P., Fung, I.Y., and Takahashi, T. (1990) Observational constraints on the global atmospheric CO_2 budget. Science, 247: 1431-1438.

Taylor, D.L., and Lee, C.C. (1971) A new cryptomonad from Antarctica, *Cryptomonas criophila* sp. nov. Archiv für Mikrobiologie, 75: 269-280.

Tierney, T.J. (1975) An externally draining freshwater system in the Vestfold Hills. Polar Record, 17: 684-685.

Tokarczyk, R. (1986) Annual cycle of chlorophyll *a* in Admiralty Bay, 1981-1982. Polish Archives of Hydrobiology, 33: 177-188.

Tréguer, P., Kamatani, A., and Guenely, S. (1988) Biogenic silica and particulate organic matter from the Indian sector of the Southern Ocean. Marine Chemistry, 23: 167-180.

Tucker, M.J. (1988) Temporal distribution and brooding behaviour of selected benthic species from the shallow marine waters off the Vestfold Hills, Antarctica. Hydrobiologia, 165: 15-159.

Tucker, M.J., and Burton H.R. (1988) The inshore marine ecosystem of the Vestfold Hills, Antarctica. Hydrobiologia, 165:129-139.

Tucker, M.J., and Burton H.R. (1990) Seasonal and spatial variations in the zooplankton community of an eastern Antarctic coastal location. Polar Biology, 10: 571-579.

Utermöhl, H. (1958): Zür Vervollkommung der quantitätiven Phytoplankton-Methodik. Mitteilungen - Internationale Vereinigung für Theoritische und Angewandte Limnologie, 9: 1-38.

Veldhuis, M.J.W., Admiraal, W., and Colijn, F. (1986) Chemical and physiological changes of phytoplankton during the spring bloom dominated by *Phaeocystis pouchetii* (Haptophyceae): Observations in Dutch coastal waters of the North Sea. Netherlands Journal of Sea Research. 20: 49-60.

Verity, P.G., Villareal, T.A., and Smayda, T.J. (1988) Ecological investigations of blooms of colonial *Phaeocystis pouchetii*. I. Abundance, biochemical composition, and metabolic rates. Journal of Plankton Research, 10: 219-248.

von Bodungen, B., Smetacek, V.S., Tilzer, M.M., and Zeitzschel, B. (1986) Primary production and sedimentation during spring in the Antarctic Peninsula region. Deep-Sea Research, 33:177-194.

von Bodungen, B., Nöthig, E., and Qingbo, S. (1988) New production of phytoplankton and sedimentation during summer 1985 in the south eastern Weddell Sea. Comparative Biochemistry and Physiology., 90B: 475-487.

von Bröckel, K. (1985) Primary production data from the south-eastern Weddell Sea. Polar Biology, 4: 75-80.

Wada, E., Terazaki, M., Kabaya, Y., and Nemoto, T. (1987) ^{15}N and ^{13}C abundances in the Antarctic Ocean with emphasis on the biogeochemical structure of the food web. Deep-Sea Research, 34: 829-841.

Wanninkhof, R. (1992) Relationship between wind speed and gas exchange over the ocean. Journal of Geophysical Research, 97: 7373-7382.

Wassmann, P. (1984) Sedimentation and benthic mineralization of organic detritus in a Norwegian Fjord. Marine Biology, 83: 83-94.

Wassmann, P., Vernet, M., Mitchell, B.G., and Rey, F. (1991) Mass sedimentation of *Phaeocystis pouchetii* in the Barents Sea. Marine Ecology Progress Series, 66: 183-195.

Watanabe, K., Satoh, H., Kanda, H., and Takahashi, E. (1986) Oceanographic and marine biological data from routine observations near Syowa Station between February 1983 and January 1984 (JARE-24). JARE Data Reports 114, 22 pp.

Watson, A.J., Robinson, C., Robertson, J.E., Williams, P.J.le B., and Fasham, M.J.R. (1991) Spatial variability in the sink for atmospheric carbon dioxide in the North Atlantic. Nature, 350: 50-53.

Weeks, W.F., and Ackley, S.F. (1982) The growth, structure and properties of sea ice. CRREL Monograph No. 82-1, US Army Corps of Engineers, Hanover, NH, USA. 130 pp.

Wefer, G., and Fischer, G. (1991) Annual primary production and export flux in the Southern Ocean from sediment trap data. Marine Chemistry, 35: 597-613.

Wefer, G., Fischer, G., Füetterer, D., and Gersonde, R. (1988) Seasonal particle flux in the Bransfield Strait, Antarctica. Deep-Sea Research, 35: 891-898.

Weiss, R.F. (1974) Carbon dioxide in water and seawater: the solubility of a non-ideal gas. Marine Chemistry, 2: 203-215.

Weiss, R.F., Ostlund, H.G., and Craig, H. (1979) Geochemical studies of the Weddell Sea. Deep-Sea Research, 26: 1093-1120.

White, W.B., and Peterson,. R.G. (1996) An Antarctic circumpolar wave in surface pressure, wind, temperature and sea-ice extent. Nature, 380: 699-702.

Williams, P.J. le B., Bauer, J., Benner, R., Hegeman, J., Ittekkot, V., Miller, A., Norrman, B., Suzuki, Y., Wangersky, P., and McCarthy, M. (1993) DOC subgroup report. Marine Chemistry, 41: 11-21.

Williams, R. (1988) The inshore marine fishes of the Vestfold Hills region, Antarctica. Hydrobiologia, 165: 161-167.

Wilson, D.L., Smith, W.O. Jr, and Nelson, D.M. (1986) Phytoplankton bloom dynamics of the Western Ross Sea ice edge. I. Primary productivity and species specific production. Deep-Sea Research, 33: 1375-1387.

Wong, A.P.S. (1994) Structure and dynamics of Prydz Bay, Antarctica, as inferred from a summer hydrographic data set. Honours Thesis, University of Tasmania. Unpublished.

Wong, W.W., and Sackett, W.M. (1978) Fractionation of stable carbon isotopes by marine phytoplankton. Geochimica et Cosmochimica Acta, 42: 1809-1815.

Zhang, H., and Byrne, R.H. (1996) Spectrophotometric pH measurements of surface seawater at in-situ conditions: absorbance and protonation behaviour of thymol blue. Marine Chemistry, 52: 17-25.

Zhang, J., Quay, P.D., and Wilbur, D.O. (1995) Carbon isotope fractionation during gas-water exchange and dissolution of CO_2. Geochimica et Cosmochimica Acta, 59: 107-114.